INVESTIGATION OF COPPER CONTAMINATION AND CORROSION SCALE MINERALOGY IN AGING DRINKING WATER DISTRIBUTION SYSTEMS

Nadja Frank Turek, Captain, USAF

AFIT/GES/ENV/06M-05

DEPARTMENT OF THE AIR FORCE
AIR UNIVERSITY

AIR FORCE INSTITUTE OF TECHNOLOGY

Wright-Patterson Air Force Base, Ohio

The views expressed in this thesis are those of the author and do not reflect the official policy or position of the United States Air Force, Department of Defense, or the United States Government

AFIT/GES/ENV/06M-05

INVESTIGATION OF COPPER CONTAMINATION AND CORROSION SCALE MINERALOGY IN AGING DRINKING WATER DISTRIBUTION SYSTEMS

THESIS

Presented to the Faculty

Department of Systems and Engineering Management

Graduate School of Engineering and Management

Air Force Institute of Technology

Air University

Air Education and Training Command

In Partial Fulfillment of the Requirements for the

Degree of Master of Science in Environmental Engineering and Science

Nadja Frank Turek

Captain, USAF

March 2006

AFIT/GES/ENV/06M-05

INVESTIGATION OF COPPER CONTAMINATION AND CORROSION SCALE MINERALOGY IN AGING DRINKING WATER DISTRIBUTION SYSTEMS

Nadja Frank Turek, BS
Captain, USAF

Approved:

_____/signed/_____	__15 March 06__
Dr. Mark N. Goltz (Chairman)	date
_____/signed/_____	__14 March 06__
Dr. Darren Lytle (Member)	date
_____/signed/_____	__09 March 06__
Dr. Ellen C. England (Member)	date

Abstract

Research has shown higher levels of copper appear in drinking water conveyed through relatively new copper piping systems; older piping systems typically deliver lower copper levels in their drinking water. This research contributes field data from a real drinking water distribution system, providing a better understanding of this phenomenon, as it relates to treatment considerations and compliance with the Lead and Copper Rule.

Copper pipes and copper levels were sampled from drinking water taps of 16 buildings with pipes ranging in age from less than 1 to 48 years. Water samples from each building were collected before and following a 16-hour stagnation period. A piece of domestic cold water pipe was cut from each building near the tap where the water samples were obtained and analyzed to determine the mineralogy of the copper scale present using x-ray diffraction (XRD) and x-ray photoelectron spectroscopy (XPS) technologies.

The samples showed remarkable variation in scale appearance and mineralogy, demonstrating the diversity of pipe scales present within a single distribution system. A mix of highly soluble and relatively insoluble copper phases were identified in the real world scale. Both stable scales, such as malachite, and relatively instable solids, such as cupric hydroxide appear in pipes irrespective of age. In many samples cupric hydroxide and cuprite appeared on the surface of the scale while malachite was in the bulk. Copper cyanide was also identified in two pipe scales. XPS and XRD are shown to be complimentary techniques for characterizing complex scales made up of a mixture of amorphous and crystalline solids.

To my Opa

Acknowledgments

I want to thank the many people that made this collaborative project possible. Dr. Mark Goltz and LtCol Ellen England were both incredibly supportive and caring advisors to me. Without the consultation and knowledge base of Dr. Darren Lytle of the EPA, this topic would never have materialized as my thesis, and without his constant enthusiasm for the topic, my spirits may have failed me. The tap water and pipe sampling were made possible by the cooperation and support of many members of the 88th Air Base Wing Civil Engineer's organization, including Randy Parker, Tom Davis, Treva Bashore, C.J. Vehorn, Jim Bundy, and Cheryl Robinson. I am indebted to Mark and Robin, the patient plumbers who cut up lots of perfectly good pipe with me for this project, and Ron Creech their supervisor. The building managers of each building in the sample deserve thanks for allowing me into their buildings and enduring the inconvenience of sampling. Linda Kasten of the University of Dayton Research Institute single-handedly taught me to analyze and understand XPS spectra, and more importantly always treated me like a respected peer and collaborator. She was more influential to this research and my personal sanity than she may ever know. Dr. Charles Bleckman and Dr. Audrey McGowin deserve thanks as supporters, teachers and sounding boards for me throughout. But my ultimate supporters, sounding boards, confidants, and cheerleaders for this effort were my beloved family; my husband, my parents and my sister. Thanks also to my fellow AFIT students who shared this journey with me.

Table of Contents

Page

Page

Page

List of Figures

Page

Page

List of Tables

INVESTIGATION OF COPPER CONTAMINATION AND CORROSION SCALE MINERALOGY IN AGING DRINKING WATER DISTRIBUTION SYSTEMS

I. INTRODUCTION

1.1 Overview

Copper is a soft, malleable, ductile, and highly conductive metal found naturally as ore. One of the main uses of copper is to make pipes and fittings for drinking water distribution systems. Water flowing through distribution systems corrodes the copper to some extent (some waters more than others) resulting in the release of copper into the drinking water (USC, 1991). Although trace amounts of copper are essential for all forms of life and are found in every human tissue, ingesting too much copper can cause stomach and intestinal distress, liver or kidney damage, and complications of Wilson's disease in genetically predisposed people (Schroeder, 1966; EPA, n.d.). Acute gastrointestinal effects of excessive copper ingestion include nausea, vomiting, stomach cramps and diarrhea, especially in children (Schroeder, 1966; Pontius, 1998). In 1991 the United States Environmental Protection Agency (USEPA) passed the Lead and Copper Rule (LCR) to "protect public health by minimizing lead and copper levels in drinking water, primarily by reducing water corrosivity" (USEPA, 2004).

1.2 Background

The Lead and Copper Rule (LCR) was passed by the USEPA to establish a mandatory monitoring program for lead and copper in drinking water. Due to the well-

understood and detrimental effects of lead consumption, much of the attention and sampling under the LCR has been focused on sites where high lead levels are anticipated, such as older buildings, where lead service lines or use of lead solder, is expected. Although copper is needed in the human body at low levels, it is also controlled under the LCR to prevent stomach and intestinal distress and liver or kidney damage caused by higher exposure. The USEPA has set the action level for copper at 1.3 mg/L or 1300 μg/L in drinking water (USC, 1991; USEPA, 2002). In contrast to lead, younger buildings may be more at risk for high copper levels in drinking water because new copper piping has not yet built up a protective scale. As water flows through copper pipe a cuprous oxide film builds up on the pipe walls. This film is important for inhibiting further copper dissolution in potable water systems (Lane, 1993). Many laboratory studies have explored copper corrosion under various water conditions (Palit and Pehkonen, 2000; Boulay and Edwards, 2001; Broo et al., 1997; Edwards et al., 1996; Feng et al. 1996a and 1996b; Schock et al., 1995; Zang et al., 2002); however, not as much is known about the evolution of copper corrosion processes in the field; that is, in the pipes of buildings.

1.3 Problem Identification

In the summer of 2004, the Wright-Patterson Air Force Base (WPAFB) Bioenvironmental Engineering Flight conducted extensive lead and copper testing of the drinking water at four Child Development Centers (CDCs) on the base. Such sampling is required by Air Force Instruction 34-248, *Child Development Centers*, every three years. Also, an October 1992 policy memo from the Air Force Director of Medical Programs

and Resources directs the Bioenvironmental Engineering Services to conduct lead sampling prior to opening a CDC that has had a plumbing line or fixture replaced or added. Since both new construction and renovation work was recently completed on the WPAFB CDCs, every tap (i.e. faucet, spigot, water fountain, etc.) in these four facilities was sampled. The study discovered elevated levels of both lead and copper in many of the CDC taps.

Table 1.1, reproduced from *Investigation/Survey of Lead and Copper in Drinking Water at Child Care Development Centers* contains the abbreviated results of the WPAFB CDCs tap tests from summer 2004 (Shaw Environmental Inc., 2004). The table compares the tap values to 15 μg/L of lead and 1300 μg/L of copper, the action levels dictated by the EPA under the Lead and Copper Rule. Between 12% and 55% of taps (depending upon the building sampled) in the CDCs exceeded the action levels of lead or copper, leading the Air Force to turn its attention to these metals.

Table 1.1 Summary of Pb and Cu Water Sampling Results from WPAFB CDCs, Summer 2004

Building Number	Number of Taps Sampled	Number of Taps Pb>15 μg/L	% of Taps Pb>15 μg/L	Number of Taps Cu>1300 μg/L	% of Taps Cu>1300 μg/L	% of Taps exceeding Pb or Cu action level*
26933	77	9	12%	2	3%	12%
11403	43	5	12%	0	0%	12%
20630	164	11	7%	53	32%	35%
31235	29	11	38%	8	28%	55%

Data reproduced from *Investigation/Survey of Lead and Copper in Drinking Water at Child Care Development Centers*
* Some taps exceeded both Cu and Pb action levels

In addition to the required CDC testing, lead and copper sampling is conducted in other WPAFB facilities every three years as required by the EPA under the LCR. Taps from 30 buildings serviced by the base's Area B water distribution systems and 30

buildings serviced by the combined Area A/C water distribution systems are sampled. The last LCR sampling at WPAFB was conducted in September 2003. Water purveyors must report the "90th percentile" results to the EPA; that is, the lead or copper levels that are exceeded by only 10% of the samples. For Area B water, the 90th percentile values for lead and copper were 2.85 μg/L and 561 μg/L, respectively. For the Area A/C water system, the 90th percentile values for lead and copper were 2.475 μg/L and 890 μg/L, respectively (Shaw, 2005). Both systems' results were well below the LCR action levels (although the only CDC tested in September 2003 slightly exceeded the action level, with a copper concentration of 1370 μg/L).

WPAFB funded further study of the lead and copper problems at the CDCs in May 2005. The high copper levels at two of the four CDCs were satisfactorily addressed by replacing individual plumbing fixtures (although follow-up testing is needed). At the other two CDCs, Shaw Environmental Inc. concluded the heightened copper levels were attributable to interaction between the buildings' new copper pipe and the drinking water. Further testing may ultimately result in a recommendation for a new water treatment system to reduce the levels of copper in these two facilities. Shaw recommends "…drinking water sampling at five or six newer buildings on base to substantiate that elevated copper levels...are a result of the combination of new pipe, low to neutral pH, and high alkalinity" (Shaw Environmental Inc., 2005).

Recent research supports Shaw's conclusion that the high copper levels on WPAFB could be caused by new copper pipe in combination with cuprosolvent water. Epidemiological studies have shown higher rates of copper related illness and higher copper concentrations in younger homes with copper piping (Knobeloch et al., 1998;

Rajaratnam et al., 2002; Sharrett et al., 1982b). Many researchers have undertaken epidemiological copper studies in an effort to estimate the general population's exposure to copper in drinking water and have gathered valuable data about buildings of different ages in the process (Sharrett et al., 1982a; Lagos et al., 1999). Much like the WPAFB CDC study, these researchers discovered higher copper exposure risk in younger buildings within their distribution area. One study found that although the water system involved had always been in compliance with the LCR, newly built or remodeled houses in the service area had very high concentrations of copper, often exceeding the action level (Cantor et al., 2000). LCR testing, which focuses on older, "high risk" buildings, including those built within five years of the leaded solder ban, and houses with lead service lines or lead interior plumbing, often misses high copper levels in the tap water of new buildings.

Such epidemiological studies support predictions of the "cupric hydroxide model" which was developed by researchers at the EPA's National Risk Management Research Laboratory, Water Supply and Water Resource Division (Schock et al., 1995). The model was designed to predict dissolved copper concentrations in drinking water, accounting specifically for the effects of pH and dissolved inorganic carbon (DIC). The model is a tool available to water purveyors to model their system's water quality, test treatment options, and predict copper concentrations cheaply and quickly. The model predicts that given identical stagnation times, equivalent water usage patterns, and the absence of any diffusion barriers such as mineral deposits, the standing copper level in tap water is predicted to decrease over time due to the development of a corrosion film on the inside of copper pipes (Schock et al., 1995). Laboratory experiments conducted by

the EPA in the process of model development and testing, and subsequent lab studies, have shown the copper concentrations in water decrease linearly with average age of the copper pipe (Schock et al. 1995; Lagos et al. 2001).

The investigators found precipitation and dissolution of a corrosive film on the inside of copper pipes to be the main causes of copper "aging" over time and diminishing copper concentrations. Electrochemical reactions between Cu metal and water cause the initial formation of solid corrosion compounds on the pipe inner walls. Copper corrosion can produce one or several copper solids that form a scale on the inner walls of copper pipe over time. The development and aging of such copper scales play an important role in determining the level of copper in drinking water (Schock et al., 1995). As highly soluble solids dissolve into drinking water, precipitation of less-soluble compounds simultaneously begins. The dissolution of a high-solubility compound enables the precipitation of a low-solubility compound, therefore aging the scale (Lagos et al., 2001). Low-solubility solids that develop later in the life of a copper pipe produce lower copper concentrations in drinking water.

Limited field data have supported an inverse correlation between age of pipe and copper concentrations in drinking water (Brandenburg et al., 1993; Lagos et al., 2001). However more well designed studies of real piping systems are needed to corroborate the predictions of the cupric hydroxide model and the applicability of controlled laboratory findings to predict behavior in real distribution systems in the field.

1.4 Copper Corrosion

Copper is used frequently in water distribution systems because, as a noble metal, it is highly resistant to corrosion (Lane, 1993). Copper forms an oxide film on its surface when exposed to water, and this film acts as a boundary between the electrolyte and metal, protecting the metal from further corrosion. Exposure to clean, debris free water of pH between 7.2 and 8.5 and containing adequate dissolved oxygen will provide optimal conditions for cuprous oxide film development (CDA, 2005). It is also essential to maintain water velocity and temperature within limits in copper pipes in order to preserve the oxide film (Lane, 1993; CDA, 2005). The main corrosion problem associated with copper is rapid pitting in cold water which leads to pipe failure (AWWA, 1985).

Copper levels will be higher in drinking water samples taken after letting the water stand in the pipes, as may occur overnight (Lane, 1993). Flushing, or allowing water to flow freely from the faucet after a period of stagnation, in the morning is often recommended to lower copper levels in drinking water (EPA, n.d.; Knobeloch et al., 1998). The principal variables affecting the amount of dissolved copper in drinking water are (Lane, 1993):

- Water quality
- Materials in the pipes (brass, copper, alloys)
- Temperature and velocity of the water
- Age of the plumbing system (new systems have higher copper dissolution while older systems have developed protective oxide/scale layers)
- Length of time water contacts the metal

Water composition, including pH, bicarbonate (HCO_3^-), chloride (Cl^-), sulfate (SO_4^{2-}) and calcium (Ca^{2+}) concentrations, affect the chemical make-up and solubility of copper solids formed on the inside of copper pipes, and therefore affect the dissolved copper concentrations that are in equilibrium with those solids in the drinking water (Lagos et al., 2001). While water quality parameters' effects on copper concentrations have been heavily researched in the lab, and in many cases are well understood (Palit and Pehkonen, 2000; Boulay and Edwards, 2001; Broo et al., 1997; Edwards et al., 1996; Feng et al. 1996a and 1996b; Schock et al., 1995; Zang et al., 2002), the question of how the age of pipe/scale is related to copper concentration levels (and hence, exposure to copper) still remains to be answered. A theory explaining this relationship has been developed and modeled by the EPA, but requires substantiation in the field (Schock et al., 1995).

1.5 Research Questions/Objectives

The purpose of this research was to increase our understanding of the development and properties of copper scale in drinking water systems as buildings age. Four main research questions were suggested by the literature reviewed.

1. How does the age of a copper piping system influence the level of copper in drinking water?
2. How does the age of the piping system affect the type of copper corrosion scale present in a pipe? How does mineralogy of the corrosion scale develop/change with time?
3. How does copper pipe scale mineralogy and composition in the field compare to the cupric hydroxide model's predictions?

4. What type of corrosive scale most effectively reduces dissolved concentrations of copper in drinking water?

1.6 Research Approach

Background facility data were collected and analyzed to choose a representative sample of Wright Patterson AFB buildings with copper drinking water piping of different ages. Wright Patterson offered a unique setting for a study of copper levels in aging drinking water systems. An area of the base was selected containing scores of buildings supplied by only one water treatment system, providing similar water quality to all the eligible buildings. Wright Patterson was first an Army and then an Air Force facility, in operation since the days of the Wright brothers, and has grown continually throughout its history. The base contains buildings and copper piping systems of all ages going back 65 years. From this population of buildings, a sample was selected and studied representing copper pipe of different ages.

Water chemistry data were analytically determined for the drinking water being delivered to each building. To answer the first research question, water samples from each building were collected following a consistent experimental protocol and copper concentrations determined by inductively coupled plasma spectroscopy. Each tap was flushed, sampled for water characterization, pH, and chlorine, and then taken out of service for 16-hours. After the 16-hour stagnation period, two 250 mL samples were collected for copper concentration measurement. The post-stagnation samples were also tested for water characterization, pH, and chlorine. After all samples were collected, an

analysis was conducted to determine if the level of copper within the drinking water could be correlated with the age of the buildings' piping.

To answer the second and third research questions, a piece of domestic cold water pipe was cut from each building in the vicinity of the tap where the water sample was obtained. The pipe walls visually examined to compare solid properties and coverage, and viewed under a stereomicroscope to ascertain qualitative information about the scales present. The pipe walls were also analyzed to determine the mineralogy of the copper scale present using X-ray diffraction (XRD) and X-ray photoelectron spectroscopy (XPS) technologies. XRD allows an analyst to compare an unknown solid sample to a database of different solid compounds to identify the mineralogy of any crystalline solids present. XPS allows identification of copper oxides and the oxidation state of the copper solids at the immediate surface of a solid. This is the first study to combine these two techniques to identify and analyze the complex scales present on the inside of a drinking water distribution system, as XPS is normally employed in the analysis of pristine scales created in a laboratory. These complementary techniques were used to confidently identify the scale solids present.

The combination of scale characterization and copper concentration data allowed a comparison of copper levels in drinking water with the mineralogy of the copper solid present in the corresponding supply pipes. These parameters were compared for copper piping systems of different ages. Data collected were also compared with predictions of the cupric hydroxide model (Schock et al., 1995).

1.7 Scope

This study was sponsored jointly by the WPAFB Civil Engineers (88 ABW/CE) and the USEPA's Water Supply and Water Resource Division, and is unique in several ways. The well documented collection of buildings on WPAFB presented a research opportunity. The base's many buildings contain copper piping of many different ages that can be dated with confidence using the thorough maintenance and construction records kept by the base Civil Engineers. With the support of the 88 ABW/CE, the researcher was able to access a variety of locations within the base water distribution system and both cut physical pipe samples and collect corresponding water samples. This is the first study to collect both water and pipe samples of many ages that have been supplied over time by the same water source. Sampling WPAFB afforded us a unique opportunity to see the development of corrosion scales over time in a single distribution system, and to be able to compare water quality with the corrosion scale in the delivery pipes.

This is also the first study to use XPS as a complementary technique to XRD to identify the corrosion scales present in real-world pipe samples. XRD is able to identify a variety of stable solids at once, making it a powerful tool often used to analyze copper pipe corrosion. However, XRD cannot recognize amorphous solids, including cupric hydroxide, thought to be a key participant in the aging phenomenon. XPS can identify amorphous solids and is therefore employed as a secondary analytical technique to XRD in this study.

The results of this research are applicable directly to water purveyors with similar water properties to those of WPAFB. This study does not aim to develop new copper

corrosion theory, but rather to help validate the laboratory studies and copper corrosion models already available in the literature by adding field data to the body of knowledge. This research is part of a collaborative effort between the Air Force Institute of Technology and the USEPA's Water Supply and Water Resource Division to better characterize corrosion scale in copper piping and improve the cupric hydroxide model. The model was developed by the USEPA as a tool for water purveyors nationwide. The model allows these purveyors to simulate the effect of changes in water quality on copper concentrations. It also is a tool that can be used by water purveyors to predict how copper levels in consumers' water will change over time.

Results of the analyses were also used to guide the leadership of the Wright Patterson AFB Base Civil Engineers in managing their water supply system. This study further characterized the copper levels delivered to the base's consumers in buildings of different ages. It also characterized the scales seen in various buildings on base. The information will help the Base Civil Engineers make future decisions about changing or maintaining water quality characteristics to combat high copper levels in drinking water.

1.8 Significance

This study also advances the overall understanding of the contribution of pipe age to the concentration of copper in drinking water. Since water testing is focused on older buildings under the LCR, it is possible copper problems in young buildings are being overlooked. Many researchers have expressed concern that the LCR is not effective in detecting and managing copper risk to drinking water consumers. Several weaknesses in

the LCR have been identified (Kimbrough, 2001; Cantor et al., 2000; Schock et al., 2001):

- Lack of a feedback mechanism in the LCR to determine whether lead and copper levels decline naturally over time
- The 90th percentile reporting requirement is not a sensitive measure to changes in lead or copper levels
- The validity of the "high-risk" predictors used to choose LCR sampling locations has been questioned, especially with respect to building age
- The LCR assumes "high-risk" buildings remain so indefinitely
- LCR compliance data are often inappropriate or misleading for determining the chemical relationships behind copper corrosion
- LCR samples may not be representative of the overall lead and copper risk

Data from the current study may be helpful in addressing some of these weaknesses. An increased understanding of the development and properties of copper scale in drinking water systems as piping systems age adds to the body of knowledge available for USEPA decision makers as they attempt to revise the LCR.

Validating the USEPA's cupric hydroxide model with field data should also bolster confidence in the model, allowing water purveyors to quickly and cheaply model their water systems. Purveyors with recognized copper problems can use the model to predict the effects of corrosion control modifications they may be considering for their water treatment regime. A validated model provides a valuable problem solving tool for the USEPA, WPAFB, and other water purveyors.

1.9 Summary

This research will synthesize information available concerning copper corrosion in drinking water systems, including theory developed in the laboratory to explain the role of aging in copper scale formation and dissolution. It aims to advance the knowledge of copper corrosion scale aging by collecting and analyzing water and solid samples to determine dissolved copper levels and copper scale mineralogy from pipes of different ages. This study is unique in several ways. It is the first to collect and analyze both copper pipe and corresponding water samples of a variety of ages from a water distribution system. It is also the first to use XPS and XRD as complementary analytical techniques to identify corrosion solids on real-world pipes. Results may be helpful to local, state, and federal regulators and water system purveyors as they manage copper piping in the nation's drinking water distribution systems.

II. LITERATURE REVIEW

2.1 Copper and Household Plumbing

Copper is a soft, malleable, ductile, and highly conductive metal that is normally light red in color (AWWA, 1985). It is the first element of Group 1B on the periodic table and is a noble metal, found in nature in its pure form. Copper in its oxidized state is extremely active, forming more water-soluble salts than any other metal in its periodic group, as well as many other compounds (Seiler et al., 1994). Copper has four natural oxidation states: Cu(0), Cu(+1), Cu(+2), and Cu(+3). Cu(+1) or cuprous ion is unstable, and it will rapidly be oxidized to Cu(+2) or reduced to Cu(0) in water. It will only be stable as a component of an insoluble compound, such as CuCl(s) or Cu_2O(s). Cuprous compounds normally are colorless unless bound to a ligand of color (USDHHS, 2004). Cupric ions, Cu(+2), are the most important oxidized form of copper. Cupric ions form a variety of compounds, most of which are water soluble, and a variety of complexes by binding to dissolved organics or inorganic ions. Virtually all complexes and compounds of Cu(+2) are blue or green. (USDHHS, 2004; Seiler et al. 1994). Finally, Cu(+3) forms many complexes which are generally short-lived and considered industrially and environmentally insignificant (USDHHS, 2004; Seiler et al. 1994).

Although there is a long list of uses for copper, one familiar application is in copper tubing used extensively to convey potable water in buildings and homes. Copper is utilized in water distribution systems because it is highly resistant to corrosion (Lane, 1993; CDA, 2005), is relatively easy to install and has been shown to kill certain bacterial

species in water (Shim, 2004). Copper has replaced alternative metals for pipes up to approximately two inches in diameter where it is cost competitive (CDA, 2005). It is more noble in the galvanic series, and therefore more corrosion resistant than any other metal used commonly in water distribution systems (AWWA, 1985). Primitive cultures use copper pots to contain and carry drinking water, perhaps understanding intuitively it helped make the water safer to drink. Indeed a study in India found that brass pitchers (brass is a copper alloy made of at least 67% copper) used by rural cultures released tiny amounts of copper that killed harmful bacteria in the water (Kaiser, 2005). Copper sulfate is also commonly used to control algae in water storage tanks (Rajaratnam, 2002) and agriculturally as a fungicide (Seiler et al., 1994).

Trace amounts of copper are essential for all forms of life and are found in every human tissue in varying amounts (Schroeder, 1966). The human body uses copper to construct a variety of enzymes and proteins many of which serve relatively undefined functions (Seiler et al., 1994). The recommended dietary allowance intake for copper is 700-900 μg/day for adults and children over four, and 200-440 μg/day for children under four years old (Institute of Medicine, 2000). However, in the 1990's the United States, the World Health Organization and the European Union enacted health-based standards for drinking water to protect against over-consumption of copper (Lagos, 1999). Copper has the potential to cause acute gastrointestinal disorders including nausea, vomiting, stomach cramps and diarrhea when consumed in too great a quantity, especially by children (Schroeder, 1966; Pontius, 1998). Additionally, people with several rare, hereditary, genetic disorders are unable to properly transport and excrete copper when over exposed and therefore store enormous amounts of copper in the liver, kidney, and

brain (Schroeder, 1966; USDHHS, 2004). These genetic disorders can lead to severe brain damage, liver failure, and death. Because of the acute health danger presented by copper overdose, the USEPA set a maximum contaminant level goal of 1300 μg/L for copper in drinking water to both provide the nutritional requirement for copper intake while protecting against acute gastrointestinal effects (USC, 1991).

2.2 The Lead and Copper Rule

Copper regulation was first mandated under the Safe Drinking Water Act amendments of 1986. The USEPA proposed a rule for lead and copper in 1988, and passed the Lead and Copper Rule (LCR) in June of 1991, establishing a mandatory monitoring program for lead and copper in drinking water. In 1986 the USEPA also banned use of lead and lead-based (containing more than 8% lead) solders in home plumbing systems (USC, 1986). The LCR directs water purveyors to identify and sample "high-risk" homes/buildings including (40 CFR 141.86(a)):

- Those containing copper pipes with lead solder installed after 1982 or containing lead pipes
- Those served by a lead service line
- When neither of the above apply, those containing copper pipes with lead solder installed before 1983
- When none of the above apply, a representative sample of buildings or homes in the water supply area

Water purveyors must report the "90^{th} percentile" results to the USEPA; that is, the lead or copper levels that are exceeded by only 10% of the samples. The sampling

requirements above focus on older buildings with lead service lines or solder where primarily high lead levels are anticipated.

In contrast to lead, younger homes may be at higher risk for elevated copper levels in drinking water because new copper piping has not yet developed a protective corrosion scale. Since water testing is focused on older homes under the LCR, it is possible copper problems in young buildings are being overlooked. As previously mentioned, many researchers have expressed concern that the LCR is not effective in detecting and managing copper risk to drinking water consumers (Kimbrough, 2001; Cantor et al., 2000; Schock et al., 2001).

In the first round of LCR monitoring, approximately 6% of the large water systems that submitted data exceeded the 1.3 mg/L action level. For the first and second rounds of monitoring combined, 7.9% of large utilities exceeded the copper action level (Schock et al., 1995). These percentages probably represent the lower bound for copper exceedances considering the testing protocol does not focus on buildings where the highest copper levels are thought to be found.

Drinking water is not the only media of concern for high copper levels. Elevated copper concentrations are also found in the sludge produced by wastewater treatment plants. In Europe and the US such sludge is often applied to agricultural fields as fertilizer as a form of recycling, but if the copper content is too high it must be disposed of as hazardous waste instead of reused. Broo et al. (1997) state that most of the copper found in wastewater originates from corrosion of the copper in private piping systems. Wastewater treatment is effective at removing copper from wastewater however, copper is concentrated in the sludge produced (Broo et al., 1997). In the United States, sludge

exceeding the ceiling concentration limit for copper, 4,300 mg/kg waste, is not allowed to be land applied. Likewise land appliers cannot exceed the cumulative pollutant loading rate of 1,500 kg Cu/hectare over the lifetime of the land application or the annual limit of 75 kg/hectare/year (USEPA, 1995). If copper corrodes from the inside of piping systems and ends up concentrated in the sludge generated at the wastewater treatment plant, land application ceases to be a sludge disposal option and additional cost is incurred to dispose of the sludge as hazardous waste.

Many researchers have investigated copper corrosion in piping systems to both protect consumers from acute copper exposure in drinking water and to limit copper concentrations in wastewater sludge. A wealth of field studies, laboratory experiments, and theories have added to the body of knowledge about copper corrosion over the past forty years.

2.3 Field Evidence of Heightened Copper Concentrations in Young Plumbing

Many field studies have provided epidemiological evidence that dissolved copper concentrations in drinking water are higher in homes with new copper pipes. Sharrett et al. (1982a, 1982b) conducted a study of copper, zinc, lead, and cadmium consumption by consumers of Seattle drinking water in 1981. They found that metal concentrations in drinking water were closely related to the type of plumbing in the resident's home. After examining many variables, the researchers found that the concentration of dissolved copper in homes with copper plumbing systems was associated with the length of copper pipe in the house and the age of the house. In standing water samples (taken after overnight stagnation in the system) longer pipes produced a median 885 μg/L of copper

while shorter pipes had a median of 446 μg/L ($P<0.01$). The age of the copper pipes was also shown to be significant. In homes newer than 5 years old the median standing sample concentration was 1379 μg/L, while the median concentration in older (>5 years) homes was only 653 μg/L ($P<0.01$) (Sharrett et al., 1982a).

A 1998 study concluded that ingestion of high levels of copper in tap water caused an outbreak of intestinal disorders in Wisconsin. The study's authors found that 69% of the houses built in the previous five years had copper levels in the tap water exceeding the 1300 μg/L standard, while only 1% of the houses built 10 years or more before the study had levels of copper exceeding standards (Knobeloch et al., 1998). An associated study found that although the water system involved had always been in compliance with the LCR, newly built or remodeled houses in the service area had very high concentrations of copper, often exceeding the action level (Cantor et al., 2000).

In a study of Contra Costa Central Sanitary District (California) aimed at estimating the impact of copper residential plumbing on levels of copper found in the city's wastewater, copper concentrations were inversely correlated with the age of the copper plumbing. Concentration of copper decreased as copper pipes aged. In this study taps were flushed the night prior to testing. Then in the morning, prior to any other water usage, the first 500 mL of tap water were discarded and the following 1000 mL were collected for sampling in order to get water that had stagnated in the copper piping system over night (Brandenburg et al., 1993). Standing times varied from 6 to 14 hours, which can cause great variation in sampling results. Since USEPA studies have shown copper concentrations increase linearly for the first 10-15 hours of stagnation, the copper amount observed was divided by the standing time to get a leaching rate (Schock et al.,

1995). These rates were then graphed, and an inverse relationship between rate and plumbing age was exhibited for plumbing ages less than 20 - 35 years. Above this age range, the data become more random. Figure 2.1 shows the rate vs. plumbing age data for two water systems, Contra Costa Water District (CCWD) and the East Bay Municipal Utility District (EBMUD), considered in the study (Brandenburg et al., 1993; Schock et al., 1995).

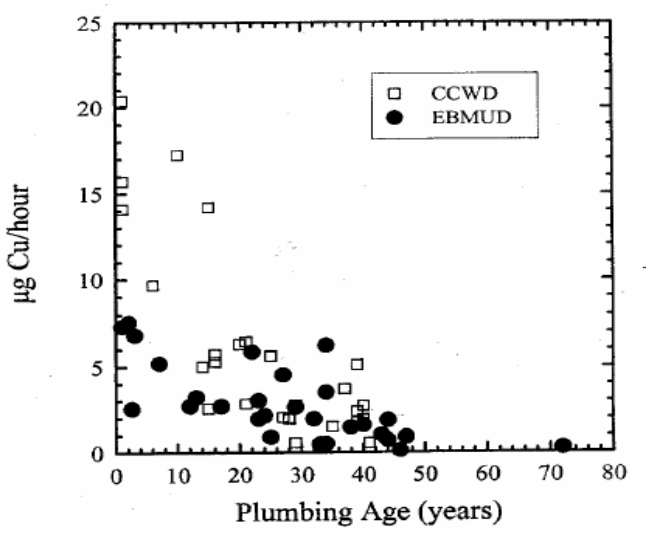

Figure 2.1 Distribution of adjusted copper leaching rates vs. age (Schock et al., 1995).

A study of pipe and drinking water samples from Santiago, Chile's water system, that will be explored in more detail later, also showed copper concentrations in water decrease linearly with the average age of the copper pipe (Lagos et al., 2001).

2.4 Corrosion and Scale Formation

The word 'corrosion' comes from the Latin term 'corrodere' meaning 'gnaw away' (Mattsson, 1989). Corrosion, in simple terms, is the degradation of a metal due to an electrochemical reaction (Lane, 1993, pg 2). The International Standard Organization

defines corrosion as a “physicochemical interaction between a metal and its environment which results in changes in the property of the metal and which may often lead to impairment of the function of the metal, the environment, or the technical system of which these form a part” (ISO, 2004). Corrosion can damage metal infrastructure, such as steam lines, condensate returns, storage tanks, hot and cold potable water delivery pipes, and heating and cooling systems. Metal corrosion can cause discolored or dirty water at the consumer’s tap, taste and odor problems, scale build-up causing clogged pipes, or pipe failure due to pits or perforations in the metal.

The term ‘scale’ refers to mineral deposits that form a coating on a metal surface. Scale formation depends on water quality parameters such as alkalinity and pH (Lane, 1993). Scale can cause a thickening of pipe walls as minerals build up deposits on the inside, reducing the diameter of the pipe available for water flow. Conversely, corrosion causes a thinning of the pipe wall, as metal dissolves into water and is removed from the inside of the pipe. Often corrosion and scaling happen in tandem, as metal is removed from the pipe itself and forms new solid scales on the inside of the pipe wall. However some metal ions will also simply dissolve into the water and not reform as solid scale.

In *Control of Scale and Corrosion in Building Water Systems*, Lane (1993) explains that four components are necessary to cause corrosion of metal: an anode or positive pole, a cathode or negative pole, an electrolyte or chemically conductive medium (e.g. water), and an electric circuit. In combination these elements create an electrochemical cell, as shown in Figure 2.2, where electrons are leaving the anode and flowing through the electrolyte into the cathode creating an electric current (Mattsson, 1989; AWWA, 1985).

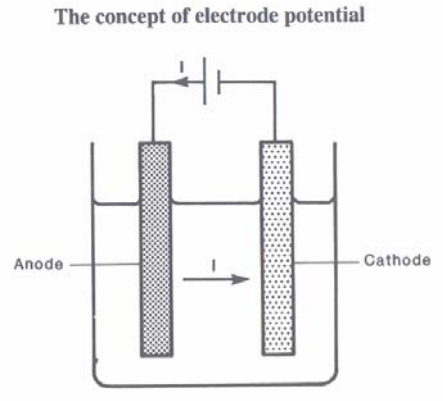

Figure 2.2 The basic electrochemical cell (Mattsson, 1985)

There are many types of corrosion depending on the circumstances of the corrosion cell's development (pitting, galvanic, dezincification, erosion-corrosion, and stress corrosion to name a few). In general or uniform corrosion, numerous small anodes and cathodes form on the metal surface causing relatively equal corrosion over the entire surface of the metal (Mattsson, 1989; Lane, 1993). This corrosion type will be the focus of this research. Uniform corrosion takes place in a generally corrosive environment, instead of having areas of heavy or localized deterioration. The rate, or corrosion current, of corrosion is dependent on several factors. Different metals have different relative electrochemical potentials based on their inherent tendency to return to the stable form in which they are found in the earth. Metals that are highly noble, meaning inert or inactive, return to a relatively stable form and are less corrosive, while less noble metals have a greater natural tendency to corrode (Lane, 1993; Mattsson, 1989).

It is helpful to quantify the corrosive potential of an electrochemical cell. The electromotive force, E, or potential to corrode, can be quantified by measuring the difference of potentials between the two electrodes (anode and cathode). However, the absolute value of the potential of each electrode alone cannot be determined experimentally, since the anode and cathode are not independent of each other. In order

to measure the potential of just the anode or the cathode alone, a relative value is discovered by experiment. The standard hydrogen electrode (SHE) consisting of a platinum wire platinized by electrolysis, surrounded by a solution with H^+ ion activity of one and bathed in hydrogen gas at one atmosphere pressure, is given a value of zero electrode potential. All other electrode potentials are measured relative to this standard. The standard potential, E^0, is the electrode potential that occurs when a metal (or redox reaction) is compared to the SHE and all substances taking part in the reaction have an activity of one. According to the International Union of Pure and Applied Chemistry convention of 1953 all SHE measurements of reactions are read in the sense of the reduction, so values are given relative to their ability to be reduced. A larger standard reduction potentials, E^0, indicates that the reaction is more thermodynamically favorable for reduction.

The standard electromotive potential of a corrosion cell can be quantified as:

$$E^o_{cell} = E^o_{anode} + E^o_{cathode}$$

and the standard potential is related to the Gibbs free energy by:

$$\Delta G^0_{cell} = - n F E^0_{cell}$$

where n is number of moles of electrons per mole of products and F is the Faraday constant. In a galvanic cell, where a spontaneous redox reaction drives the cell to produce an electric potential, Gibbs free energy ΔG^0 must be negative, and therefore the E^o_{cell} must be positive.

The corrosion rate is also dependent on the properties of the electrolyte, most often water. According to Lane (1993), “the corrosiveness of a water depends entirely on its degree of saturation with the ions or molecules of the metal or compound with which

it is in contact". Certain water properties can further promote corrosion including (Lane, 1993):

- Low pH
- Low alkalinity
- Soft water, with hardness below 60 mg/L
- High concentrations of chloride and/or sulfate
- High dissolved oxygen
- Low buffer intensity
- Low pH combined with high conductivity (>500 μS/cm)
- Free chlorine above 1 mg/L or free chloramines above ~2 mg/L
- The presence of suspended solids (like sand or crud)

The appearance of dissolved copper in drinking water is the result of both corrosion of copper pipe and the affiliated process of scale development on pipe walls. An understanding of both processes as they relate to copper is necessary to answer our research questions.

2.5 Electrochemistry of Copper Corrosion

Electrochemical reactions, where electrons are being transferred between elements, are the basis of corrosion chemistry. In an electrochemical reaction, the electron donor is oxidized, thereby transferring an electron, to the electron acceptor, which is reduced. For a metal, Me^{n+}, in a corrosion cell surrounded by an electrolyte such as water, electrode reactions will occur at the metal surface until equilibrium is reached:

$$Me \Leftrightarrow Me^{n+} + ne^{-}$$

Electrons leave the anodic portion of the metal surface and flow through the electrolyte into the cathodic region. The anode is the location of metal loss due to corrosion. At the anode conditions are favorable for chemical oxidation, whereby electrons release from the metal molecules, leaving behind positively charged metal ions. The loss of electrons causes a flow of electrical current from anode to cathode, the magnitude of which is measured to quantify corrosion. Some common oxidation reactions involving copper are:

$$Cu \Leftrightarrow Cu^{+} + e^{-}$$
$$Cu \Leftrightarrow Cu^{+2} + 2e^{-}$$

Since electrons cannot exist free in solution in any significant concentration, an oxidation reaction must take place simultaneously with a reduction reaction, presumably when there is contact between the oxidizing and reducing agents. Most often oxygen dissolved in water is the oxidizing agent, in the following reaction:

$$\tfrac{1}{2} O_2 + H_2O + 2e^{-} \Leftrightarrow 2OH^{-}$$

Since copper plumbing is exposed to a wide spectrum of conditions, including potential-pH variation, deposition of solids, ever-changing redox reactions, over various lengths of time, it is reasonable to assume that three common copper valance states (0, +1, and +2) will occur in drinking water delivery pipes (Schock et al., 1995). Cuprous (Cu^{+1}) and cupric (Cu^{+2}) ions form as a result of oxidation of copper metal in drinking water (Palit, 2000):

$$Cu(s) \Leftrightarrow Cu^{+} + e^{-}; E^{0} = -0.52V$$
$$Cu^{+} \Leftrightarrow Cu^{+2} + e^{-}; E^{0} = 0.16V$$

Copper metal in contact with pure water will not corrode (Lane, 1985; Schock et al., 1995). It is the presence of a oxidizing agent in the water that causes corrosion of the

metal. The dominant electron acceptors in drinking water are dissolved oxygen and aqueous chlorine and chloramine species (Palit, 2000; Schock et al., 1995) with oxygen being the primary reactant in the usual pH range of drinking water (6.5 to 9.5):

$$O_2(g) + 4H^+ + 4e^- \Leftrightarrow 2H_2O; E^0 = 1.23V$$

When copper oxidation and oxygen reduction occur together in a corrosion cell, recall that standard potential (E^0) values are additive and E^0_{cell} will be a positive number due dominantly to the positive E^0 of the oxygen reaction. Corrosion will proceed until either the available dissolved oxygen is consumed (as can occur in water that stands stagnant in pipes for long times), or a copper oxide film retards the corrosion (Palit, 2000). A copper oxide film grows rapidly for approximately the first 200 hours of contact between copper and oxygenated water, with slower growth thereafter. Film growth typically passivates corrosion before oxygen and chlorine are depleted as reducing agents, and diffusion of copper ions in the film has been shown to control the overall corrosion rate thereafter (Feng et al., 1996). Film and scale formation will be discussed further in subsequent sections.

The oxidation of cuprous ion into cupric ion in water can be expressed as:

$$Cu^+ \rightarrow Cu^{+2} + e^-; K = 518.8 \quad \text{at } 25^0 \text{ C}$$

The large equilibrium constant shows the instability of cuprous ion as it moves dominantly to the cupric form in water without precipitating agents (AWWA, 1985). The concentration of total aqueous copper can be approximated by summing the concentrations of the dominant aqueous cupric species of Cu^{+2}, $Cu(OH)_2(aq)$, $CuCO_3(aq)$, and $CuHCO_3^+$ (Edwards et al., 1996). Between pH 7 and 8.5, which is the pH range of drinking water, the concentrations of other cupric or cuprous species are

negligible (Schock et al., 1995). The dominant cupric reactions with corresponding log K values (at 25^{o}C) are:

$$Cu^{+2} + 2H_2O \leftrightarrow Cu(OH)_2{}^{0} + 2H^{+} \quad \text{Log K = -16.24}$$

$$Cu^{+2} + CO_3{}^{-2} \leftrightarrow CuCO_3{}^{0} \qquad \text{Log K = 6.82}$$

$$Cu^{+2} + H^{+} + CO_3{}^{-2} \leftrightarrow CuHCO_3{}^{+} \qquad \text{Log K = 12.13}$$

Here it becomes easy to see the pH and dissolved inorganic carbon (DIC) (which can be calculated from alkalinity and pH) dependence of the corrosion and solubility processes. In order to have corrosion in the first place dissolved oxygen must be present, but the extent of uniform corrosion is very pH and DIC dependent (AWWA, 1985; Schock, 1995).

Thus, during uniform corrosion of copper on the inner walls of drinking water delivery pipes, the pipe acts as an anode, releasing cuprous and cupric ions into solution. The predominant oxidizing agent in this reaction is the dissolved oxygen that is present in the water. Since cuprous ions will preferentially be oxidized to cupric ions in solution, cuprous ions are found almost exclusively at the immediate metal-water interface while cupric ions are dominant in the bulk solution away from the metal surface.

2.6 Electrochemistry of Copper Scale Formation

Cuprous ion can form a few stable complexes in solution with ammonia ($Cu(NH_3)_2^{+}$ for instance) and chloride ($CuCl_2^{-}$, $CuCl_3^{-2}$, $CuCl_4^{-3}$) and can form the solid cuprous oxide or 'cuprite' [$Cu_2O(s)$] before being oxidized to cupric form. Electrochemists assert that cuprite is formed on contact between copper metal and water with the reduction of oxygen in the overall anode reactions (Ives and Rawson, 1962):

$$\tfrac{1}{2}O_2 + H_2O + 4Cu^0 \Leftrightarrow 2Cu_2O(s) + 2H^+ + 2e^-$$
$$2OH^- + 2Cu^0 \Leftrightarrow Cu_2O(s) + H_2O + 2e^-$$

These reactions at the anode lead to the creation of an oxide film of cuprite on the surface of the metal. If the film grows thick enough to retard the contact between dissolved oxygen and the metal surface, passivation occurs, and the rate of corrosion is slowed. The thin $Cu_2O(s)$ film is thought to remain at the immediate metal surface throughout the development of young scale. Feng et al. (1996a; b) determined that diffusion of copper ions through the oxide film is the rate limiting process in the corrosion of copper, and the presence of the cuprite film can significantly retard the corrosion process (Zhang et al., 2002).

Our interest is primarily in the level of dissolved copper in drinking water and dissolution of copper scale, not the rate of metal corrosion, because dissolution of copper scale is the main mechanism by which copper is released into drinking water. (Schock et al., 1995; Lagos et al., 2001). Therefore the concentration of aqueous copper depends heavily on the solubility and physical properties of the copper solids present in the scales on the walls of copper pipes. Copper forms into two categories of solid compounds, Cu^{+1} and Cu^{+2} species. Cupric compounds are soluble in water while cuprous compounds are less so (AWWA, 1985). The most common copper solids found on pipe walls are cuprite (Cu_2O), tenorite (CuO), malachite [$Cu_2(CO_3)(OH)_2$], langite [$Cu_4(OH)_6SO_4H_2O$], atacamite [$Cu_2(OH)_3Cl$], brochanite [$Cu_4(SO_4)(OH)_6$], azurite [$2CuCO_3Cu(OH)_2$], and cupric hydroxide [$Cu(OH)_2$] (Lagos et al., 2001). The equilibrium reactions for these solids and their solubility constants are shown in Table 2.1. More than one solid species

is almost always present and several compounds can and will precipitate simultaneously during the copper corrosion process (Lagos et al., 2001).

Table 2.1: Solubility Reactions for Common Copper Solids

Common Name	Equilibrium Reaction	Log K at 25°C
cuprite	$Cu_2O(s) + 2H^+ \leftrightarrow 2Cu^+ + H_2O$	-1.62
tenorite	$CuO(s) + 2H^+ \leftrightarrow Cu^{2+} + H_2O$	7.98
malachite	$Cu_2(CO_3)(OH)_2(s) + 2H^+ \leftrightarrow 2Cu^{2+} + 2H_2O + CO_3^{-2}$	-5.48
langite	$Cu_4(OH)_6SO_4H_2O(s) + 6H^+ \leftrightarrow 4Cu^{2+} + 7H_2O + SO_4^{-2}$	17.34
atacamite	$Cu_2(OH)_3Cl(s) + 3H^+ \leftrightarrow 2Cu^{2+} + Cl^- + 3H_2O$	14.68
brochanite	$Cu_4(SO_4)(OH)_6(s) + 6H^+ \leftrightarrow 4Cu^{2+} + 6H_2O + SO_4^{-2}$	15.38
cupric hydroxide	$Cu(OH)_2(s) + 2H^+ \leftrightarrow Cu^{2+} + 2H_2O$	8.89

Values from Schock et al., 1995 and used in the cupric hydroxide modeling program

2.7 Scale Aging

Cupric ions are formed preferentially in solution and contribute to important solubility-controlling solids. Copper concentrations in drinking water are heavily dependent on the solubility and physical properties of cupric oxide, hydroxide, and carbonate solids which make up most scales not at the immediate pipe surface in drinking water supply pipes (Palit, 2000). Maximum soluble copper concentrations are attained in equilibrium with the solid cupric hydroxide [$Cu(OH)_2(s)$], formed through the reaction (Shock et al., 1995; Broo et al., 1997):

$$Cu^{+2} + 2H_2O \Leftrightarrow Cu(OH)_2(s) + 2H^+$$

It is believed that in drinking water systems where aqueous copper concentrations reach elevated levels, particularly when the systems are young, the dominant solid in the scale is $Cu(OH)_2(s)$. Equilibrium copper concentrations will begin to fall as copper precipitates to form more thermodynamically stable copper solids (Broo et al., 1997). Aqueous copper concentrations in equilibrium with tenorite (CuO) are predicted to be an order of magnitude lower than concentrations in equilibrium with cupric hydroxide, and concentrations in equilibrium with malachite [$Cu_2(OH)_2(CO_3)$] are two orders of magnitude lower, as shown in Figure 2.3. An extensive explanation of the aqueous chemistry involved in both copper scale formation and dissolution is provided in the referenced work of Schock et al., (1995).

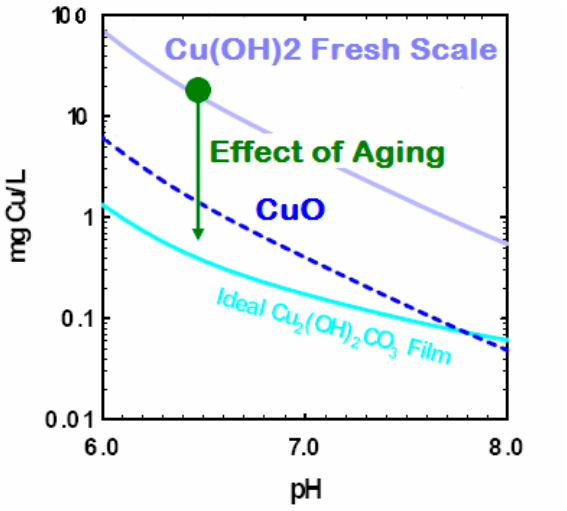

Figure 2.3 Effects of Aging on Dissolved Copper Concentration (Lytle, 2005)

A series of studies have examined the initial formation of copper solids and the aging process they undergo in an effort to effectively precipitate copper ions out of wastewater or wastewater sludge. The conclusions from these studies give us greater insight into the aging process on the inside of distribution pipes as well. Schindler et al. (1965) laid the foundation for later work by quantifying the influence of molar surface

area and surface tension on the solubility of certain solids, including $Cu(OH)_2(s)$ and CuO(s). They determined the thermodynamic activity of each solid in terms of molar surface area, S (m^2/mol), and surface tension, γ (ergs/cm^2). Schindler et al. (1965) found that when molar surface is large (when particles are initially forming), growth of $Cu(OH)_2$ is favored over CuO. As solid particles grow and reach a critical size (about 4 nm) $Cu(OH)_2(s)$ becomes thermodynamically less stable than CuO(s) and $Cu(OH)_2(s)$ will dehydrate to form CuO(s) according to the equation (Schindler et al., 1965):

$$Cu(OH)_2(s) \rightarrow CuO(s) + H_2O$$

The transition of matter from a disordered to an ordered state, or the transition from the liquid (or vapor) phase to the solid phase, is called crystallization (Brecevic, 2002). Although generally small particles crystallize in a system initially, larger particles are thermodynamically favored over small ones because small crystals have a larger surface area to volume ratio than large crystals. Surface molecules are energetically less stable than molecules already well ordered and packed in the interior of a large particle, so a lower surface area to volume ratio leads to a lower energy state. The spontaneous growth of small $Cu(OH)_2$ particles into larger ones over time is explained by the thermodynamic favorability of large crystals over small ones (Boistelle and Astier, 1988).

Patterson et al. (1991) studied cupric hydroxide formation and aging in controlled laboratory studies and identified a likely evolution of solids in accordance with Schindler et al.'s (1965) predictions. Patterson et al. (1991) observed three stages of growth. First, when saturation of Cu^{+2} was reached, a blue precipitate identified as $Cu(OH)_2(s)$ formed. Next, the solids change from blue to yellow as $Cu(OH)_2(s)$ dehydrated to form CuO(s), as predicted by Schindler et al. (1965). Finally, the solids grew in size and turbidity

increased as the color transitioned from yellow to brown to black, consistent with the growth of CuO(s) crystals. After a month of aging the copper concentration and solution properties were consistent with a system that would be in equilibrium with only CuO(s). Hidmi and Edwards (1999) studied the effects of pH and temperature on the aging of copper solids and used X-ray diffraction (XRD) to confirm the aging sequence proposed by Patterson et al. (1991). pH and temperature affected the rate of aging, but the stages were the same. At pHs 7, 8, and 9, and between 5 and 96 hours of aging, they observed predominately cupric hydroxide solids precipitating out of solution. After one month of aging at all pHs, tenorite, CuO(s), was the dominant solid.

In each of the controlled experiments described above, nitrate, sodium, cupric ions, and water were the only species present in the solutions as they aged. Therefore the role of carbonates, natural organic materials, chloride, or other important species in drinking water was not studied. While these experiments provide a valuable understanding of the aging sequence of copper solids, real drinking water systems are considerably more complex and scale aging within them is still not fully understood, especially with respect to the time required for aging to take place.

To review, when corrosion begins, $Cu_2O(s)$ forms at the metal surface, the outer layers of which are quickly oxidized in the presence of excess oxygen and chlorine to cupric aqueous species and solids such as $Cu(OH)_2(s)$. While the immediate $Cu_2O(s)$ film grows rapidly thick enough to passivate the corrosion process, equilibrium with $Cu(OH)_2(s)$ at the water interface controls the aqueous concentration of copper during the early stages of scale development. Then, as cupric hydroxide particles grow larger in

size, the outer scale transitions to tenorite (CuO), or at lower pHs, malachite, which lowers the aqueous copper concentration by one to two orders of magnitude.

If oxygen and chlorine become depleted over time as they oxidize the copper metal (for instance, due to water stagnating in pipes for long periods of time), then Cu^{+1} and Cu^{+2} metal in the surface film layer would be reduced, converting Cu^{+2} and $Cu(OH)_2(s)$ back into the cuprous forms $Cu_2O(s)$ or CuOH(s), thereby causing a decrease in the soluble copper concentration, as the cuprous form of copper is generally less soluble (Schock et al., 1995).

2.8 Modeling Cuprosolvency

The principal variables affecting the amount of dissolved copper in drinking water are (Lane, 1993):

- Water quality (AWWA, 1985)
- Materials in the pipes (brass, copper, alloys)
- Temperature and velocity of the water
- Age of the plumbing system
- Length of time water contacts the metal

It is commonly understood that aqueous copper concentration decreases as the pH of the water increases, and that copper concentration will increase as water temperature increases (AWWA, 1985; Lane, 1993; Edwards, 2002; Boulay and Edwards, 2001). It is widely believed that ammonia, sulfate, chloride, phosphate, and dissolved inorganic carbon (meaning CO_3^{-2}, HCO_3^-, and H_2CO_3) are the primary inorganic species that affect the concentration of dissolved copper in drinking water systems (Palit, 2000). High

concentrations of HCO_3^- will lead to higher copper corrosion by-product release. At a constant pH, copper concentration increases linearly with the HCO_3^- concentration (also reported as alkalinity) (Schock et al., 1995; Edwards et al., 1996; 2001). The presence of dissolved oxygen and chlorine residual species is essential for the copper corrosion process, as discussed earlier. Schock et al. (1995) found that copper-carbonate and oxide species had the dominant effect on cuprosolvency in drinking water, predicting that chloride, sulfate and ammonia species of Cu^{+2} would have little effect on the over all Cu^{+2} solubility when compared to carbonate.

Experimental evidence has shown that due to the dynamic environment inside a drinking water system, water chemistry does not reach equilibrium with copper and copper corrosion solids present unless long stagnation takes place. Broo et al. (1997) tudied copper coupons in contact with synthetic drinking water and compared their behavior with water samples taken from an operational drinking water system. Their findings implied that copper concentrations in drinking water did not reach equilibrium until at least 8 hours of stagnation in the piping system. It is widely assumed that the most significant health risk for high copper exposure occurs in water that has stagnated overnight, and therefore “first draw” water samples are analyzed for the LCR, and also in most copper studies, after a long stagnation. Therefore to be conservative most modeling of copper in water assumes copper levels have reached equilibrium with the copper solids present in the pipes.

Water chemistry modeling for this research included all relevant copper solid and aqueous species including ammonia, sulfate, chloride, phosphate, and carbonate. Computer modeling was based on fundamental aqueous chemistry relationships, using

thermodynamic solubiltiy and equilibriums constants. Model equilibrium equations, thermodynamic and solubility data, and development assumptions are described thoroughly elsewhere (Schock et al., 1995). The presence of organic matter has also been shown in some circumstances to increase cuprosolvency (Boulay and Edwards, 2001), although more study is needed to further the understanding of the role of organics and biofilms. Organic matter is not considered in the modeling associated with this work, as it is assumed to have negligible effect as compared to inorganics. The presence of a chlorine residual in drinking water distribution systems is intended to prevent most bacterial growth.

Much of the current understanding of the "aging" phenomenon of copper drinking water systems has been developed through water sampling and modeling. The USEPA's National Risk Management Research Laboratory, Water Supply and Water Resource Division developed the "cupric hydroxide model" based on copper coupon aging experiments and pipe rig studies (Schock et at, 1995). Experimental data demonstrated the dominance of $CuOH_2(s)$ in controlling copper levels in drinking water in young scales. The USEPA's modeling showed that given identical stagnation times, equal water usage patterns, and the lack of interfering mineral deposits, standing copper concentrations will decrease over time (Schock et al., 1995). In their analysis of copper concentrations in piping systems of various ages in Santiago, Chili, Lagos et al. (2001) collected field data supporting some of the model's predictions. They collected drinking water samples in 217 Santiago homes, measuring copper levels and water quality (the water system sampled had a mean pH of 7.9 and a mean hardness of 220 mg/L as $CaCO_3$). They then modeled the water in each home and predicted a "dominant copper

solid" that would best correspond to the copper levels found by measurement. In other words, they chose one particular copper solid by how well the model's prediction of the copper level in equilibrium with that solid corresponded to the real copper concentration. The distribution of 207 samples are shown in Figure 2.4, demonstrating a downward trend in copper concentration with age, similar to that shown earlier in the field data from the Contra Costa Central Sanitary District (Figure 2.1).

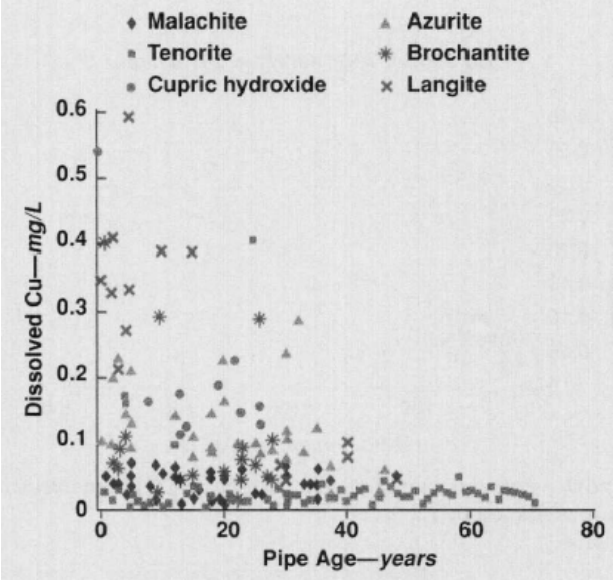

Figure 2.4 Copper concentration vs. pipe age from Lagos et al. (2001) study

Having assigned each sample a predicted equilibrium solid, Lagos et al. (2001) then sorted the data by solid and found a mean copper concentration for each dominant solid. When copper concentration data were thus sorted, the average 8-hour stagnant copper concentration in drinking water decreased linearly with age, as Schock et al. (1995) had predicted (Lagos et al., 2001). Figure 2.5 shows the mean values and shows the downward trend of copper concentration with age.

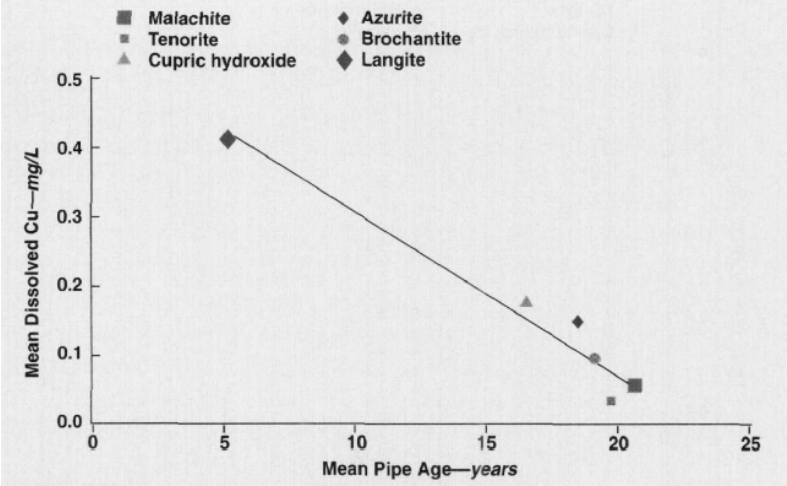

Figure 2.5 Plot of mean dissolved copper conc. vs. pipe age (Lagos et al., 2001), sorted by predicted copper solid

Understanding that copper concentrations should decrease with time as copper scales age, the question then is, how long does it take for the scale to 'age' and the copper concentrations to decrease? In the past it was thought malachite [$Cu_2(CO_3)(OH)_2(s)$] played the key role in determining the concentration of cupric species in drinking water in pipes of any age. As explained earlier, in newer pipes soluble copper levels are now thought to be controlled by equilibrium with $Cu(OH)_2(s)$ scale. Models employing $Cu(OH)_2(s)$ instead of CuO(s) as the controlling cupric solid have proven more realistic in the short term. Additionally if orthophosphate is present in the water, the lower solubility solid $Cu_3(PO_4)_2(s)$ can form instead of $Cu(OH)_2(s)$ and control copper solubility (Schock et al., 1995; Edwards et al., 2001). In the conclusions of their report on the cupric hydroxide model, Schock et al. (1995) recommend that water purveyors aiming to understand and control copper concentrations in their water supply should assume equilibrium with $Cu(OH)_2(s)$ for new pipes and should model equilibrium with

malachite or tenorite in older piping systems. But in what timeframe does this shift happen in real systems?

This question can only be partially answered. Schock et al.'s (1995) model is based on research showing that cupric hydroxide will slowly convert to tenorite through recrystallization and aging. If the pH falls below the range of tenorite stability, malachite will slowly form as well (Schock et al., 1995). Zhang et al. (2002) analyzed the corrosion of pure copper coupons in simulated tap water using x-ray photoelectron spectroscopy (XPS) and scanning electron microscopy. They found that for the first six days of immersion in water the polarization resistance of the copper metal increased steadily, then slowed from days 8 to 30 indicating growth of a passivating film primarily in the first six days. By day 8 of the experiment the copper surface was heavily covered with a cupric and cuprous oxide film. The intensity of XPS spectra peaks corresponding to $Cu_2O(s)$ in the film fell from day 8 to day 30 and as $Cu_2O(s)$ oxidized to Cu^{+2} solid species including $CuO(s)$, $CuCO_3(s)$ or $Cu(OH)_2(s)$. At day 30 an XPS nitrogen peak at binding energy 399.6 eV was attributed to ammonia incorporated into the film via the adsorption of ammonia copper complexes, and there was no evidence of chloride ion being incorporated into the film. In Zhang et al.'s (2002) control experiments observing copper coupon corrosion at pH 8 they observed that the polarization resistance was low in the first 8 days of the experiment, but was almost 100 fold higher than the initial value after 30 days of corrosion. Effective inhibition of corrosion was achieved by 30 days. At the 30 day mark the scale at the coupon surface was comprised of approximately 45% CuO, 30% Cu_2O, and 25% $CuCO_3$ or $Cu(OH)_2$ as estimated from XPS spectra (Zhang et al., 2002). Recall that Himdi and Edwards (1999) also observed that tenorite was

dominant and that copper concentrations were relatively low at the one month mark. However both of the above studies were controlled laboratory experiments with fewer variables than real pipe systems.

Lagos et al.'s (2001) study used x-ray diffraction (XRD) to examine copper coupons corroded experimentally for 69 days. They detected cuprite after 46 days of aging and langite, malachite, and hydrated cupric hydroxide [$Cu(OH)_2H_2O(s)$] after 69 days. They also cut several samples from buildings 30 and 40 years old served by the Santiago water system and analyzed the solids present in the pipe scale with XRD. Langite was the most soluble and youngest film found inside the copper pipes, while cupric hydroxide, azurite, brochantite, malachite, and tenorite were the next oldest films, respectively. The most stable solids found – malachite and tenorite – were 8 and 16 times less soluble than the most soluble compound, langite. The modeling work done in Lagos et al.'s (2001) study shows copper concentrations in water falling over the span of approximately 20 years of aging (Figure 2.4).

Recall the study in the Contra Costa Central Sanitary District (California) aimed at estimating the impact of copper residential plumbing on levels of copper found in the city's wastewater. Researchers found copper concentrations were inversely correlated with the age of the copper plumbing, with copper concentrations decreasing with age, up to the 20 to 35 year range (Brandenburg et al., 1993; Schock et al., 1995). In Sherrett et al.'s (1981) study of Seattle drinking water, the investigators noted that copper concentrations continued to decline "even after 10 or 20 years." Therefore there is ample reason to believe that copper corrosion and scale formation affect aqueous copper concentrations for at least 10 and possibly up to 35 years after construction.

Lagos et al.'s (2001) study is the only one to take pipe samples out of a functioning distribution system and analyze the solids present. Only three pipes were analyzed (aged 30 and 40 years) showing a diverse mix of corrosion solids present, and no accompanying water samples were taken from those locations. All other work presented in this literature review has relied on controlled coupon studies, short term (less than 5 years) pipe rig experiments, or water modeling to further the knowledge of the aging process. No studies were found where pipes and corresponding water samples were collected from an operational drinking water distribution system.

2.9 Research Needs

Clearly there is still much to learn about the development and properties of copper corrosion in drinking water systems as buildings age. Although age clearly plays a role in copper corrosion by-product levels in drinking water, as demonstrated by the epidemiological studies discussed earlier, the mechanisms associated with aging in real world systems are not well understood. Great variability has been found in the relationship of pipe age to dissolved copper concentrations (Lagos et al., 2001). Although experiments show cupric hydroxide forming in a matter of hours and tenorite or malachite developing within a month, field studies show high copper concentrations (indicative of cupric hydroxide) lasting for 10 to 35 years.

In their work developing the cupric hydroxide model, Schock et al. (1995) identified several gaps in our present knowledge of copper corrosion. They identified the need to analyze pipe deposits from copper plumbing systems of various ages. Such a study would determine pH, dissolved inorganic carbon, and time dependent stability

domains of $Cu(OH)_2$ (cupric hydroxide), CuO (tenorite), and $Cu_2(OH)_2CO_3$ (malachite). As noted earlier, no studies were found in the literature where pipes and corresponding water samples were collected from an operational drinking water distribution system. This study aims to fill the gap identified by Schock et al. (1995) by collecting and analyzing pipe and water samples from copper plumbing systems of different ages.

With the sponsorship of the WPAFB Civil Engineers (88 ABW/CE), the researcher was able to access a variety of locations within the WPAFB water distribution system and both cut physical pipe samples and collect corresponding water samples. This is the first study to collect both water and pipe samples of many ages that have been supplied over time by the same water source. Having examined the relationship between pipe age and dissolved copper levels in the literature, this research will endeavor to:

1. Identify the copper corrosion solids present in a real-world distribution system containing copper piping of different ages
2. Show how the copper solid mineralogy of the corrosion scale develops/changes with time
3. Compare real copper pipe scale mineralogy and composition to the USEPA's cupric hydroxide model's predictions
4. Examine what type of corrosive scale most effectively reduces dissolved concentrations of copper in drinking water

2.10 Solids Analysis

Two analytical techniques have proven particularly useful in analyzing and characterizing corrosion films and scales. X-ray diffraction (XRD) is commonly used to identify the composition of films on metal surfaces. It is able to identify a mix of solids present based on their structure since each x-ray diffraction pattern is unique for every crystalline structure (Skoog and West, 1971). Analytes can be multilayer thin films or powders, and produce diffraction patterns that are compared to a library of known structures. Thus determination of crystals is empirical. Limits of detection of a phase in a sample depend on the relative diffracting ability of the phase, peak overlap, and counting statistics. XRD works best with a flat sample surface without irregularities (often made with a packed powder). An important limitation of XRD is that it is not able to accurately characterize amorphous solids such as cupric hydroxide, a key solid of concern in this study (Settle, 1997). Schock et al. (1995) point out that during pipe removal, scraping, and the sample mounting process involved with XRD, changes in scale mineralogy are likely to occur, especially the change of cupric hydroxide to cupric oxide. Nonetheless XRD has been used in many studies of copper corrosion to identify scale solids present on pipe walls or experimental coupons (Schock et al., 1995; Lagos et al., 2001; Adeloju and Hughes, 1986; Hidmi and Edwards, 1999; Edwards et al., 2002).

X-ray Photoelectron Spectroscopy (XPS) is often used in corrosion surface film analyses. It detects only the top one to two nanometers of depth in a film in a small (several square millimeters) area. XPS is sensitive to all elements of importance in this study. It has typical detection limits between 1.0 and 0.1 percent of the total composition and therefore some corrosion constituents such as chloride or phosphate are barely or not

at all detectable with XPS (Briggs and Seah, 1983). XPS is a tool for identifying the major phases (mainly oxides) in corrosive films at the immediate solid surface. It is especially useful in differentiating between the different types of oxygen present, especially metal oxide and metal hydroxide, and in determining oxidation state (Cu^{+1} from Cu^{+2} solids). Some limitations include that XPS utilizes an ultra high vacuum environment and an x-ray source, both of which can cause partial reductions in some metal oxides or decomposition of hydroxides. However the unique ability of XPS to distinguish between CuO, Cu_2O, and amorphous $Cu(OH)_2$ makes it a useful tool in this study and a complement to XRD.

The vast majority of the surface analysis literature involving copper and XPS describe analyses of specimens from contrived experiments rather than study of material from actual corrosion situations. There exists a healthy body of literature for identifying XPS patterns for the copper oxides and sulfates generated from pure samples (Moudler et al., 1995; Deroubaix and Marcus, 1992; Shim and Kim, 2004; Chawla, Sankarraman and Payer, 1992). Several papers employed XPS to analyze non-homogenous copper corrosion films on archeological artifacts with some success (Squarcialupi et al., 2002; Paparazzo and Moretto, 1999). No literature was found where XPS was used to study malachite, an important compound in corrosion films. Only one source was found that had previously identified copper carbonate ($CuCO_3$) using XPS (Moulder et al., 1995). In this research, we analyzed a pure malachite sample to provide a means of comparison for identifying it in this study.

2.11 Summary

Research has shown higher levels of copper appear in drinking water conveyed through relatively new copper piping systems; older piping systems typically deliver lower copper levels in their drinking water. It is believed that precipitation and dissolution of a corrosive film on the inside of copper pipes is the main cause of copper "aging" over time. Some cuprosolvency theories suggest that relatively soluble, young cupric hydroxide [Cu(OH)2] scale produces high dissolved copper concentrations while the low-solubility solids that develop later in the life of a copper pipe, such as tenorite or malachite, produce lower dissolved copper concentrations at equilibrium. The USEPA Water Supply Water Resource Division's "cupric hydroxide model," which is based on fundamental chemistry and experimental observation of the solubility of Cu(+2) in new copper pipes, shows that over time the cupric hydroxide phase transforms into less soluble mineral solids. This model provides a foundation for research targeting the effects of water quality parameters on copper solubility and aging. This research expands on the current cupric hydroxide model by contributing field data from a real drinking water distribution system, providing a better understanding of cuprosolvency and the formation of soluble copper particles as it relates to treatment considerations and compliance with the Lead and Copper Rule. Through a unique combination of water and solid characterization it is hoped this and further research will ultimately result in the ability to control water quality in a distribution system in such a way as to build protective copper scale on the inside of new copper pipe rapidly, protecting drinking water consumers from high levels of copper at the tap.

III. EXPERIMENTAL MATERIALS AND METHODS

3.1 Introduction

In order to address the research questions developed in Chapter II, a group of buildings on Wright-Patterson Air Force Base (WPAFB) containing copper pipe of different ages was sampled. WPAFB is home to scores of buildings with copper pipe of different ages, all of which are supplied by the same water source. The 88th Air Base Wing Civil Engineers (88 ABW/CE) are charged with maintaining and constructing WPAFB's built environment, including all facilities and infrastructure. The 88 ABW/CE maintains a consolidated collection of building construction, maintenance, and repair records for all of its buildings, enabling accurate dating of many buildings' plumbing systems. Such a collection of buildings, supplied over time by the same water source and with good records of installations and repairs, makes an ideal field site for a study of the aging of copper pipe scale over time and its effect on copper levels in drinking water.

A sample of 16 buildings was chosen on WPAFB because they contained copper drinking water distribution pipes of a variety of ages (from less than one year old to 44 years old) and allowed access to that piping for sampling. Three types of data were collected to answer the research questions. Tap water sampling was conducted in order to determine the copper concentration in the potable water of each building. The tap water was also characterized for pH and total inorganic carbon, as input data for application of the EPA's cupric hydroxide model, and 13 other inorganic constituents as

well (Appendix B). Finally, physical pipe samples were retrieved from each building's copper system in order to characterize the solids formed as scale on the inside of each pipe.

3.2 Building Selection and Pipe Dating

3.2.1 Area B Water Supply

WPAFB is divided geographically into three areas: A, B, and C. Areas A and C abut one another and are supplied by two separate but connected water systems. Area B is geographically separated and is supplied by its own water supply and treatment system. Because of the independence of Area B's water supply, this area was chosen for building sampling. Prior to 1980, Area B's water came from two well fields, one of which is now inactive. The current water supply comes from four wells located on base. In 1989 air strippers were added to the Area B water treatment process to eliminate volatile organic compounds. 1~2 mg/L of polyphosphate is added to the water prior to air stripping to control scale build up in the strippers themselves. According to personal interviews with the base water engineer, polyphosphate addition is intermittent depending on how reliable the treatment plant operators are in ordering chemicals (Vehorn, 2005). Just after air stripping, fluoride is added, and next CO_2 is added to replace the CO_2 removed during air stripping. The base water engineer says the CO_2 treatment was included when air stripping was found to raise the water's pH to approximately 8. It was desired that the water pH in the distribution system be at about 7.2, to avoid scaling problems. Chlorine is added just prior to the water entering a 370,000 gallon chlorine contact reservoir and from that reservoir it is distributed to the base system or pumped to elevated storage tanks

(Vehorn, 2005). Typical water parameters for WPAFB Area B from the time of this study are provided in Table 3.1.

Table 3.1 Source Water Analysis from Area B Water System

Parameter	Unit	Nov-05 Monthly Avg	Dec-05 Monthly Avg
Phosphate*	ppm	**0.154**	**0.162**
Total Alkalinity*	ppm as CaCO3	276	280
Flouride*	ppm	1.16	0.945
Sodium	ppm	59	252
Chlorine: Free (leaving plant)	ppm	0.8	0.8
Chlorine: Total	ppm	0.9	0.9
Chlorine: Combined	ppm	0.1	0.1
pH**		7.4	7.3
Chlorine: Free (at tap)**	ppm	0.25	0.2

* one time value
** field measurements

3.2.2 Building Records

Three sources of data were utilized to date the copper water pipes in the buildings selected for sampling in this study. The 88 ABW/CE maintains a digital database of all of their building drawings called the Record Drawings system. Record Drawings contains scanned images of older architectural drawings and computer aided drafting drawings of more recent construction. The drawings are cataloged by building number, date, project title, drawing name, drawing number, and other descriptors. These drawings were used as a baseline for examining when piping systems were constructed, renovated, added to, or replaced. The 88 ABW/CE also maintains data for construction and renovation projects in the Automated Civil Engineer System (ACES) database. ACES contains project titles, descriptions, costs, design and construction milestone dates, as well many other project parameters. ACES was searched for additional plumbing related projects that might have happened in a building for which no drawings were available in the Record Drawing system. ACES also contains a real property module where 88

ABW/CE personnel track facility construction dates, square footage, and usage. The real property records were used to find the year in which the building was occupied. Next the 88 ABW/CE maintains another database, similar in function to ACES, called the Interim Work Information Management System (IWIMS) which contains maintenance records for each building. IWIMS contains records on each building of the daily work orders completed by the in-house plumbing staff and of other minor construction projects that fall below the threshold for tracking in the ACES database. IWIMS also provides dates of changes to the plumbing system. These three sources of building data were used to date the copper pipes sampled in each of the selected buildings.

Additionally, the building manager of each building was interviewed to corroborate the building data gleaned from 88 ABW/CE's records. Each building on an Air Force Base is assigned a building manager who oversees and coordinates all maintenance, repair, and construction actions with 88 ABW/CE. In some cases the building managers had been in a facility for only a short time and in those cases other workers who had been in the building longer were interviewed.

Buildings were eliminated from consideration for the study for a number of reasons. Some buildings on WPAFB are laboratory facilities with specialized water treatment systems. Any building with a water softener, an ion-exchange system, or another special water treatment system was eliminated. If insufficient drawings and records existed to confidently date the copper pipes, the pipes would not be sampled. In several cases sampling was deemed too disruptive to the facility's mission and the facility was therefore eliminated. Every effort was made to sample a basement or first floor

faucet, usually in bathrooms where there was a reasonable assurance of frequent usage. Only cold, domestic water and copper delivery pipes were sampled.

Information for each building sampled is contained in Appendix A. A data sheet on each building shows construction and modification project information, maps and pictures of the sampling location and building manager/occupant interview data.

3.3 Chemicals

The chemicals used to preserve samples and calibrate measurement instruments were procured from commercial sources and no additional purification was attempted. Specific chemicals are described below.

3.3.1 Nitric Acid

Each tap water sample was acidified per EPA guidelines with enough nitric acid (HNO_3) to bring the sample's pH below two. Fisher Scientific nitric acid (OPTIMA grade for HPLC, GC, plasma/ICP, spectrophotometry, and pesticide residue analysis, Cole Parmer) was used for acidification of samples, calibration standards, blanks and to make 1+1 nitric acid solution used to clean sample bottles before sampling.

3.3.2 pH Probe Calibration Standards

An Oakton Instruments pHTestr pH meter was used to periodically test the pH of preserved samples to assure acidification to a pH less than two. The pHTestr was calibrated per instructions using buffer solutions obtained from Fisher Scientific including pH 4, pH 7, and pH 10 buffers.

3.3.3 Field Test Kit for pH, free chlorine residual, and total chlorine residual

To measure pH, free chlorine residual, and total chlorine residual on site in each building, a field test kit manufactured by LaMotte (Model LP-8, code 6980) was utilized. The kit provided colorimetric readings accurate to 0.1.

3.3.4 Deionized (DI) Water

DI water used to create sample blanks and to rinse bottles and other glassware was produced by a Millipore DirectQ-5 purification system. The Millipore unit consistently produced 18.2 MΩ-cm resistivity DI water.

3.3.5 XPS solid standards

Several solid standards were analyzed in the XPS machine in order to establish reference values for comparison with the pipe samples. The standards were also compared to literature reference values to assure instrument and methodological accuracy in analysis. The solid standards analyzed by XPS are listed in Table 3.2. The malachite sample was also analyzed with XRD to affirm that it was pure malachite.

Table 3.2 Copper Solids Standards for XPS

Analyte	Supplier
Tenorite (CuO)	Fisher Scientific Co, ESA Tested Purity Reagent
Malachite [$Cu_2CO_3(OH)_2$]	J.T. Baker, Mallinkrodt Baker, Inc, Phillipsburg, NJ
Pure Copper (Cu^0)	Physical Electronics, XPS Calibration Standard

Many literature references are available for some of the prominent copper solids under investigation. Several literature reference values were used as a basis of comparison for the spectra gathered from the WPAFB pipe samples. Their values are tabulated in Table 3.3 and graphed following convention in a chemical state plot in Figure 3.1.

Table 3.3 Literature Values for XPS Spectra of Copper Solids

Copper Species	Cu2p3/2 In binding energy, eV	Cu(LMM) In kinetic energy, eV	Δα	Reference
Cu	932.5	918.9	0	Chawla et al., 1992
Cu	932.7	918.6	0.1	Deroubaix and Marcus, 1992
Cu	932.6	918.6	0.15	Moulder et al., 1995
Cu	932.6	918.7	0	Moulder et al., 1995
Cu	932.6	918.6	1.5	Moulder et al., 1995
Cu	932.6	918.7	2.3	Moulder et al., 1995
Cu	932.7	918.6	2.6	Moulder et al., 1995
$Cu(OH)_2$	934.5	916.6	-0.3	Chawla et al., 1992
$Cu(OH)_2$	934.7	916.7	0.2	Deroubaix and Marcus, 1992
$Cu(OH)_2$	934.75	916.3	-0.15	Deroubaix and Marcus, 1992
$Cu(OH)_2$	935.1	916.2	0.25	Moulder et al., 1995
Cu_2O	932.4	917.3	-1.7	Chawla et al., 1992
Cu_2O	932.5	916.5	-2.2	Deroubaix and Marcus, 1992
Cu_2O	932.5	916.2	-2.35	Moulder et al., 1995
Cu_2O	932.5	916.2	-2.35	Moulder et al., 1995
Cu_2O	932.5	916.6	-1.95	Moulder et al., 1995
Cu_2O	932.5	917.2	-1.35	Moulder et al., 1995
$CuCO_3$	935	916.3	0.25	Moulder et al., 1995
CuO	933.7	918.1	0.4	Chawla et al., 1992
CuO	933.6	917.8	0.2	Deroubaix and Marcus, 1992
CuO	933.7	918.1	0.75	Moulder et al., 1995

All values relative to C1s peak at 284.6 eV, using Mg x-ray source

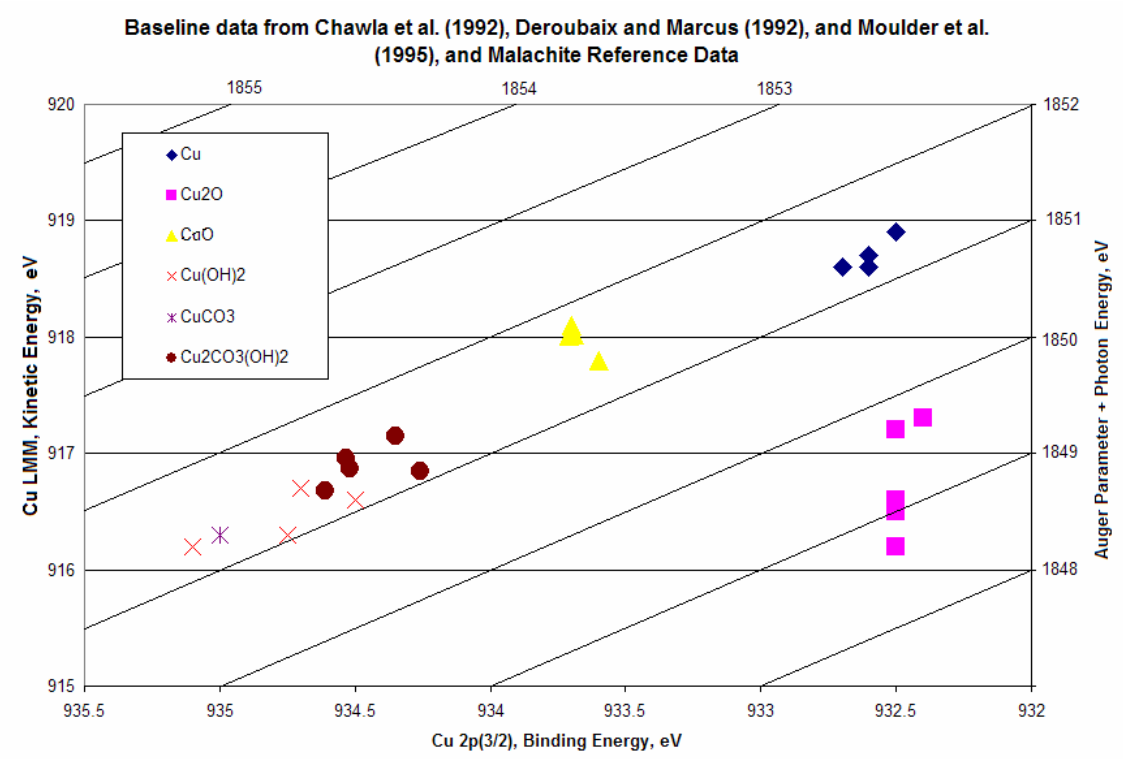

Figure 3.1 Chemical State Plot for Copper Solids

3.4 Analyses

3.4.1. Copper Concentration in Drinking Water

Copper levels in the drinking water samples were determined by GEL Laboratories of Ohio, LLC, a USEPA certified lab under contract with the 88 ABW/CE. The lab used inductively coupled plasma (ICP) analysis following USEPA method 200.7 and their internal standard operating procedures including quality control and assurance guidelines.

3.4.2. Water Characterization and Modeling

Metals analysis of the flushed water samples was done on a Thermo Jarrel Ash (Franklin, MA) 61E® purged inductively coupled argon plasma spectrometer (ICAPS) according to USEPA standard method 200.7 (USEPA, 1994). Total inorganic carbon was analyzed via a coulometric procedure on a UIC Model 5011 CO_2 coulometer (Joliet, IL) with Model 50 acidification module, operated under computer control according to ASTM Standard D-513-92 (ASTM, 1994). Total alkalinity and chloride was determined via potentiometric titration employing Standard Methods 2320 b.4.6 and 4500-Cl D respectively (Eaton et al., 1992). The titrations were performed on a Metrohm 751 GPD Titrino autotitrator. Ammonia analyses were performed on an Alpkem RFA/2 autoanalyzer employing USEPA method 350.1 (USEPA, 1993). Finally, nitrate, nitrite, and orthophosphate were determined via a colorimetric test according to USEPA method 353.1 and 365.2 (USEPA, 1993). The results of water characterization for the 16 buildings in the sample are in Appendix B.

Water modeling utilized the thermodynamic and solubility constants developed and tabulated by Schock et al. (1995) for the cupric hydroxide model. Changes and

updates to the model's thermodynamic data since the original publication are tabulated in Appendix C. The dissolved inorganic carbon and pH levels for each building were modeled assuming the presence of either cupric hydroxide or malachite respectively. An aqueous copper concentration was predicted for each combination of copper solid and water quality in each building. Dissolved inorganic carbon used for modeling was computed using the total alkalinity determined for each sample. Alkalinity was converted to dissolved inorganic carbon using WaterPro software, published by ChemSW, Inc (www.chemsw.com). Modeling results are discussed in Chapter 4.

3.4.3. X-ray Photoelectron Spectroscopy (XPS)

XPS analysis was performed using the Physical Electronics (PHI) 5700 Multi-Probe. This instrument is equipped with a dual-anode type (Mg and Al) soft x-ray source. The study utilized unmonochromatized radiation from the Mg anode (Mg Kα) at characteristic energy 1253.6 eV and full width at half maximum (FWHM) was used for obtaining binding energy values. The anode was operated at a total power dissipation of 400 W and 15 kV. Spectral analysis was performed with a hemispherical analyzer and a 16-channel detector. The aperture was set to an 800 μm diameter and the sample was positioned at an electron take-off angle of 45^{o} from the analyzer. Samples were analyzed in an ultra high vacuum chamber with pressure at 10^{-9} Torr during analysis. Quantitative analysis was carried out using manufacturer supplied sensitivity factors. The XPS machine was calibrated using magnesium against the Cu $2p_{3/2}$ peak at 932.67 ± 0.1 eV and the Cu 3p peak at 75.13 ± 0.1 eV.

XPS spectra were collected using a scan range of 0 and 1200 eV binding energies and an analyzer pass energy of 187.85 eV. In multiplex mode, spectral data were

collected in five or six energy bands with an analyzer pass energy of 23.50 eV. Each multiplex scan included the Cu $2p_{1/2}$ and Cu $2p_{2/3}$ peaks in band range 928-970 eV, the O 1s peak in band range 525-540 eV, the Cu LMM Auger peak in band range 325-355 eV, and the C 1s peak in band range 279-294 eV. The S 2p peak was also measured in band range 155-175 eV, the Cl $s_{1/2}$ peak in band range 192-210 eV, the Zn $2p_{1/2}$ and Zn $2p_{2/3}$ peaks in band range 1010-1040 eV, P 2p peak in band 130-140 eV, and N 1s peak in band 395-405 eV when each of those respective elements was detected in quantity on the preliminary survey scan.

A common problem in distinguishing various copper compounds using XPS is the build up of surface charge during analysis which results in shifting all binding energies to higher values (Wagner et al., 1979; Deroubaix and Marcus, 1991). The C 1s line of carbon contamination has a binding energy of 286.4 eV on metallic copper and the electrostatic charge was assumed to be equal to the difference between the measured C 1s binding energy and the reference value. Therefore all binding energies were referenced to the C 1s peak at 286.4 eV and shifted accordingly (Wagner et al., 1979; Deroubaix and Marcus, 1991). The peak positions and FWHM values from the multiplex scans were tabulated and used for solids determination.

A piece of pure copper was analyzed along side all the pipe samples in the study. Upon introduction of each set of samples into the XPS chamber, the pure copper was first analyzed and compared to standards to assure binding energy accuracy. The pure copper was sputtered with argon ions occasionally for one minute to remove any surface contamination and/or surface oxidation that may have formed over time. Sputtering was used minimally to avoid changes in near-surface stoichiometry or oxidation state.

3.4.4. X-ray Diffraction Spectroscopy

X-ray diffraction (XRD) was used to identify crystalline phases of the solids present on the inner walls of the pipe samples. A Scintag (Scintag, Inc., Santa Clara, CA) XDS-2000 theta-theta diffractometer with a copper X-ray tube was used to acquire X-ray patterns. The tube was operated at 30 kV and 40 mA and scans were typically over the range of 5 to 60 degrees 2 theta, with 0.03 degree step sizes that were held for 3 seconds each. Pattern analysis was performed using the computer software provided by the manufacture, which generally followed ASTM procedures.

Two methods of XRD analysis were used. First, small pieces of the copper pipe were put in the XRD machine and analyzed directly to try to obtain a pattern from the wall of the pipe without disturbing the corrosion scale present. The small pieces of pipe were the same ones that were used for XPS analysis. After analyzing several buildings this way, the XRD results from the pipe pieces did not appear to provide complete characterization of the solids present. The pipe pieces had curvature that may have disrupted the peak locations and intensities during XRD analysis. Analyzing a powderized, homogenized sample presents a flat sample surface to the x-ray beam (Settle, 1997). Therefore we decided to powderize the corrosive scale, when enough scale was present, for XRD analysis. The corrosive scale was scraped using a stainless steel spatula from the pipe sections, finely ground using a synthetic ruby or agate mortar and pestle, and passed through a 200-mesh sieve (approximately 75 μm). The resulting powder was then suspended as a slurry with amyl acetate, and deposited on zero-background quartz plates with disposable pipettes for mounting in the diffractometer.

3.4.5. Photography

Magnified images of the pipe halves were collected with a Nikon E8400 camera taken at a focal length of 11.5mm. All photos were taken at the same time under the same light source in order to present a consistent picture of the various colors and corrosion types on the different pipes. Detailed pictures of the corrosion were obtained under the magnification of a Nikon SMZ800 stereomicroscope, taken with a Spot Insight Color camera, model 3.2.0 made by Diagnostic Instruments, Inc. Stereomicroscope images were gathered with Spot version 3.3 for Windows software.

3.5 Sample Collection, Preservation and Preparation

Both liquid and solid sampling followed a uniform written protocol (Appendix D) for consistency from location to location.

3.5.1 Liquid Samples

Water samples for each location were collected both before and after a 16 hour stagnation period. Upon arrival at a sampling location, the cold water faucet was allowed to run for one minute in order to flush water that had been sitting in the pipes and introduce fresh water from the distribution system into the pipes immediately leading up to the faucet. Next, 60 mL and 250 mL water samples were collected. The 60 mL sample was later acidified (within 24 hours) in accordance with EPA method 200.7 for ICP analysis. The 250 mL was not acidified and was later used for wet chemistry analysis to determine total inorganic carbon (TIC), alkalinity, nitrate, and ammonia levels. Next, the water was tested using a colorimetric field test kit (see section 3.3.5) for pH, free chlorine residual and total chlorine residual. After testing the first six buildings in the study and finding

consistently identical readings for free and total chlorine, only free chlorine readings were taken for the remainder of the sample locations. Next, the faucet was wrapped in a clear plastic bag which was taped around the faucet neck, and marked "temporarily out of order" with a sign. The plastic bag allowed identification of any human interference during the stagnation time (none was found) and also identified leaky faucets which slowly released water overnight instead of stagnating completely (two faucets in the study).

After 16 hours of stagnation the bag was observed for tampering or leaking and removed from the faucet. Any irregularities were noted and photographed. Two 250 mL bottles were filled with first and second draw water from the faucet. Both the first and second 250 mLs of water were collected in order to compare the results of water that had stagnated in or near the faucet fixture itself, and were perhaps influenced by the fixture materials (1^{st} draw) with water that had stagnated in the copper distribution pipes immediately leading up the faucet (2^{nd} draw). Both samples were acidified and analyzed for total copper concentration according to EPA method 200.7 by a certified lab. Water from the first draw sample (20~30 mL) was also analyzed colorimetrically to determine pH and free/total chlorine with the field test kit.

The 60 mL sample for ICP analysis and the two 250 mL samples for AAS analysis were acidified within 24 hour per EPA methods 200.2, 200.7, and 200.9. EPA method 200.2 section 8.1 states the requirement to acidify drinking water samples for total recoverable metals analysis to pH<2 using 1+1 nitric acid. The acidification must be done within two weeks of field collection and then the sample must be held for at least 16 hours before analysis. Once acidified, samples can be held for up to six months. The

pH of each sample was checked immediately prior to withdrawing an aliquot for analysis to assure the pH was less than two. Samples were acidified with 0.15% by volume nitric acid (see section 3.3.1). This amount was found sufficient to bring the pH to below 2. Water samples were stored at room temperature.

3.5.2 Pipe Samples

Pipe sampling locations were determined based on several criteria. A 3" to 12" piece of copper pipe was cut from the cold water distribution system either directly leading to the fixture where the water sampling took place, or near to it. The location of the pipe piece sampled was chosen based on the location of near-by shut-off valves and the ability to access the pipe for cutting and replacement. Pipes were generally accessed either above a drop ceiling, in a pipe chase, or via a plumbing access panel. In several cases the pipes sampled were exposed, either under, or leading to, the fixture, as in a basement or janitors closet. In each instance a pipe was chosen that either provided water directly to the water sampling location, or was nearby in the piping system and received similar usage as the pipes leading to the fixture. Each pipe sampling location is described and pictured in Appendix A. Pipes and fixtures where water had likely stagnated for long periods (infrequently used locations) were avoided when possible. Deviations are discussed in section 4.2.3.

In many cases insulation around the pipe was removed to reach the pipe for sampling. Then the water was shut off to the affected area with a valve and a piece of copper pipe was cut using a handheld pipe cutter. Compression fittings were used to place a new pipe section back into the distribution system before restoring the water flow. The piece of pipe removed was placed in a clear plastic Ziploc bag, labeled, and

photographed. The pipe sampling process and location was also photo documented. Each sampling location is documented in Appendix A.

To prepare the pipes for analysis they had to be cut into small pieces that would fit in the XPS and XRD sample chambers. The pipes were cut lengthwise on a band saw exposing the insides of the pipes. Pictures were taken of the scale. Next small, approximately ¼" square chips, were cut from the pipe. In early samples (buildings 441, 553, and 571) six chips were cut encompassing the entire pipe perimeter, but as the experiment progressed and corrosion was found to be relatively uniform from chip to chip on the same side of the pipe, only two chips were cut. Each of the two chips were cut from opposing sides of the pipe to capture visually different corrosion solids on the top and bottom of many pipes. When a sample was obtained from a horizontal pipe, one square chip was from the bottom of the pipe and the other from the top. In vertical pipe samples, two squares were chosen from opposing sides of the pipe. In early sample preparation, the chips were cut with the combination of a band saw and a hand-held hacksaw. Pipe cutting was accomplished in a fairly dusty, multipurpose fabrication workshop. The hand hack-sawing of the small pieces was accomplished on a rubber padded vice grip causing small flakes of rubber to fall onto the sample surface. A burst of compressed air was used to remove unattached dust and flakes from the samples before the samples were introduced into the sample chamber of the XPS or XRD machine. For later samples, only the band saw was used to eliminate possible contamination due to use of the hand hacksaw and the rubber pad. Each square was placed in a labeled, plastic bag for storage until analysis.

The remaining pipe halves were stored in a labeled, Ziploc plastic bag until they were prepared for XRD analysis. The corrosive material was scrapped off of the pipes and used for XRD analysis, as described in Section 3.4.4.

3.5.3 Bottles

The bottles used to collect water samples were newly procured Nalgene LDPE plastic bottles (Cole Parmer catalogue number C-06033-50 and C-06033-20). Bottles were washed with 1+1 nitric acid (Section 3.3.1) before sampling. A small amount of 1+1 nitric acid was poured into the bottle, which was then capped and agitated for approximately 15 seconds. The acid was then removed from the bottle and it was rinsed three times with DI water. The bottles were allowed to dry under a lab hood and then capped until sample water was added.

3.5.4 Blanks

Each time the researcher washed a set of sampling bottles an extra bottle was washed as a blank. The bottle was prepared identically to the other bottles and also transported to the sampling location with the other bottles. Upon return to the lab the bottle was filled with DI water and labeled as a blank. The blanks were analyzed for copper alongside the first and second draw water samples to identify any copper contamination possibly present in the bottles themselves or in the washing process.

3.6 Sequential Water Sampling

After the initial copper concentration data were analyzed from the 16 buildings in the sample, questions arose about the source of the copper in the water from the first and second draw samples. This dilemma is discussed further in section 4.2.3 of Chapter IV.

Briefly, the researcher desired to determine if the high copper levels found in the first draw samples was a result of stagnant water contact with the faucet fixture (usually brass, not pure copper), while the lower copper levels found in the second draw samples were attributable to overnight contact with the copper distribution system. To attempt to answer the question of where the copper contamination was coming from, another series of water samples was collected for a single building. The sink originally sampled in building 641 was resampled by taking more water samples of smaller size in sequence. The researcher flushed the faucet for one minute and sampled the free chlorine and pH levels, consistent with the experimental protocol described in Appendix D. The faucet was put out of service overnight for 16 hours of stagnation. The following day two 30 mL samples, followed by six 60 mL samples were collected from the faucet. A diagram of the faucet is shown in Appendix E.

IV. RESULTS AND DISCUSSION

4.1 Introduction

This chapter outlines the analytical findings of the water and solids analyses and discusses the meaning of the results. Key findings are summarized in figures and tables, while more detailed data are included in several appendices.

4.2 Copper Concentration in Drinking Water

Water samples were collected before and after a 16 hour stagnation period from taps in each of 16 different buildings.

4.2.1 Water Characterization

The initial water samples were collected after flushing the tap for one minute and before the stagnation period. These samples were used to characterize the water delivered to each building during normal use and establish a background level of copper in the water of each building, without stagnation. The water characteristics of each sample building are tabulated in Appendix B. The values that are bolded in the chart are significantly different from the average values of the other samples. Two buildings, 571 (2002) and 306 (1997), had copper levels exceeding the LCR action level after a one minute flush of the tap and before stagnation. Two buildings had high iron (Fe) levels and seven out of the sixteen had high zinc (Zn) concentrations relative to the other buildings in the sample. Phosphorous and especially orthophosphate are known to reduce copper levels in drinking water by contributing to a copper-phosphate solids scale that is

protective of the water (Schock et al., 1995; McNeill and Edwards, 2004; Edwards et al., 2002). The water from buildings 676 (1985) and 11A (1984) exhibited relatively high background levels of phosphate and orthophosphate. No statistical correlation between orthophosphate, total phosphate, or zinc with the 2nd draw copper concentration data, presented in the next section, were found. Building 441B (1993) water had a relatively high concentration of NO_3 while building 553 (2001) had a higher pH at 7.6 than the rest of the buildings which averaged 7.3. The water is well buffered, with high alkalinity, so there is very little variation in pH through the system. In several cases the researcher found no chlorine residual in the water even before stagnation (buildings 571, 837, 306, 556, and 11A). Again, no statistical correlation was found between the chlorine residual levels and the 2nd draw copper concentration data. In all cases the chlorine residual was gone after 16 hours of stagnation either because of a demand from bacteria in the water or possibly from corrosion. In general no water quality parameter was found to significantly correlate with the 2nd draw copper concentration data. The water quality in the base supply system was relatively consistent between sampling locations and none of the water quality parameters significantly contributed to the variability found in the copper concentration data, presented in the next section.

4.2.2 Copper Concentration in Drinking Water

Table 4.1 lists the copper concentrations found in the first and second draw water samples taken after 16 hours of stagnation from each of the 16 buildings.

Table 4.1 Copper Concentrations in Drinking Water after 16 Hour Stagnation

Building	Year of Pipes	1st Draw Sample Copper Level (mg/L)	2nd Draw Sample Copper Level (mg/L)
441S	2005	1.74	2.46
837	2004	2.72	2.83
571	2002	2.55	2.99
553	2001	2.36	2.18
645	1998	2.48	2.05
306	1997	2.23	2.17
556	1995	1.74	1.85
620 PII	1994	1.86	2.13
441B	1993	2.80	0.44
620 PI B	1992	2.13	2.53
620 PI	1992	1.32	0.80
642	1989	1.93	0.67
676	1985	2.21	2.36
11A	1984	1.64	1.95
641	1977	1.96	0.53
653	1975	0.93	0.42
464	1962	1.39	0.95

In the case of building 620 Phase I, water samples were collected in two different locations within the building so both results are reported. Sample "620 PI" was taken from a sink in a first floor men's restroom. It was later determined that the pipes leading to this bathroom were unreachable to obtain a sample of copper pipe, so a different location in Phase I of building 620 was chosen. The second round of water sampling, labeled "620 PI B" was taken from a janitor's sink in the basement of 620 Phase I. The "620 PI B" data correspond to the pipe sample, documented in Appendix A. The researcher had some concern that the janitor's sink was not used regularly. Both 1st and 2nd draw copper concentrations were lower in the men's bathroom sample than in the janitor's sink sample, probably because of infrequent use of the janitor's sink. All other buildings were sampled only once.

The review of current literature in Chapter II revealed that many researchers have shown copper concentrations in drinking water decrease as the copper plumbing system ages, although there is no consensus about the timeframe of this decline. Researchers

have proposed an inverse, linear relationship between aqueous copper concentration and plumbing system age (Lagos et al., 2001; Schock et al., 1995). Such a decline with age is demonstrated by both 1st and 2nd draw data sets, though more dramatically with the 2nd draw data (Figure 4.1).

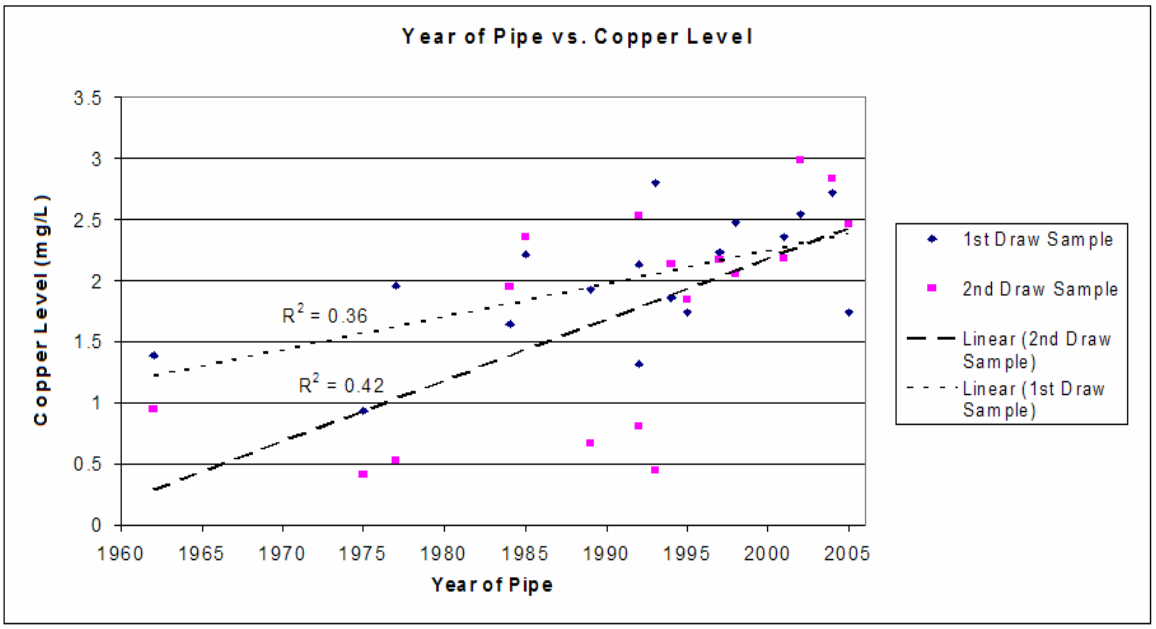

Figure 4.1 Copper Concentration Plotted vs. Age of Copper Plumbing

In both 1st and 2nd draw data sets there is wide variability in the copper levels, though the copper concentrations trend down in older pipes. Linear regressions of the two data sets are also plotted in Figure 4.1 with their respective R^2 values. Both visual inspection and the low R^2 values evidence only a weak linear correlation. The variability in these data is reminiscent of Figure 2.1, the data from Contra Costa Water District and the East Bay Municipal Utility District study, and Figure 2.4, the Lagos et al. (2001) study data.

4.2.3 Sequential Sampling

Initially 250 mL 1st and 2nd draw samples were collected from each location to differentiate copper levels in water that had possibly stagnated in contact with the faucet

fixture (the 1st draw), which is often brass or another alloy and not pure copper, and water that had stagnated in contact solely with the copper delivery pipe (the 2nd draw). Therefore, the hypothesis was that 2nd draw samples would provide a more accurate picture of copper concentrations caused by contact with nearly pure copper delivery pipes. Indeed, as shown above, the 2nd draw samples exhibit a more pronounced decline in copper level with pipe age. It is important to note that the theory that copper levels and pipe age are inversely correlated, developed in Chapter II, assumes contact with pure copper and not alloys, such as brass, where galvanic interactions may be important.

The researcher conducted additional sampling to affirm that the 2nd draw samples were indicative of water in contact with pure copper pipe, and the 1st draw samples were affected by contact with the fixture. In the same location in building 641 as the 1st and 2nd draw samplings, a second set of water samples were collected. Again, the faucet was flushed for one minute and background water samples were collected. After 16 hours of stagnation the researcher returned and took two 30 mL samples followed by six 60 mL water samples in sequence from the faucet. The diagram in Appendix E shows the faucet sampled and the cold water domestic pipe leading up to the faucet. The sequential sampling shows the copper concentrations at different locations in the distribution system leading up to the tap. Table 4.2 lists the results of this sequential sampling.

Table 4.2 Sequential Sampling of Building 641

Sequential Sampling of building 641		
	Location of Stagnation	**Cu (mg/L)**
Background	(taken after 1 min flush, before stagnation)	0.114
1st 30mL	Faucet fixture and 1/4" supply line	1.28
2nd 30mL	1/4" faucet supply line and supply line within wall	1.07
1st 60mL	Supply line in wall	1.08
2nd 60mL	1/2" cold water domestic copper pipe	0.866
3rd 60mL	1/2" cold water domestic copper pipe	0.431
4th 60mL	1/2" cold water domestic copper pipe	0.285
5th 60mL	1/2" cold water domestic copper pipe	0.264
6th 60mL	1/2" cold water domestic copper pipe	0.294

The copper concentrations of water in the ½" cold water domestic supply line are significantly lower than the copper concentration in the water that stagnated in the faucet fixture itself and in the connection supply lines (1/4" copper) that come with the fixture and connect the fixture to the cold water domestic lines. Building 641 was constructed in 1977, however the bathrooms were more recently renovated so the faucet and corresponding supply lines are newer than the domestic cold water lines, which are original to the building. Table 4.3 shows the relationship between the sequential sampling in 641 and the 1st and 2nd draw 250 mL samples.

The copper (in mg) in the two 30 mL samples and the first three 60 mL samples are added together and divided over the combined 240 mL to arrive at the mg/L concentration in the first 240 mL of sequential sampling. The same calculation was done for the last three 60 mL samples. These copper concentrations are compared to the 1st and 2nd draw data that were obtained earlier for building 641. Although the

concentrations are larger in the 1st and 2nd draw data than in the sequential sampling, the order of magnitude drop between the first 240~250 mL samples and the subsequent samples are very close, 68.4% compared to 73.1%.

Table 4.3 Comparison of Sequential Sampling to 1st and 2nd Draw Sampling

Copper Concentration (mg/L)	
Cu in first 240mL from sequential sampling	1st Draw 250 mL
0.888	1.96
Cu in last 180 mL from sequential sampling	2nd Draw 250 mL
0.281	0.528
Percent Decrease	
68.4%	73.1%

The sequential sampling data demonstrate that the 1st draw sample data from the 16 sample buildings are probably most indicative of the copper concentration corresponding to the faucet fixture itself and its associated supply piping. In many cases the bathrooms sampled had been renovated and the fixture age does not correspond with the pipe age listed in Table 4.1. In a study of the aging of pure copper pipe, the 2nd draw samples are of most interest because they are more indicative of the water's contact with pure copper.

Reexamining only the 2nd draw data, shown in Figure 4.2, one sees again the declining trend in the data. The decline with time has a slope of -0.05 milligrams of Cu per liter per year, so on average, with each year a copper pipe ages the copper concentration in the drinking water will fall 0.050 mg/L according to this data set.

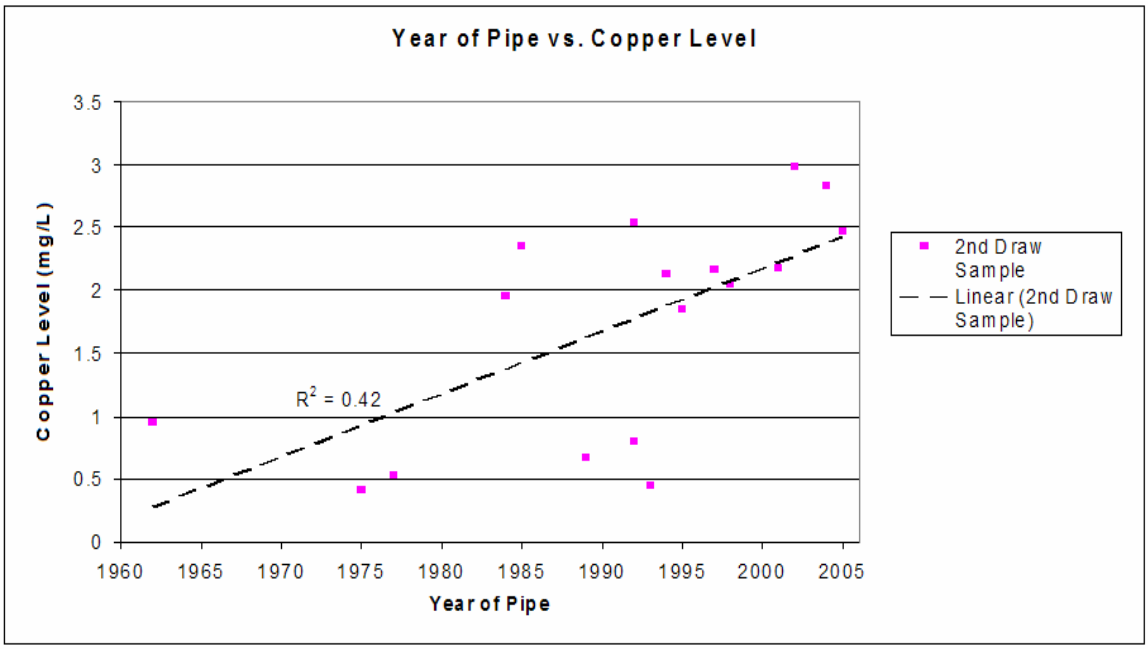

Figure 4.2 2nd Draw Copper Concentration vs. Age of Copper Plumbing

A few data points in the water sampling are worthy of special mention. In two of the sampling locations the water did not stagnate completely over night. When the researcher returned after the stagnation period the plastic bag over the faucet was filled with water, indicating leaking. The two affected buildings were 642 (1989) and 441B (1993). If the leaks had an effect on the copper level, it is likely to have falsely lowered the concentrations measured in those two buildings.

These two data points (1989 and 1993) flank the two data points for building 620 Phase I (1992). As mentioned earlier, the "620 PI B" point corresponds to a janitor's sink in the building's basement that likely received less use than the men's restroom sink sampled as "620 PI." This might explain the disparity between the copper concentrations at the two locations. The apparent effect of water usage on the measured copper concentrations in building 620 Phase I beg a discussion of how water usage affects the other buildings in the sample. The majority of the sampling locations were points of

frequent water usage such as bathroom sinks, kitchen sinks, an actively utilized shop sink. In three buildings, 441B (1993), 620 PI B (1992), and 620 PII (1994), basement janitor's sinks were chosen. These sinks probably received less usage than the majority of other locations. The janitor's sinks were picked because the cold water domestic delivery pipe to the sinks could be reached for sampling. These buildings provided no other accessible location, such as a bathroom or kitchen, for pipe sampling. A basement sink in building 11A (1984) was also chosen for sampling. The building manager of 11A was confident that the basement sink sampled was used daily from its installation until approximately one year before sampling. For the past year the room where the sink is located has been used for storage and the sink is now only infrequently used. Finally, a kitchenette sink in the basement of building 556 was chosen, again because of the ability to reach and sample the supply pipe leading to it. The building manager could not say how often the sink was used in the recent past, and it did not seem well utilized. These five sampling locations are the only places where water usage was suspect of being less than daily.

Figure 4.3 depicts the 2nd draw data with questionable data points (where water usage was low or the faucet dripped) removed. In the reduced data set of 10 buildings, a decline with time is still evident. A linear fit is better for these data ($R^2 \sim 0.6$) than for the complete 2nd draw data set ($R^2 \sim 0.4$). This experiment certainly supports the conclusion of earlier researchers that copper concentrations decline with increasing age of copper piping systems, and the assertion that the relationship is linear is weakly supported by these data. The decline in concentration in time is -0.052 mg/L/year for this data set. It also shows that variation in water usage may contribute to some of the

variation in the copper concentration data. Controlling usage in a future study might provide a better picture of how much variation in the copper data is caused by the age of the pipe alone. It would also be interesting to learn if the amount of usage of a fixture, which relates to the amount and frequency of flow through the pipes, plays a dominant role, compared to age, in reducing copper concentrations in drinking water.

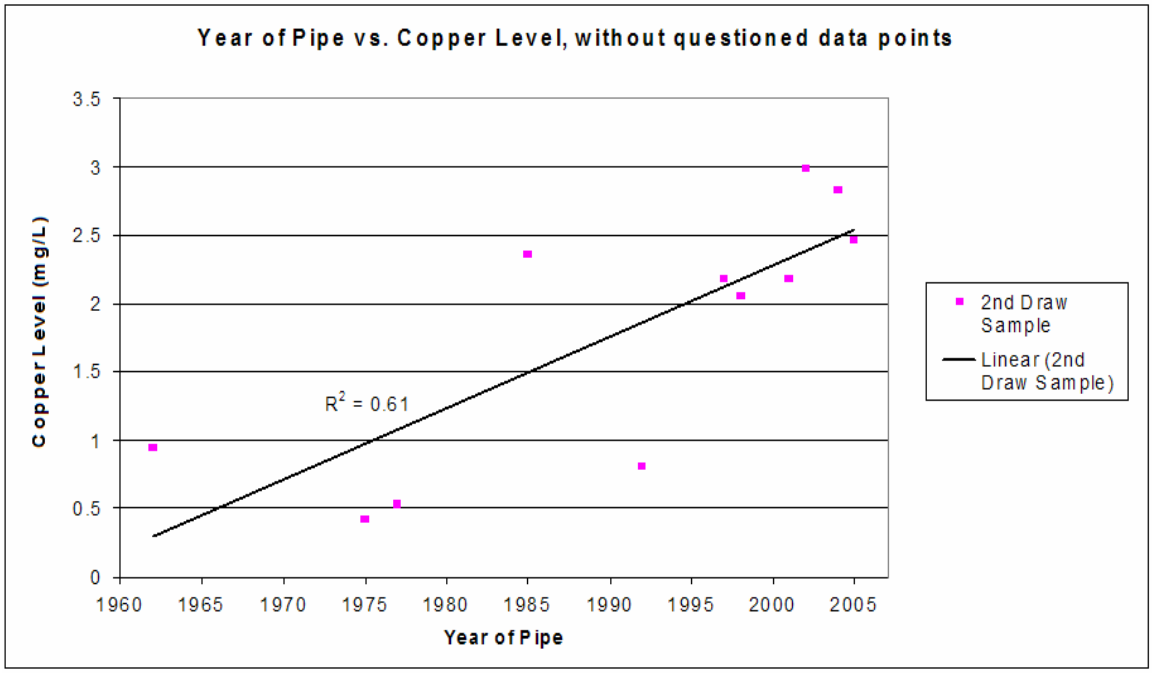

Figure 4.3 Abbreviated 2nd Draw Copper Concentration Data vs. Age

The sequential sampling experiment's findings are also relevant to Lead and Copper Rule (LCR) sampling. The LCR calls for the first liter of water to be collected and analyzed after a minimum six hour stagnation period in the distribution system. The sequential findings indicate that the LCR one liter sample is a mix of water from the distribution system and water which stagnated in the fixture. This phenomenon explains why LCR compliance data can be misleading for determining the chemical relationships behind copper corrosion (Schock et al., 1995). Dezincification of yellow brass in fixtures has been suggested as the main source of both lead and copper in LCR samples before

(Kimbrough, 2001). Certainly this study suggests that a 1st draw sample indicates the consumer's exposure to copper from the faucet fixture (see Tables 4.2 and 4.3), while a sample drawn after a short flush would better indicate the risk posed by the copper distribution system. The graph in Figure 4.4 depicts the different copper concentrations that would have been reported for the water from building 641 as measured in the sequencing experiment for different sample sizes.

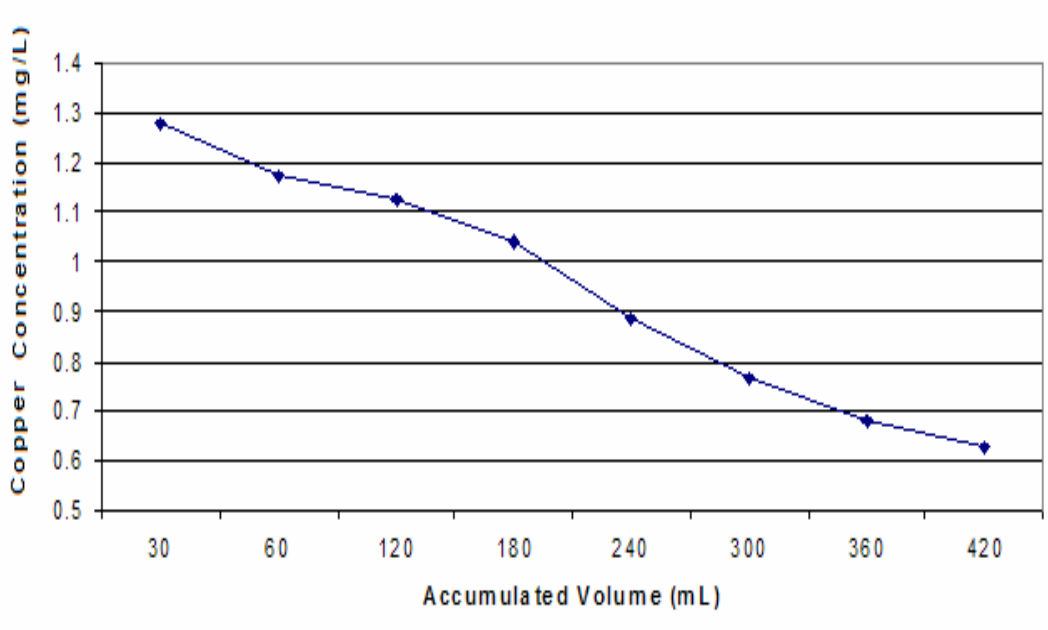

Figure 4.4 Change in Reported Copper Concentration with Sample Volume

If a researcher had taken only a 30 mL sample from the sink in building 641 they would have determined the copper level to be close to the LCR action level at 1.3 mg/L. However, if a researcher took a 420 mL sample from the same sink with the same stagnation time they would determine the copper level to be 0.63 mg/L, well under the LCR action level. Clearly the sample size can significantly affect the copper concentration determined in a study because of the effect of the faucet. Studies vary as to whether they follow the LCR protocol in collecting samples or not, depending on what is

being studied. This effect is certainly something to be considered in designing a sampling study.

4.3 Modeling

Having characterized the water quality being delivered to each building and having determined the 2nd draw copper concentration in the water after stagnation in each building, the question becomes, what role are the corrosive solids on the inside of the delivery pipes playing? Recall that this research endeavors to identify the corrosion solids present in a real-world distribution system containing piping of different ages, show how the copper solid mineralogy of the corrosion scale changes with time, compare real copper pipe scale mineralogy to the USEPA's cupric hydroxide model's predictions, and finally, examine what type of corrosive scale most effectively reduces dissolved concentrations of copper in drinking water.

The water quality data from each building were used as input parameters for the model to predict the copper concentration in the presence of different copper compounds. The measured dissolved inorganic carbon (DIC) and pH levels for each building were input to the model, and the presence of cupric hydroxide [$Cu(OH)_2$] and malachite [$Cu_2CO_3(OH)_2$] respectively, was assumed. Table 4.4 shows the model's prediction of the aqueous copper concentration in the presence of either cupric hydroxide or malachite scale on the inside of the delivery pipe. The model only takes into account one solid at a time, and not a mix of solids, as are almost certainly present in reality. This approach is consistent with the work of Shock et al. (1995) in development of the cupric hydroxide model and in Lagos et al.'s (2001) work.

Table 4.4 Modeling of Water for Each Building

Building	Plumbing Date	Model Predictions Cu (mg/L) in presense of… $Cu(OH)_2$	Model Predictions Cu (mg/L) in presense of… $Cu_2CO_3(OH)_2$	Actual Cu (mg/L) 2nd Draw
441S	**2005**	4.40	0.091	2.46
837	**2004**	3.54	0.083	2.83
571	**2002**	4.32	0.090	2.99
553	**2001**	2.42	0.073	2.18
645	**1998**	4.26	0.090	2.05
306	**1997**	4.33	0.090	2.17
556	**1995**	3.42	0.082	1.85
620 PII	**1994**	4.34	0.091	2.13
441B	**1993**	2.90	0.071	0.442
620 PI B	**1992**	4.38	0.091	2.53
642	**1989**	4.25	0.089	0.668
676	**1985**	4.99	0.096	2.36
11A	**1984**	4.04	0.087	1.95
641	**1977**	4.35	0.090	0.528
653	**1975**	4.06	0.088	0.417
464	**1962**	4.08	0.088	0.946

Next, the actual copper level measured from the 2nd draw water analysis is compared to the copper values predicted by the model. Figure 4.5 graphs the model values along side the 2nd draw copper concentrations. All of the 2nd draw values fall in between the model's predicted values. This is consistent with the belief that a mix of solids, including both cupric hydroxide and malachite, are expected to be present on the pipe. Equilibrium with these solids is what is assumed to determine the copper concentration in drinking water, and indeed, the copper concentrations do not exceed the values predicted by the presence of pure cupric hydroxide. Nor are they ever less than those predicted in the presence of a pure malachite scale. It is reasonable to think the 2nd draw copper concentrations were caused by the presence of a mix of these solids. We can also see in Figure 4.4 that the 2nd draw concentrations are closer to the model's

values for cupric hydroxide and with age lessen until the copper levels in older pipes are closer to the model's values for a pure malachite scale. The 2nd draw data appear consistent with the predictions of the cupric hydroxide model.

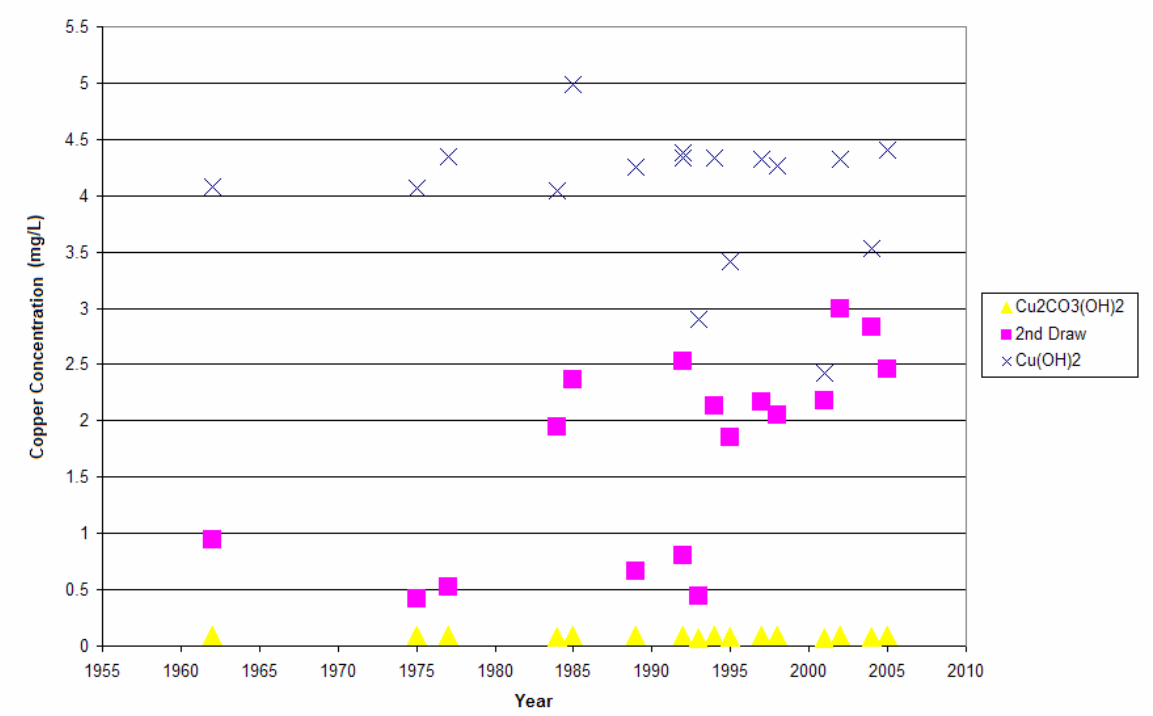

Figure 4.5 2nd Draw Copper Concentrations Compared to Model Values

Tenorite was originally included in this analysis since so much of the theoretical work behind the aging phenomenon shows cupric hydroxide aging to tenorite over time (Schindler et al., 1965; Patterson et al., 1991; Hidmi and Edwards, 1999). In reality, WPAFB's water supply system is maintained at a lower pH (approximately 7.3) and higher alkalinity than that associated with tenorite formation. It is expected that, instead of tenorite, cupric hydroxide would age to malachite at WPAFB's pH and alkalinity. Indeed, the solids analysis, explained in the following section, found no evidence of tenorite on the WPAFB pipes. Therefore only malachite and $Cu(OH)_2$ are considered in the model.

4.4 Solids Analysis

The sample of copper drinking water delivery pipe cut from each building was prepared for analysis by cutting it in half lengthwise, and then cutting several small (approximately one cm^2) pieces from each pipe (see Section 3.5.2). The halved pipes were photographed and the small pieces were analyzed using x-ray diffraction (XRD) and x-ray photoelectron spectroscopy (XPS) to identify the copper solids forming the interior corrosive scale. Scale solids identified with XRD and XPS are listed in Table 4.5 and will be discussed in subsequent sections. Note from the XPS and XRD analyses that tenorite was, as expected, not found in the pipe scales.

Table 4.5 Results of XRD and XPS analysis

Building	Plumbing Date	XRD Results	XPS Results
441S	**2005**		Cu_2O, C with Cl, N, S and O with Si, N, P
837	**2004**	Cu_2O, Malachite	$Cu(OH)_2$ and Cu_2O with P, Ca, Si, Cl present
571	**2002**	*Cu_2O, Cu*	$Cu(OH)_2$ and Cu_2O with P present
553	**2001**	*Cu_2O, Cu*	Cu_2O or Cu_2S, CuCN or $CuC(CN)_3$ with small amount of $CaCO_3$ and Zn or ZnO
645	**1998**	*Cu_2O, Cu, Malachite*	$Cu(OH)_2$
306	**1997**	*Cu_2O, Cu, Malachite, $CaCO_3$*	CuCN or $CuC(CN)_3$, P and Ca present
556	**1995**	*Cu, Cu_2O*	$Cu(OH)_2$ and Cu_2O with Ca and P present
620 PII	**1994**	Cu_2O, Malachite	$Cu(OH)_2$
441B	**1993**	*Cu_2O, Cu*	$Cu(OH)_2$ (Lot of C)
620 PI B	**1992**	Cu_2O, Malachite	$Cu(OH)_2$ and Cu_2O, Carbide, Ca and P
642	**1989**	Cu_2O, Malachite *Cu_2O, Cu, Malachite*	$Cu(OH)_2$
676	**1985**	Cu_2O, Malachite, Quartz	Cu_2O, P and Cl also present
11A	**1984**		$Cu(OH)_2$, small CO_3; P, Si, Cl present
641	**1977**	Cu_2O, Malachite *Cu_2O, Cu, Malachite*	$Cu(OH)_2$ with P, Cl, small amount of CO3
653	**1975**	Cu_2O, Malachite	Malachite, Cu_2O, with Fe-oxide, Ca and P
464	**1962**	Cu_2O, Malachite	$Cu(OH)_2$

4.4.1 Photography

Photos of the halved pipes reveal a remarkable diversity among the pipe scales present in a single water distribution system. From dark brown, to green, to yellow, to white, the pipe scales are visually very different from each other. A timeline of the pipe photos is presented in Appendix F. Despite efforts to engineer water chemistry to produce beneficial scale in distribution systems and to reduce detrimental scale build up, this photo montage shows that even in one system supplied by a single treatment plant, corrosive scale is widely varied. Pipes less than five years old have spotty or incomplete scale coverage on the inside, but all pipe older than five years appear to have complete scale coverage of some type. Based on visual evidence alone, it appears to take at least five years for pipes exposed to WPAFB-type water to develop 100% scale coverage.

Appendix G summarizes the XRD and photographic analysis of each of the pipes. Photos of the pipe halves as well as close up, stereomicroscope pictures of the scales on each pipe are shown. The stereomicroscope pictures provide another visual impression of the scale. When viewed on a 2 mm or 0.7 mm scale, the scales consistently appear as a collection of small corrosion pods that have grown together. In some pipes one sees only small, separate circles of corrosion developing. On other pipes the circles have grown together to provide seemingly continuous coverage. In each case the scale is made up of small circles of localized corrosion, not an expanding sheet or front of corrosion.

4.4.2 X-ray Diffraction Analysis (XRD)

XRD is a commonly used surface chemistry technique for identifying unknown solids. It is able to identify a mix of solids based on their structure since each x-ray diffraction pattern is unique for every crystalline structure (Skoog and West, 1971).

Analytes can be multilayer thin films or powders, and produce diffraction patterns that are compared to a library of known structures to determine crystals empirically. XRD analysis began by placing the small pieces of pipe directly into the XRD machine to ascertain the scale make-up without disturbing the scale. Six of sixteen samples were initially analyzed in this fashion with limited success. On each of the six samples XRD identified pure copper (Cu) and cuprous oxide or cuprite (Cu_2O). Pure copper was certainly present in the wall of the pipe and perhaps in small fragments of pipe dusted on the sample surface, created in the process of sawing the pipes in half. Cuprite is also expected to be present on each pipe as it is created and remains at the immediate copper-oxygen interface where water meets the pipe wall. It is believed cuprite underlies all other copper scales. Therefore finding cuprite and pure copper in the XRD scans was not surprising, but also uninformative. Three of the six samples analyzed directly with XRD also had weak peaks indicating malachite, a solid of interest since it controls or influences the aqueous copper concentration when in contact with water.

Because the sample pieces were cut from a round pipe, they were curved. We were concerned the XRD results from the pipe pieces were not providing a complete characterization of the solids present because the curvature could disrupt the peak locations and intensities during XRD analysis. Analyzing a powderized, homogenized sample presents a flat sample surface to the x-ray beam and is a more conventional analytical technique for XRD (Settle, 1997). Therefore we decided to scrape the scale off of each pipe, when enough was present, and powderize it for analysis (see Section 3.4.4 for procedure). The results shown in the XRD column of Table 4.5 in italics are results obtained after scraping the scale from the pipe. Results shown in plain font for six

buildings are the results of intact sample analysis. The XRD spectra for each building are shown in Appendix G.

XRD identified malachite and cuprite on 10 of 16 samples, including a pipe less than a year old and the oldest pipe in the sample. Theory suggests that malachite would develop over time in the copper pipes and perhaps not appear in young or new pipes. One aim of this work was to identify the period of time necessary to develop a protective copper scale in WPAFB water. Although XRD identified malachite in scale as young as one year old in building 837, the copper concentration in that building's water (both 1st and 2nd draw) far exceeded the LCR action level. If malachite were dominating the copper scale, the copper level is predicted to be much lower (0.083 mg/L by the model's prediction in Table 4.4). Therefore, although malachite is present, it does not seem to be "protecting" the water by containing copper in the scale. This is the case for the other seven pipes where XRD detected malachite, but cupric hydroxide was predicted by the model. In each of these buildings the presence of malachite is not protecting the water. Rather, copper is being released to the water, most likely via contact with another copper scale compound not detected by XRD. The model predominately predicted the presence of cupric hydroxide, which XRD cannot detect. However in three cases it predicted malachite as the dominant solid. In two of those three cases, XRD did identify malachite in the scale.

4.4.3 X-ray Photoelectric Spectroscopy (XPS)

An important limitation of XRD is that it is not able to accurately characterize amorphous solids such as cupric hydroxide, a key solid of interest in this study (Settle, 1997). X-ray Photoelectron Spectroscopy (XPS) detects only the top one to two

nanometers of depth in a film with a lateral resolution of 100-800 micrometers. XPS is sensitive to all elements of importance (except hydrogen) in this study and can distinguish between CuO, Cu_2O, and amorphous $Cu(OH)_2$, making it a complementary technique to XRD. XPS is a tool for identifying the major phases (mainly oxides) in corrosive films at the immediate solid surface and for determining oxidation state (i.e. it can differentiate between Cu^{+1} and Cu^{+2} solids). Many good reference texts for basic XPS terminology and techniques are available (Settle, 1997; Briggs and Seah, 1983). The only literature identified where researchers used XPS to analyze "real world" copper corrosion films were two studies of bronze archeological artifacts (Squarcialupi et al., 2002; Paparazzo and Moretto, 1999). XPS has been used to analyze corrosion of copper coupons exposed to fabricated drinking water over short periods of time in the laboratory and has helped to explain the mechanisms of copper corrosion (Feng et al., 1995; Shim and Kim, 2004).

This study is the first to utilize XPS to try to identify naturally formed, heterogeneous scales on the inside of real-world drinking water pipes. Two pieces of each pipe were analyzed by XPS, usually from opposite sides of the pipe. One survey scan and three high resolution scans were taken of each piece. The three high resolution scans were taken in three different locations on the piece. Carbon, oxygen, and copper (both the Auger and photoelectron peaks) were always high resolution scanned. The initial survey scan often identified additional elements of interest which were high resolution scanned as well. Almost every pipe sample had silicon, Si, present, but usually in such small concentration it was not multiplexed. The "XPS results" column in Table 4.5 lists the major elements present in each pipe's scale. The most common elements

observed were phosphate, chlorine, calcium or sulfate. Two samples had pronounced nitrogen peaks, while one building had iron, Fe, and one had zinc, Zn, present.

The XPS spectra of interest for each building are summarized in Appendix H. Both peak shape and binding energy values were used to identify the solids listed in Table 4.5. Each peak's binding energy (BE) was measured using the full-width half max (FWHM) function provided in the Multipak software program. The copper photoelectron and Auger BEs were compared to reference values found in the literature (see Table 3.3), and also plotted in chemical state plots (such as Figure 3.1) along side the reference values. BEs for oxygen, carbon, and nitrogen when applicable were compared to reference values as well to identify what type of molecules those elements were bonded to on the sample surface. The peak binding energy data were combined with a qualitative look at each peak for characteristic shape to make a final determination of the solid present. Often the sample's chemical state plot and curve shape could seem at odds unless carefully considered.

Building 620 Phase I is a good example of the combination of chemical state and curve shape analysis necessary for scale identification. The chemical state plot for building 620 PI's six data points (three multiplexes on each of two pieces taken from the pipe) is shown in Figure 4.6. The FWHM determined peak locations for the Cu $2p_{3/2}$ peaks and Cu LMM Auger peaks place the samples in a neat cluster close to the reference values for Cu_2O.

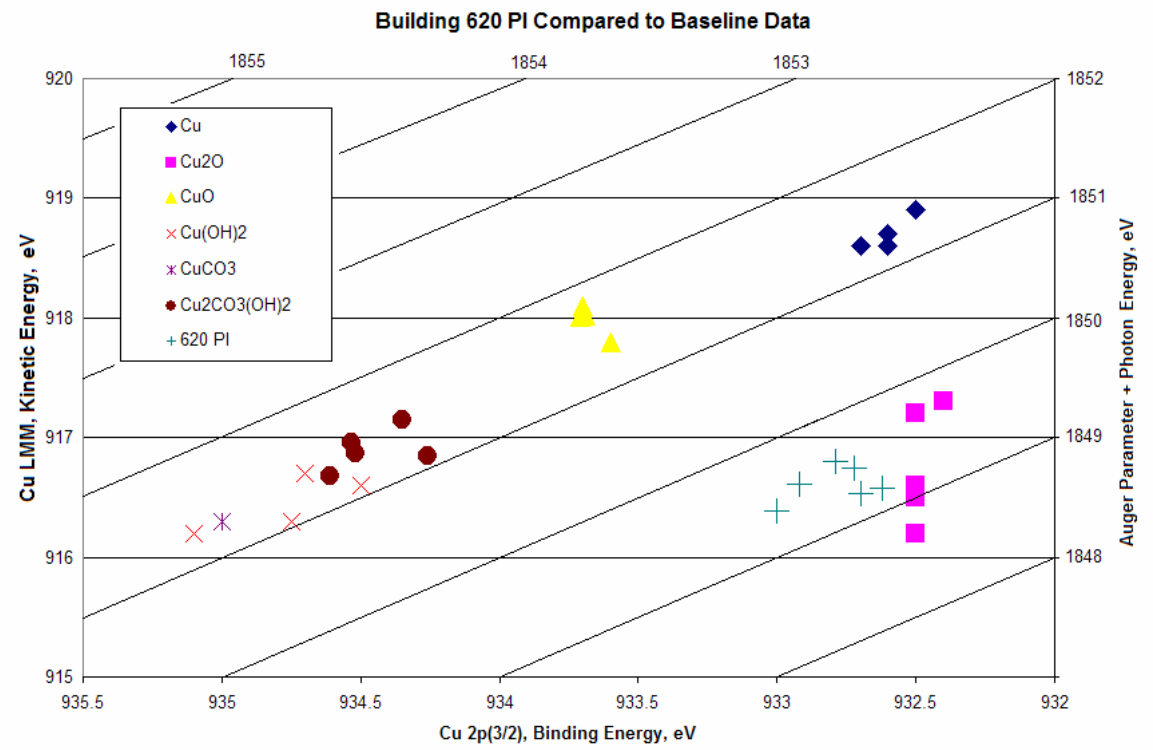

Figure 4.6 Chemical State Plot for Building 620 PI with Reference Data

Looking at this chemical state plot alone, one would ascertain that XPS identified Cu_2O on the samples from building 620 PI. However, a qualitative look at the peak shapes for the Cu 2p and Cu LMM peaks for these samples provides additional information about the solids present. Figure 4.6 shows the Cu 2p area of the XPS spectra for three multiplex scans taken on the same pipe sample in slightly different locations, one after the other.

The software's FWHM function calculates the binding energy at the maximum height of the peak. Therefore the three spectra in Figure 4.7 would have their maximum binding energy at or near 932.6 eV which corresponds to the cluster of values in Figure 4.6 for building 620 PI which occur between 932.5 and 933.0 eV on the abscissa. However, qualitatively we can see the peak is broad at 934.4 eV.

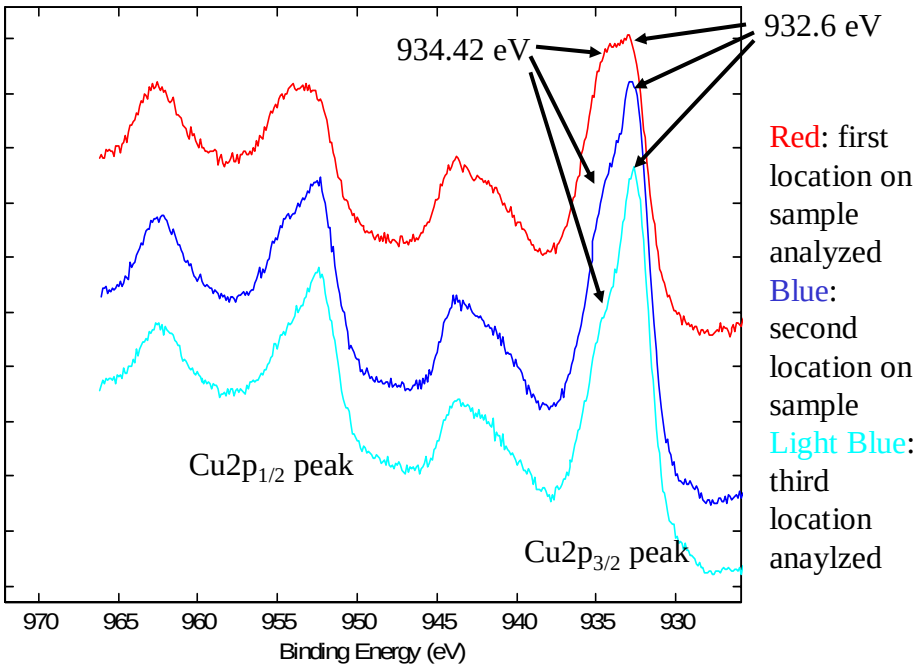

Figure 4.7 Stack Plot of XPS Cu 2p Spectra of Building 620 PI

In the first scan the peak at 932.6 eV is only slightly more intense than the peak at 934.42 eV. In each progressive scan the peak at 934.42 eV gets smaller, while the peak at 932.6 eV remains pronounced. Why would the curve shape be changing with each subsequent x-ray scan? XPS utilizes an ultra high vacuum environment and an x-ray source, both of which can cause partial reductions in some metal oxides or decomposition of hydroxides. It is well documented that x-ray exposure causes the reduction of copper species from Cu^{+2} to Cu^{+1} oxide over time (McIntyre and Cook, 1975; Frost et al., 1972; Klein et al., 1984; Iijima et al., 1996; McIntyre et al., 1981). In the spectra of first, second, and third analyses of the building 620 PI sample there appears to be decomposition occurring of the Cu^{+2} oxide, probably $Cu(OH)_2$, to a Cu^{+1} oxide. Based on this explanation, when we analyzed each building's samples, the most confidence was

placed in the peak locations and shapes from the first of three spectra taken, as they were the least affected by possible x-ray reduction.

Note that in the first scan in Figure 4.6 both Cu^{+2} and Cu^{+1} oxides were present in almost equal amounts. Looking again at the chemical state plot in Figure 4.5 one can see that Cu $2p_{3/2}$ binding energies in the neighborhood of 934.42 correspond to $Cu(OH)_2$ while 932.6 corresponds to Cu_2O. Therefore the curve shape provide evidence that both $Cu(OH)_2$ and Cu_2O are present, though the chemical state plot identified only Cu_2O.

Another visual method of determining what copper species is present is to compare the curve shape to published standards. Figure 4.8 shows one such published montage from Chawla et al. (1992).

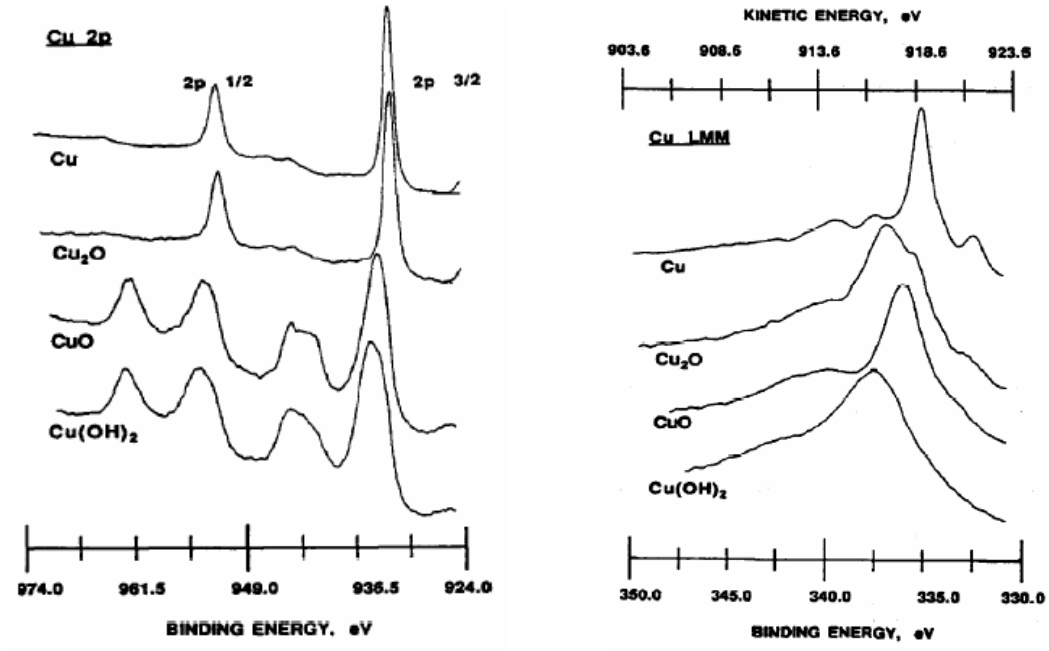

Figure 4.8 Montage of Copper Oxide Spectra (Chawla et al., 1992)

Comparing the peak shapes from building 620 PI in Figure 4.7 to this montage, it become clear that the Cu^{+2} compound present is $Cu(OH)_2$. Cu^{+2} compounds all exhibit characteristic shake-up peaks on the higher BE side of both Cu 2p peaks, while Cu^{+1}

compounds do not. The shake-up next to the Cu $2p_{3/2}$ peak of building 620 PI in Figure 4.7 is identical to the $Cu(OH)_2$ standard in Figure 4.8. Figure 4.9 shows the Cu LMM peak for building 620 PI. Again the qualitative shape of the peak matches the published $Cu(OH)_2$ standard, while the binding energy quantitatively corresponds to both Cu_2O and $Cu(OH)_2$. Therefore the researcher concluded that the copper solids observed by XPS were both $Cu(OH)_2$ and Cu_2O.

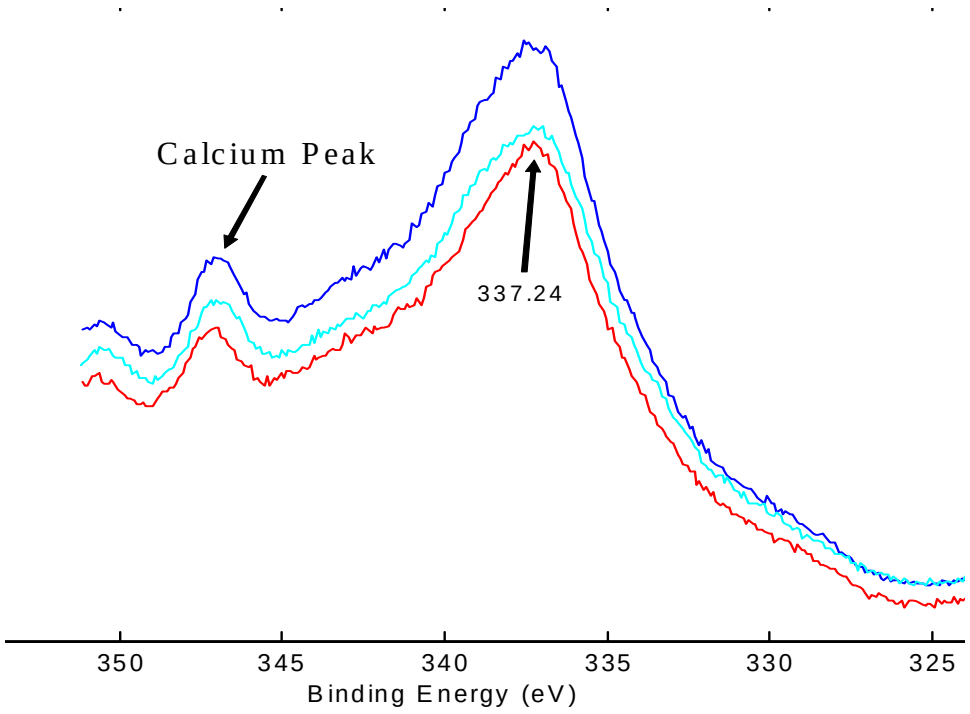

Figure 4.9 Cu LMM Peak Montage from Three Building 620 PI High Resolution Scans

Note that Figure 4.9 also identifies a characteristic calcium peak on the high binding energy side of the Cu LMM peak. The researcher was able to identify and analyze several other peaks in addition to copper to aid in species identification. Nitrogen, carbon, oxygen, zinc, iron, calcium, chlorine, silicon, and phosphorous were all recorded when identified. Often the location and shape of the carbon, oxygen and

nitrogen peaks were important in identifying the presence of cyanide (CN^-), hydroxyl ions (OH^-), and carbonate (CO_3^{-2}) when present.

Only one published source was found identifying the characteristic binding energies for the Cu $2p_{3/2}$ and Cu LMM peaks of copper carbonate [$CuCO_3$]. No published source identified the peak shapes for $CuCO_3$ and no references were found of any sort for XPS data on malachite [$Cu_2CO_3(OH)_2$]. Since malachite was a key solid to identify in this study, a malachite standard was obtained and analyzed as a means of comparison for the study samples. The malachite standard was confirmed as pure malachite by XRD analysis as well. The montage of curve shapes from the malachite analysis, as well as a chemical state plot for malachite are provided in Appendix I. This provides at least one reference for identifying malachite in future XPS work in this field. Note the major distinguishing characteristic of malachite were two carbon 1s peaks. One peak is corrected to 284.6 eV (as described in Section 3.4.3) for pure carbon and the other peak occurs at approximately 289.3 eV, the location of carbonate (CO_3^{-2}). In all other respects the malachite shape and chemical state plot location are virtually identical to $Cu(OH)_2$. This is logical considering malachite contain two hydroxyl ions bound to copper just as $Cu(OH)_2$ does – the carbonate ion bound to copper differentiates the two.

4.4.4 Solids Analysis Conclusions

Copper concentrations in drinking water are heavily dependent on the solubility and physical properties of cupric oxide, hydroxide, and carbonate solids which make up most scales not at the immediate pipe surface in drinking water supply pipes (Palit, 2000). Maximum soluble copper concentrations are attained in equilibrium with the solid cupric hydroxide [$Cu(OH)_2(s)$]. Thus in drinking water systems where aqueous copper

concentrations reach unhealthy levels, particularly young systems, theory says $Cu(OH)_2(s)$ is present. Equilibrium copper concentrations will begin to fall as copper precipitates to form more stable copper solids such as tenorite and malachite. Copper concentrations in equilibrium with malachite [$Cu_2(OH)_2(CO_3)$] are predicted to be two orders of magnitude lower than with $Cu(OH)_2$.

The solids analysis work aimed to answer the following questions, from Chapter II:

1. Identify the corrosion solids present in a real-world distribution system containing piping of different ages
2. Show how the copper solid mineralogy of the corrosion scale develops/changes with time
3. Compare real copper pipe scale mineralogy and composition to the USEPA's cupric hydroxide model's predictions
4. Examine what type of corrosive scale most effectively reduces dissolved concentrations of copper in drinking water

Let's examine each question individually. First, the copper solids present in the corrosion scale on the inside of 16 drinking water delivery pipes were identified with XPS and XRD analysis. Both pure copper (Cu) and cuprite (Cu_2O) are anticipated constituents of any copper oxide scale on the inside of a drinking water delivery pipe. Of more interest to the researcher was the additional presence of either cupric hydroxide, malachite, or both. XRD identified malachite on 10 of 16 pipes, regardless of age. Due to its inability to recognize amorphous solids, XRD tells us nothing of the presence or absence of cupric hydroxide.

Interestingly XPS identified $Cu(OH)_2$ on eleven out of sixteen pipes and malachite on only one pipe (building 653). The other four buildings that did not have $Cu(OH)_2$ had Cu^{+1} solids present instead. Two buildings had Cu_2O and two had a cuprous cyanide solid present, possibly CuCN or $CuC(CN)_3$. Finding copper-cyanide on the wall of two drinking water pipes is surprising. No literature examined in this study identified copper cyanide as a possible scale constituent in a drinking water system. Copper cyanide is used industrially in electroplating operations (CDA, 2006). There is no known connection to drinking water delivery pipes.

XPS identified the presence in many cases of phosphorus, sulfur, chlorine, zinc, iron and calcium, as noted in Table 4.5. The atomic percent of these species were usually very low and their peaks were often very small, with a high signal to noise ratio. Sulfur, chlorine, zinc, and calcium rarely exceeded 1% of the total composition. In samples where phosphorus, iron or nitrogen were seen they constituted anywhere between 1% and 15% of the total composition. Due to the limited counting time (usually half an hour in this study) corrosion products such as chlorine or phosphate were barely detected. Unless the count rates were increased substantially, XPS is best utilized for studying the major phases in the corrosion, in this case mainly copper, oxygen, and carbon (Briggs and Seah, 1983). Thus XPS has been used to identify copper-oxide species. Despite seeing sulfur and chlorine at times, no determination of other corrosion solids in the literature such as langite $[Cu_4(OH)_6SO_4H_2O]$, atacamite $[Cu_2(OH)_3Cl]$, brochanite $[Cu_4(SO_4)(OH)_6]$ was attempted with XPS. These species should have been recognized by XRD if they have been prevalent in the scales and were not seen at all with that technique.

Question two asks how the copper solids change with age. No clear aging pattern is recognizable from the available data. Both malachite and cupric hydroxide were identified on seven out of sixteen pipes, including the oldest pipe, the one year old pipe and others spread in between. Thus, no relationship between solid type and pipe age is obvious. Without being able to determine if the coverage of malachite versus cupric hydroxide is changing on the pipe surface over time, we cannot say if cupric hydroxide is precipitating to malachite over time. It is impossible to tell in what ratio malachite and cupric hydroxide are present, or whether one dominates over the other. We know only that both were identified. Visually, one sees it takes at least five years to develop complete scale coverage of the pipe walls.

Question three asks how the real world scales compare to the understanding of scale development presented in current literature, underlying the cupric hydroxide model, and summarized in Chapter II. A review of the literature from Chapter II tells us that when copper metal comes in contact with oxygenated water corrosion begins, and $Cu_2O(s)$ forms at the metal surface. While the immediate $Cu_2O(s)$ film grows rapidly thick enough to passivate the corrosion of the copper pipe, the outer layers the $Cu_2O(s)$ film in contact with water are quickly oxidized in the presence of excess oxygen and chlorine to cupric aqueous species and solids such as $Cu(OH)_2(s)$. Equilibrium with $Cu(OH)_2(s)$ at the water interface controls the aqueous concentration of copper during the early stages of scale development. Then, as cupric hydroxide particles grow larger in size, the outer scale transitions to malachite (in WPAFB water) which lowers the aqueous copper concentration. This concept of scale development paints the picture of a Cu_2O

film at the metal surface, underlying a Cu^{+2} solid film, made of $Cu(OH)_2$, malachite, and other cupric solids that interact with the water.

The data collected in this study paint a slightly different picture of the scale layers present on the inside of drinking water pipes. Remember that XPS is a surface technique that only "sees" the top 5 to 50 Angstroms (0.5-5 nanometers) of scale depth, whereas XRD analyzes the constituents of the entire powderized sample. Therefore XPS tells us what is at the immediate surface of the corrosive scale, while XRD tells us what is present throughout the scale bulk, regardless of location. Because malachite on most pipes was identified by XRD but not by XPS implies that the malachite was not in the surface layer. Rather XPS found $Cu(OH)_2$ or a cuprous oxide at the surface in most cases. This implies that cuprite and malachite are present in the bulk of the scale, and $Cu(OH)_2$ is more likely to develop at the scale surface, in immediate contact with water. Cuprite and copper-cyanide solids, Cu^{+1} compounds, were found at the surface in four scales, in one case with malachite present in the bulk of the scale below them (building 676). Therefore cuprous compounds can occur naturally overlaying cupric solids in contact with drinking water.

Finally, what do the solids analysis data tell us about which scales are most protective of drinking water? Table 4.6 shows the solids analysis results along side the aqueous copper concentration measured for each building. Again, without knowing which solid is present in highest concentration or with the most coverage it is hard to relate the copper solid to the copper concentration in water. Neither XRD or XPS are able to ascertain the quantities of solid present, only to identify which solids are seen. XPS is able to do depth profiling of corrosion films and this is an interesting area for

further work. If the researcher could ascertain which solids form at which layer in the corrosion film it could provide further information about the interaction between water and solid. At the moment we are only able to say which solids are present and that there is a mix of solids present on all pipes. Recall that in most scales XPS identified $Cu(OH)_2$ in the top Angstroms of scale depth. This could mean that $Cu(OH)_2$ is dominating the interaction between the scale and the water, as it is present at the surface. This result is consistent with the high copper concentrations in many buildings.

Table 4.6 Solids Results Compared with Aqueous Copper Concentration

Building	Plumbing Date	Cu (mg/L) 2nd Draw	XRD Results	XPS Results
441S	**2005**	2.46		Cu_2O, C with Cl, N, S and O with Si, N, P
837	**2004**	2.83	Cu_2O, Malachite	$Cu(OH)_2$ and Cu_2O with P, Ca, Si, Cl present
571	**2002**	2.99	*Cu_2O, Cu*	$Cu(OH)_2$ and Cu_2O with P present
553	**2001**	2.18	*Cu_2O, Cu*	Cu_2O or Cu_2S, CuCN or $CuC(CN)_3$ with small $CaCO_3$ and Zn or ZnO
645	**1998**	2.05	*Cu_2O, Cu, Malachite*	$Cu(OH)_2$
306	**1997**	2.17	*Cu_2O, Cu, Malachite, $CaCO_3$*	CuCN or $CuC(CN)_3$, P and Ca present
556	**1995**	1.85	*Cu, Cu_2O*	$Cu(OH)_2$ and Cu_2O with Ca and P present
620 PII	**1994**	2.13	Cu_2O, Malachite	$Cu(OH)_2$
441B	**1993**	0.442	*Cu_2O, Cu*	$Cu(OH)_2$ (Lot of C)
620 PI B	**1992**	2.53	Cu_2O, Malachite	$Cu(OH)_2$ and Cu_2O, Carbide, Ca and P
642	**1989**	0.668	Cu_2O, Malachite *Cu_2O, Cu, Malachite*	$Cu(OH)_2$
676	**1985**	2.36	Cu_2O, Malachite, Quartz	Cu_2O, heavy C, P and Cl also present
11A	**1984**	1.95		$Cu(OH)_2$, small CO_3; P, Si, Cl present
641	**1977**	0.528	Cu_2O, Malachite *Cu_2O, Cu, Malachite*	$Cu(OH)_2$ with P, Cl, small CO3
653	**1975**	0.417	Cu_2O, Malachite	Malachite, Cu_2O, with Fe-oxide, Ca and P
464	**1962**	0.946	Cu_2O, Malachite	$Cu(OH)_2$

Note: For XRD: normal text = scraped/powderized sample results and italics = pipe pieces

Based on fundamental chemistry and experimental observation of the solubility of Cu^{+2} solids, malachite is still the solid scale which should contribute the lowest amount of aqueous copper to drinking water. However this research has shown that within one distribution system a surprisingly wide variation in scale color, coverage, and chemical

make-up exists. Promoting the homogenous coverage of a malachite scale throughout a distribution system in order to protect consumers from elevated copper levels in drinking water seems extremely difficult. Even in water that promotes malachite growth, such as Wright-Patterson Air Force Base's high alkalinity and 7.3 pH, scales show remarkable variation after less than one year, and up to 44 years, of exposure in the distribution system.

V. DISCUSSION

5.1 Conclusions

The conclusions drawn from this research are summarized below.

- The water sampling data collected support the hypothesis that copper concentrations decline in drinking water as the copper delivery system ages. The data between copper concentration and pipe age exhibited a negative correlation that was weakly linear.
- The sequential sampling showed that 2nd draw samples would provide a more accurate picture of copper concentrations caused by contact with copper delivery pipes. 1st draw samples are more indicative of the copper concentration in water in contact with the tap fixture, which is often made of an alloy of several metals.
- The one liter sample collected per the LCR is a mix of water from the distribution system and water which stagnated in the fixture. Therefore compliance data can be misleading for determining the relationship between dissolved copper levels and corrosion in pure copper pipes. 2nd draw samples are preferable in that regard.
- Photos of the halved pipes reveal a remarkable diversity among the pipe scales present in a single water distribution system. Even in one system supplied by a single treatment plant, corrosive scale is widely varied.
- Based on visual evidence alone, it appears to take at least five years for pipes exposed to WPAFB-type water to develop 100% scale coverage. The scales

appear as a collection of small corrosion pods that have grown together. The scale is made up of small circles of localized corrosion, not an expanding sheet or front of corrosion.

- When possible it is recommended to scrape the scale off of drinking water pipes and powderize it for XRD analysis. It is not known if this approach is beneficial to XPS analysis.
- XPS and XRD have been shown to be complementary techniques for identifying the constituents of "real world" pipe scale. In combination, they are able to identify both crystalline and amorphous solids of interest including copper oxides, hydroxides, and carbonates.
- This research adds XPS reference data, including Cu2 p, C 1s, O 1s, and Cu LMM peak locations and shapes, for malachite [$Cu_2CO_3(OH)_2$] to the literature to support further study and identification of this important solid in drinking water delivery systems.
- Both peak locations and peaks shapes must be considered to accurately identify copper solids within complex, real world scales using XPS.
- In future XPS studies of complex, naturally formed scales, limiting the sample's exposure to x-rays is recommended. In this study, the first multiplex scan of each sample appeared to be the most reliable, while subsequent scans showed degradation of Cu^{+2} compounds to Cu^{+1} solids. Although it is statistically favorable to have multiple scans of each pipe, there is a trade-off in that the sample degrades with prolonged x-ray exposure. Use of a monochrometer to lessen x-ray effects may be helpful.

- The water sampling and solids analysis results generally support the predictions of the cupric hydroxide model and the copper aging theory behind the model (Schock et al., 1995).
- This study identified copper-cyanide solids in the scale of two drinking water delivery pipes. No literature examined in this study identified copper cyanide as a possible scale constituent in a drinking water system.

5.2 Future Research

Much work remains in the study of copper aging and cuprosolvency in drinking water. This study was unique in collecting both pipe and corresponding water samples from a distribution system to examine the aging phenomenon. However more pipe and water samples would contribute to a more statistically significant sample and would provide even more information about aging. This study could be replicated in other distribution systems with different water quality characteristics. The number of sampling locations was low (16 buildings) and more heavily distributed in young buildings than in old buildings. A statistically driven study would include more sampling locations, multiple water samples in each location, and perhaps a longitudinal component that sampled water and pipe over time. A sample of buildings could be chosen at random and include more older buildings. The difficulties in finding building records and sampling locations would be the most significant the barrier to such a study.

XPS has been demonstrated as a useful complementary technique for solids identification of drinking water scales in copper pipes. This study has only scratched the surface of what can be learned from XPS research in this area. A logical next step would

be to try depth profiling copper scales with XPS to determine what scales are forming at what layers of the film. Important considerations for future study designs will be sample degradation under x-ray exposure and also the danger of changing the solids' oxide state by argon sputtering. Experimental controls will be necessary to assure samples are not being degraded. One way to reduce x-ray exposure during XPS analysis would be to use a monochromated aluminum x-ray source, which confines x-ray exposure to a smaller area of the sample being analyzed.

This study also demonstrated that high copper concentrations in drinking water are partially caused by copper contributions from individual tap fixtures. Fixtures are often made of one of many types of brass. Little is known about the fundamental chemistry and corrosion mechanisms of copper alloys, including brass. Copper leaching from fixtures is a fruitful area for future research.

Appendix A

Building Information Sheets

The building information sheets describe the background information gathered on each building, the point(s) of contact for each facility, and shows the location of the water and pipe samples gathered. The buildings are listed by age, from youngest to oldest.

Building Information Sheet – 441S, Shower Installation

Building Number: 20441

Real Property Date: The building was constructed in 1957

Building Manager: Glenda Tool, AFRL/HEOC, Mary McClellan, AFRL/HEOC

Interviewed on: 12 December 2005

Relevant Construction or Renovation Project Drawings:

Per e-mail with Mary McClellan the shower in the 1st floor women's restroom was installed in September 2005. Project number was 051972 per CE records.

Location of Sampling (room number): The new shower was installed in the 1st floor women's restroom. The pipes to the shower were access via the drop ceiling in the basement hallway, beneath the location of the shower. Because they were newly installed, there was a shut-off valve in easy reach.

Date of pipe sampled: 2005
According to what reference: Project 051972, as built drawings dated October 2005, Sheet 3A and the interview with Mary McClellan

Is there a water softener or an ion-exchange system in the building: No

Photos taken:

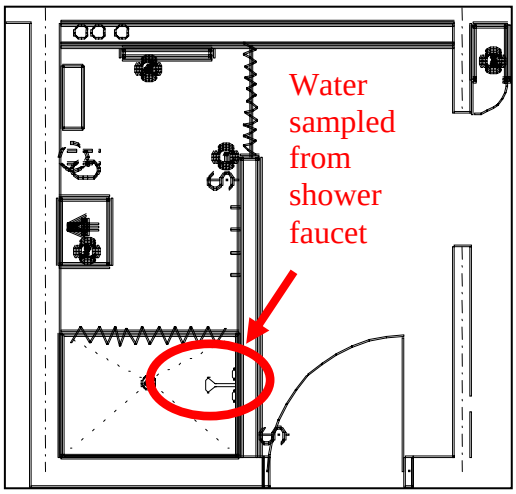

Building Information Sheet – 837

Building Number: 20837

Real Property Date: 2004

Building Manager: MSgt Ellen Ebel, AFRL/HEPB

Interviewed on: 19 December 2005

Relevant Construction or Renovation Project Drawings:

Construction drawings for the building:

Building Number	Project	Sheet	Title
20837	27-01-C-0031	A2.01	First Floor Plan East
		A2.15	First Floor - Room Number/Room ID
		P2.03	Plumbing First Floor Plan East - Overhead

Location of Sampling (room number): I sampled the first sink in the women's restroom on the first floor. I sampled the cold water domestic pipe leading to a drinking water fountain across the hall from the bathroom. The pipes to the bathroom itself were unreachable, however the drinking fountain feed pipe branches off near-by from the sample cold water domestic line that feeds the bathrooms. The pipe to the drinking water fountain was overhead, above the drop ceiling in the hallway.

Date of pipe sampled: 2004 According to what reference: Project 27-01-C-0031

Is there a water softener or an ion-exchange system in the building: No

Photos taken:

Sampling the cold water domestic pipe in the ceiling over the hallway.

Building Information Sheet – 571

Building Number: 20571, renovated hanger housing the Area B fitness center

Real Property Date: Constructed in 1942. Renovated in 2002

Building Manager: Mr. Julian Bell, MSG/SVMPD

Interviewed on: 12 October 2005

Relevant Construction or Renovation Project Drawings:

Renovation drawings for the building:

Building	Project	Sheet	Title
20571	883259	P0-1	Plumbing Legend & Schedules
		P2-2	Plumbing Ground Floor - Area C

Location of Sampling (room number): I sampled the only sink in room 155. This sink is in a sampling lab of Health and Wellness Center that is used daily. The pipes leading to this sink were accessible above the drop ceiling in the reception area of the HAWC.

Date of pipe sampled: 2002 According to what reference: Project 883259

Is there a water softener or an ion-exchange system in the building: No

Photos taken: Sampling location above the drop ceiling in the reception/hallway area of the HAWC

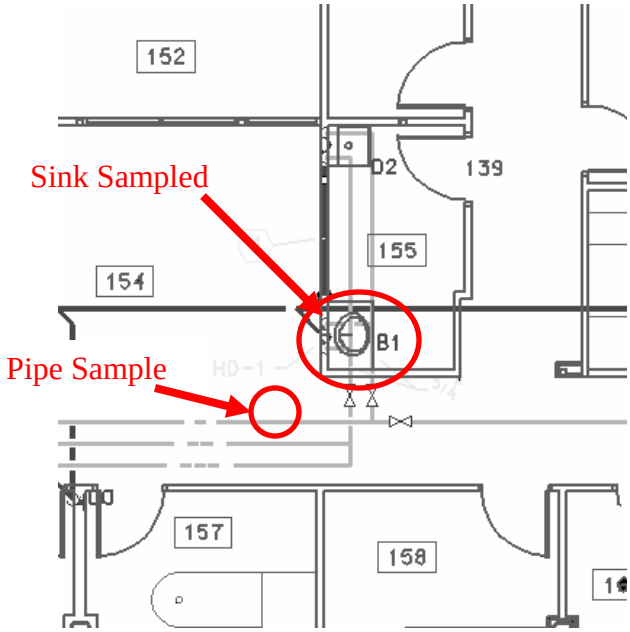

Building Information Sheet – 553

Building Number: 20553

Real Property Date: Constructed in 2001

Building Manager: Mr. Arlyn "Art" Johnson, FASW/OM

Interviewed on: 12 October 2005

Relevant Construction or Renovation Project Drawings:

Construction drawings for the building:

Building	Project	Sheet	Title
20553	983205	M0.01	Legend & General Notes
		P1.01	Basement - Area A
		P1.02	Basement - Area B
		P1.03	First Floor - Area A

Location of Sampling (room number): I sampled a sink in the men's bathroom, room 125D, on the first floor of building 553. The pipe sample was taken from the pipe chase between the men's and women's restrooms.

Date of pipe sampled: 2001 According to what reference: Project 983205

Is there a water softener or an ion-exchange system in the building: No

Photos taken:

The pipe sample was retrieved from a cold water domestic line in the pipe chase between the men's restroom sampled and the neighboring women's room bathroom.

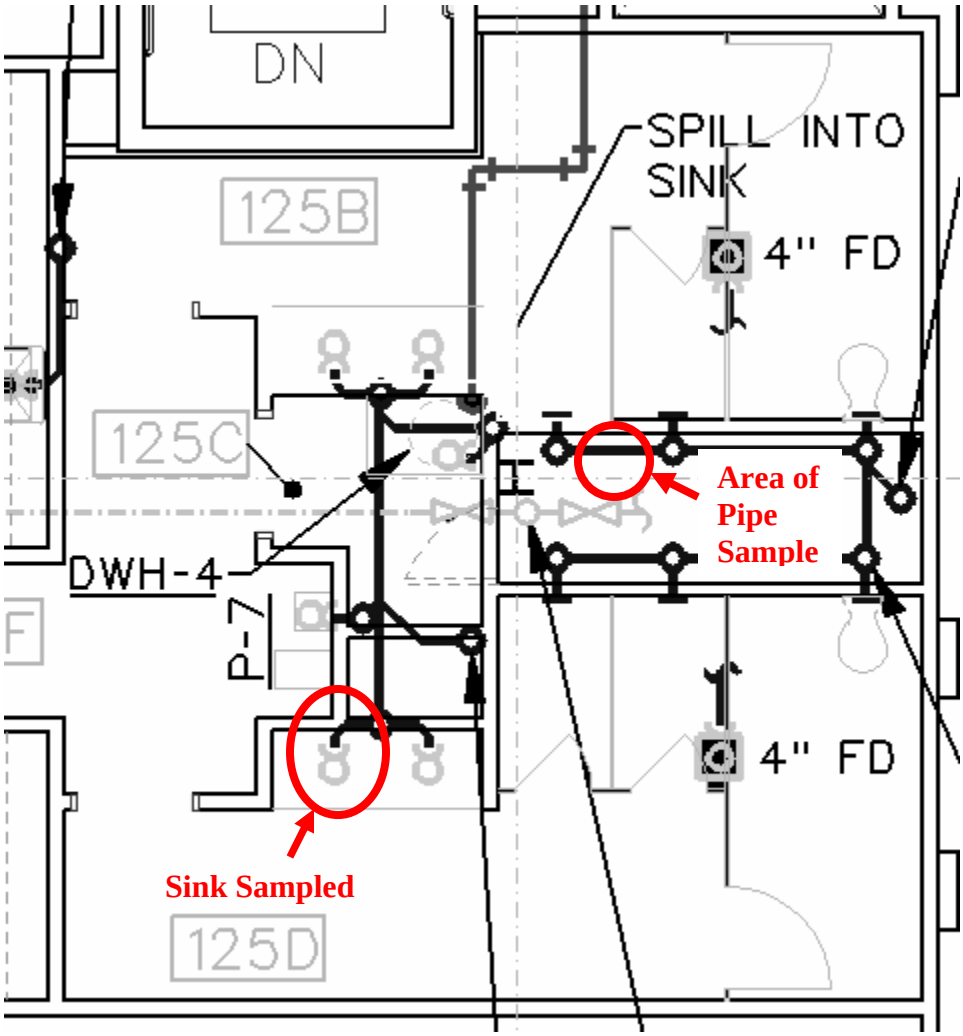
DN
SPILL INTO SINK
4" FD
125B
125C
Area of Pipe Sample
DWH-4
P-7
4" FD
Sink Sampled
125D

Building Information Sheet - 645

Building Number: 20645

Real Property Date: 1998

Building Manager: Dr. Philip Westfall

Interviewed on: 17 November 2005

Relevant Construction or Renovation Project Drawings:

From the original construction of the building:

Building	Project	Sheet	Title
20645	9604	A1	Schedules, Floor Plan and Elevation and Section

Location of Sampling (room number): Water samples were taken from the only sink in the only bathroom in this building. The pipe sample was taken from the copper pipe leading to the urinal. The sink and urinal are fed by the same cold water line, however there was a shutoff valve for the urinal.

Date of pipe sampled: 1977 According to what reference: Project 9604

Is there a water softener or an ion-exchange system in the building: No

Photos taken:

Location of the pipe sampling, above the ceiling over the sink and urinal.

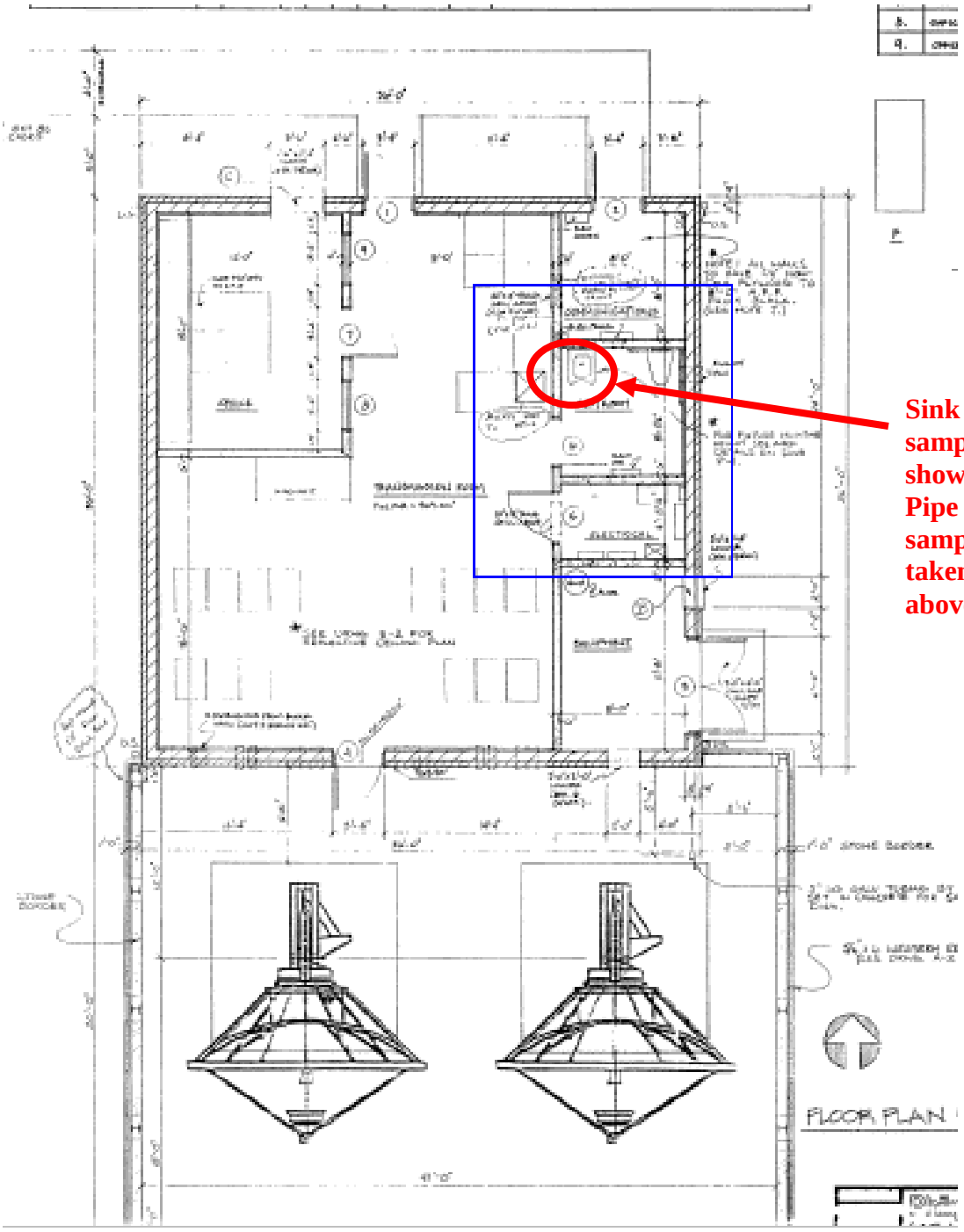
Sink sampled shown. Pipe sample taken above sink
FLOOR PLAN

Building Information Sheet – 306

Building Number: 20306, incinerator

Real Property Date: Constructed in 1997

Building Manager:

Interviewed on: 19 December 2005

Relevant Construction or Renovation Project Drawings:

Construction drawings for the building:

Building	Project	Sheet	Title
20306	940111	P1.1	Floor Plan, Legend, Details & Schedule, Notes

Location of Sampling (room number): This small building has only one office and one restroom. The water supply comes into the building and one branch goes to the water heater and another branch takes cold water to the bathroom. I sampled water from the only bathroom sink. The cold water pipe going to the bathroom was unreachable so we took a pipe sample from the line going into the water heater.

Date of pipe sampled: 1997 According to what reference: Project 940111

Is there a water softener or an ion-exchange system in the building: No

Photos taken:

We sampled the cold water domestic line feeding into the water heater.

Building Information Sheet - 556

Building Number: 20556

Real Property Date: 1995

Building Manager: Mr. Dan Litteral, LRSSW/OM

Interviewed on: 3 January 2006

Relevant Construction or Renovation Project Drawings:

From the original construction of the building:

Building Number	Project	Sheet	Title
20556	973301	P001	Index, general notes, Legend
		P401	Basement floor plan area a
		P402	Basement floor plan area a

Location of Sampling (room number): Kitchen 003. The sink sampled is in a kitchenette in the basement of building 556. The pipes leading up to the sink were accessible above the drop ceiling directly above the sink.

Date of pipe sampled: 1995 According to what reference: Project 973301

Is there a water softener or an ion-exchange system in the building: No

Photos taken:

Sampling above the ceiling above the kitchenette sink.

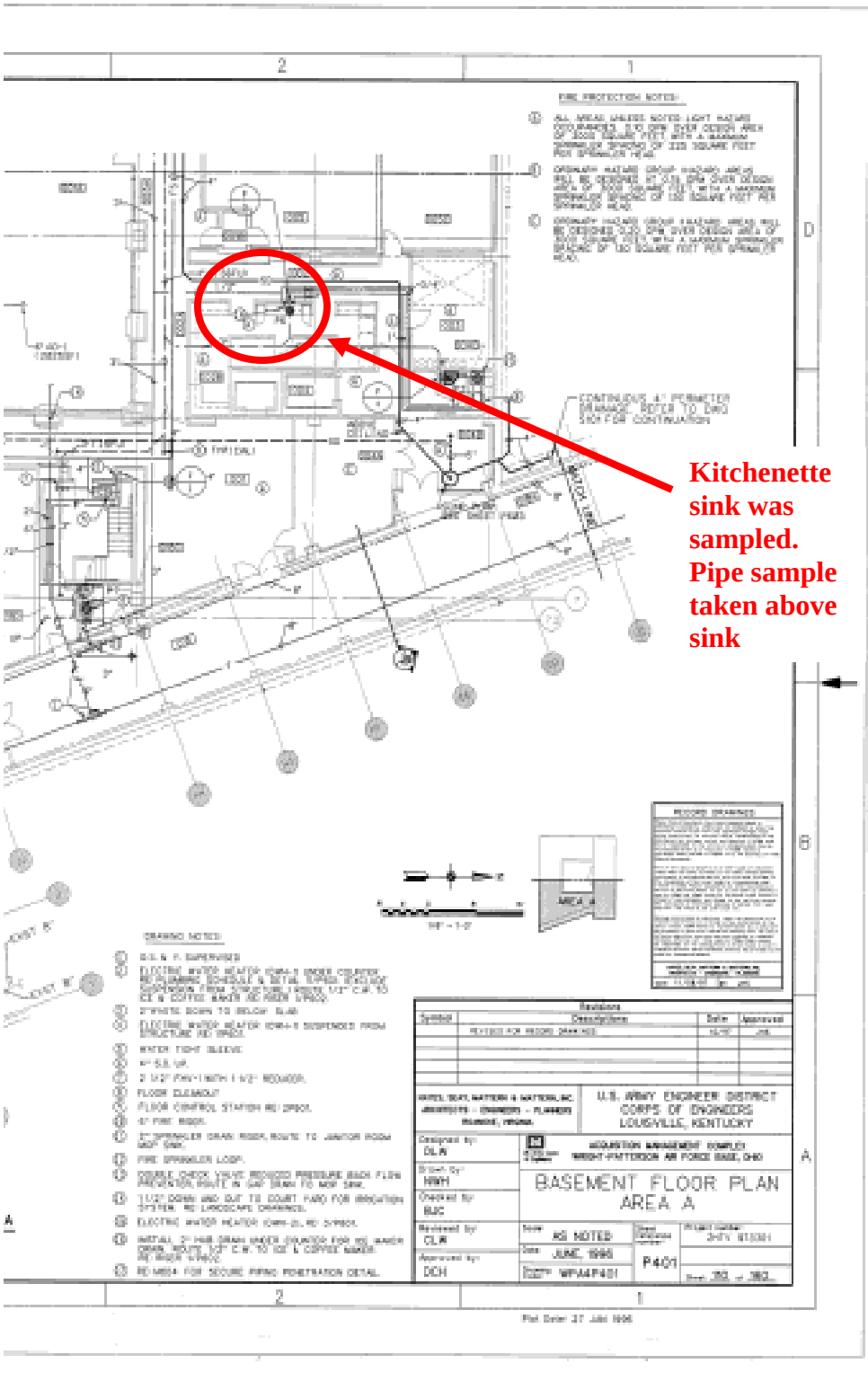
Kitchenette sink was sampled. Pipe sample taken above sink
BASEMENT FLOOR PLAN AREA A
U.S. ARMY ENGINEER DISTRICT CORPS OF ENGINEERS LOUISVILLE, KENTUCKY
P401

Building Information Sheet – 620 PII

Building Number: 20620, Phase II

Real Property Date: Constructed in 1966, Added onto in 1994

Building Manager: Amy Haddock and Ken Sizer, AFRL/SNOD

Interviewed on: 12 December 2005

Relevant Construction or Renovation Project Drawings:

From the construction of the Phase II addition to the building:

Building Number	Project	Sheet	Title
620	923304	A-103	First Floor Plan
		P-102	First Floor Plan - Supply and DWV
		P-401	Enlarged Floor Plans

Location of Sampling (room number): A janitor sink in the basement was selected for sampling because the pipes leading to the sink were exposed and accessible. No bathrooms offered accessible pipes in this building. The janitors sink was being used daily by an elevator repair crew at the time of sampling, but it is not clear what usage this sink gets otherwise. No drawings were found showing this sink.

Date of pipe sampled: 1994 According to what reference:

Is there a water softener or an ion-exchange system in the building: No

Photos taken:

Building Information Sheet – 441 B

Building Number: 20441

Real Property Date: Constructed in 1957. Plumbing renovations completed in 1993

Building Manager: Glenda Tool, AFRL/HEOC, Mary McClellan, AFRL/HEOC

Interviewed on: 1 November 2005

Relevant Construction or Renovation Project Drawings:

Renovation of the basement plumbing of the building:

Building	Project	Sheet	Title
20441	880059	P-1 P-2	Replace Cold Water Piping Replace Cold Water Piping

Location of Sampling (room number): Basement mechanical room 0-24. A janitors sink in the basement mechanical room was sampled because the piping leading to it is exposed. There are doubts this sink is used very often. This sink also leaked overnight (see picture below).

Date of pipe sampled: 1993 According to what reference: Project 990059

Is there a water softener or an ion-exchange system in the building: No

Photos taken:

Faucet leaked overnight and filled the bag.

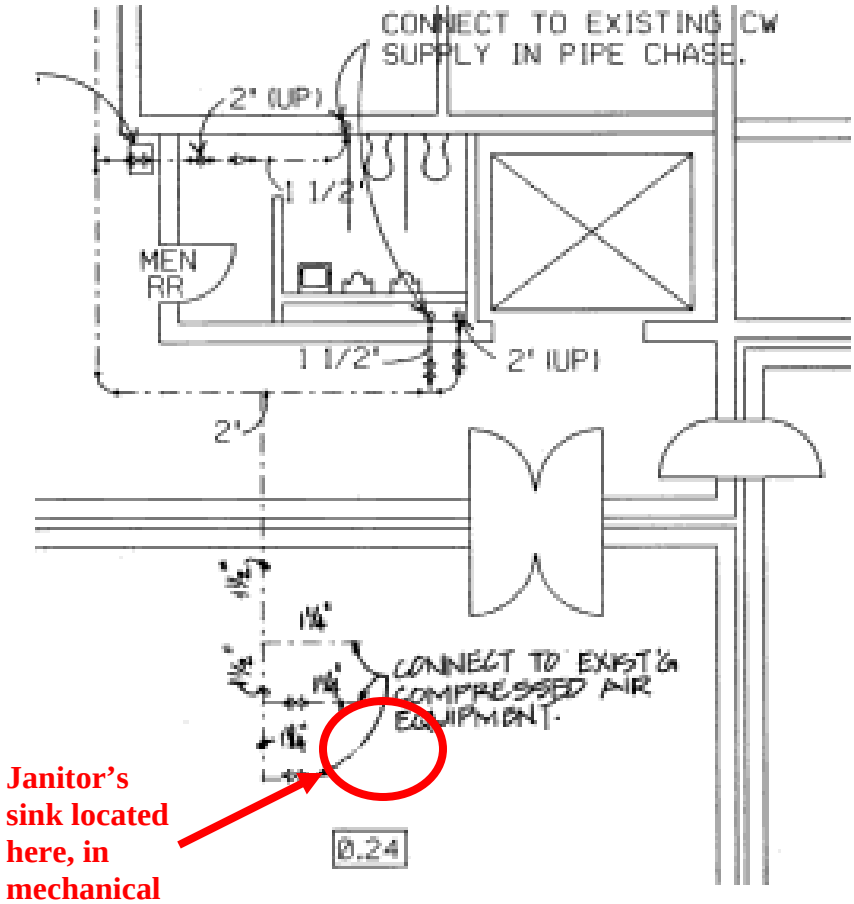

Janitor's sink located here, in mechanical room

Building Information Sheet – 620 PI B

Building Number: 20620, Phase I

Real Property Date: Constructed in 1966, Added onto in 1992

Building Manager: Amy Haddock and Ken Sizer, AFRL/SNOD

Interviewed on: 12 December 2005

Relevant Construction or Renovation Project Drawings:

From the construction of the Phase I addition to the building:

Building Number	Project	Sheet	Title
20620	913302	P-2	First Floor Plumbing Plan
		A-2	First Floor Plan

Location of Sampling (room number): Originally a sampling location in a first floor men's room (room 15) was chosen for sampling. A sink in this bathroom was sampled. However the plumber determined that cutting pipe through the bathroom access panel was impossible. Next a janitors sink in the basement was selected for sampling because the pipes leading to the sink were exposed and accessible. It is not clear what usage this sink gets regularly. No drawings were found showing this sink.

Date of pipe sampled: 1992 According to what reference:

Is there a water softener or an ion-exchange system in the building: No

Photos taken:

Building Information Sheet - 642

Building Number: 20642

Real Property Date: 1989

Building Manager: Capt Michael Wethington and Mr. Harry Peterman

Interviewed on: 10, 17 November 2005

Relevant Construction or Renovation Project Drawings:

From the original construction of the building:

Building Number	Project	Sheet	Title
20642	863276	A-3	First floor plan - Seg. 2
		A-54	Toilet Room Plan and Elevations
		P-5	First floor plan - Seg. 2 Plumbing
		P-11	Flow Diagram, Domestic Water & Fire Protection

Location of Sampling (room number):

Date of pipe sampled: 1989 According to what reference: Project 863276

Is there a water softener or an ion-exchange system in the building: No

Photos taken:

AAFES kitchen sink. Sample taken from under the sink

Location of sampling under the sink. Seen after sampling with the new pipe and compression fittings in place.

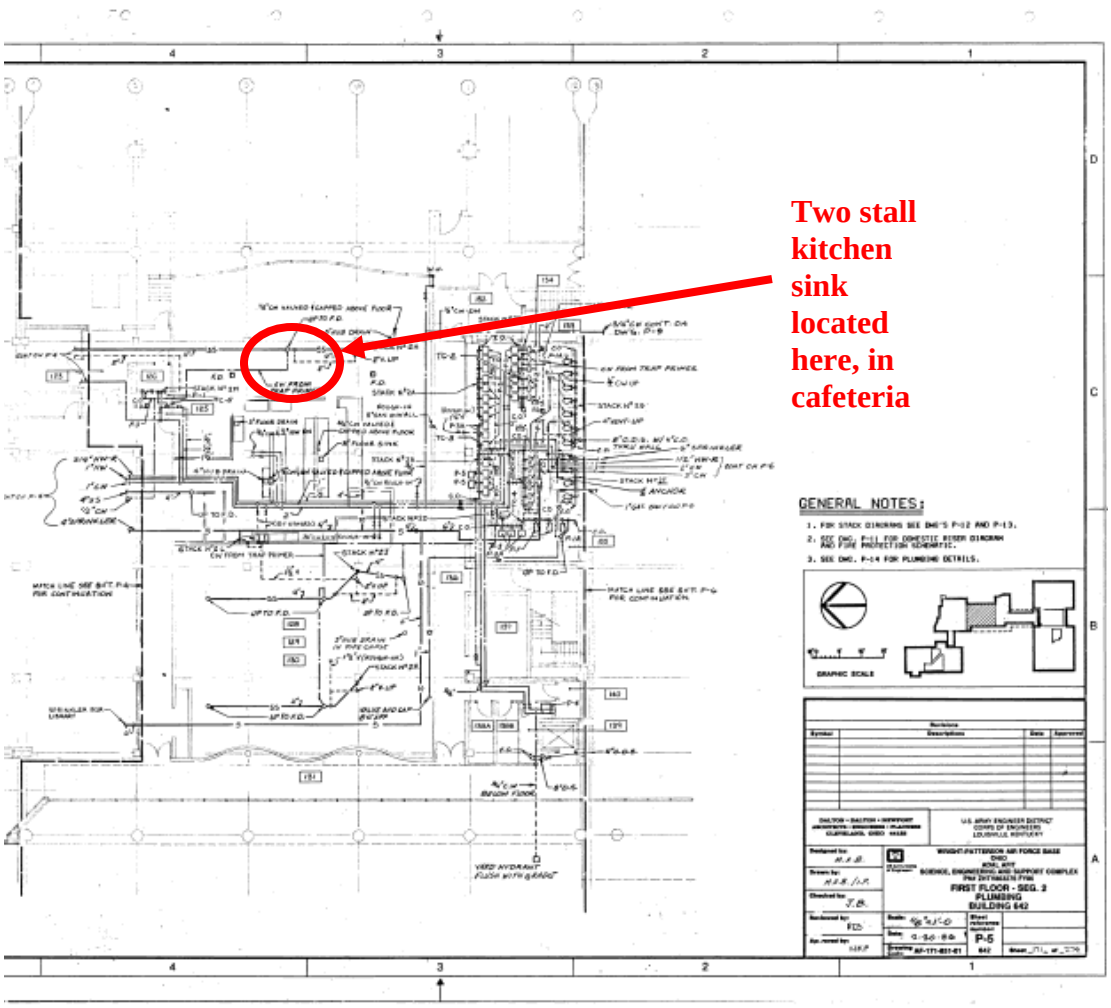
Two stall kitchen sink located here, in cafeteria
GENERAL NOTES:
1. FOR STACK DIAGRAMS SEE DWG'S P-12 AND P-13.
2. SEE DWG. P-11 FOR DOMESTIC RISER DIAGRAM AND FIRE PROTECTION SCHEMATIC.
3. SEE DWG. P-14 FOR PLUMBING DETAILS.
GRAPHIC SCALE
WRIGHT-PATTERSON AIR FORCE BASE
OHIO
FIRST FLOOR - SEG. 3
PLUMBING
BUILDING 642
P-5

Building Information Sheet - 676

Building Number: 20676

Real Property Date: 1985

Building Manager: Mr. David Sweet, 88 CG/SCX

Interviewed on: 13 January 2006

Relevant Construction or Renovation Project Drawings:

From the addition to the building:

Building Number	Project	Sheet	Title
20676	AF-610-711-0	P-1	Plumbing First Floor Plan
		P-3	Plumbing Schematics and Schedule

Location of Sampling (room number): A sink in the men's restroom was sampled and the cold water pipe leading into the men's restroom was sampled above the ceiling in the janitors closet adjacent to the men's room.

Date of pipe sampled: 1985 According to what reference: Project AF-610-711-0

Is there a water softener or an ion-exchange system in the building: No

Photos taken:

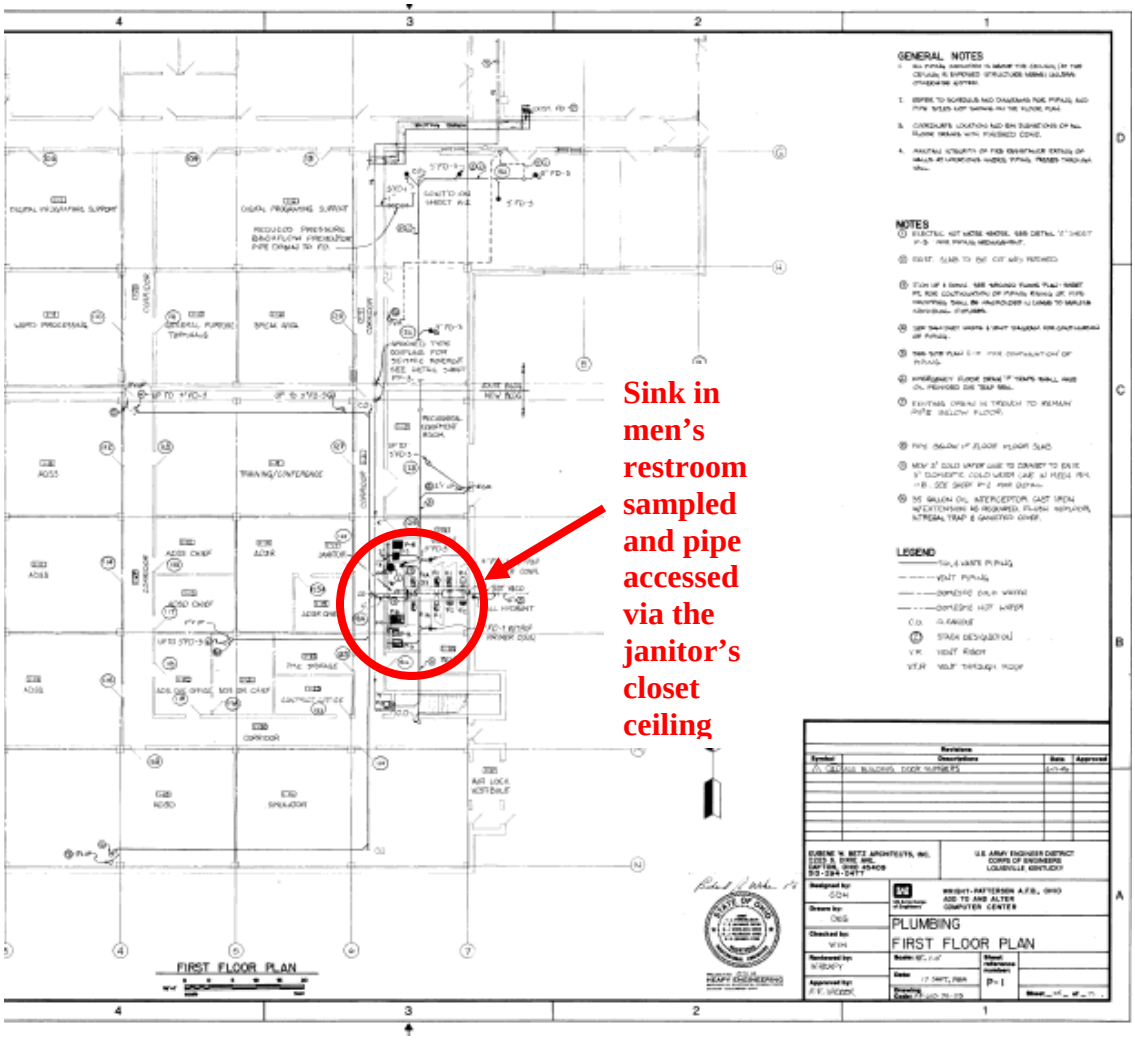
Sink in men's restroom sampled and pipe accessed via the janitor's closet ceiling
GENERAL NOTES
NOTES
LEGEND
FIRST FLOOR PLAN
PLUMBING
FIRST FLOOR PLAN

Building Information Sheet – 11A

Building Number: 20011A

Real Property Date: Constructed in 1930

Building Manager: Mario Gutierrez, AFMCLO/JAB

Interviewed on: 13 January 2006

Relevant Construction or Renovation Project Drawings:

Installation of a sink in building 11A:

Building Number	Project	Sheet	Title
20011	84wa3395	1	mechanical

Location of Sampling (room number): The sink shown in the drawing above was installed in 1984 and used daily in a shop until 2004. For the last year it has not been used since the room it is in has been used as a storage area by the JAG.

Date of pipe sampled: 1984 According to what reference: Project 84wa3395

Is there a water softener or an ion-exchange system in the building: No

Photos taken:

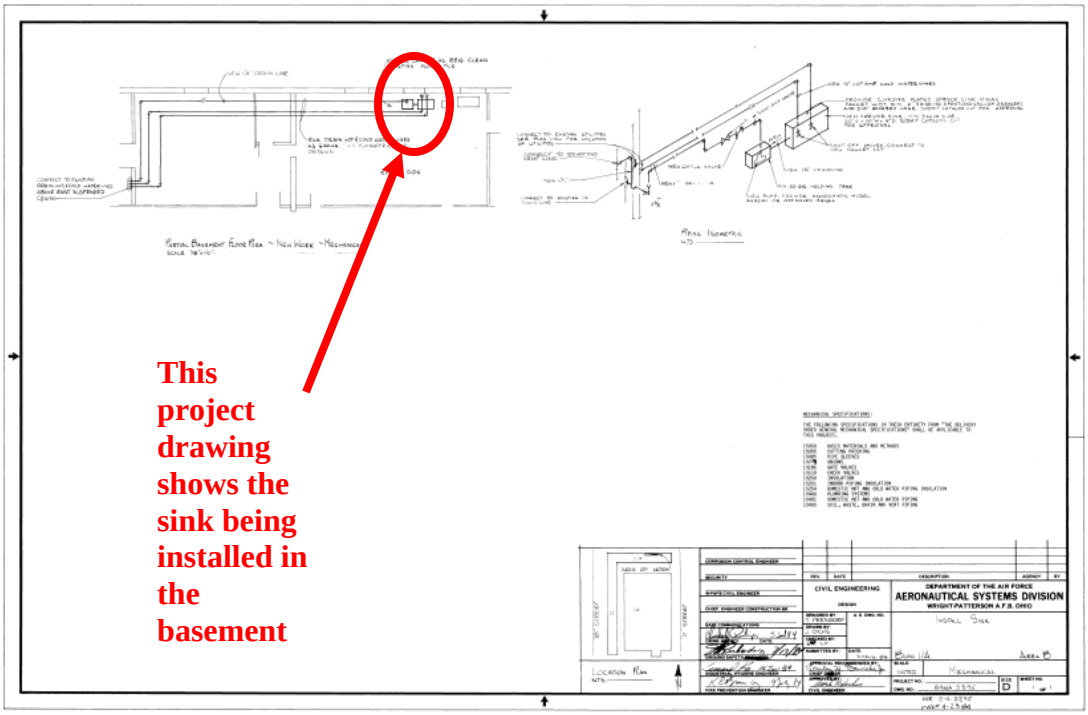
This project drawing shows the sink being installed in the basement
CIVIL ENGINEERING
DEPARTMENT OF THE AIR FORCE
AERONAUTICAL SYSTEMS DIVISION
WRIGHT-PATTERSON A.F.B. OHIO
INSTALL SINK
MECHANICAL

Building Information Sheet - 641

Building Number: 20641

Real Property Date: 1977

Building Manager: Capt Michael Wethington and Mr. Harry Peterman

Interviewed on: 10, 17 November 2005

Relevant Construction or Renovation Project Drawings:

From the original construction of the building:

Building Number	Project	Sheet	Title
20641	AW-29-01-05	A-1	First Floor Plan
		SK-1	Bathroom Layout
		P-2	Water Piping Plan
		P-4	Second Floor Plumbing Plan

Location of Sampling (room number): The sink sampled was in the 2nd floor women's restroom in the south east corner of the building. The pipe sampled leads directly to the sink sampled. The pipe an vertically down the wall in the janitor's closet in women's restroom.

Date of pipe sampled: 1977 According to what reference: Project AW-29-01-05

Is there a water softener or an ion-exchange system in the building: No

Photos taken:

Pipe sample taken from the cold water domestic line coming down the wall in the janitor's closet and feeding the sinks on the other side of the wall.

Sink sampled for building 641, and for the sequential sampling.

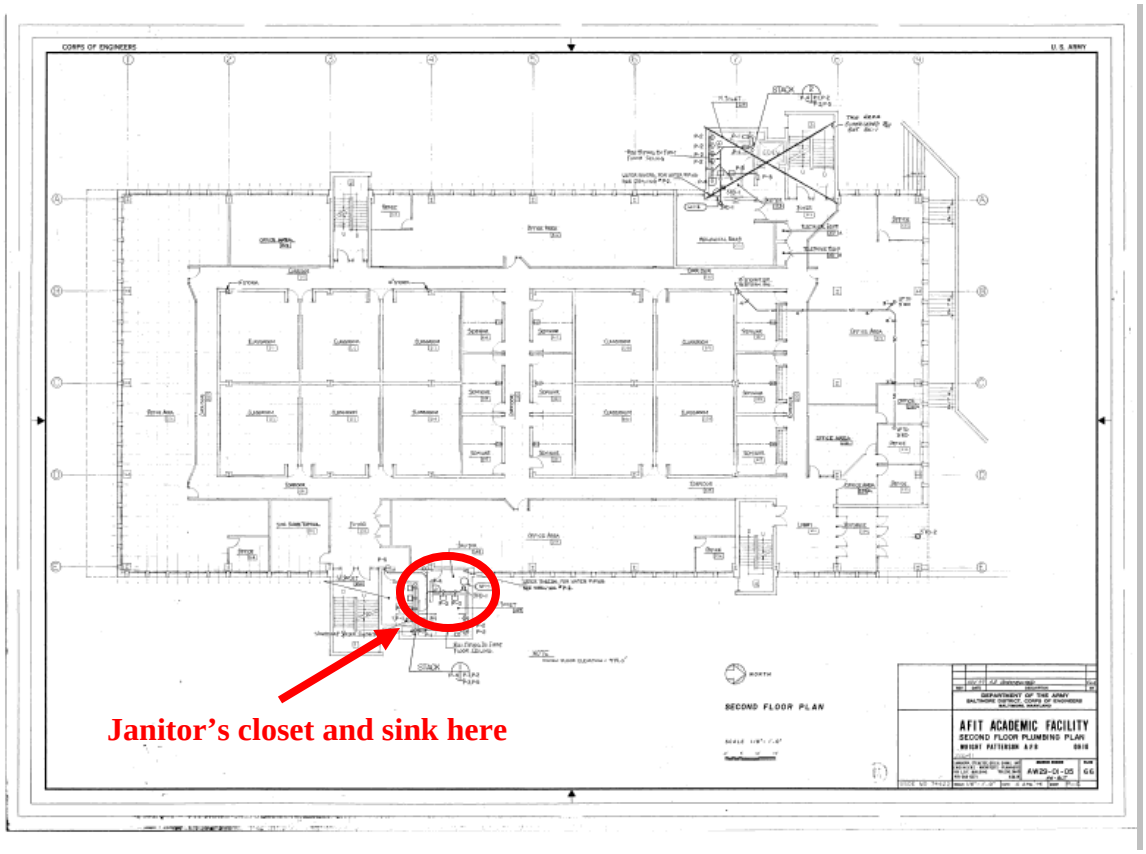

Building Information Sheet - 653

Building Number: 20653

Real Property Date: 1975

Building Manager: Jesse Genetin, AFRL/MLOF

Interviewed on: 11 January 2006

Relevant Construction or Renovation Project Drawings:

From the original construction of the building:

Building Number	Project	Sheet	Title
20653	AW-35-65-01	148	Plumbing - Administration Wing
		149	Plumbing - Administration Wing
		150	First Floor Plan - East Admin. Plumb

Location of Sampling (room number): The sink sampled and the CMU wall that it is on are not on the original plans for the building. It is in the south west corner of the basement in the fabrication shop. A gentleman working in the shop has been with the building since it was built since 1975. The gentleman stated that although the wall and sink are not on the drawings they were built with the original building at the request of the shop chief at the time. The CMU wall and the pipes to the sink looked original to the building. There was no evidence that the wall was a retrofit, and the insulation around the pipes and the valve leading to it were identical to the other building plumbing that did appear on the drawings.

Date of pipe sampled: 1975 According to what reference: Building manager and a coworker who has worked in the building since its construction

Is there a water softener or an ion-exchange system in the building: No

Photos taken:

We cut a section of the cold water domestic pipe leading to the utility sink in the fabrication ship in the SW corner of basement.

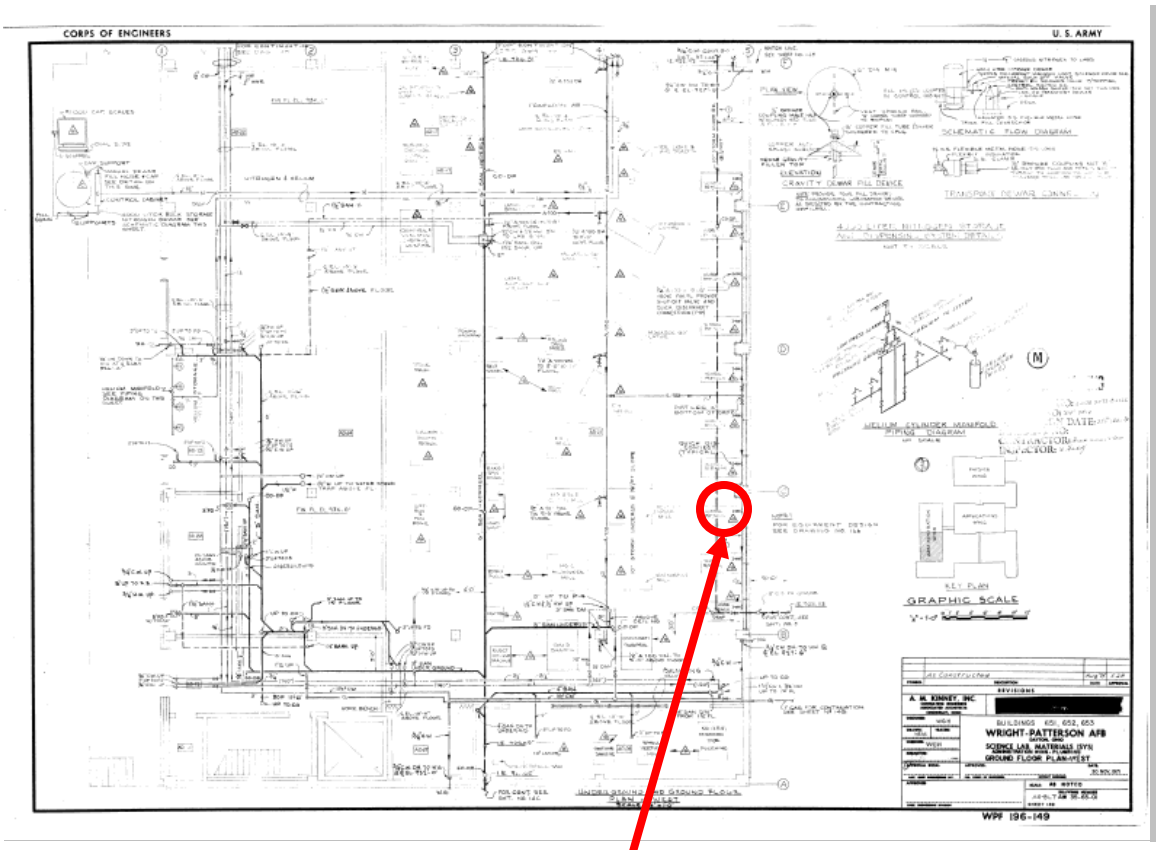

Shop sink located approximately here. Pipe sample taken from pipe on wall leading to sink

Building Information Sheet - 464

Building Number: 20464, AAFES gas station

Real Property Date: Occupied in 1962 per real property manager

Building Manager: AAFES store clerks on duty

Interviewed on: 12 January 2006

Relevant Construction or Renovation Project Drawings:

From the original construction of the building:

Building Number	Project	Sheet	Title
20464	None	4	Foundation Plan and Details
		3	Floor Plan - Details - Schedule

Location of Sampling (room number): No renovations have been done to the water suppy pipes since construction of this facility. I sampled the only sink in the only restroom in the building. We took the pipe sample from the cold water line as it comes into the building, before it branches off to the bathroom and water heater.

Date of pipe sampled: 1970? Or 58? According to what reference:

Is there a water softener or an ion-exchange system in the building: No

Photos taken:

Cutting the sample from the cold water line leading into the water heater.

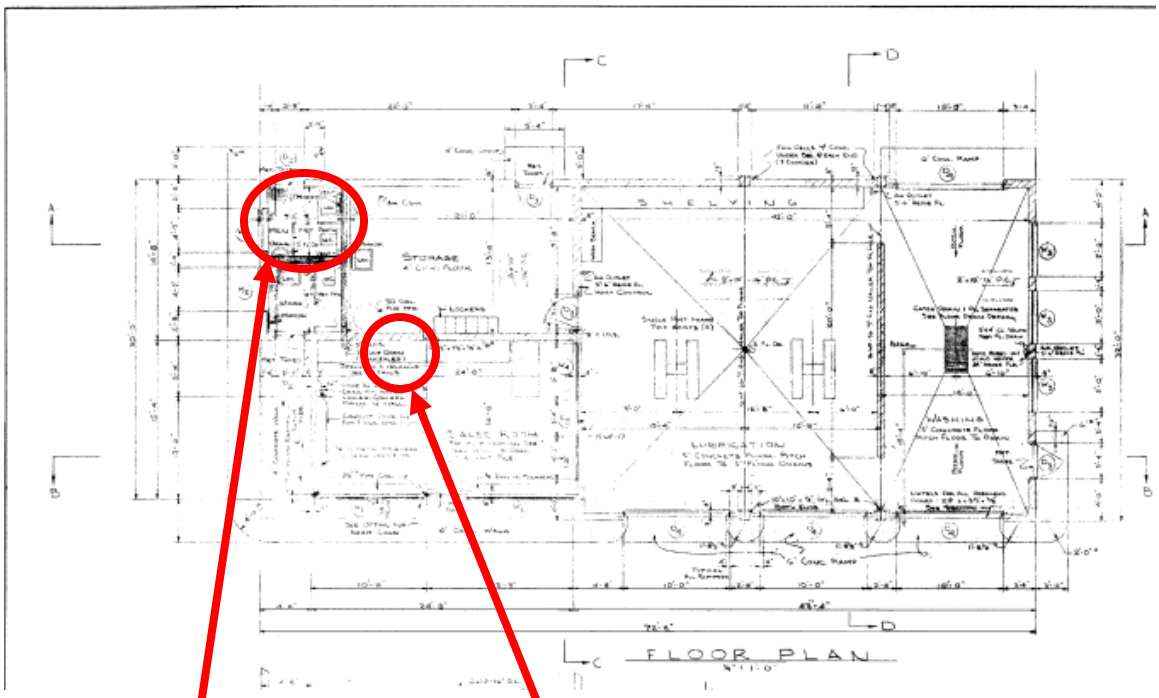

Bathroom sampled

Location of water pipes

Appendix B

Water Characterization

Building	Plumbing Date	Water Characterization Data in Each Building, Before Stagnation (mg/L) pH	Ca	Cl	Cu	Fe	NH3 as N	NO3 as N	P
441S	**2005**	7.3	87.42	68.77	0.26	0.01	0.00	1.69	0.10
837	**2004**	7.4	83.31	60.54	0.69	0.00	0.00	1.78	0.11
571	**2002**	7.3	86.47	61.54	**2.38**	0.01	0.04	1.72	0.09
553	**2001**	**7.6**	86.14		0.16	0.03			0.00
645	**1998**	7.3	86.08	58.93	0.90	0.00	0.00	1.97	0.09
306	**1997**	7.3	84.24	61.00	**1.37**	**0.64**	0.00	1.71	0.11
556	**1995**	7.4	84.12	52.12	0.32	0.01	0.00	1.79	0.12
620 PII	**1994**	7.3	87.73	68.35	0.23	0.02	0.00	1.69	0.08
441B	**1993**	7.5	87.11	60.89	0.49	**3.82**	0.04	**5.09**	0.18
620 PI	**1992**	7.3	86.95	60.16	0.48	0.01	0.00	1.67	0.00
620 PI B	**1992**	7.3	86.18	68.60	0.50	0.03	0.00	1.47	0.07
642	**1989**	7.3	86.26	59.61	0.11	0.00	0.00	1.80	0.08
676	**1985**	7.2	82.66	56.76	0.42	0.01	0.00	1.79	**0.31**
11A	**1984**	7.3	81.73	56.06	0.29	0.02	0.00	1.77	**0.59**
641	**1977**	7.3	88.11	68.83	0.15	0.00	0.03	1.75	0.09
641 (add. smp)	**1977**		82.81	61.04	0.11	0.01	0.00	1.86	0.61
653	**1975**	7.3	82.27	55.81	0.14	0.00	0.00	1.71	0.10
464	**1962**	7.3	82.87	55.34	0.18	0.02	0.00	1.64	0.14
	Average	7.3	85.1	60.8	0.5	0.3	0.0	1.9	0.2
	Std. dev	0.09	2.11	5.13	0.57	0.90	0.01	0.82	0.17

Building	Plumbing Date	Water Characterization Data, Before Stagnation (mg/L) PO4	S	Si	SiO2	SO4	Zn	Total Alkalinity mg/L as $CaCO_3$	DIC mg/L as C
441S	**2005**	0.14	15.93	5.40	11.56	47.78	0.0194	295.04	80.06
837	**2004**	0.17	16.60	5.18	11.10	49.80	0.0166	288.99	76.53
571	**2002**	0.08	15.51	5.08	10.90	46.52	0.0346	289.53	78.56
553	**2001**	0.19	15.07	4.91	10.52	45.20	**0.2697**	283.46	72.41
645	**1998**	0.15	15.94	5.18	11.11	47.82	0.0116	285.12	77.37
306	**1997**	0.11	16.59	5.15	11.03	49.77	**0.1163**	289.71	78.62
556	**1995**	0.18	16.58	5.13	11.00	49.75	**0.1254**	279.16	73.92
620 PII	**1994**	0.16	16.71	5.34	11.44	50.12	0.0256	294.23	79.84
441B	**1993**	0.27	15.53	5.37	11.51	46.59	**0.6771**	285.55	74.14
620 PI	**1992**	0.16	16.75	5.33	11.41	50.25	**0.2352**	290.63	78.87
620 PI B	**1992**	0.13	16.12	5.25	11.26	48.37	**0.5921**	293.89	79.75
642	**1989**	0.14	15.90	5.18	11.11	47.69	0.0130	284.35	77.18
676	**1985**	**0.63**	16.36	5.06	10.84	49.07	0.0143	269.07	75.23
11A	**1984**	**1.17**	16.36	5.07	10.86	49.09	0.0612	269.40	73.11
641	**1977**	0.16	16.17	5.33	11.42	48.50	0.0132	291.59	79.13
641 (add. smp)	**1977**	1.29	16.52	5.05	10.81	49.55	0.0059	267.02	72.46
653	**1975**	0.23	16.38	5.08	10.88	49.14	0.0192	271.02	73.54
464	**1962**	0.25	16.40	5.19	11.12	49.21	**0.2892**	272.05	73.82
	Average	0.3	16.2	5.2	11.1	48.6	0.1	283.3	76.4
	Std. dev	0.35	0.47	0.13	0.28	1.40	0.20	9.61	2.77

Appendix C

Selected Solubility Constants for Cupric Hydroxide Model

Values not listed in this table are reported in the original publication (Schock et al., 1995)

Species	log K value	Reaction	Reference
$CuOH^+$	-7.96	$Cu^{2+} + H_2O \rightarrow CuOH^+ + H^+$	[1]*
$Cu(OH)_2$	-14.1	$Cu^{2+} + 2H_2O \rightarrow Cu(OH)_2^o + 2H^+$	best fit
$Cu(OH)_3^-$	-26.9	$Cu^{2+} + 3H_2O \rightarrow Cu(OH)_3^- + 3H^+$	[2]*
$Cu(OH)_4^{2-}$	-39.56	$Cu^{2+} + 4H_2O \rightarrow Cu(OH)_4^{2-} + 4H^+$	[3]*
$Cu_2(OH)_2^{2+}$	-10.58	$2Cu^{2+} + 2H_2O \rightarrow Cu_2(OH)_2^{2+} + 2H^+$	[3]*
$Cu_3(OH)_4^{2+}$	-20.76	$3Cu^{2+} + 4H_2O \rightarrow Cu_3(OH)_4^{2+} + 4H^+$	[3]*
$CuCO_3$	6.73	$Cu^{2+} + CO_3^{2-} \rightarrow CuCO_3^o$	[4]
$Cu(CO_3)_2^{2-}$	10.6	$Cu^{2+} + 2CO_3^{2-} \rightarrow Cu(CO_3)_2^{2-}$	[5]
$CuHCO_3^+$	12.13	$Cu^{2+} + H^+ + CO_3^{2-} \rightarrow CuHCO_3^+$	[5]
$Cu(OH)CO_3^-$	-4.25	$Cu^{2+} + CO_3^{2-} + H_2O \rightarrow Cu(OH)CO_3^- + H^+$	[6]
$Cu(OH)_2CO_3^{2-}$	-13.14	$Cu^{2+} + CO_3^{2-} + 2H_2O \rightarrow Cu(OH)_2CO_3^{2-} + 2H^+$	[7]*

*Model values were computed from referenced ΔG_f° by Schock et al.

References

[1] Computed from log β values given in: Paulson, A.J. and D.R. Kester, Copper(II) Ion Hydrolysis in Aqueous Solution. J. Solution Chem., 1980. 9(4): p. 269-277

[2] Computed from log β values given in: Vuceta, J. and J.J. Morgan, Hydrolysis of Cu(II). Limnol. & Oceanog., 1977.22:p.742-746

[3] Computed from log β values given in: Martell, A.E. and R.M. Smith, Critical Stability Constants. Vol. 5: First Supplement.1980, New York, New York: Plenum Press.

[4] Schindler, P., M. Reinert, and H. Gansjäger, *Löslichkeitskonstanten und Freie Bildungsenthalpien von $Cu_2(OH)CO_3$ (Malachit) und $Cu_3(OH)_2(CO_3)_2$ (Azurit) bei 25·C.* Helvetica Chim. Acta, 1968. 51(2): p. 1845-1856.

[5] Byrne, R.H. and W.L. Miller, *Copper(II) Carbonate Complexation in Seawater.* Geochim. Cosmochim. Acta, 1985.49: p.1837-1844.

[6] Symes, J.L. and D.R. Kester, *Thermodynamic Stability Studies of the Basic Copper Carbonate Mineral, Malachite.* Geochim. Cosmochim. Acta, 1984. 48: p. 2219-2229.

[7] Either the only value tabulated, or the average of values tabulated in: Woods, T.L. and R.M. Garrels, Thermodynamic Values at Low Temperature for Natural Inorganic Materials: An Uncritical Summary. 1987, New York, New York: Oxford University Press.

Appendix D

Sampling Protocol

The following sampling steps were taken at each chosen sampling location:

End of day prior to sampling (approximately 1600):

1. Flush faucet to be sampled for 1 minute.
2. Fill 60mL sample bottle with water (for ICP analysis).
3. Cap bottle minimizing the air in the sample
4. Fill 250mL sample bottle with water (for wet chemistry)
5. Cap bottle minimizing the air in the sample
6. Use test kit to determine pH of faucet water
7. Use test kit to determine free and total available Chlorine of faucet water (free and total Chlorine were consistently equal, so only free was read in later sampling)
8. Record pH and Cl readings in field notebook
9. Record bottle numbers/data in field notebook
10. Wrap plastic bag around faucet and tape bag in place
11. Hang "Temporarily out of Order" sign on faucet

Day of sampling (approximately 0800):

1. Return to faucet exactly 16 hours after sampling the night before
2. Check tape and plastic bag for tampering. Record any discrepancies.
3. Remove bag, sign, and tape
4. Take first draw 250mL sample from faucet
5. Cap bottle minimizing the air in the sample
6. Take second draw 250mL sample from faucet
7. Cap bottle minimizing the air in the sample
8. Pour off a small amount of first draw sample for pH and Cl testing. Use field test kit to take pH and free and total available Chlorine readings (free and total chlorine were consistently equal, so only free was read in later sampling)
9. Record pH and Cl readings in field notebook
10. Record bottle numbers/data in field notebook

Day of sampling continued:

Back at the AFIT labs acidify the all samples *except the wet chemistry sample* using nitric acid to bring the pH to <2.

1. Add 0.15% nitric acid to each sample by adding 0.09 mL of nitric acid to 60mL sample and 0.375mL of nitric acid to 250mL sample
2. Add cap to bottles and mix by inverting bottles 10 times
3. Pour small amount of sample from bottles into individual, clean beakers
4. Take pH readings with calibrated (per instructions) automatic pH meter.

5. If pH is <2 stop. (After first several samples had <2 pH testing each sample was stopped. 0.15% nitric acid was sufficient to achieve <2 pH).

Store acidified samples at room temperature for at least 16 hours before analytical testing

Pipe sample collection:

1. Use shut off valve to cut off water to pipe section, drain water, and cut approximately 3" to 12" pipe segment.
2. Handle pipe segment with gloves, dry any water on pipe exterior, and sealed it in a plastic Ziploc bag
3. Take digital pictures to record pipe sampling and sampling location
4. Record and note sampling location on building plumbing drawing(s)
5. Record whether pipe was vertical or horizontal in the plumbing system

Appendix E

Diagram of Sequential Water Sampling Experiment

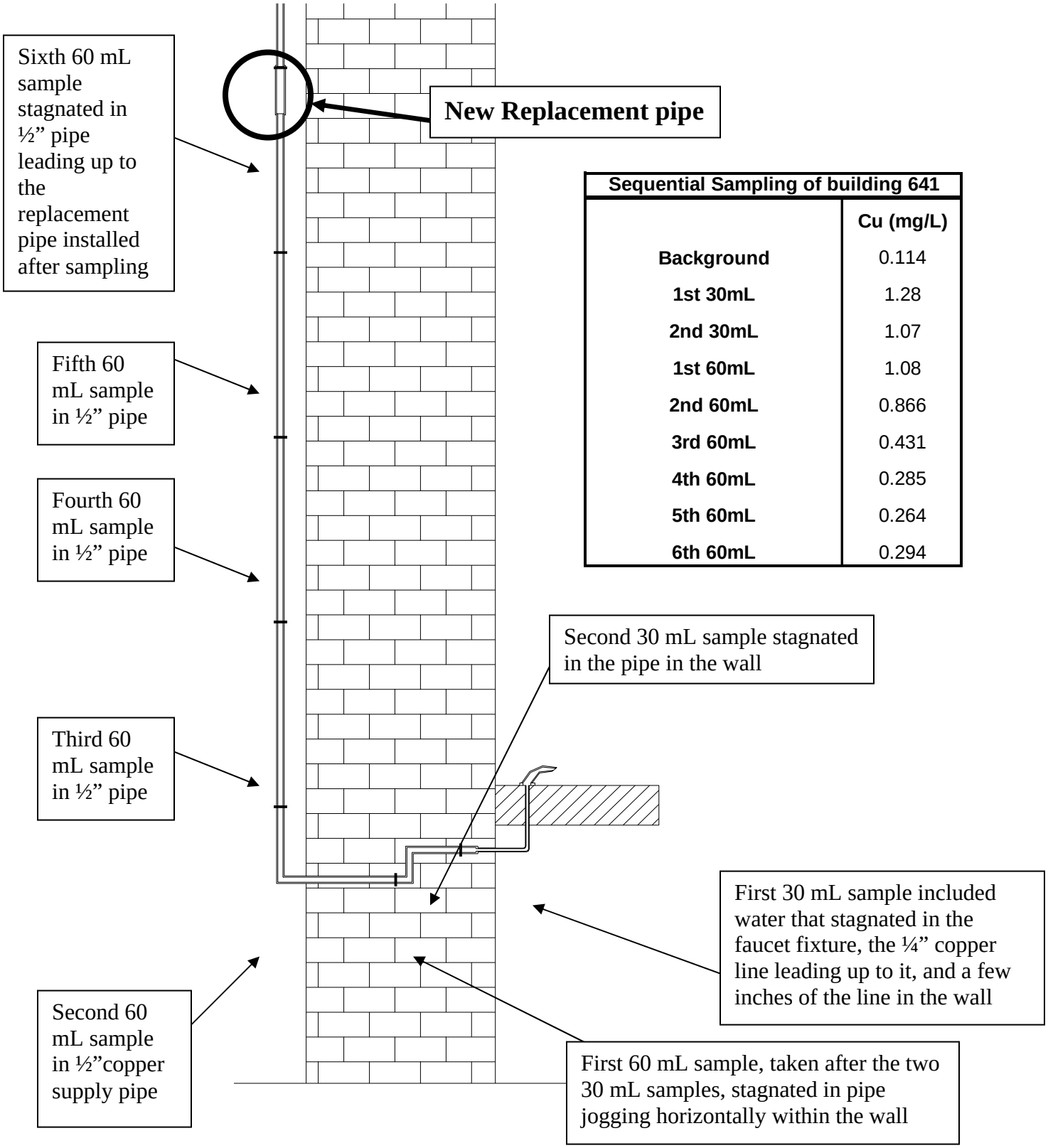

Sequential Sampling of building 641	
	Cu (mg/L)
Background	0.114
1st 30mL	1.28
2nd 30mL	1.07
1st 60mL	1.08
2nd 60mL	0.866
3rd 60mL	0.431
4th 60mL	0.285
5th 60mL	0.264
6th 60mL	0.294

Appendix F: Copper Pipe Timeline

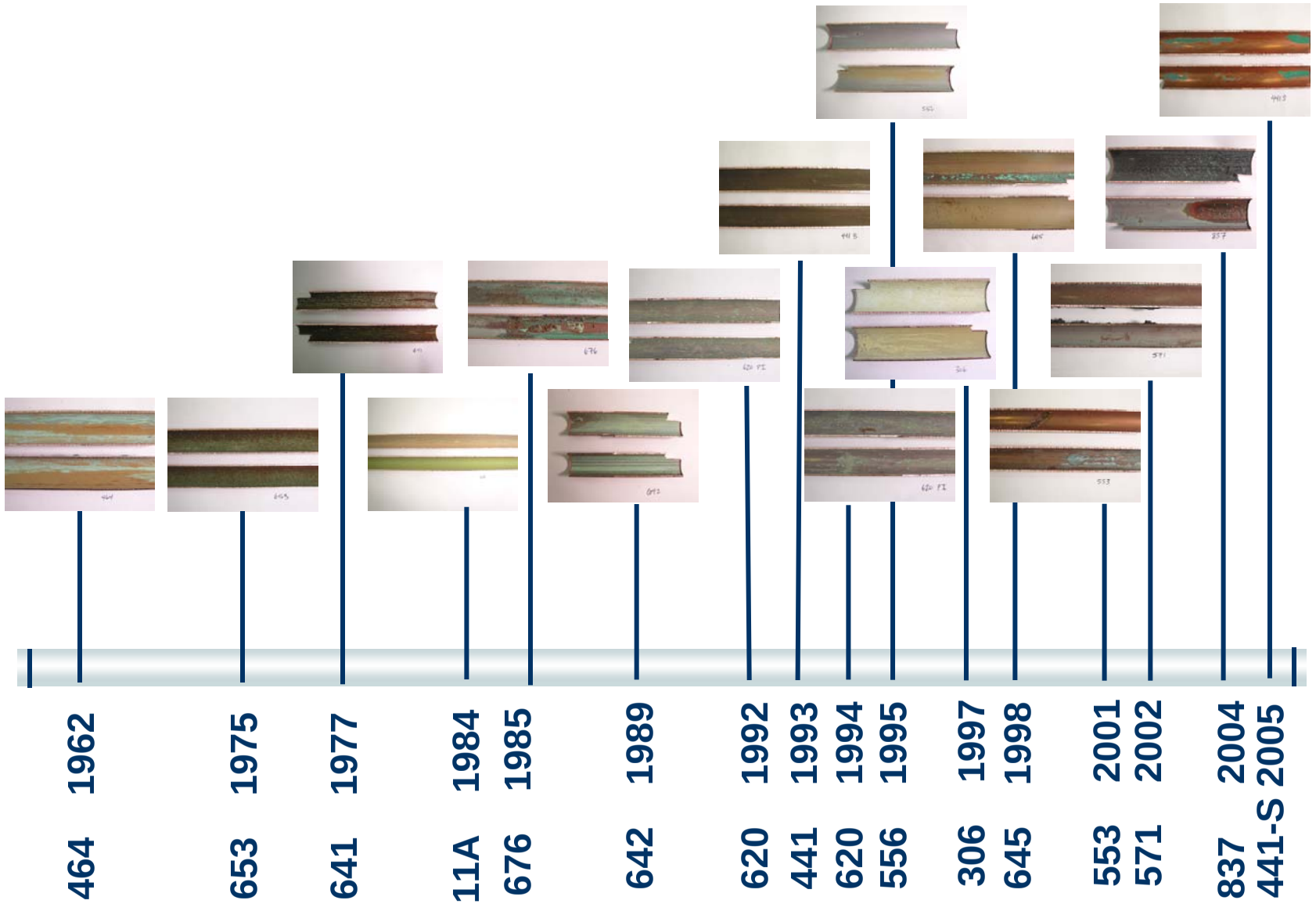

Appendix G

XRD Spectra and Photography of each Pipe Sample

The pipe samples are listed by age, from oldest to youngest.

Page

Building 464 (1962) Figures

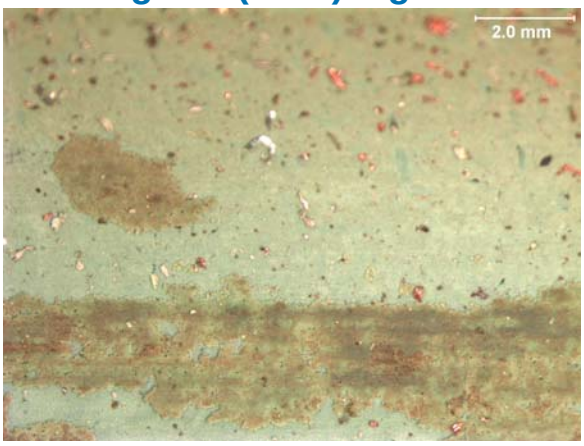

Figure G.1. Digital picture of the interior of copper recirculation pipe.

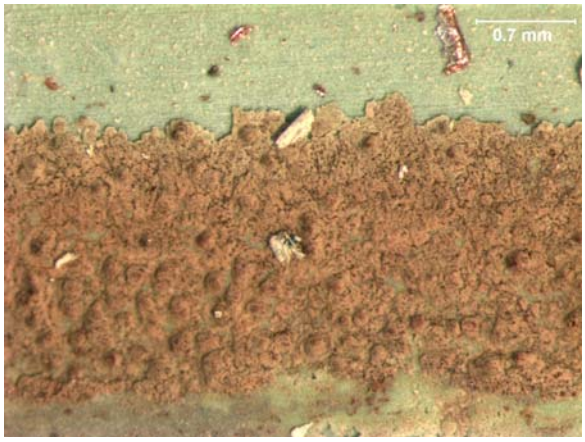

Figure G.2. Stereo-microscope picture of copper pipe wall.

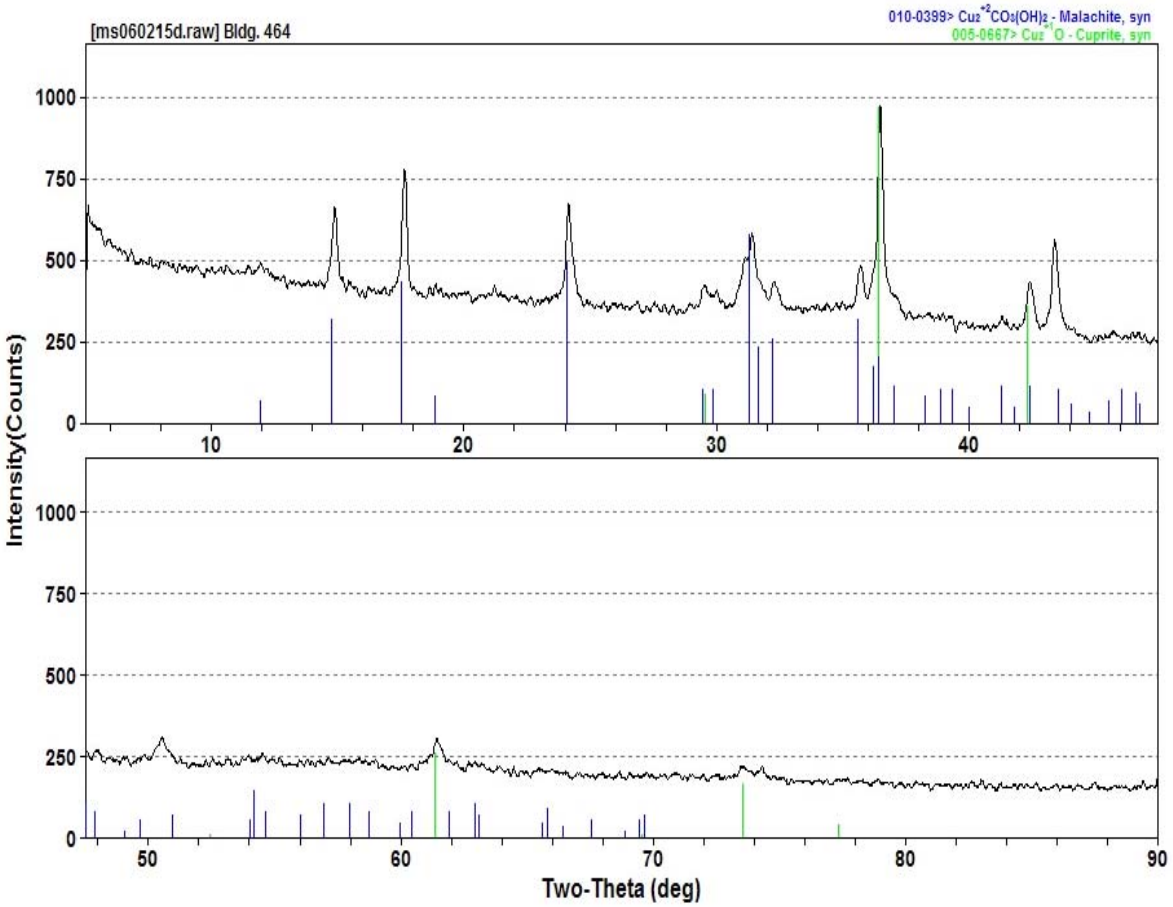

Figure G.3. Scrapings XRD scan.

Building 464 (1962) Figures

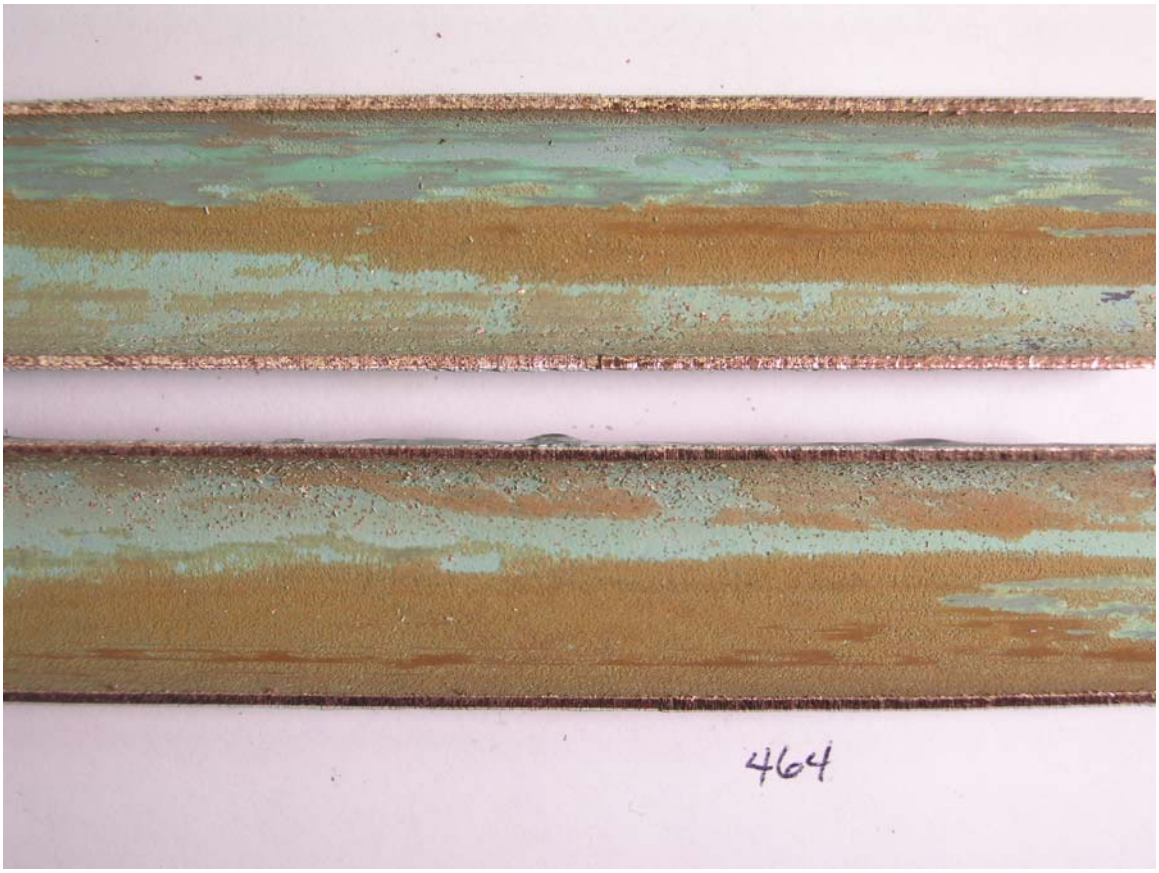

Figure G.4. Digital picture of the copper pipes.

Building 653 (1975) Figures

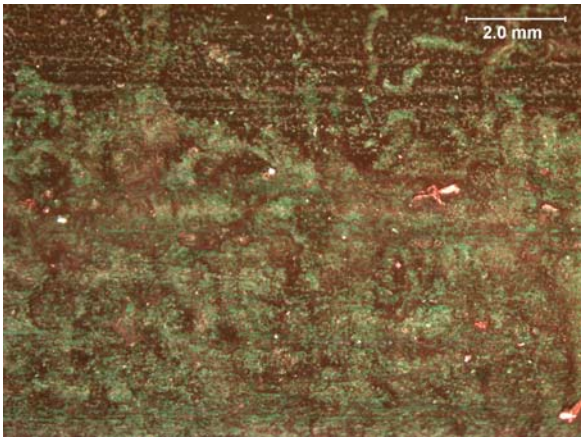

Figure G.5. Digital picture of the interior of copper recirculation pipe.

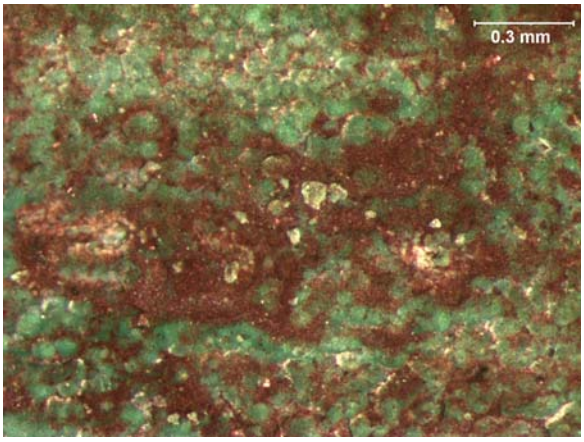

Figure G.6. Stereo-microscope picture of copper pipe wall.

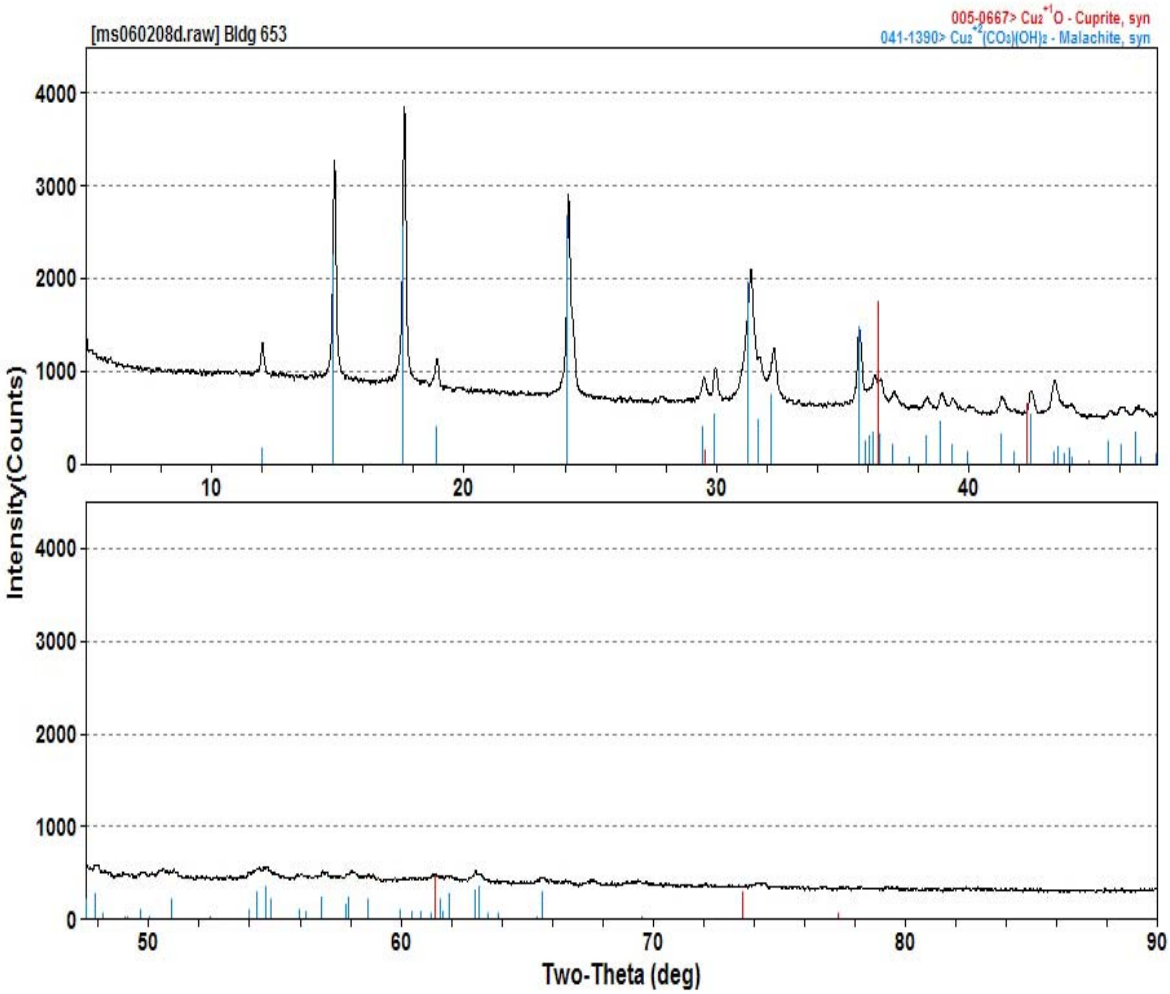

Figure G.7. Scrapings XRD scan.

Building 653 (1975) Figures

Figure G.8. Digital picture of the copper pipe.

Building 641-01 (1977) Figures

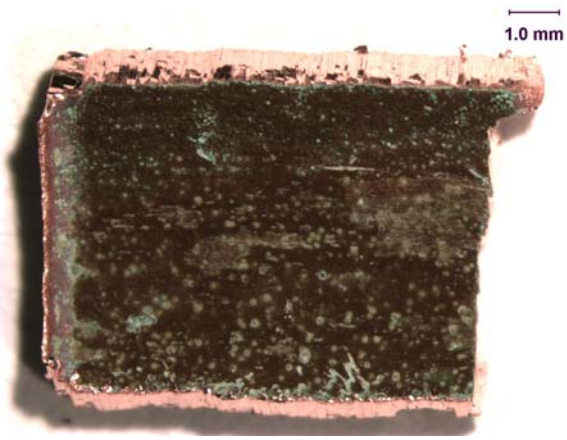

Figure G.9. Digital picture of the interior of copper recirculation pipe.

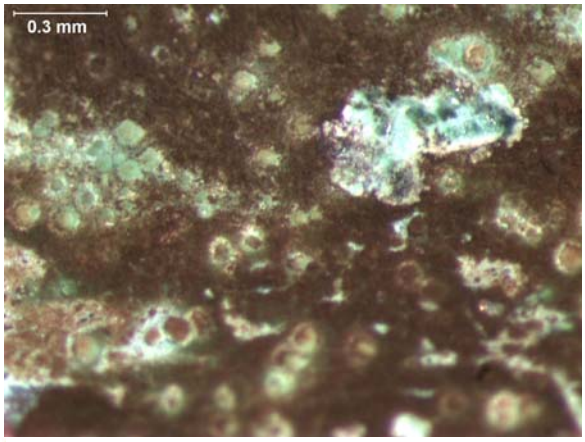

Figure G.10. Stereo-microscope picture of copper pipe wall.

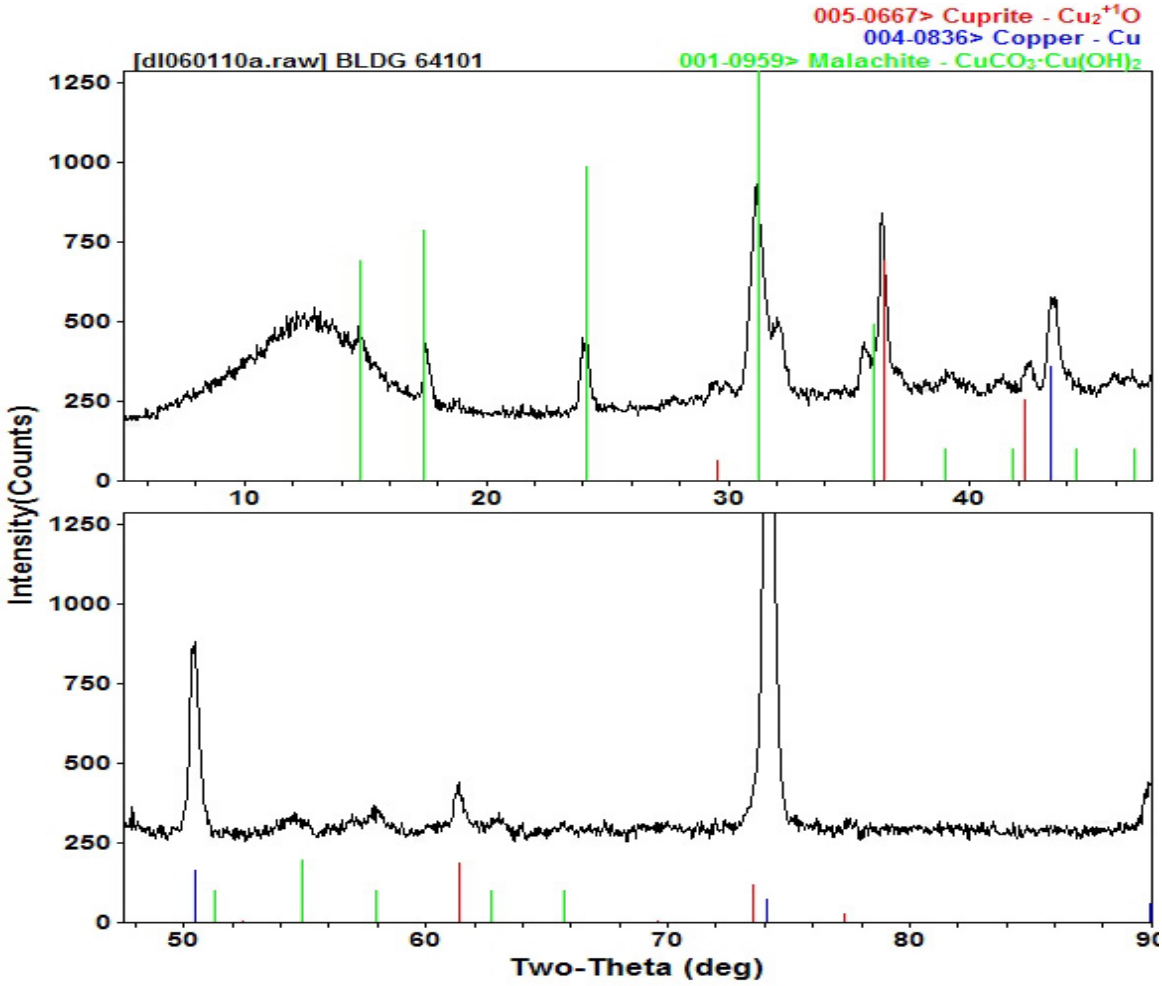

Figure G.11. Cutout XRD scan.

Building 641-02 (1977) Figures

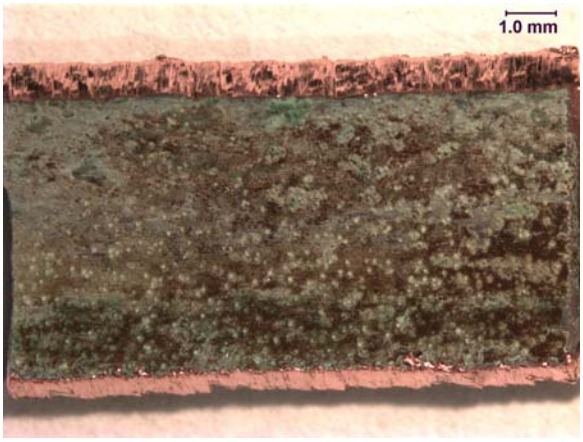

Figure G.12. Digital picture of the interior of copper recirculation pipe.

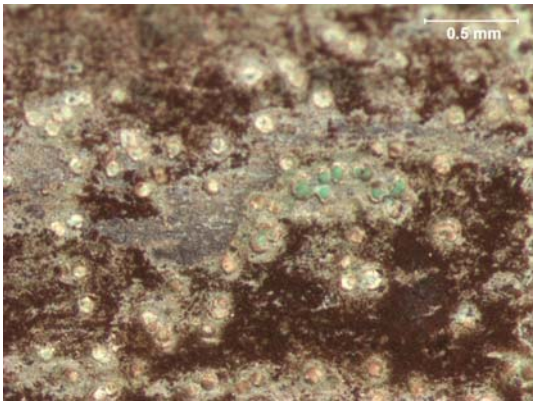

Figure G.13. Stereo-microscope picture of copper pipe wall.

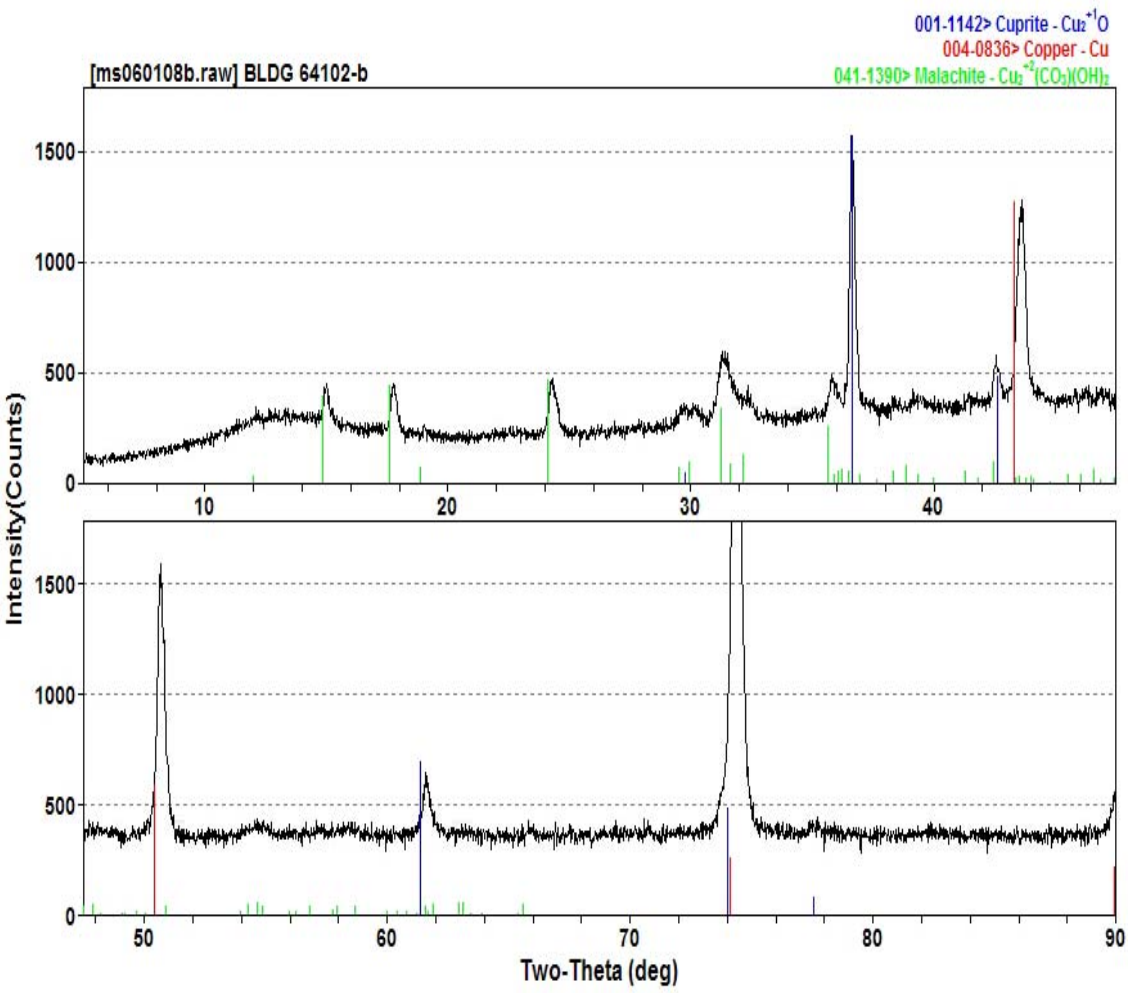

Figure G.14. Cutout XRD scan.

Building 641 (1977) Figures

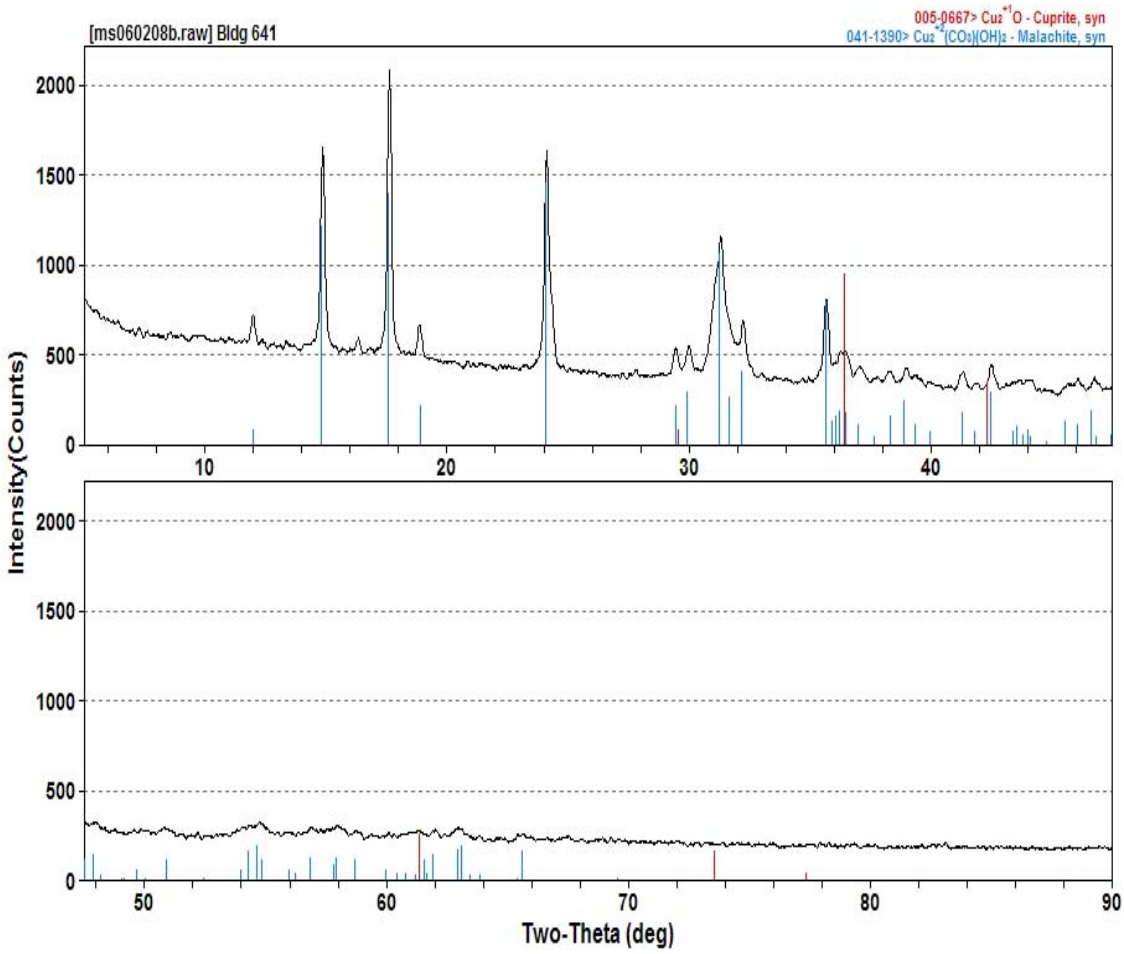

Figure G.15. Scrapings XRD scan.

Building 641 (1977) Figures

Figure G.16. Digital picture of the copper pipe.

Building 11A (1984) Figures

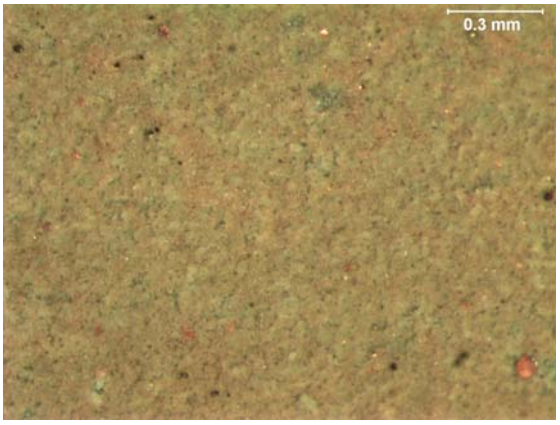

Figure G.17. Digital picture of the interior of copper recirculation pipe.

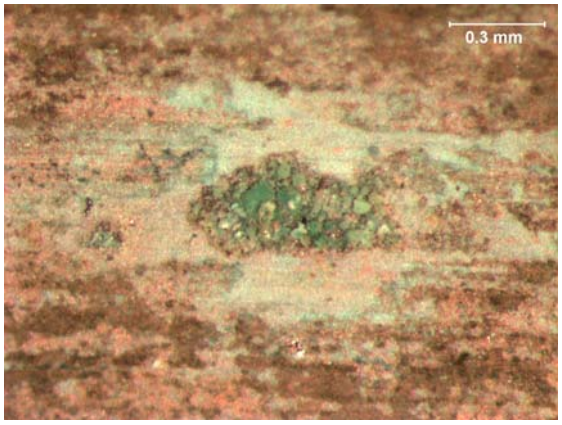

Figure G.18. Stereo-microscope picture of copper pipe wall.

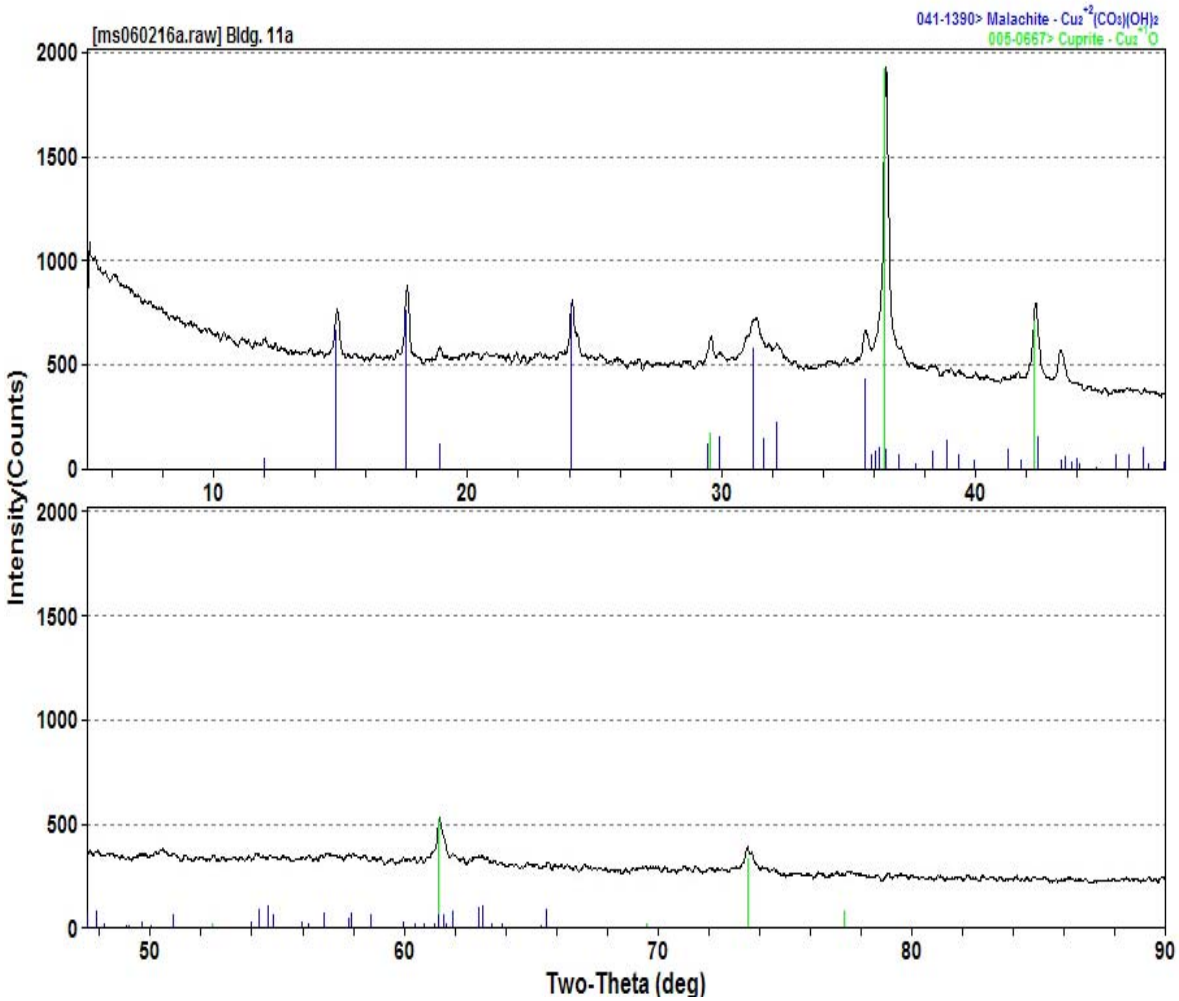

Figure G.19. Scrapings XRD scan.

Building 11A (1984) Figures

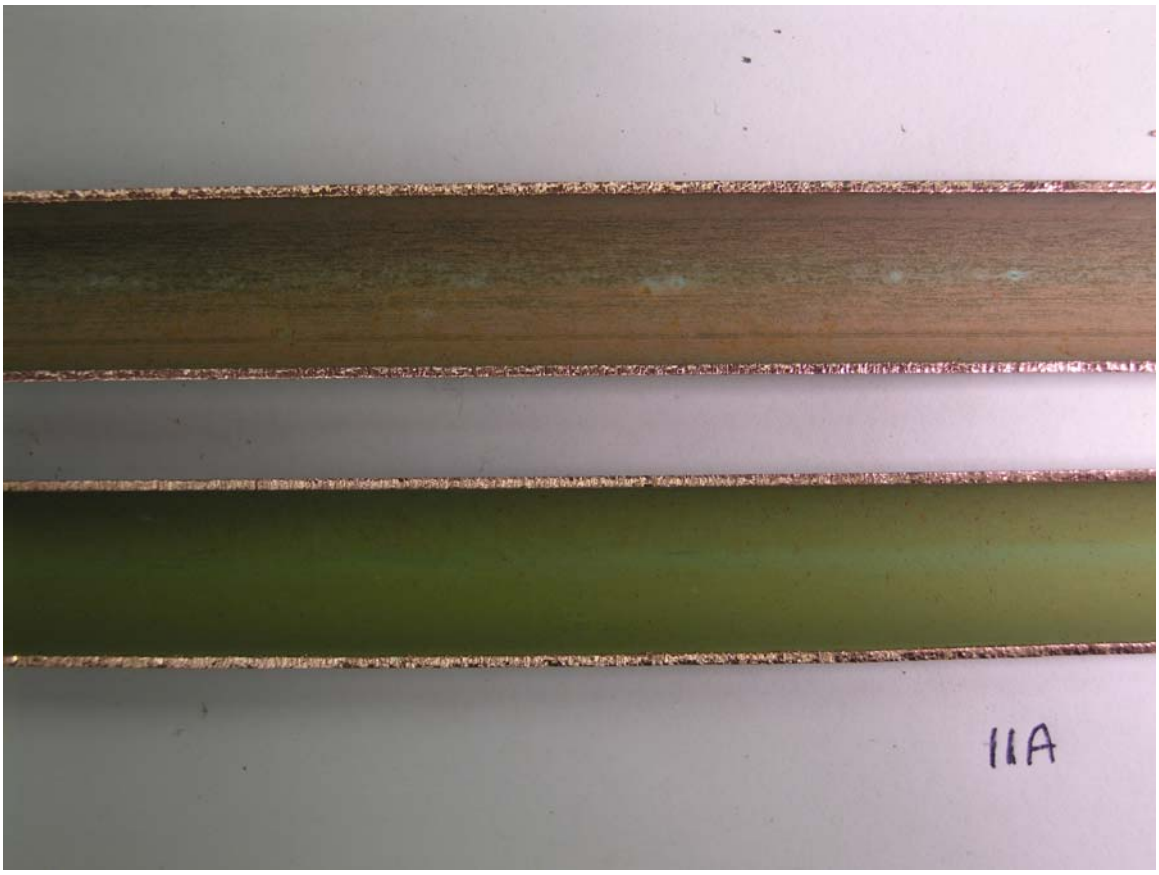

Figure G.20. Digital picture of the copper pipes.

Building 676 (1985) Figures

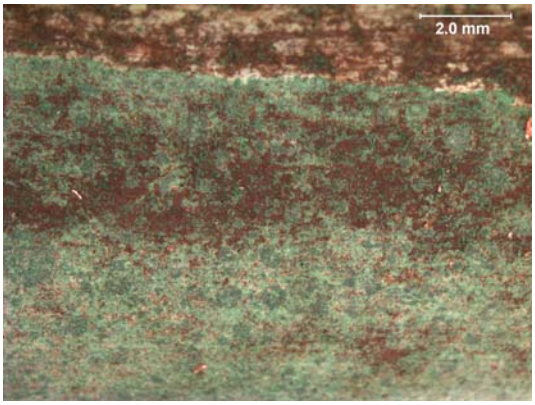

Figure G.21. Digital picture of the interior of copper recirculation pipe.

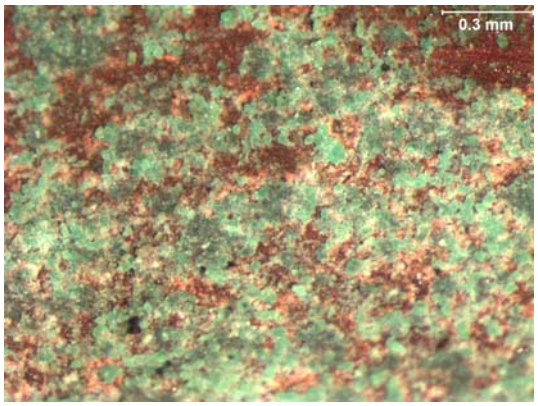

Figure G.22. Stereo-microscope picture of copper pipe wall.

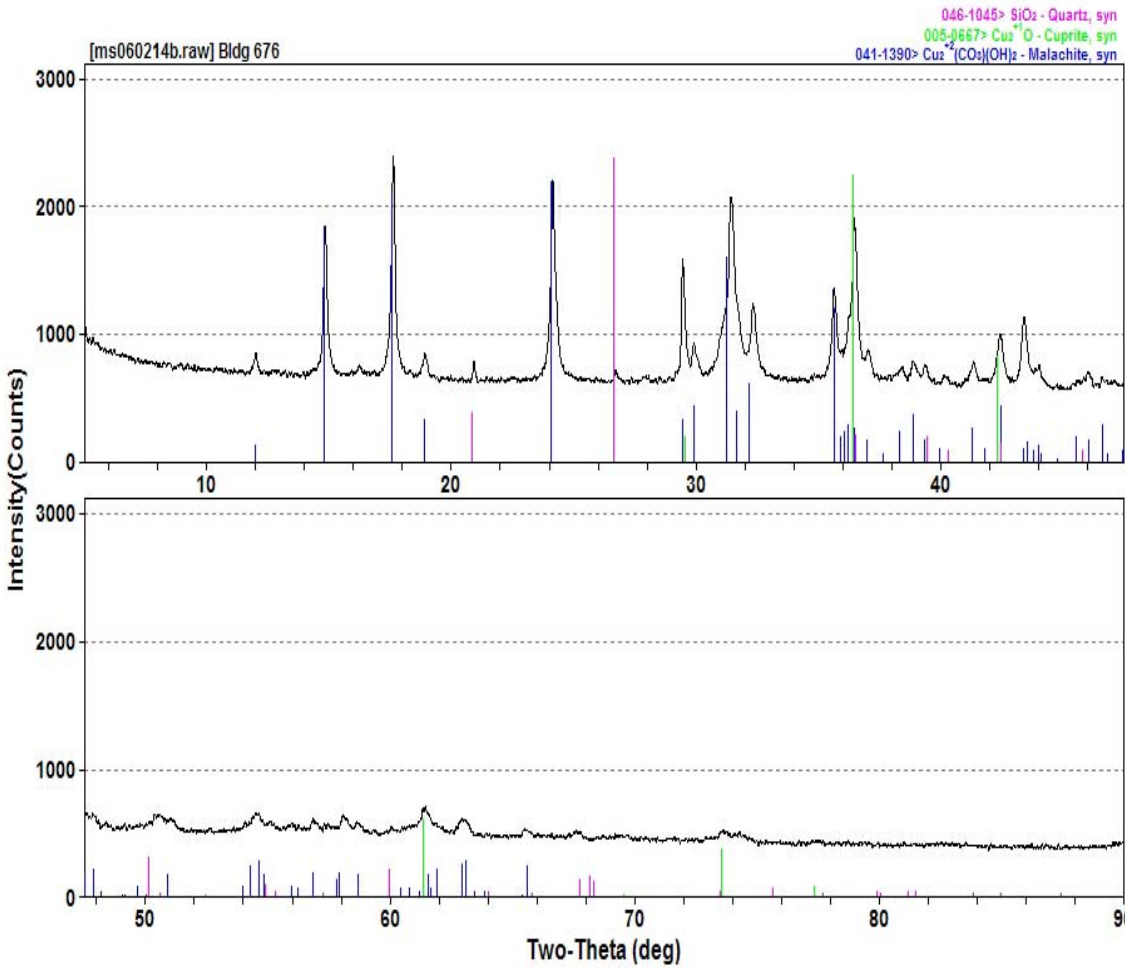

Figure G.23. Scrapings XRD scan.

Building 676 (1985) Figures

Figure G.24. Digital picture of the copper pipes.

Building 642-01 (1989) Figures

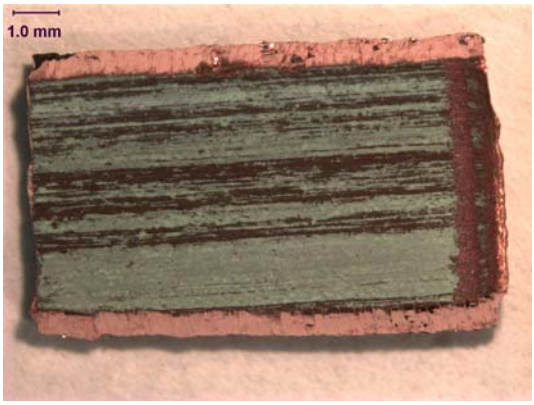

Figure G.25. Digital picture of the interior of copper recirculation pipe.

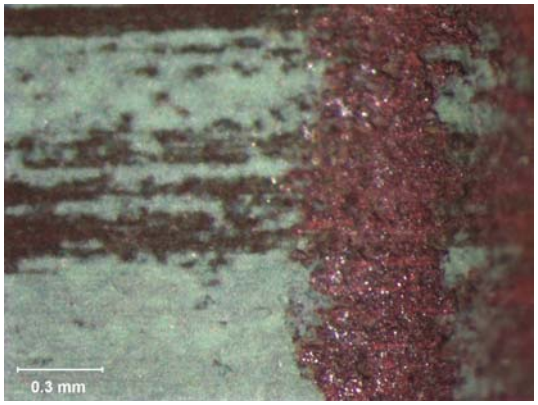

Figure G.26. Stereo-microscope picture of copper pipe wall.

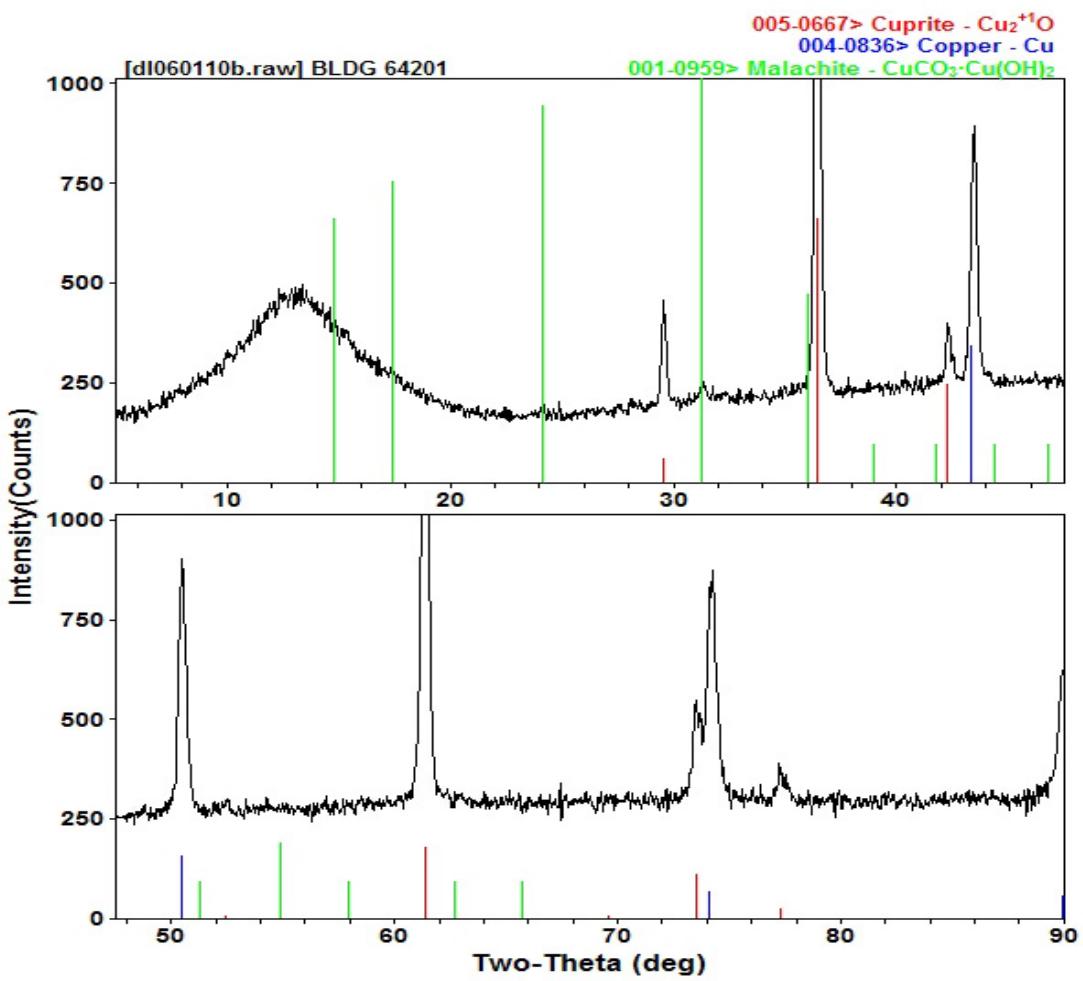

Figure G.27. Cutout XRD scan.

Building 642-02 (1989) Figures

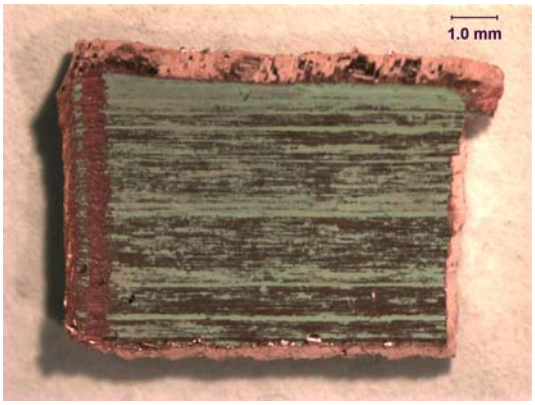

Figure G.28. Digital picture of the interior of copper recirculation pipe.

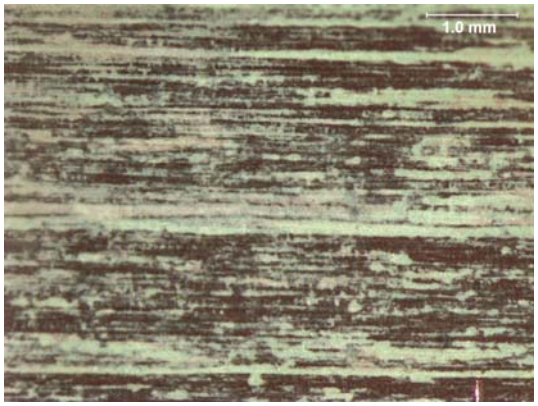

Figure G.29. Stereo-microscope picture of copper pipe wall.

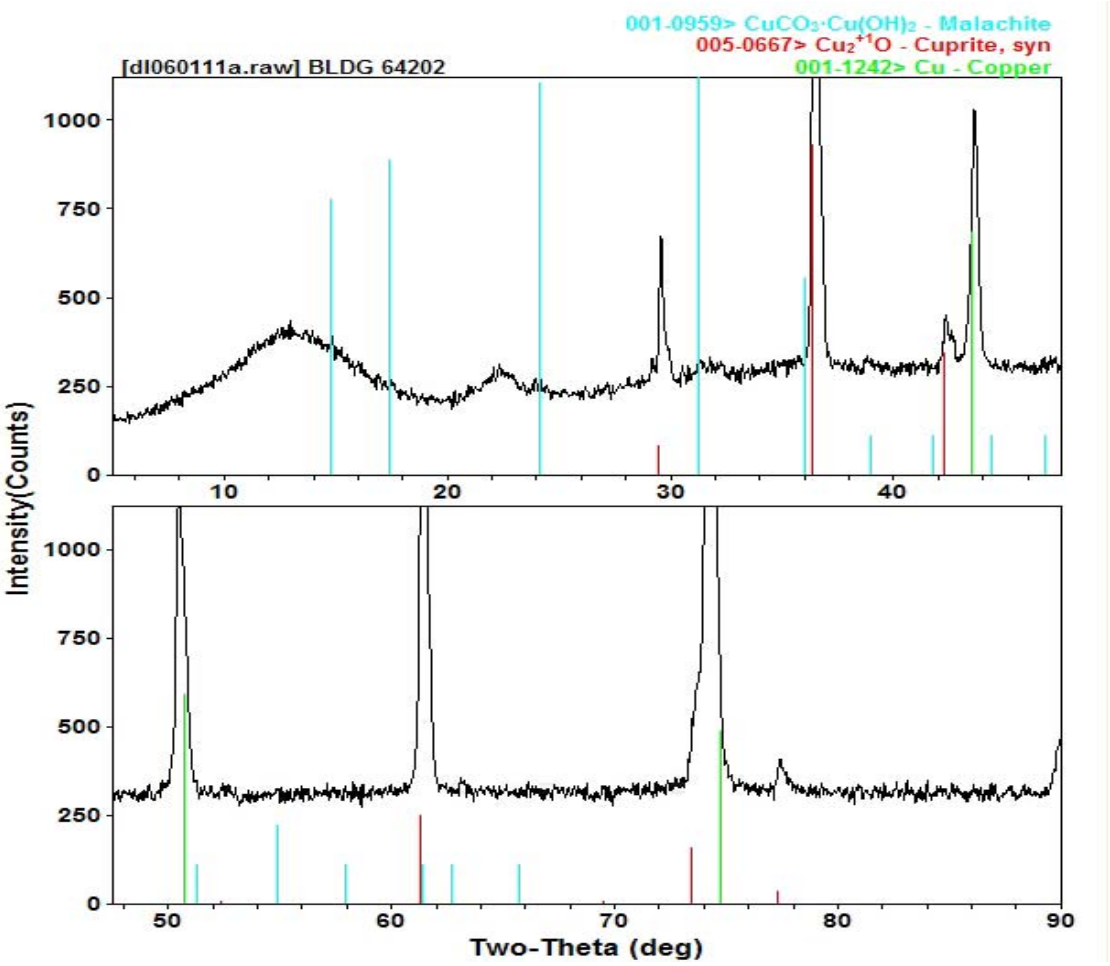

Figure G.30. Scrapings XRD scan.

Building 642 (1989) Figures

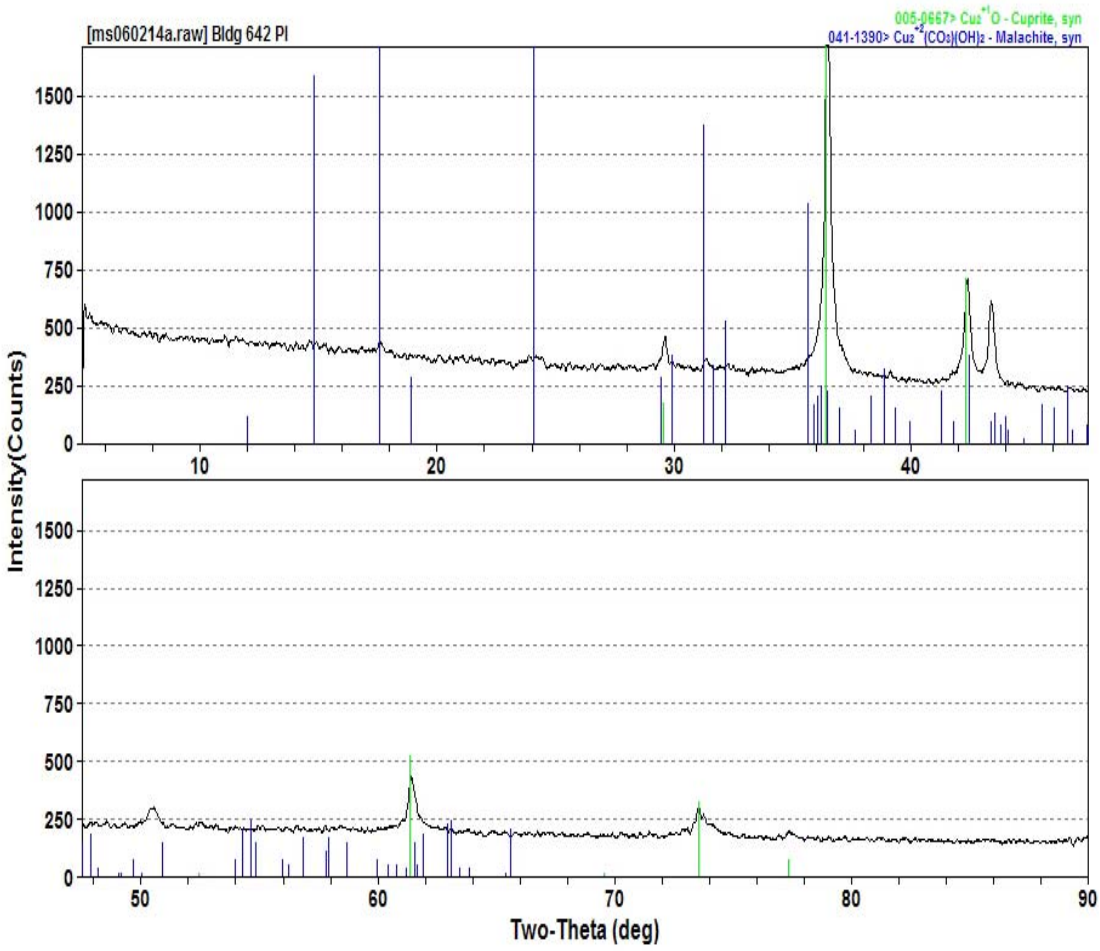

Figure G.31. Scrapings XRD scan.

Figure G.32. Digital picture of the copper pipe.

Building 620 PI (1992) Figures

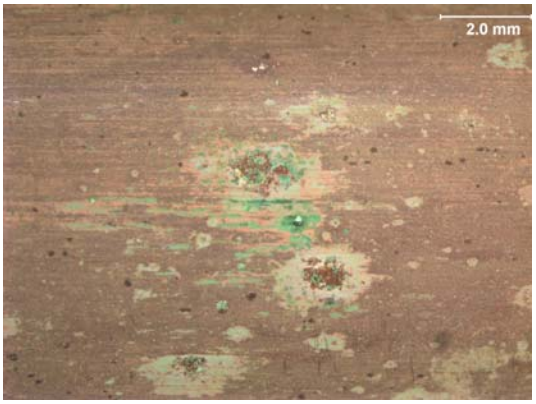

Figure G.33. Digital picture of the interior of copper recirculation pipe.

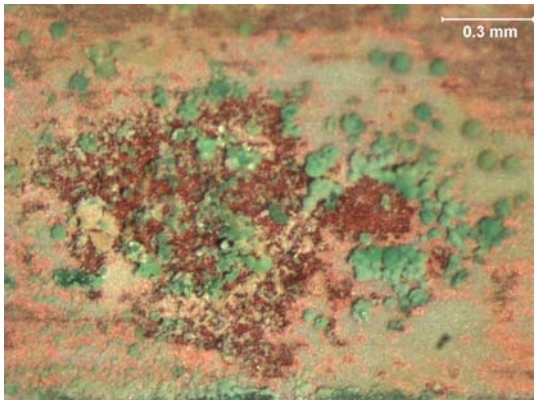

Figure G.34. Stereo-microscope picture of copper pipe wall.

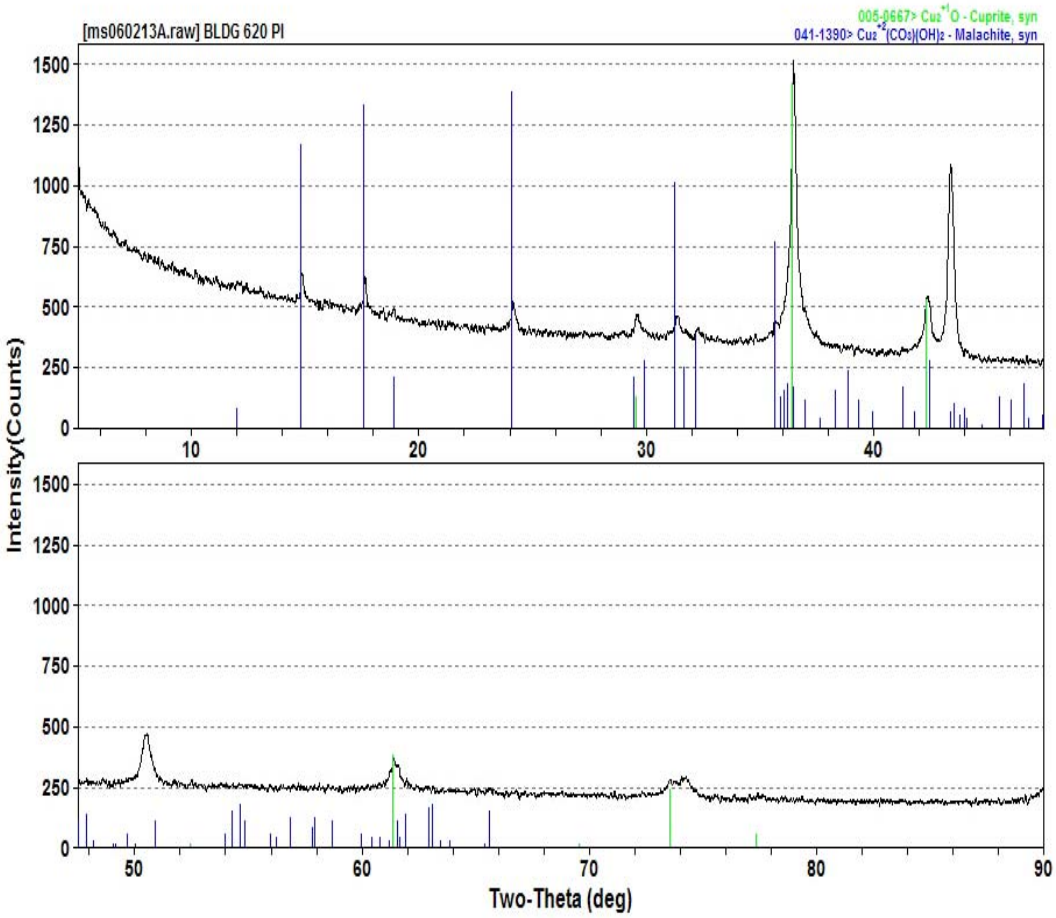

Figure G.35. Scrapings XRD scan.

Building 620 PI (1992) Figures

Figure G. 36. Digital picture of the copper pipes.

Building 441-B (1993) Figures

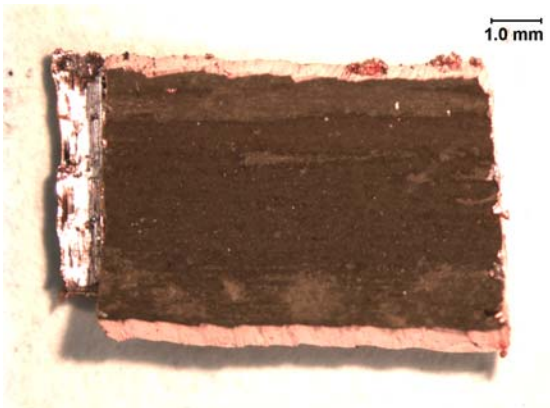

Figure G.37. Digital picture of the interior of copper recirculation pipe.

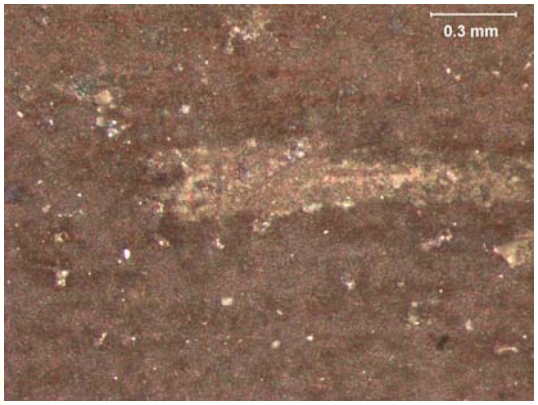

Figure G.38. Stereo-microscope picture of copper pipe wall.

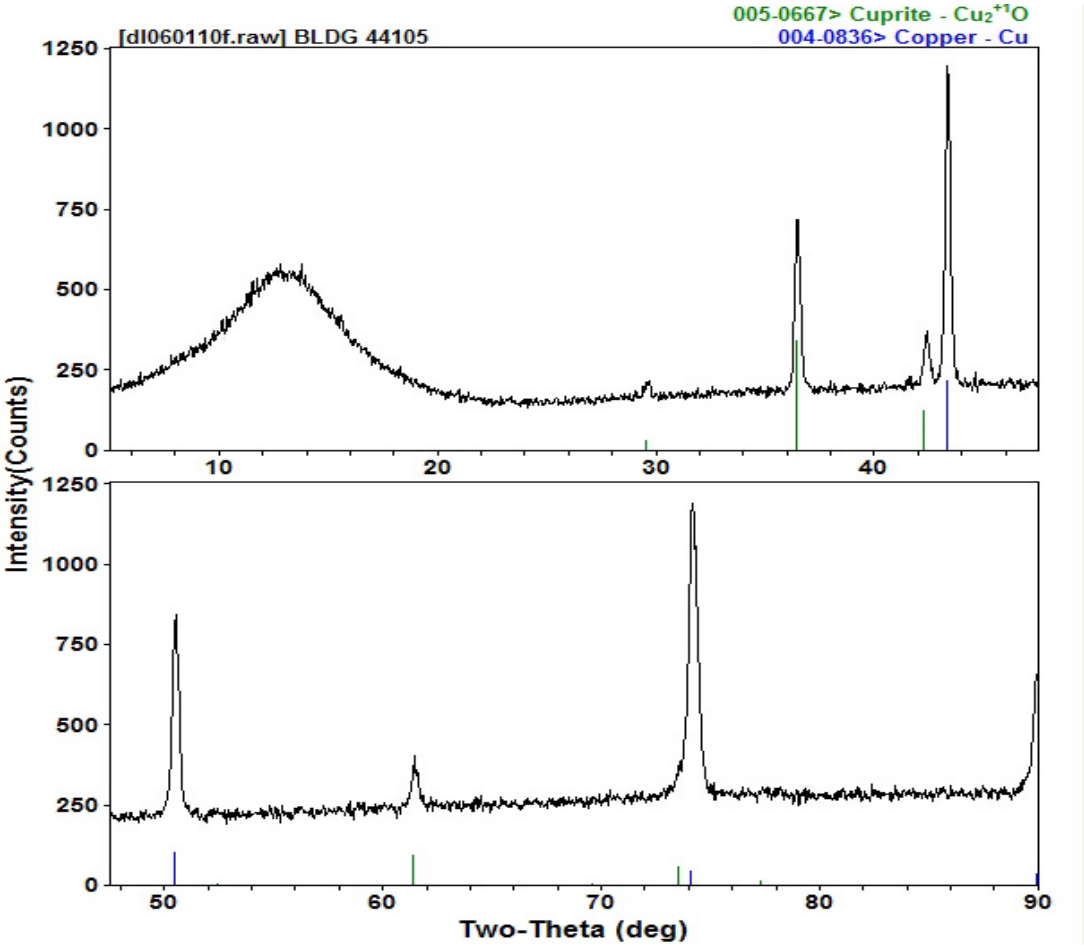

Figure G.39. Cutout XRD scan.

Building 441-B (1993) Figures

Figure G.40. Digital picture of the copper pipe.

Building 620 PII (1994) Figures

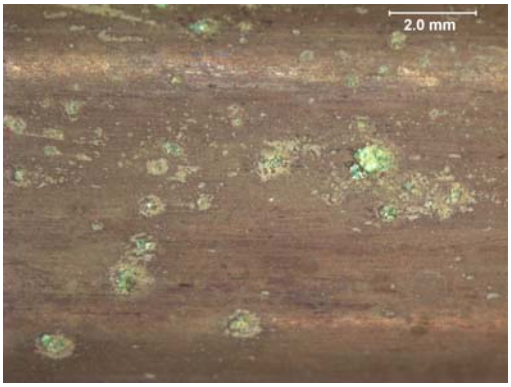

Figure G.41. Digital picture of the interior of copper recirculation pipe.

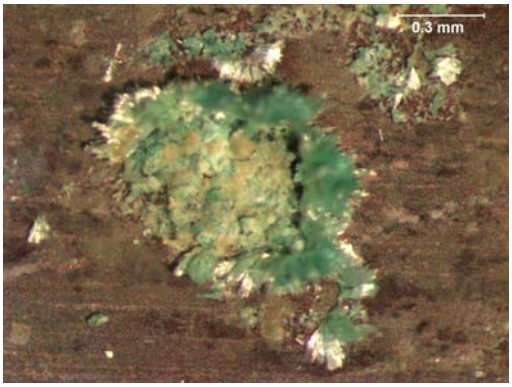

Figure G.42. Stereo-microscope picture of copper pipe wall.

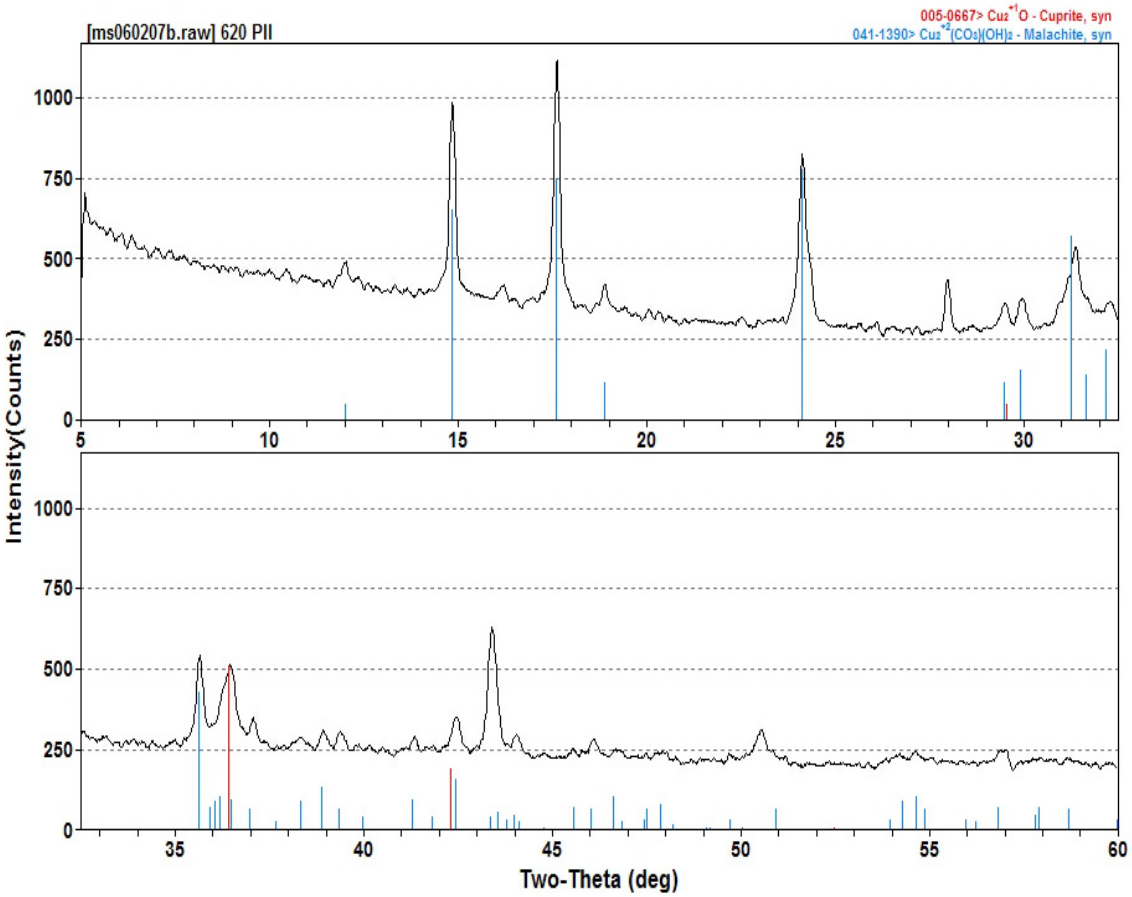

Figure G.43. Scrapings XRD scan.

Building 620 PII (1994) Figures

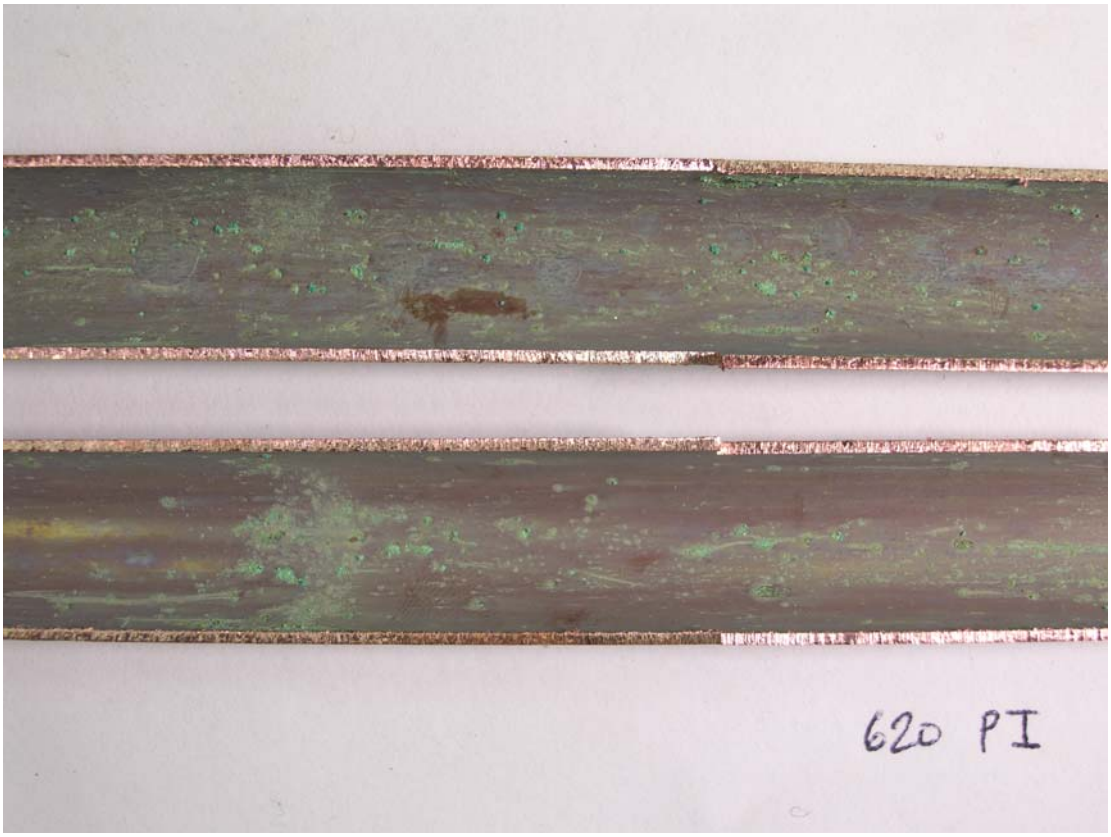

Figure G.44. Digital picture of the copper pipes.

Building 556 (1995) Figures

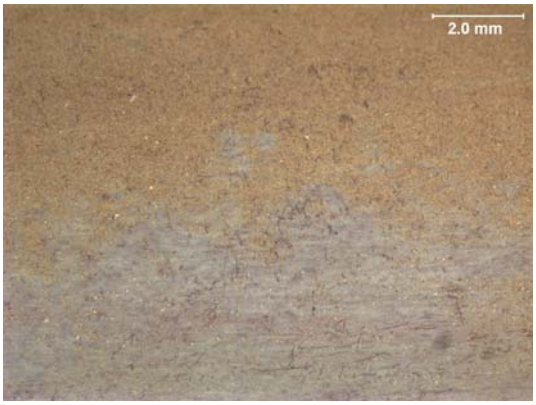

Figure G.45. Digital picture of the interior of copper recirculation pipe.

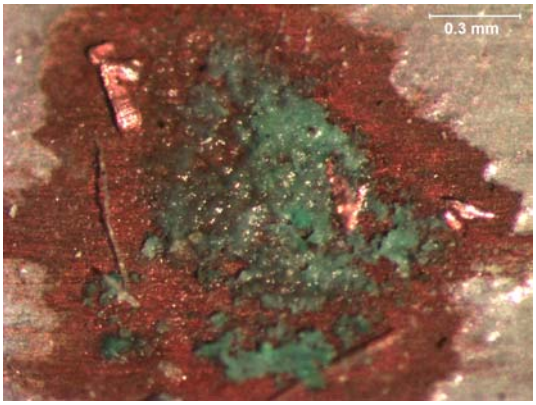

Figure G.46. Stereo-microscope picture of copper pipe wall.

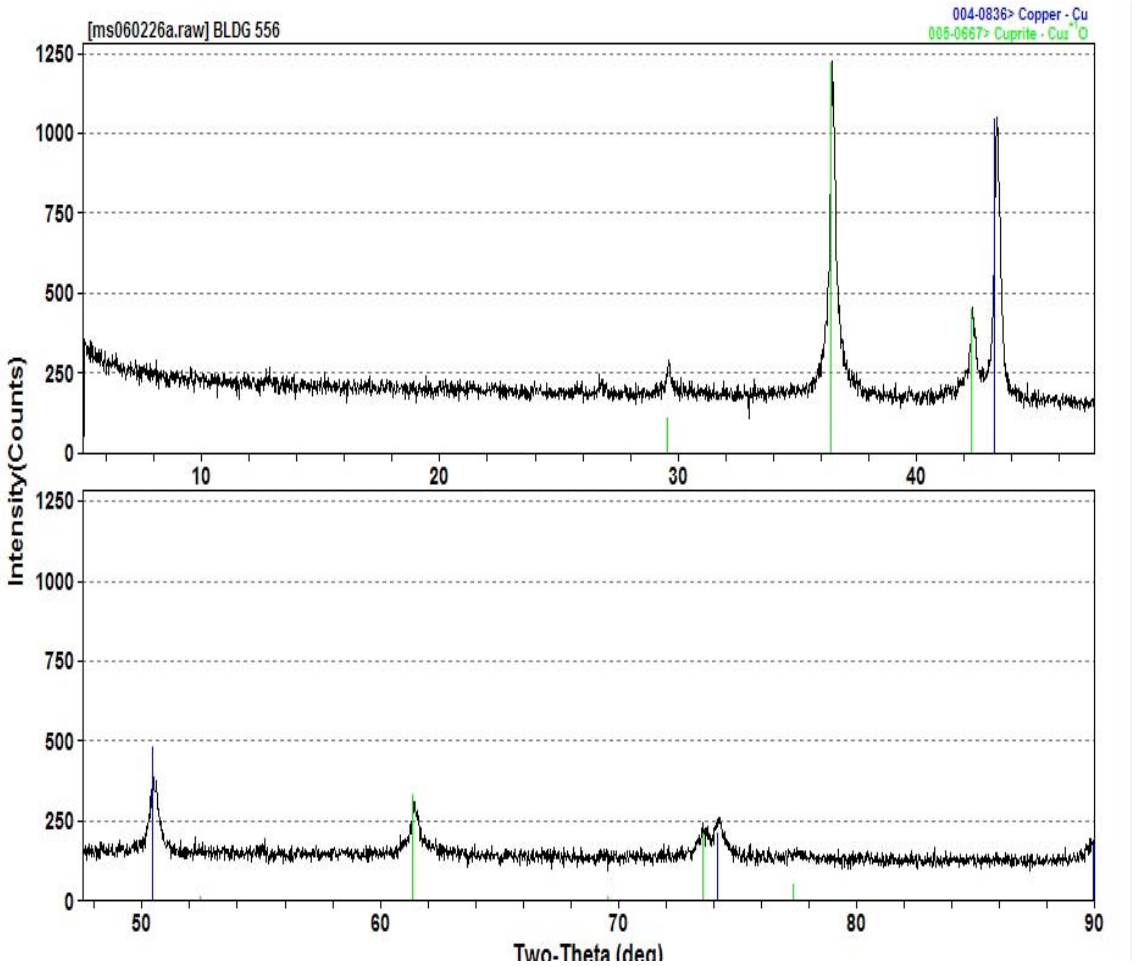

Figure G.47. Scrapings XRD scan.

Building 556 (1995) Figures

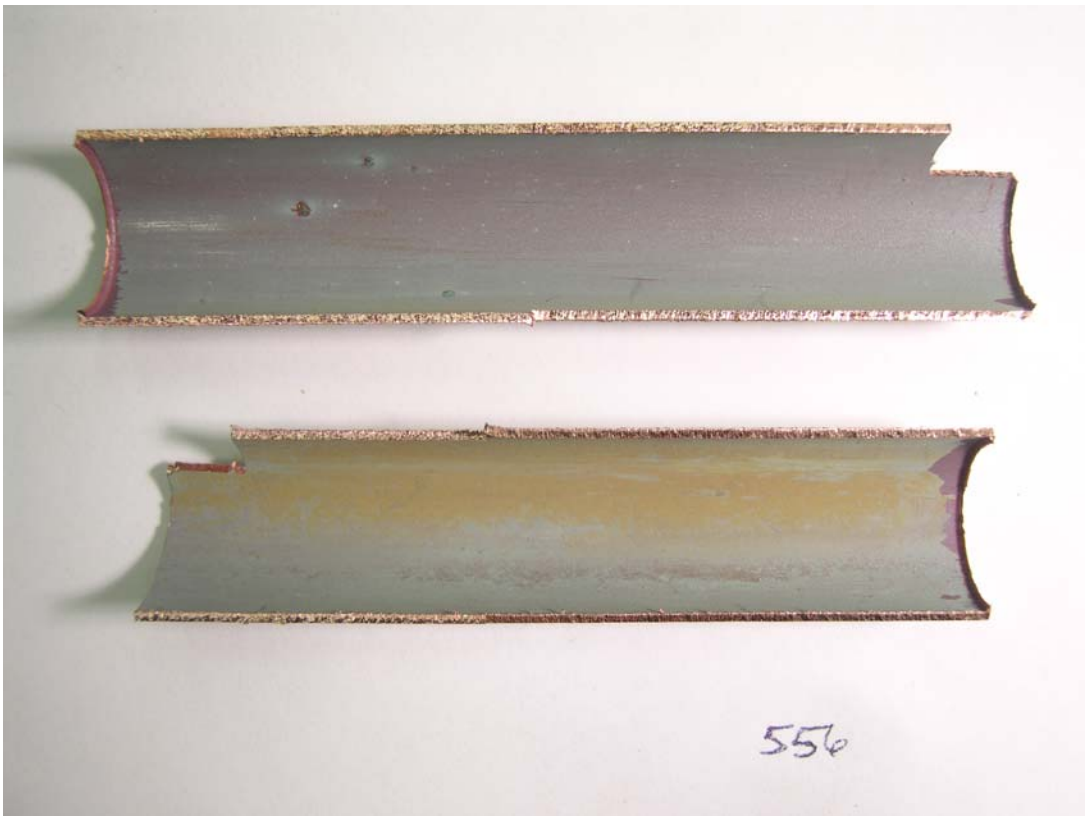

Figure G.48. Digital picture of the copper pipe.

Building 306 (1997) Figures

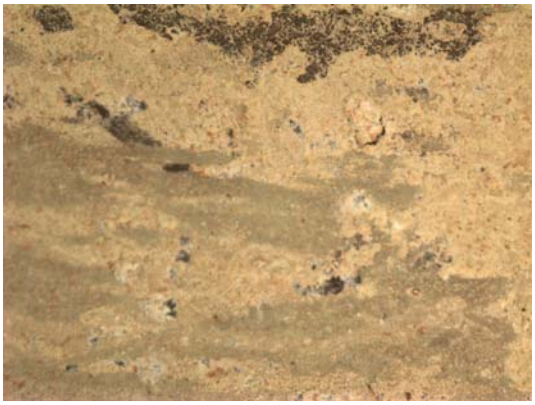

Figure G.49. Digital picture of the interior of copper recirculation pipe.

Figure G.50. Stereo-microscope picture of copper pipe wall.

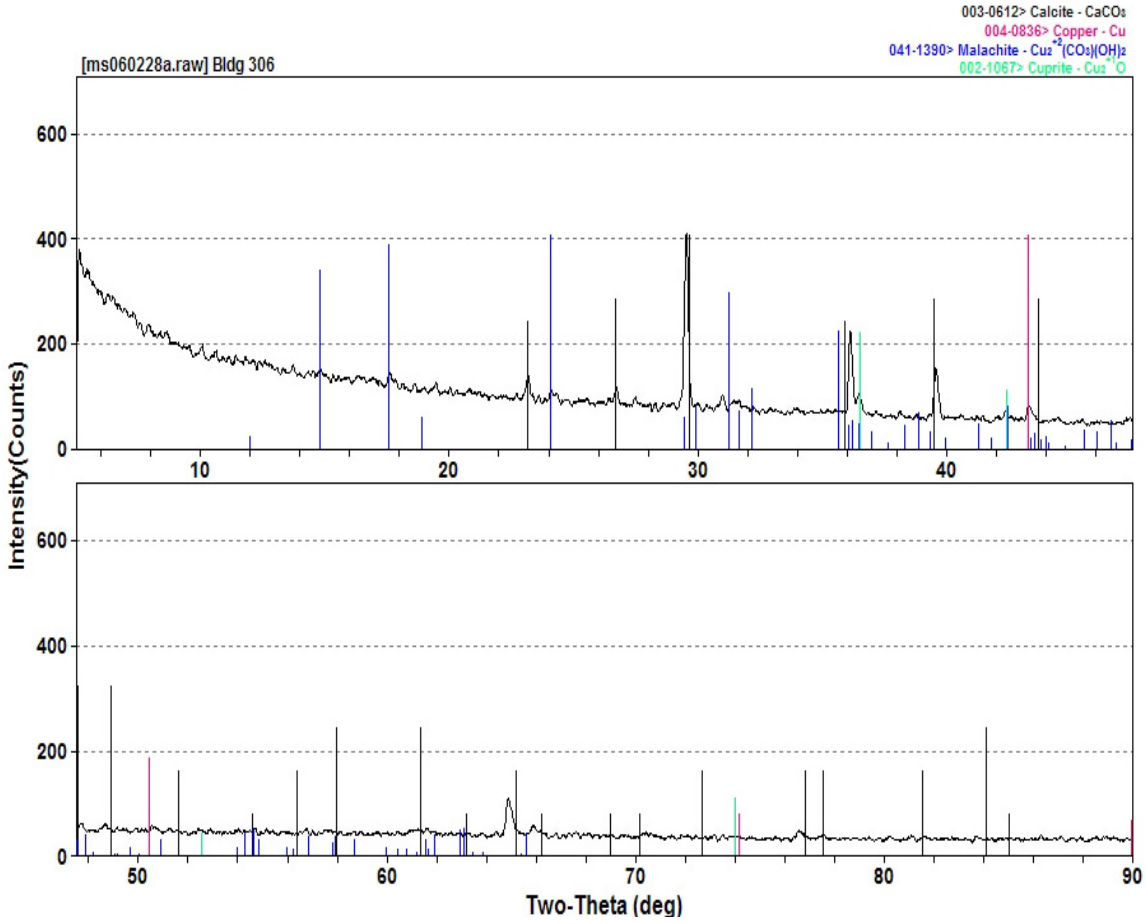

Figure G.51. Scrapings XRD scan.

Building 306 (1997) Figures

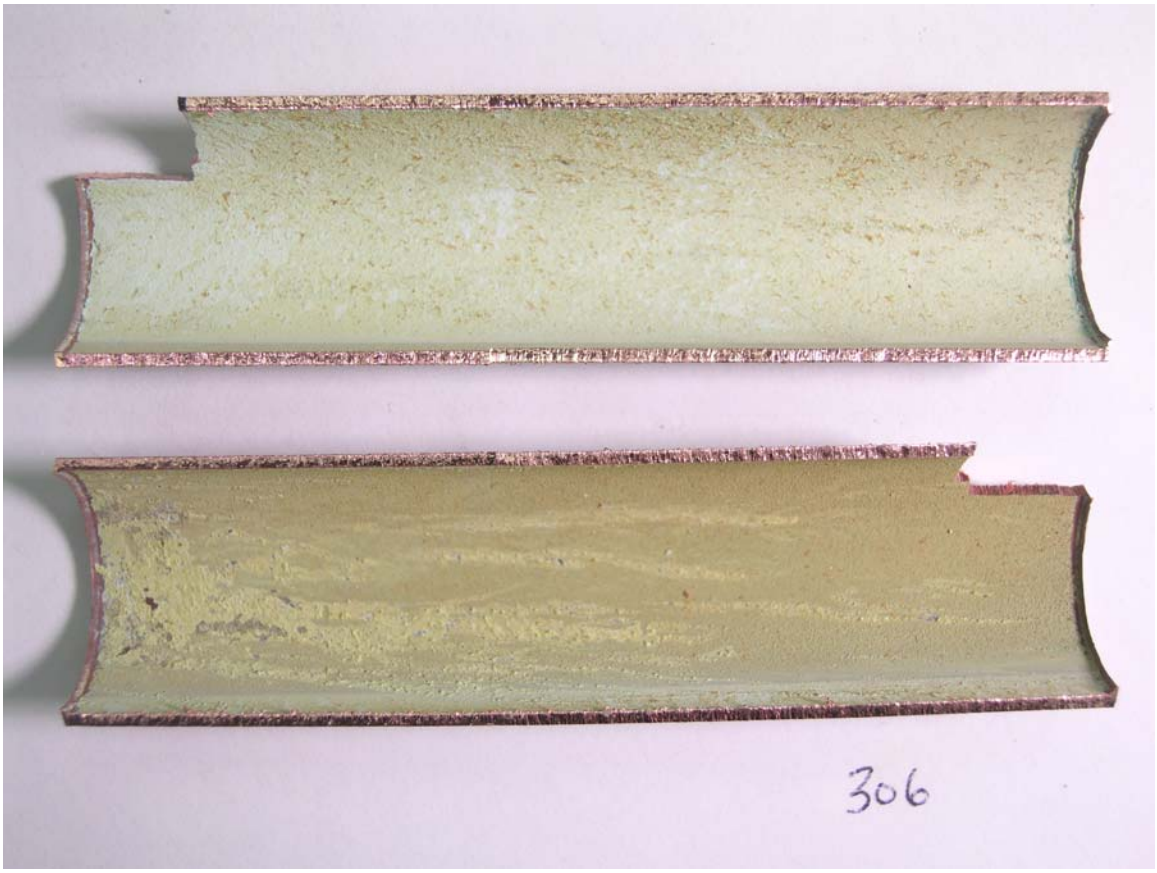

Figure G.52. Digital picture of the copper pipe.

Building 645-01 (1998) Figures

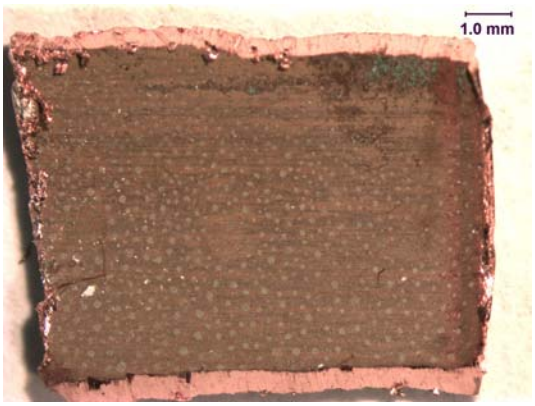

Figure G.53. Digital picture of the interior of copper recirculation pipe.

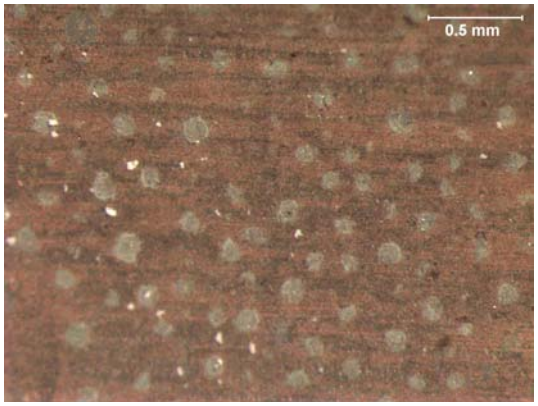

Figure G.54. Stereo-microscope picture of copper pipe wall.

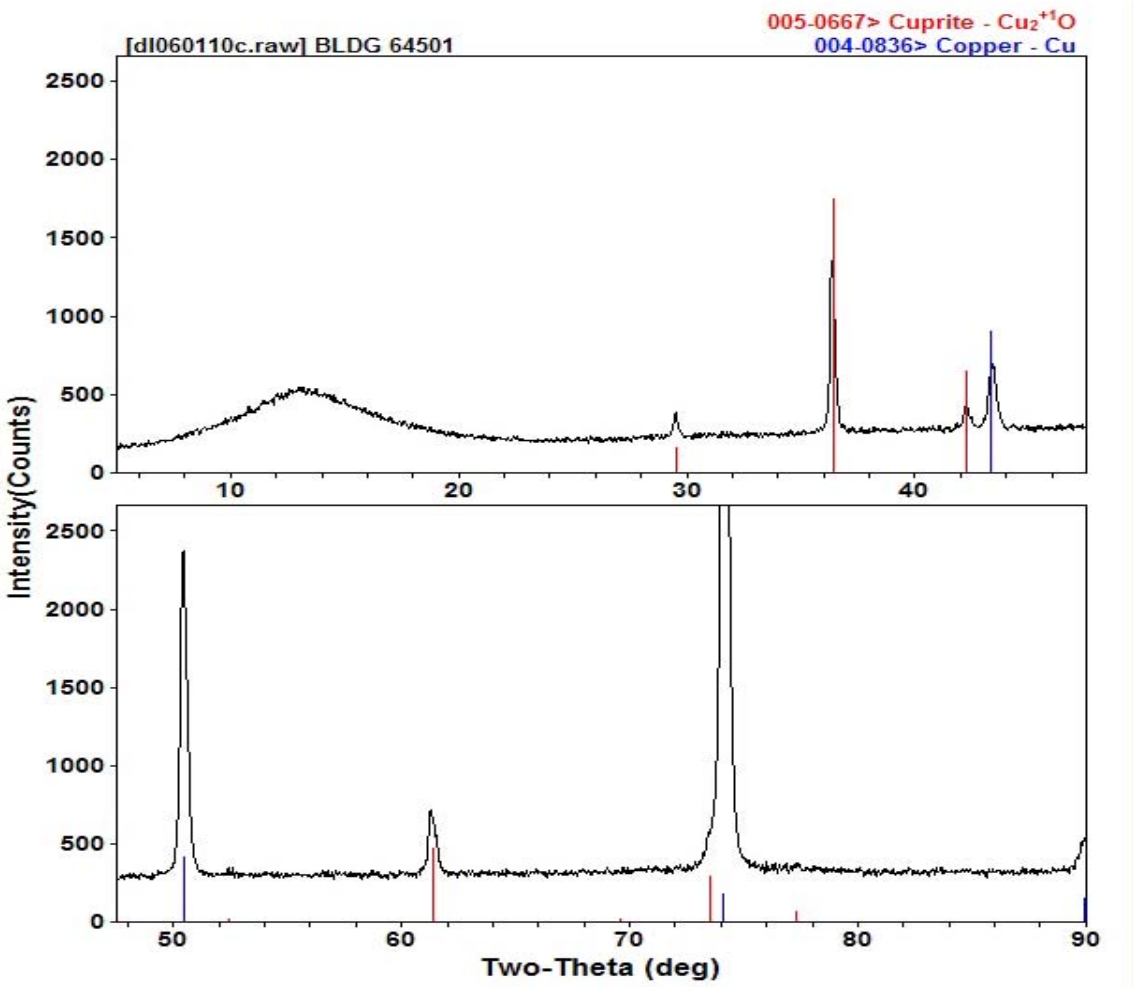

Figure G.55. Cutout XRD scan.

Building 645-02 (1998) Figures

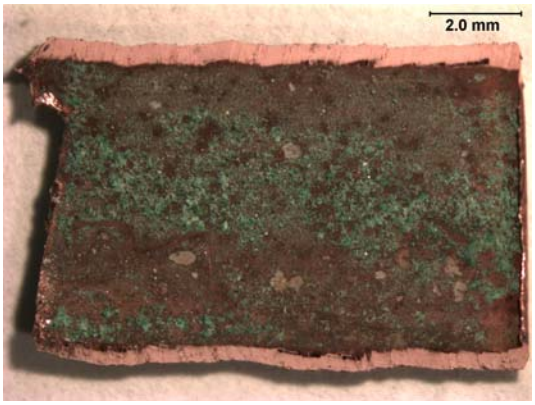

Figure G.56. Digital picture of the interior of copper recirculation pipe.

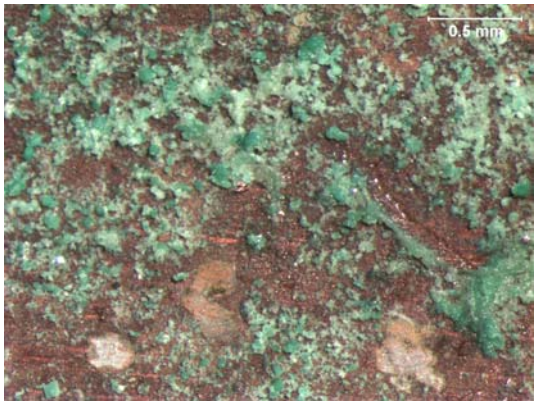

Figure G.57. Stereo-microscope picture of copper pipe wall.

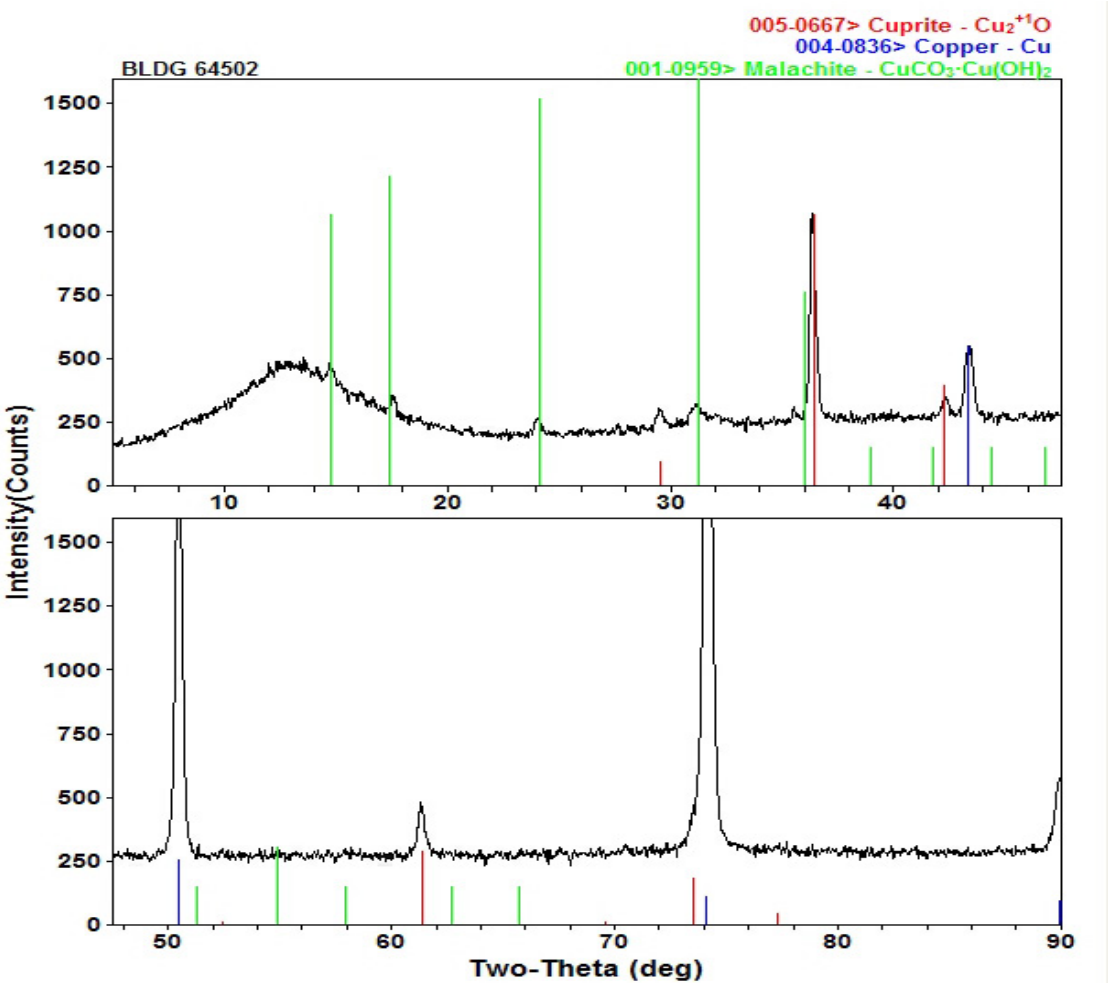

Figure G.58. Cutout XRD scan.

Building 645 (1998) Figures

Figure G.59. Digital picture of the copper pipe.

Building 553 (2001) Figures

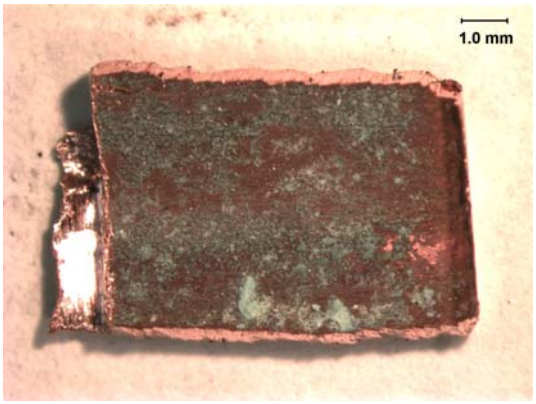

Figure G.60. Digital picture of the interior of copper recirculation pipe.

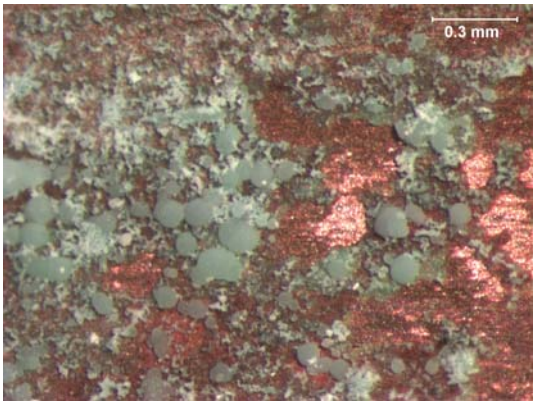

Figure G.61. Stereo-microscope picture of copper pipe wall.

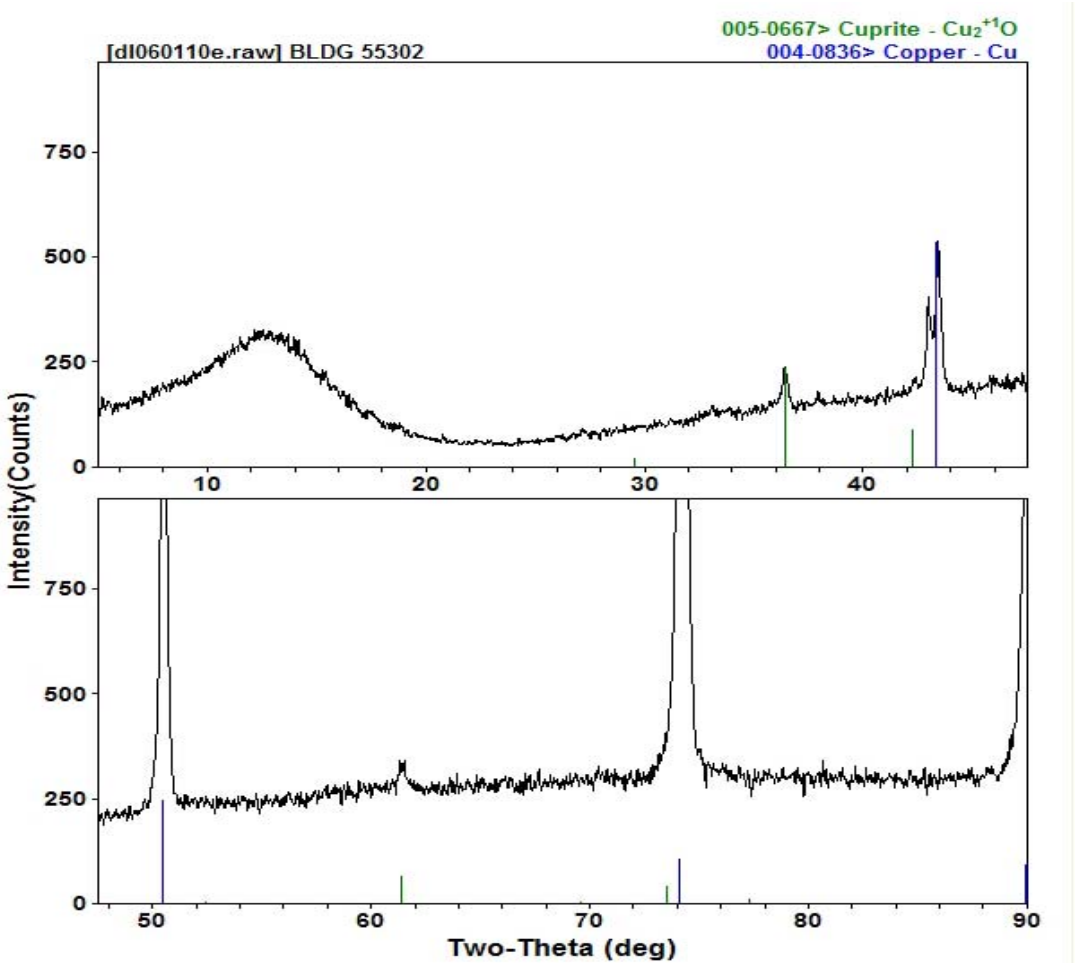

Figure G.62. Cutout XRD scan.

Building 553 (2001) Figures

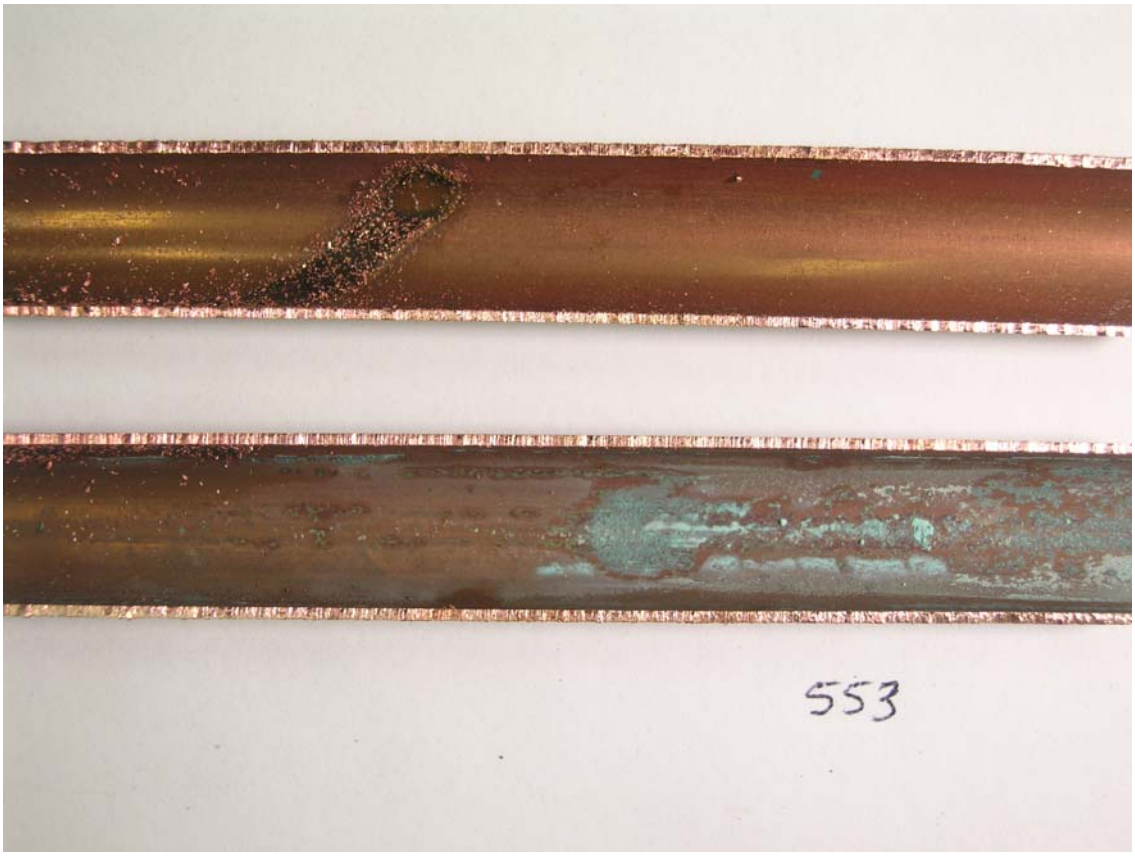

Figure G.63. Digital picture of the copper pipe.

Building 571 (2002) Figures

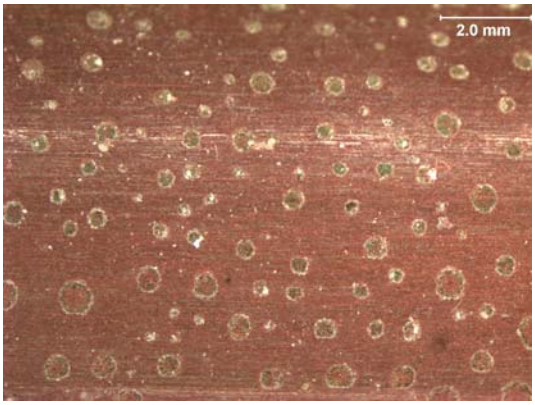

Figure G.64. Digital picture of the interior of copper recirculation pipe.

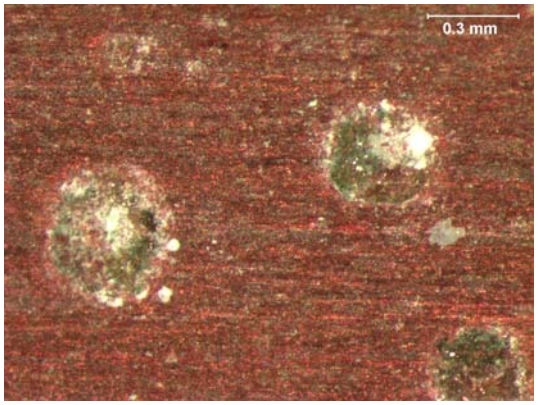

Figure G.65. Stereo-microscope picture of copper pipe wall.

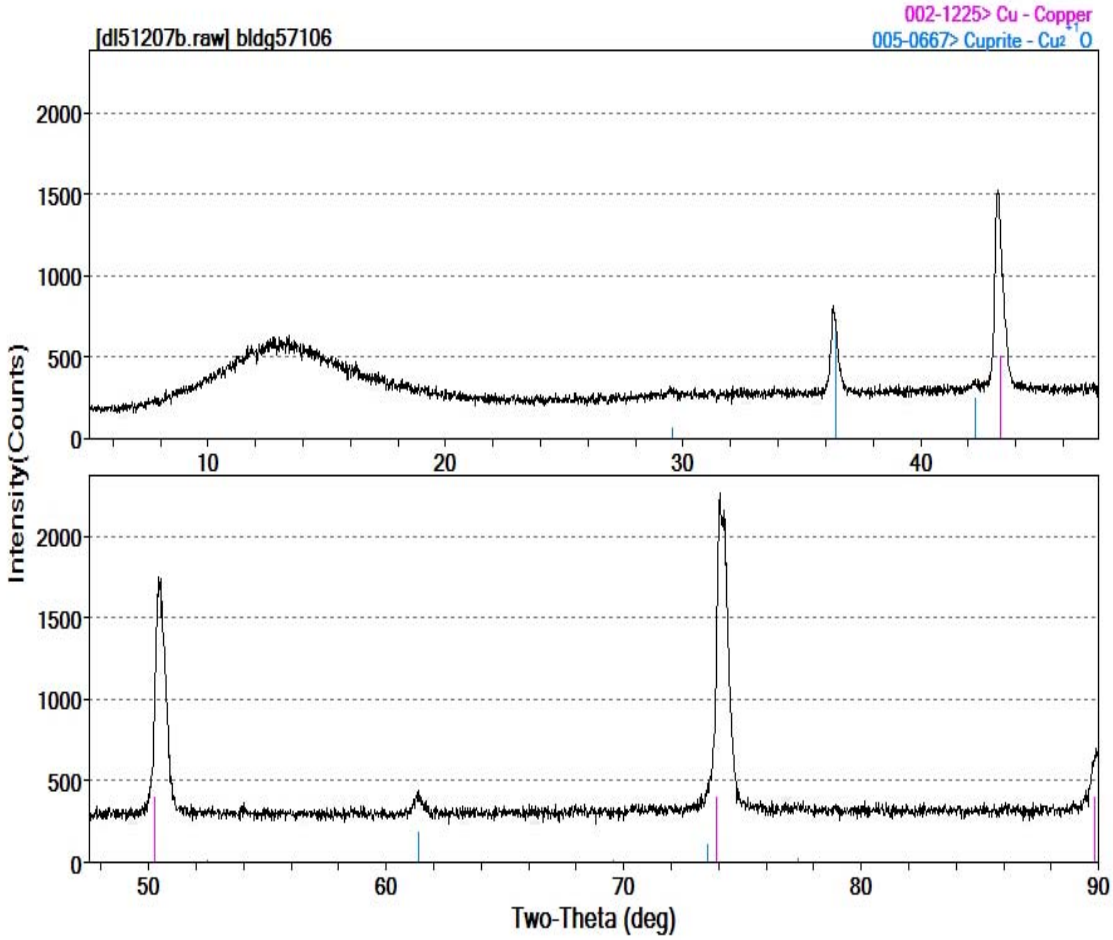

Figure G.66. Cutout XRD scan.

Building 571 (2002) Figures

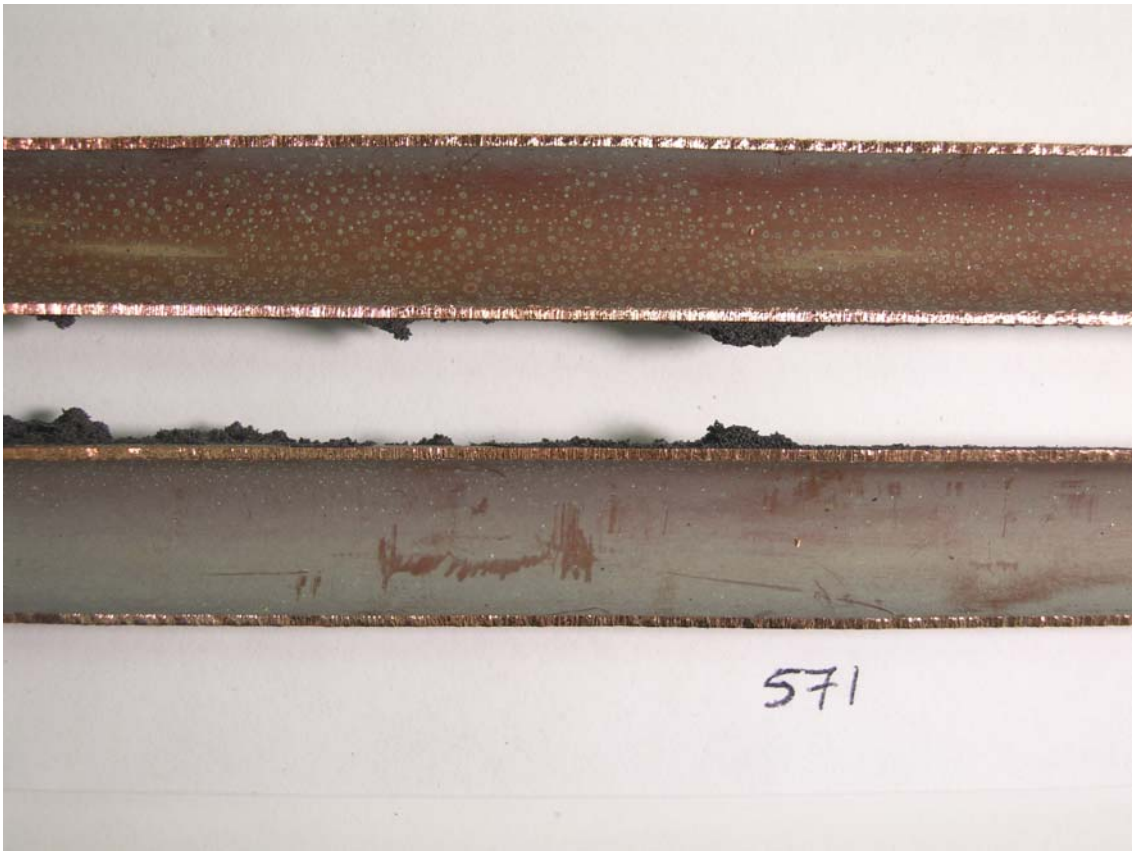

Figure G.67. Digital picture of the copper pipe.

Building 837 (2004) Figures

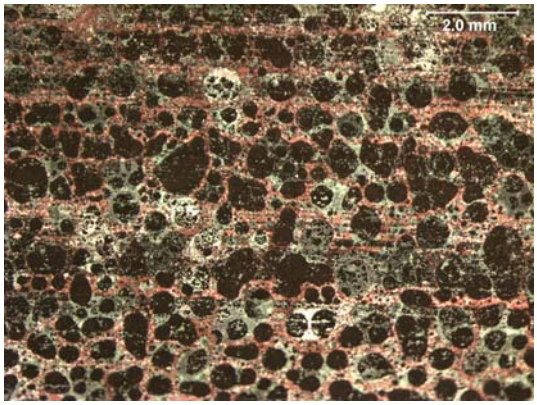

Figure G.68. Digital picture of the interior of copper recirculation pipe.

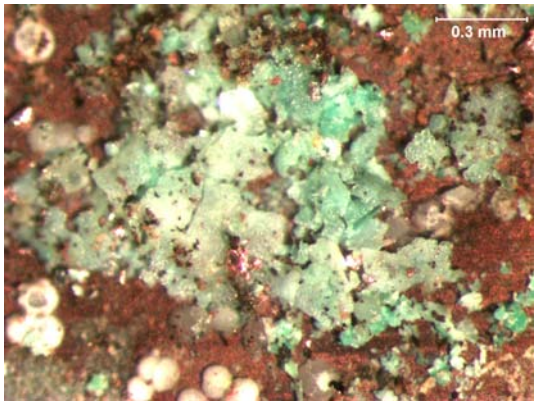

Figure G.69. Stereo-microscope picture of copper pipe wall.

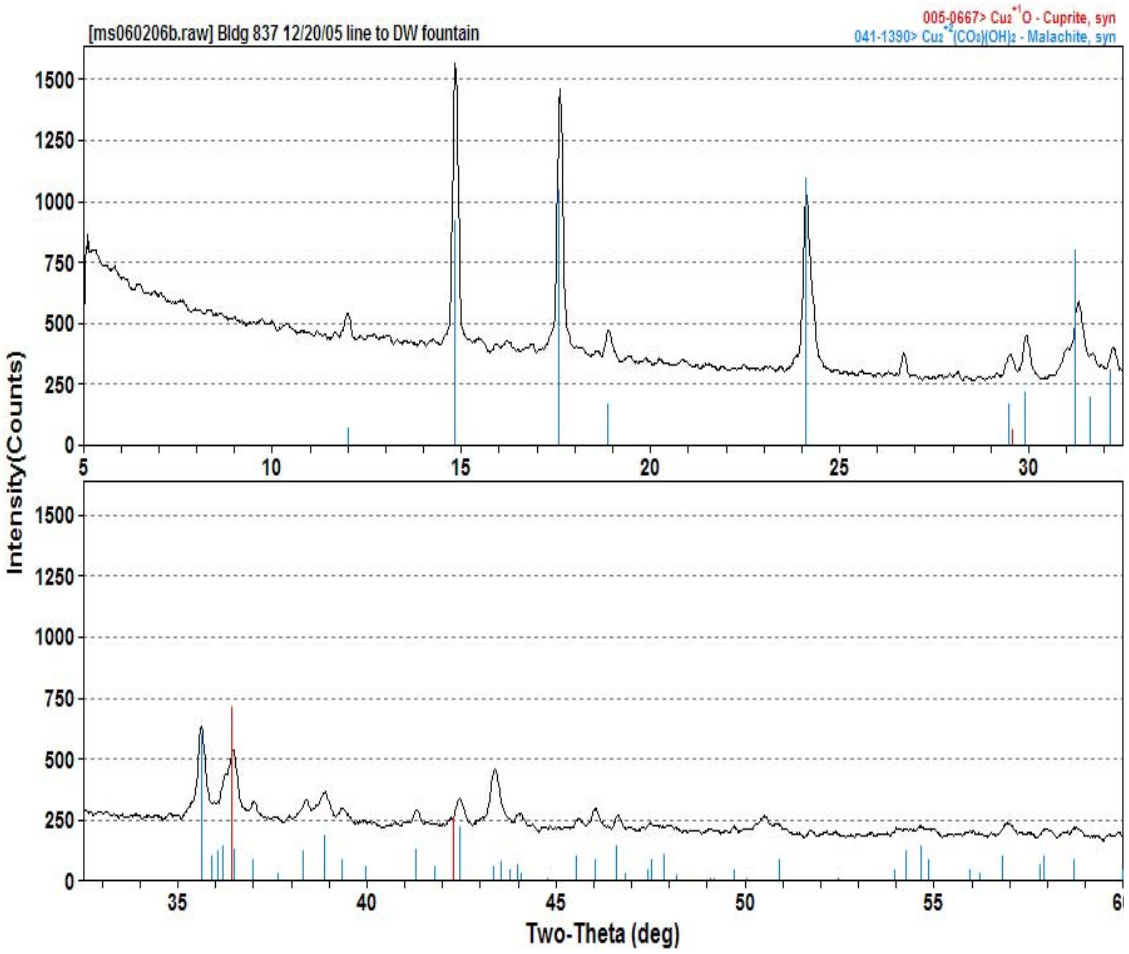

Figure G.70. Scrapings XRD scan.

Building 837 (2004) Figures

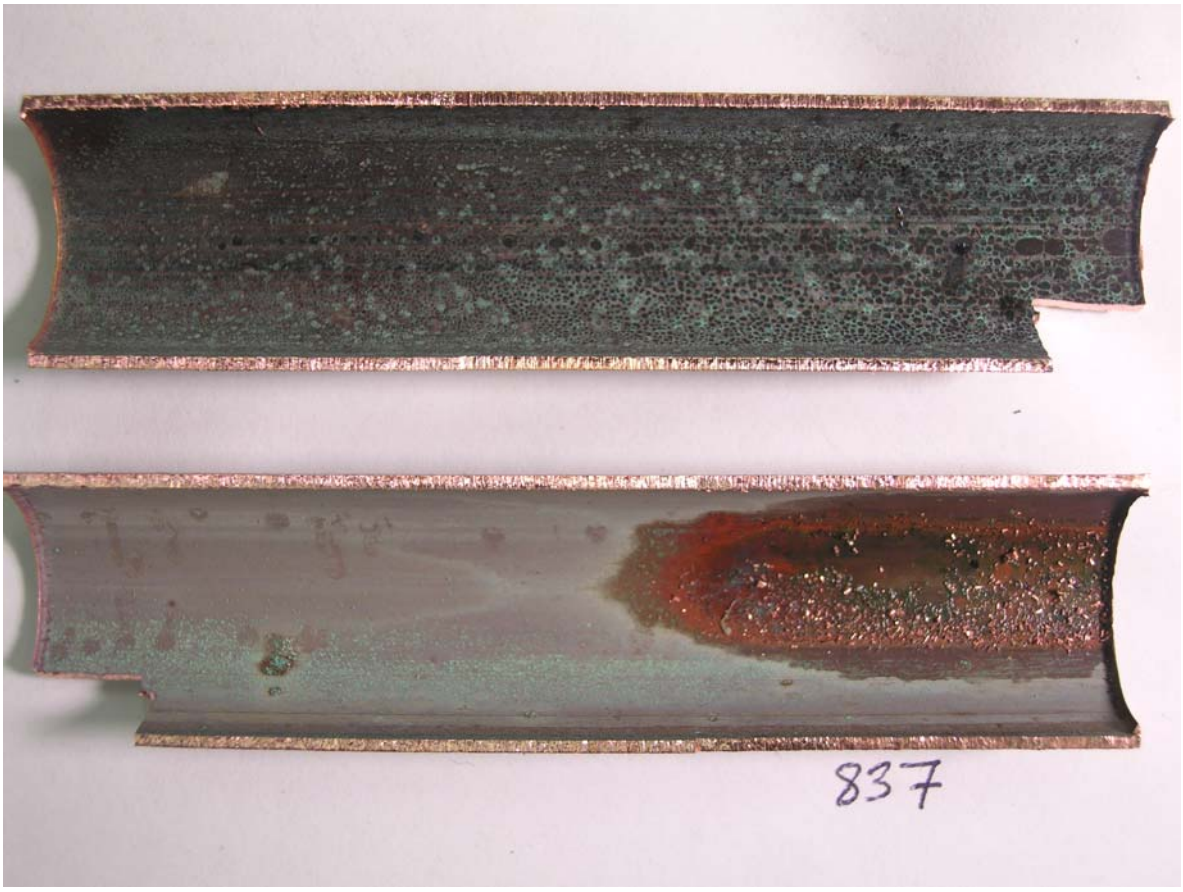

Figure G.71. Digital picture of the copper pipe.

Building 441-S (2005) Figures

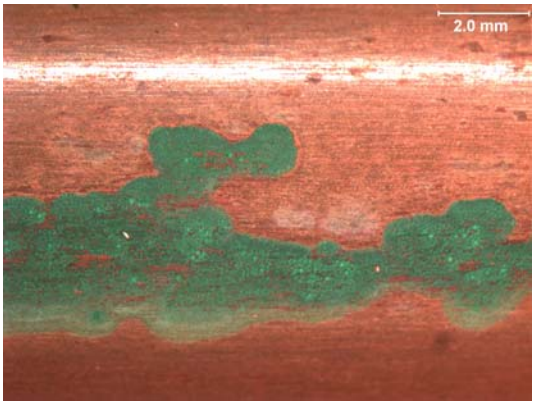

Figure G.72. Digital picture of the interior of copper recirculation pipe.

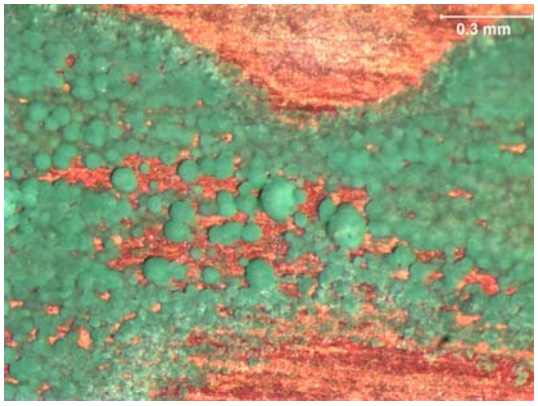

Figure G.73. Stereo-microscope picture of copper pipe wall.

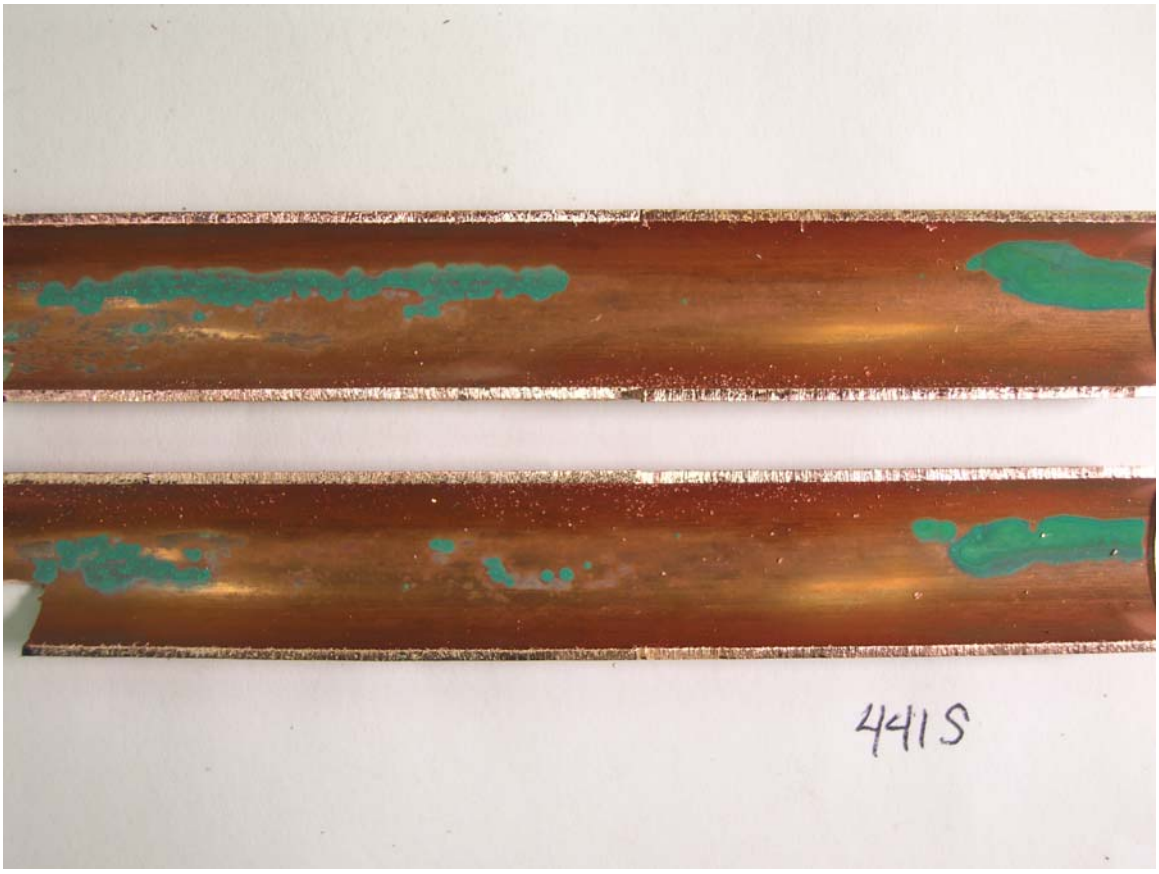

Figure G.74 Digital picture of the copper pipe.

Appendix H

X-ray Photoelectron Spectroscopy Spectra and Analysis by Building

Page

Building 464 (1962): $Cu(OH)_2$, Reducing to Cu_2O

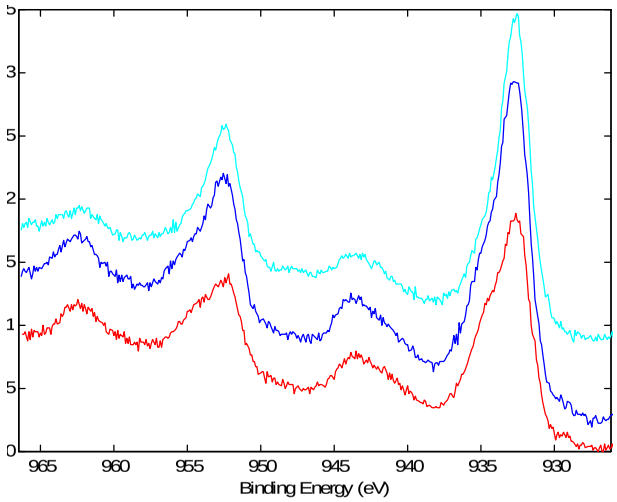

Figure H.1. Cu 2p peak (one sample)

Red: first scan, Blue: second scan, Light blue: third scan

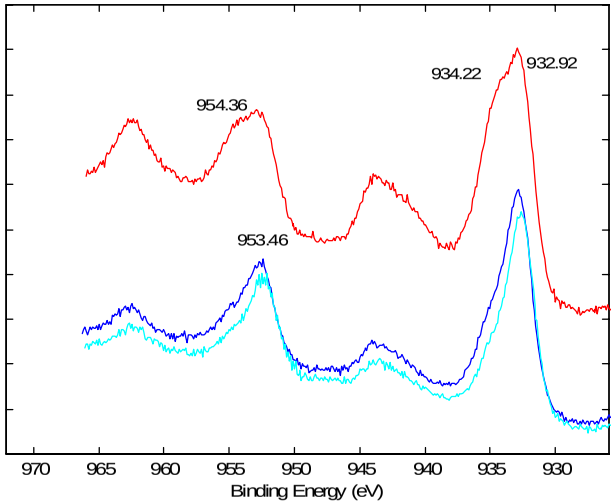

Figure H.2. Cu 2p peak (second sample)

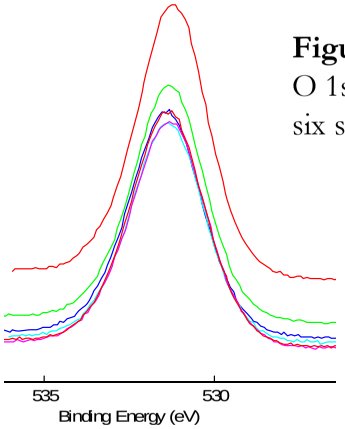

Figure H.4. O 1s peak (all six scans)

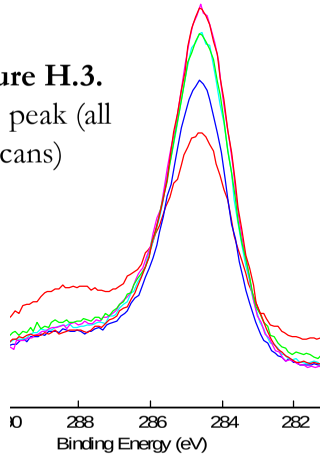

Figure H.3. C 1s peak (all six scans)

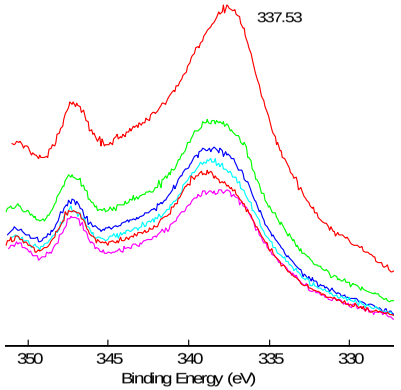

Figure H.5. Cu LMM peak (all six scans)

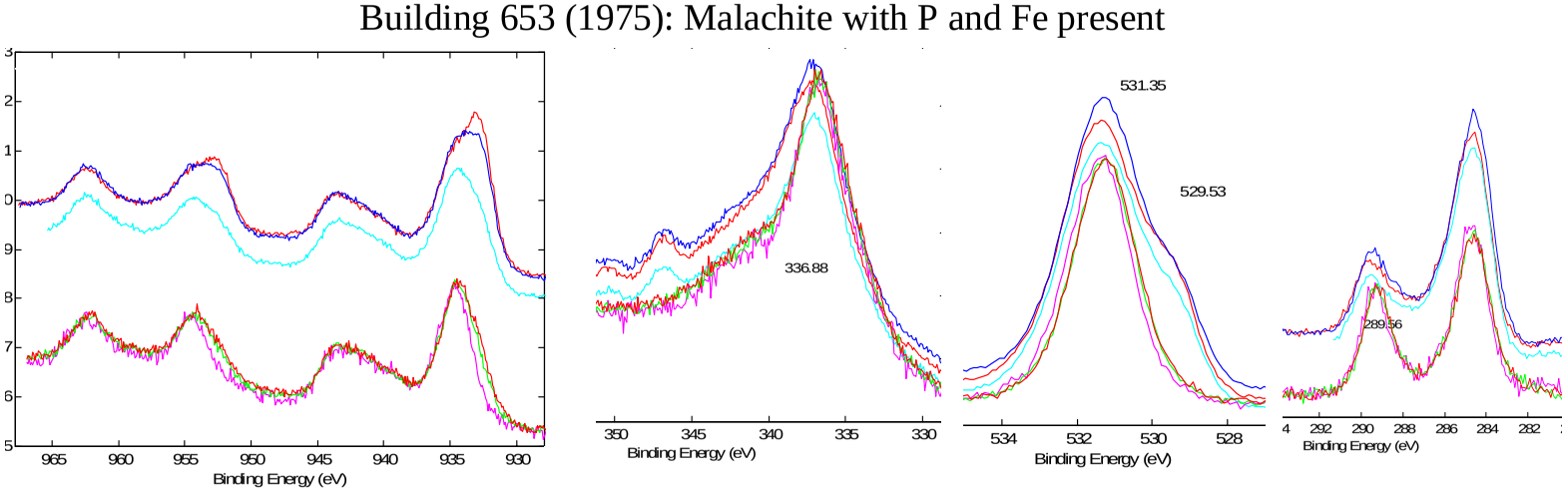

Figure H.6. Sample 02 Cu 2p (left), Cu LMM (middle left), O 1s (middle right), and C 1s (right) peaks compared to malachite (bottom). Light blue is the first run, then blue second, and red third.

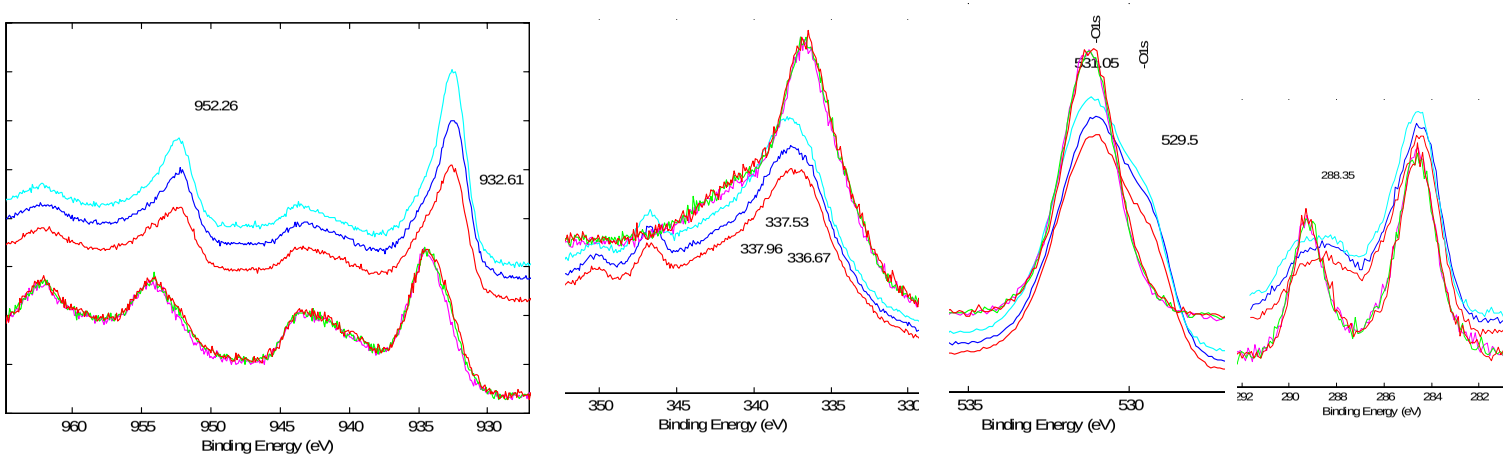

Figure H.7. Sample 01 Cu 2p (left), Cu LMM (middle left), O 1s (middle right), and C 1s (right) peaks compared to malachite (bottom). Light blue is the first run, then blue second, and red third.

Building 641 (1977): $Cu(OH)_2$ with P, Cl, and a small CO_3 peak

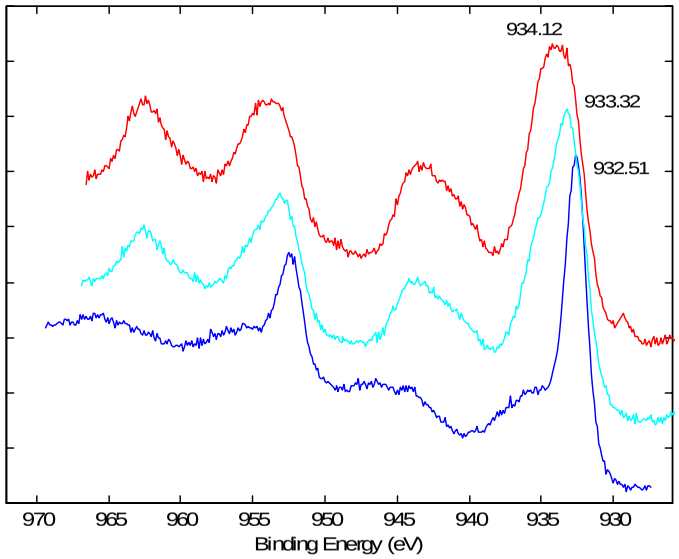

Figure H.8. Cu 2p peaks (one sample)

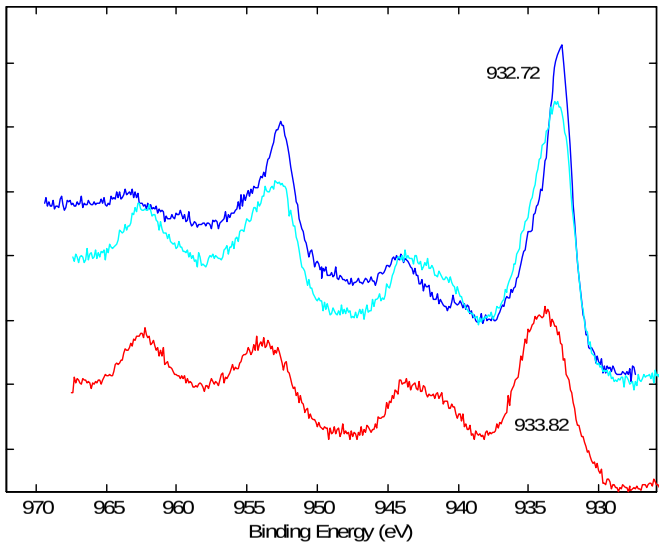

Figure H.9. Cu 2p peaks (second sample)

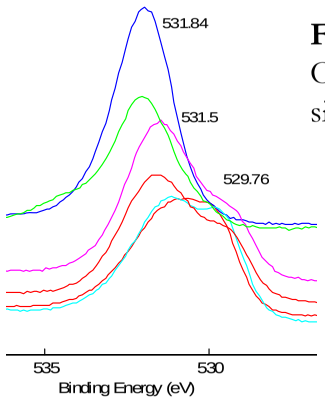

Figure H.10. O 1s peak (all six scans)

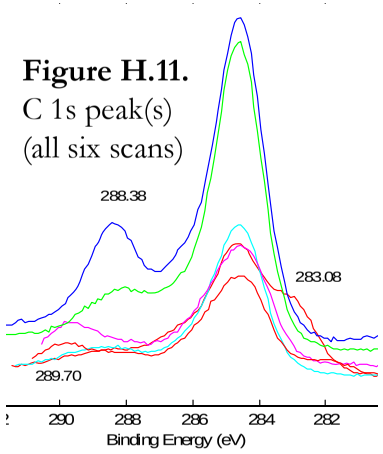

Figure H.11. C 1s peak(s) (all six scans)

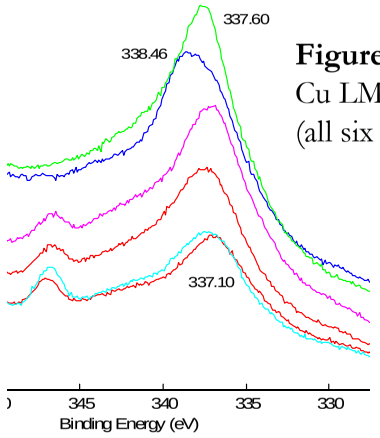

Figure H.12. Cu LMM peak (all six scans)

Building 11A (1984): Mix of $Cu(OH)_2$ and Cu_2O, some $CuCO_3$, Si, P, Ca present

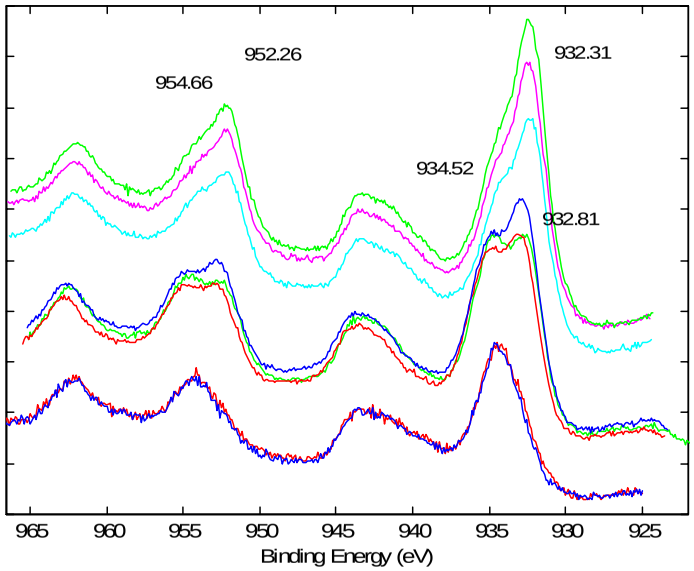

Figure H.13. Cu 2p peaks

Note. For all spectra on this page the top three curves are sample 02, middle three curves are sample 01, and blue/red on bottom is malachite

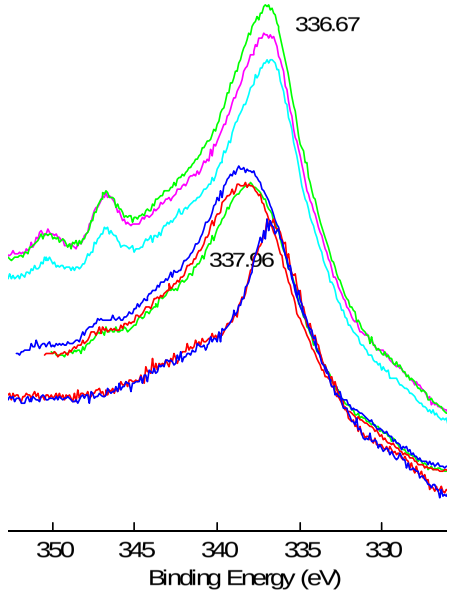

Figure H.14. Cu LMM peak

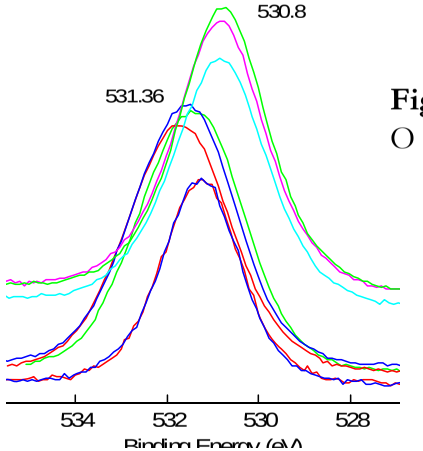

Figure H.15.
O 1s peak

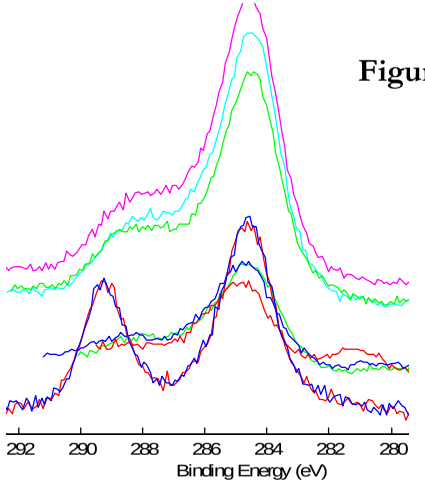

Figure H.16.
C 1s peak(s)

Building 676 (1985): Cu_2O, with P and Cl also present

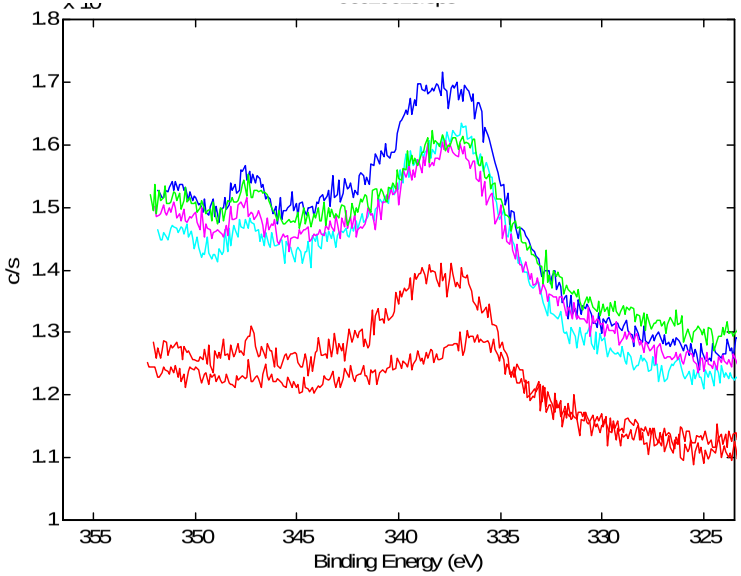

Figure H.17. Cu LMM peak

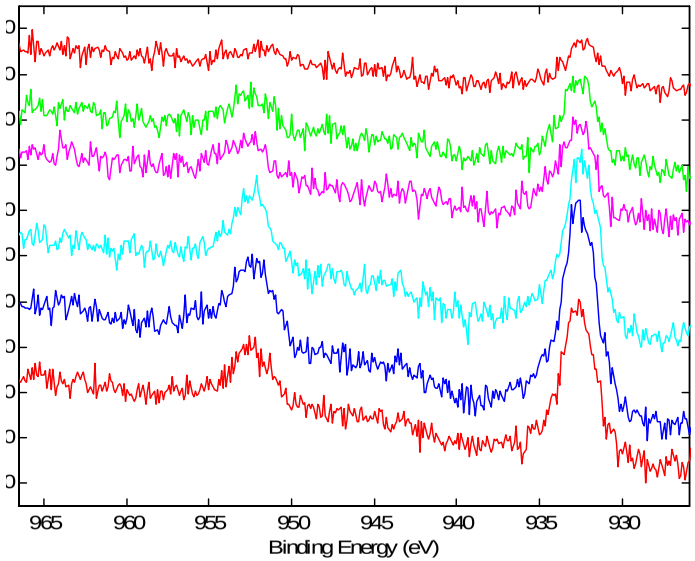

Figure H.18. Cu 2p peaks

Building 642 (1989): $Cu(OH)_2$

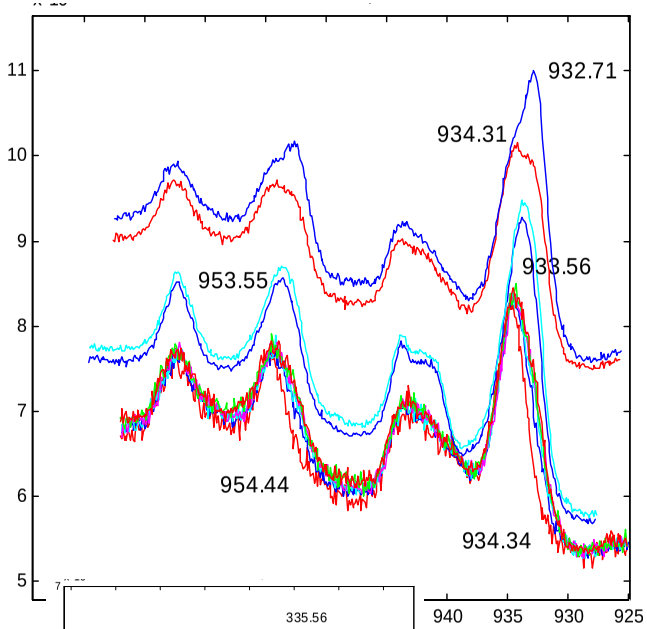

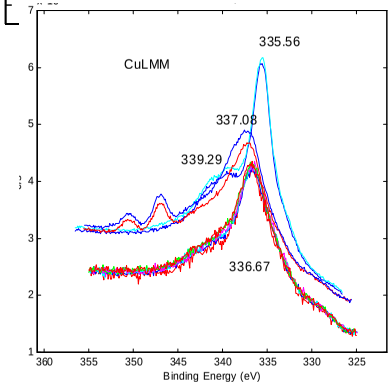

Note. Top blue spectra is the second run, red is the first run, the two middle scans are tenorite, bottom scans are malachite

Figure H.19. Cu 2p peaks (one sample)

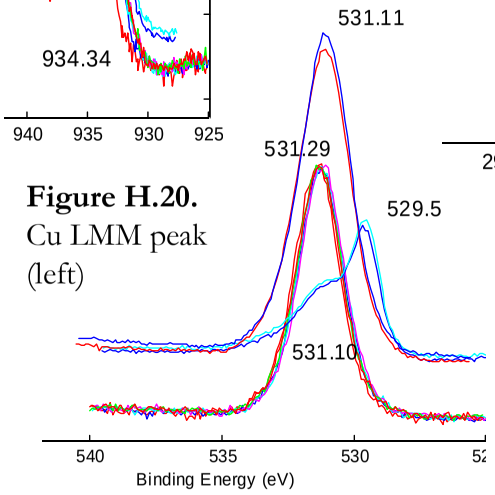

Figure H.20. Cu LMM peak (left)

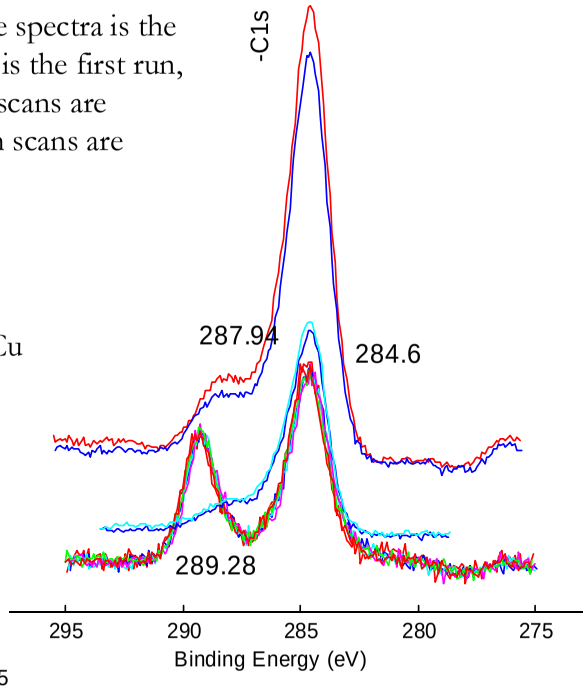

Figure H.21. C 1s peak

Figure H.22. O 1s peak

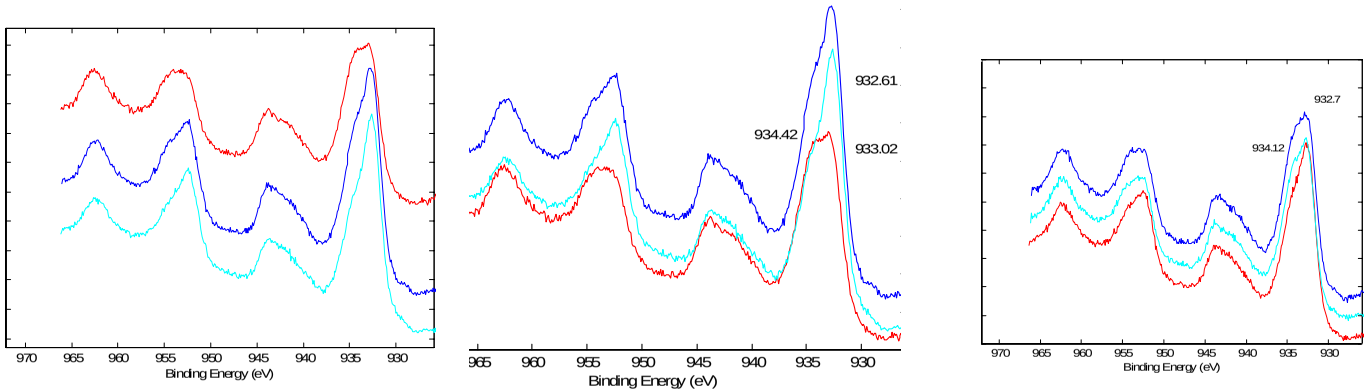

Figure H.23. Cu 2p peaks for both samples from building 620 PI (red is the first scan, blue second, light blue third)

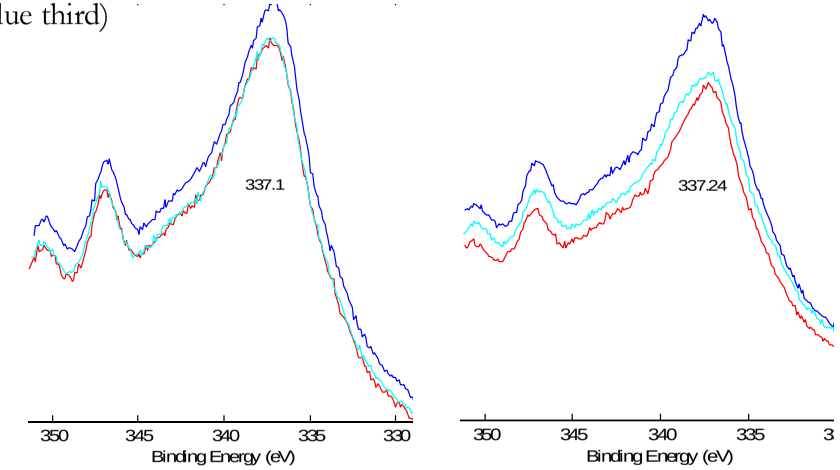

Figure H.24. Cu LMM peak for both samples

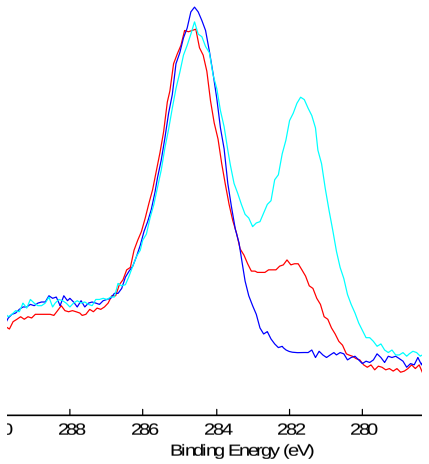

Figure H.25. C 1s peak(s), with possible carbide bond in light blue

Building 441B (1993): Sample 06, Cu(OH)2

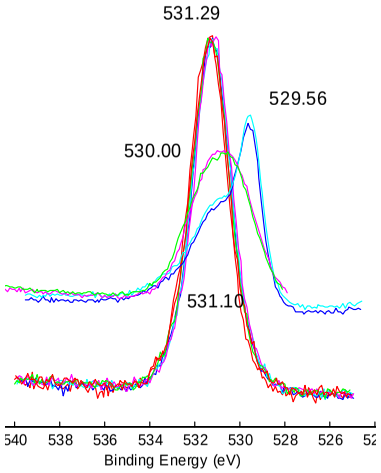

Figure H.27. O 1s peak. Building 441 on top, tenorite curves in the middle, malachite on bottom

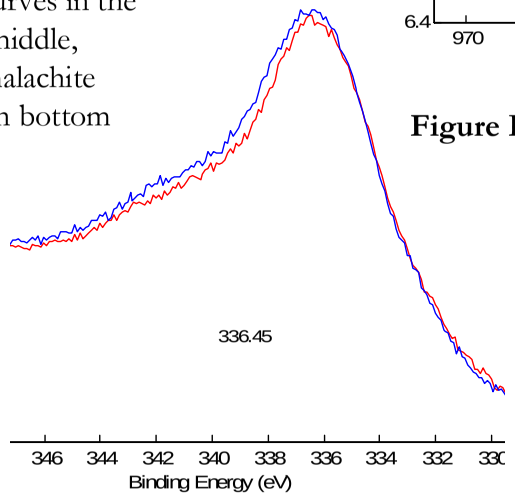

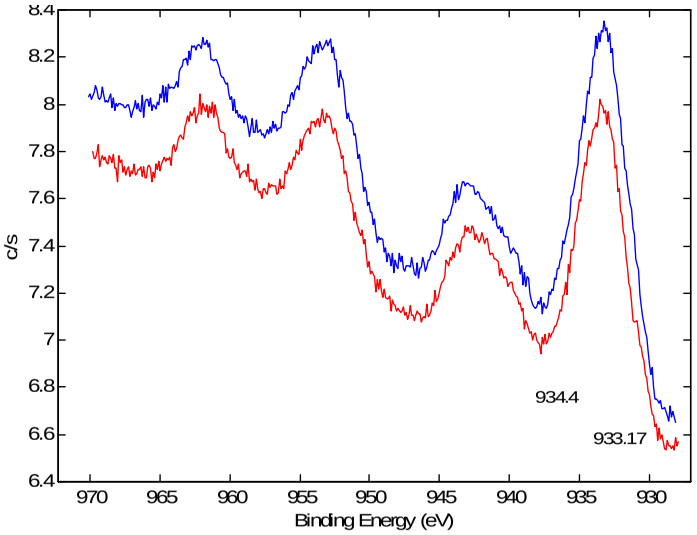

Figure H.28. Cu LMM peak

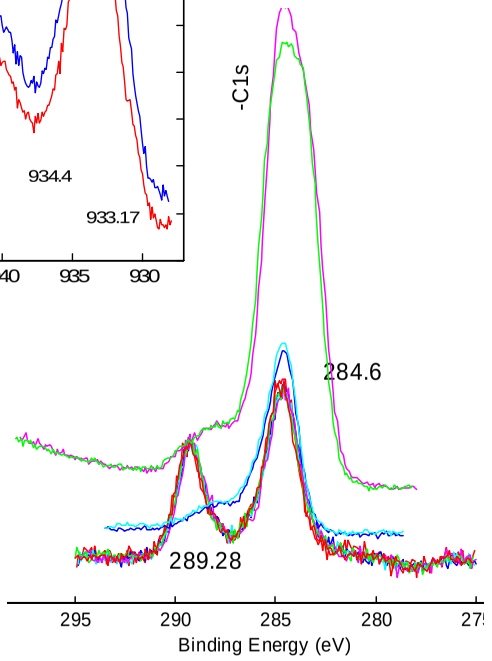

Figure H.29. C 1s peak(s), building 441 on top (pink is first run, green is second), tenorite curves in the middle, malachite on bottom

Figure H.26. Cu 2p peaks

Building 620 Phase II (1994): $Cu(OH)_2$, reducing over time to Cu_2O

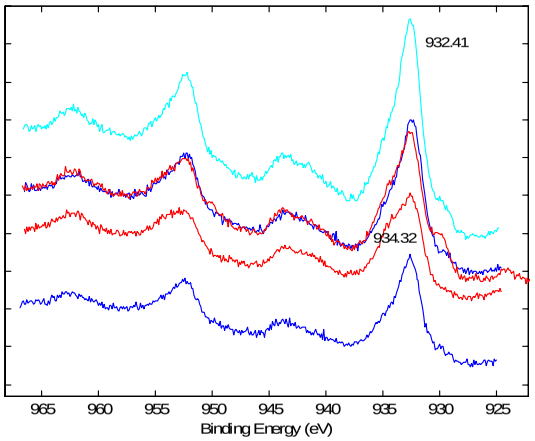

Figure H.32. Cu 2p peaks (all scans)

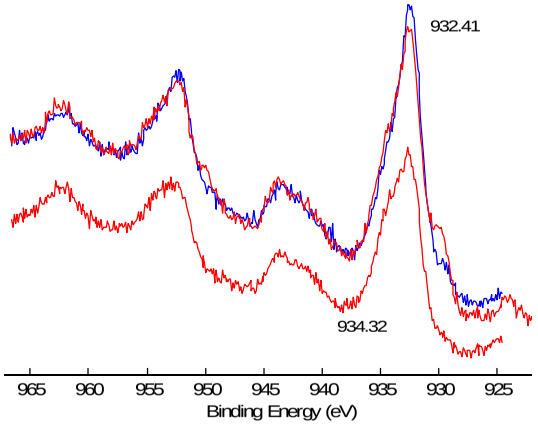

Figure H.34. Cu 2p peaks (single sample)

Figure H.30. Cu LMM peak (all six scans)

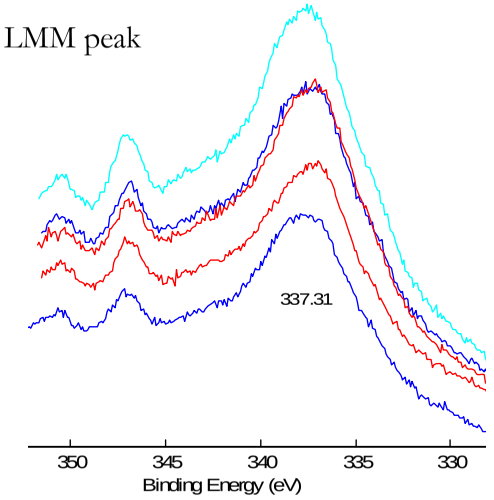

Figure H.31. O 1s peak (all six scans, below)

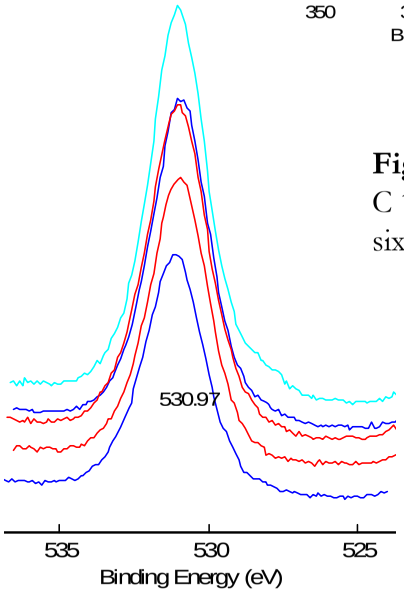

Figure H.33. C 1s peak (all six scans)

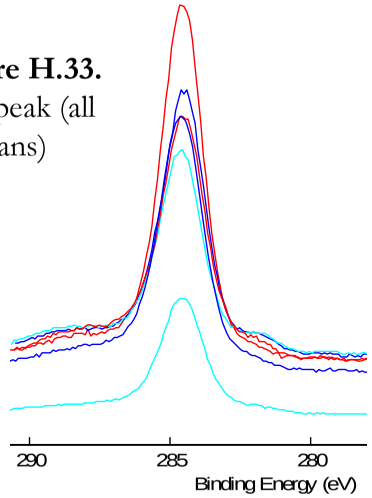

Building 556 (1995): $Cu(OH)_2$ and Cu_2O, with Ca and P present

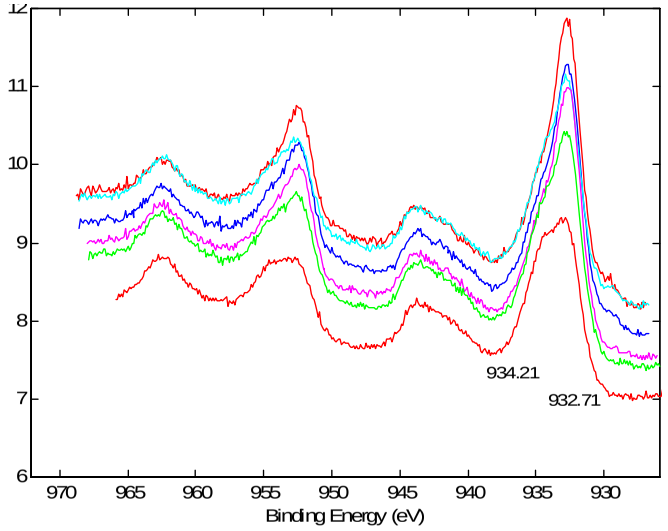

Figure H.35. Cu 2p peaks (all scans)

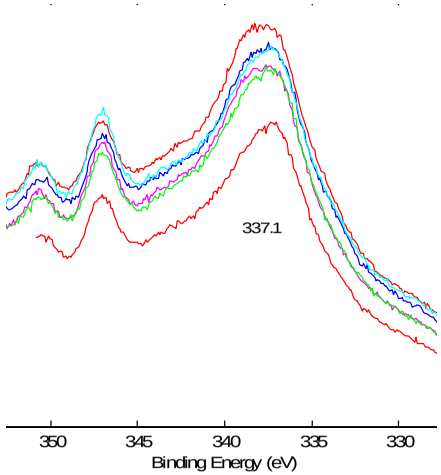

Figure H.36. Cu LMM peak (all six scans)

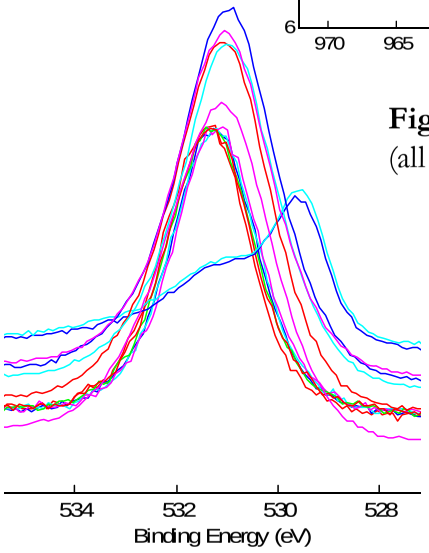

Figure H.37. O 1s peak. Building scans on top, tenorite curves in the middle, malachite on bottom

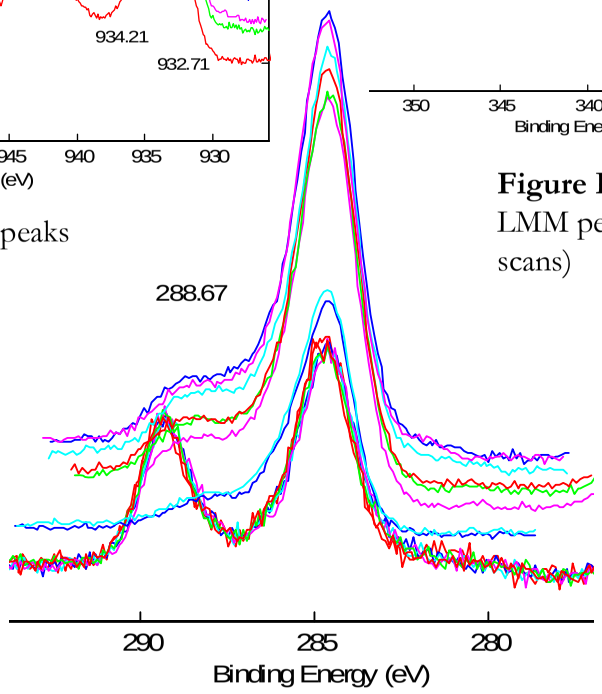

Figure H.38. C 1s peak(s). Building scans on top, tenorite curves in the middle, malachite on bottom

Building 306 (1997): CuCN or CuC(CN)3, with P and Ca present

Figure H.39. Cu 2p peaks (all scans)

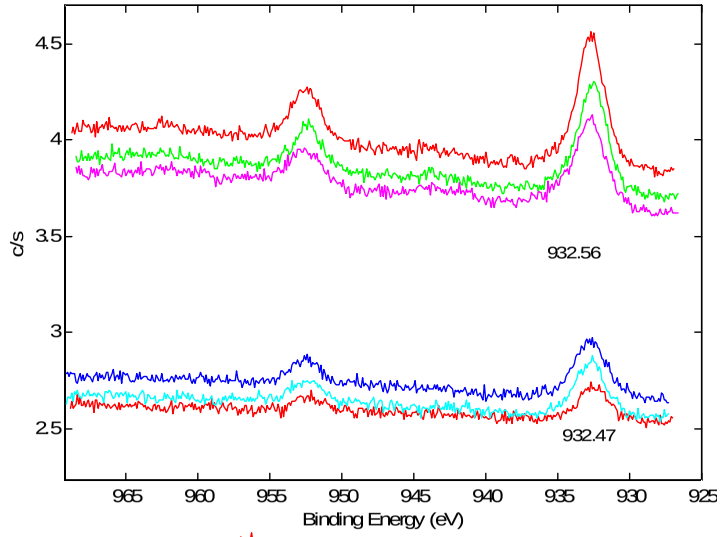

Figure H.40. C 1s peaks (below), building scans on top, tenorite curves in the middle, malachite on bottom

Figure H.41. N 1s peak, located at the binding energy for cyanide or an organic matrix

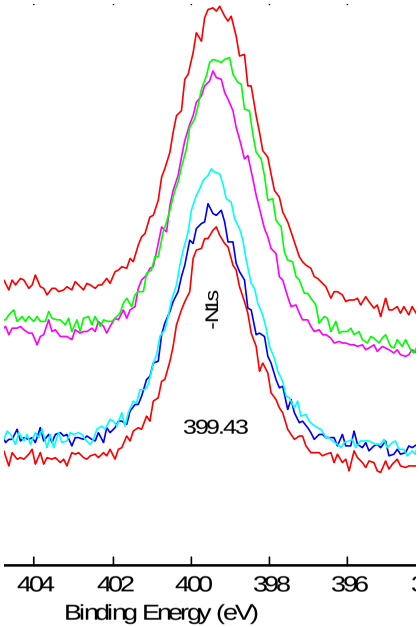

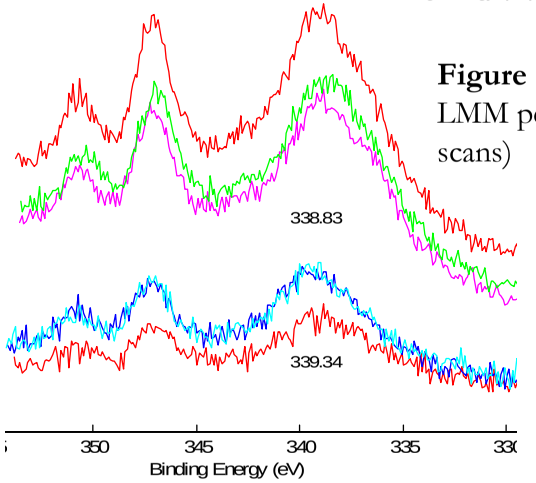

Figure H.42. Cu LMM peak (all six scans)

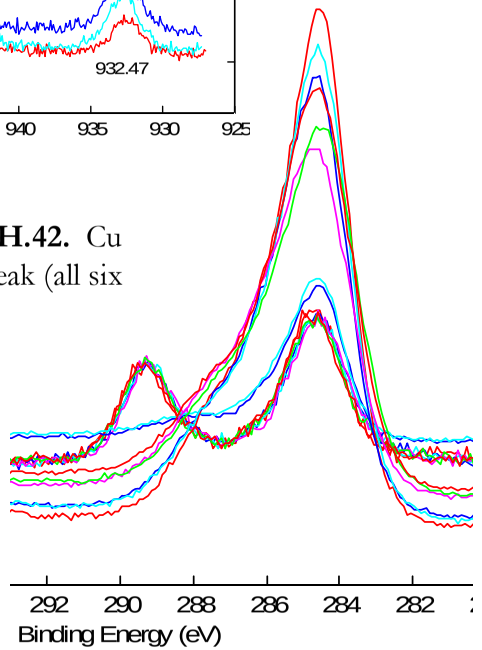

Building 645 (1998): $Cu(OH)_2$, with Cl, P present

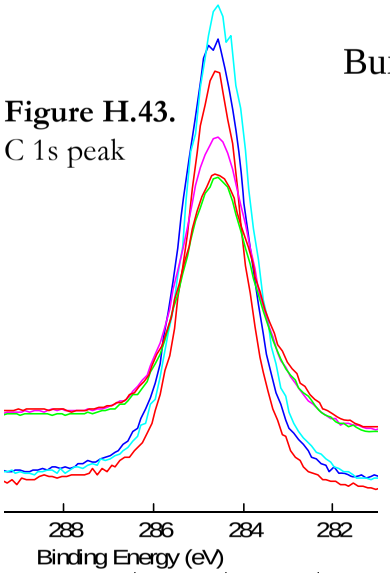

Figure H.43.
C 1s peak

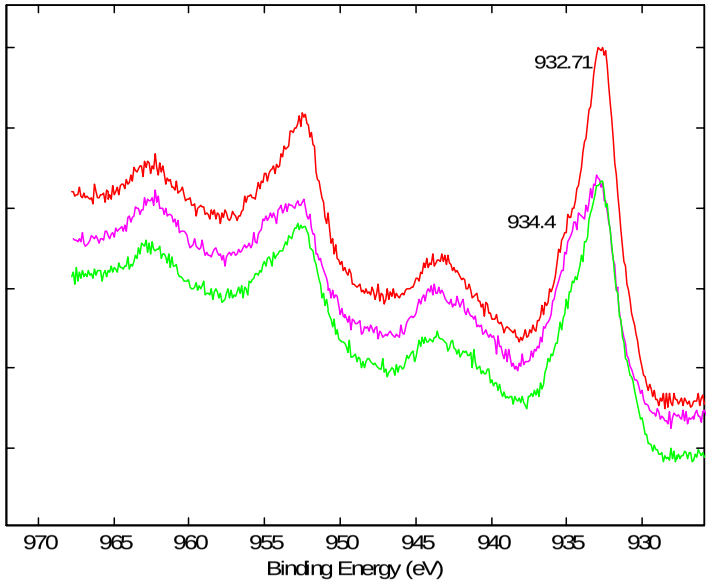

Figure H.44.
Cu 2p peaks. Pink is the first scan, green the second, red the third.

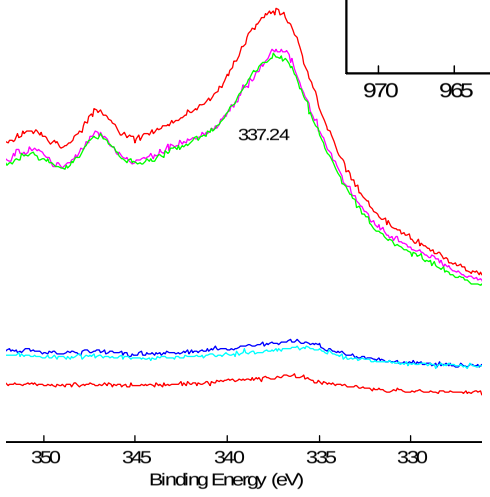

Figure H.45. Cu LMM peak (all six scans)

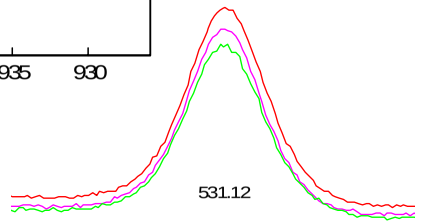

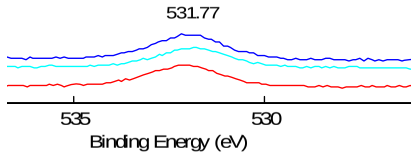

Figure H.46.
O 1s peak

Building 553 (2001) Sample 02: CuCN or $CuC(CN)_3$, $CaCO_3$ may be present, and Zn or ZnO present

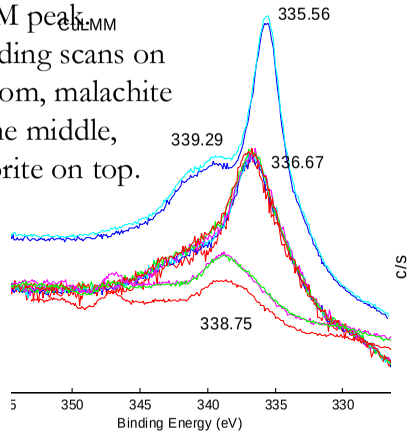

Figure H.47. Cu LMM peak. Building scans on bottom, malachite in the middle, tenorite on top.

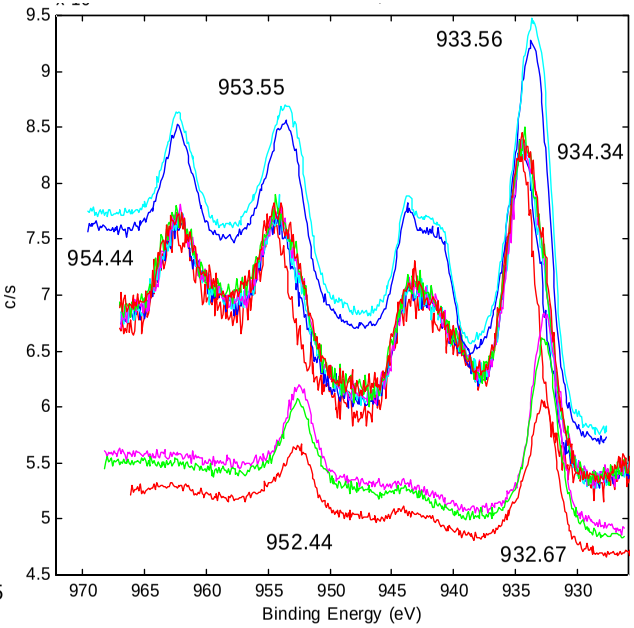

Figure H.50. Cu 2p peaks (above). Building scans on bottom, malachite in the middle, tenorite on top.

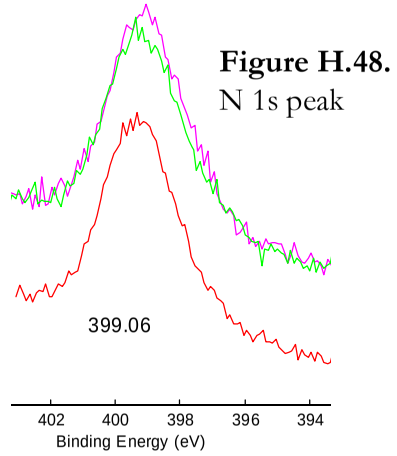

Figure H.48. N 1s peak

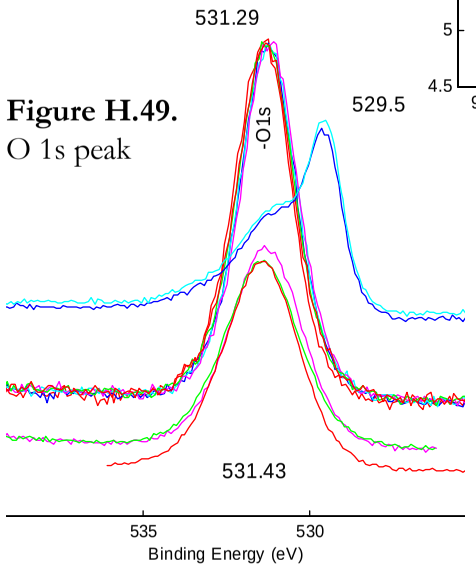

Figure H.49. O 1s peak

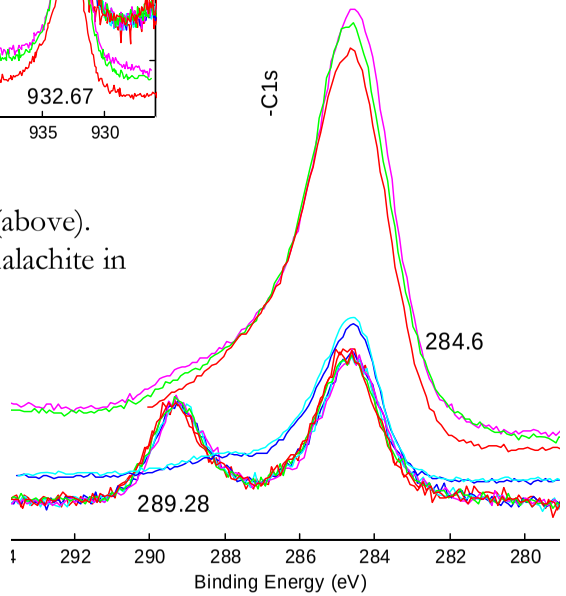

Figure H.51. C 1s peaks (right). Building scans on top, tenorite in the middle, malachite on bottom.

Building 553 (2001) Sample 05: Sulfur present, Cu_2O or Cu_2S

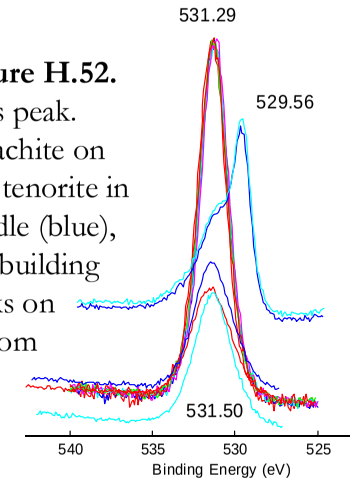

Figure H.52. O 1s peak. Malachite on top, tenorite in middle (blue), and building peaks on bottom

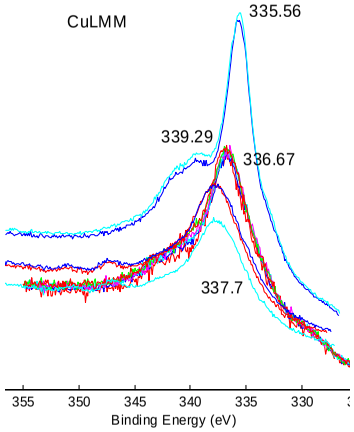

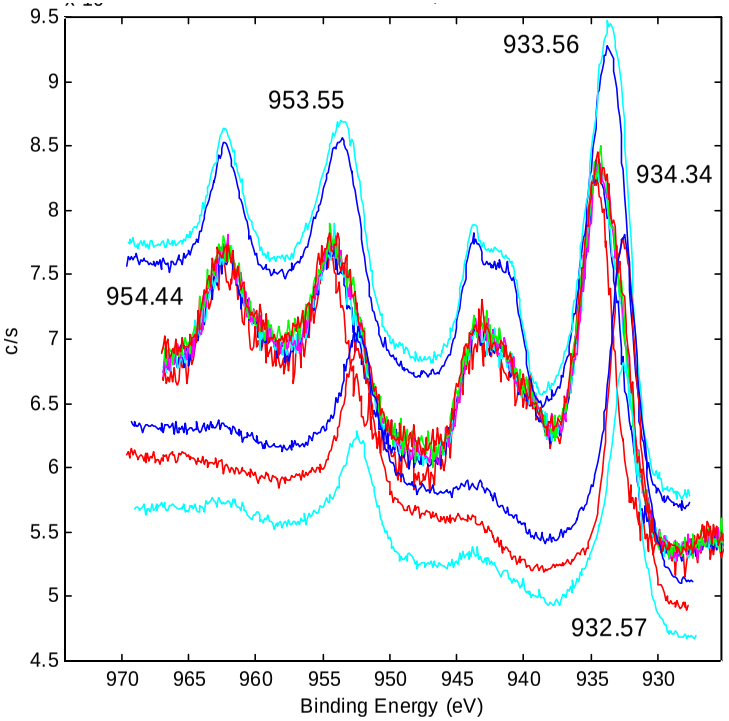

Figure H.54. Cu 2p spectra (above). Building scans on bottom (light blue first run, red second, dark blue third), malachite in the middle, tenorite on top.

Figure H.55. Cu LMM spectra (left). Building scans on bottom, malachite in the middle, tenorite on top.

Figure H.53. C 1s spectra (below). Building scans on top, tenorite in the middle, malachite on bottom.

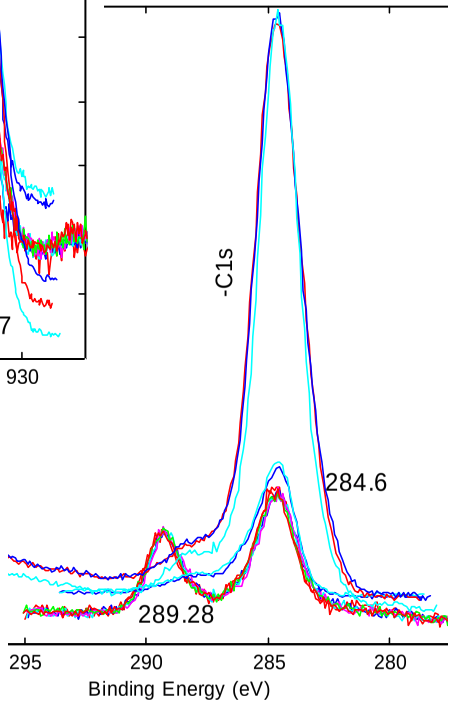

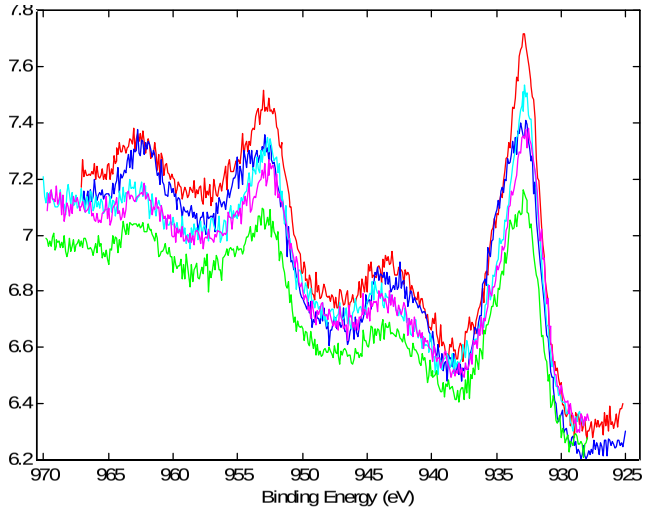

Figure H.57. Cu 2p peaks.

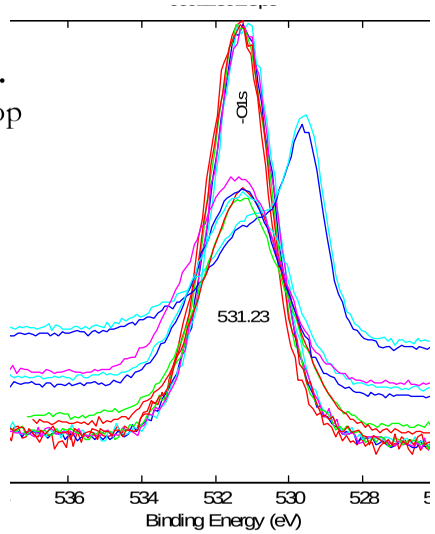

Figure H.56. C 1s peak. Top spectra are malachite, middle (blue) spectra are tenorite for comparison

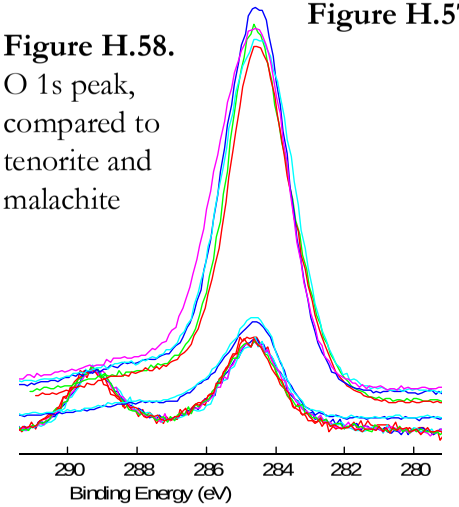

Figure H.58. O 1s peak, compared to tenorite and malachite

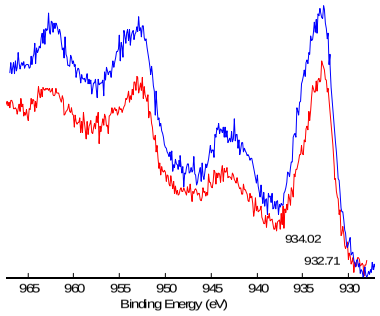

Figure H.60. Cu 2p peaks of the first run on each sample

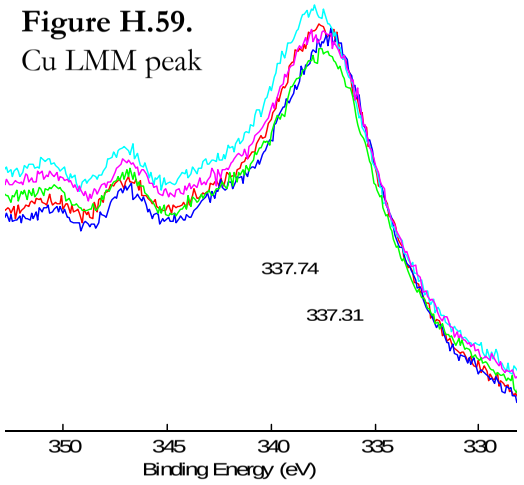

Figure H.59. Cu LMM peak

Building 837 (2004): Sample 02, $Cu(OH)_2$ shape; Sample 01: Cu_2O shape, with P, Ca, Si, Cl present

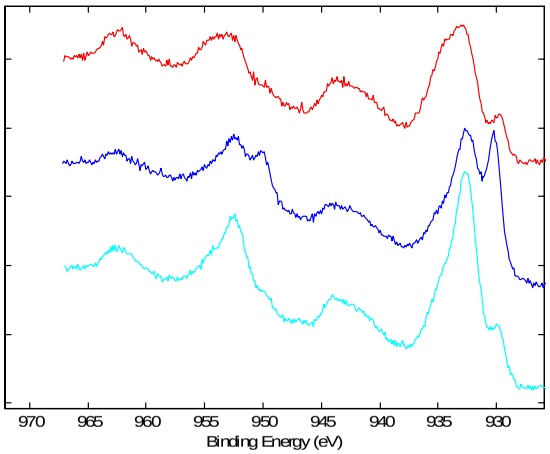

Figure H.61. Cu 2p peaks. Red first, blue second, light blue third spectra

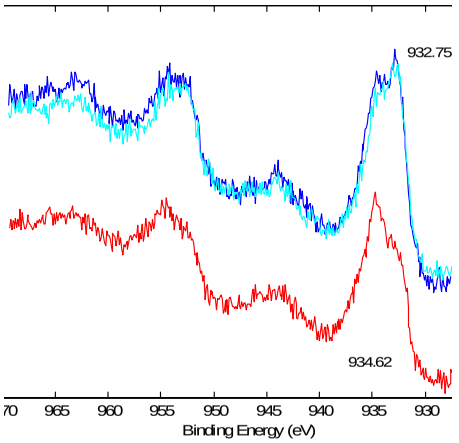

Figure H.62. Cu 2p peaks of the first run on each sample

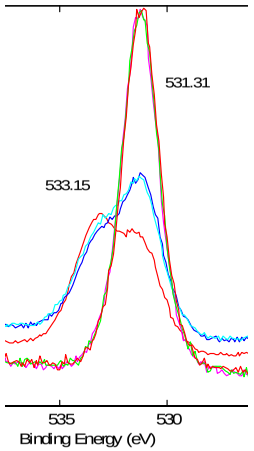

Figure H.63. O 1s peak. Top peak is malachite for comparison

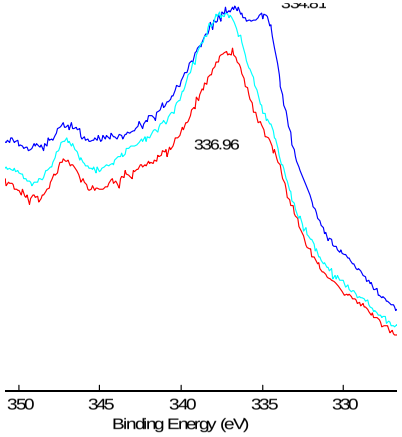

Figure H.65. Cu LMM peak

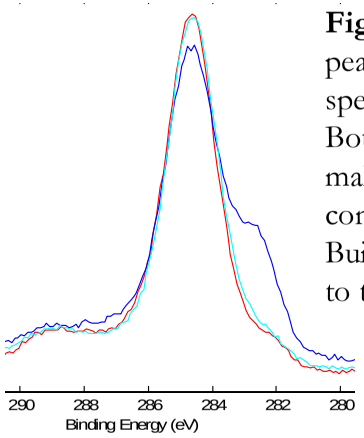

Figure H.64. C 1s peak (right and left). In spectra to the right, Bottom spectra are malachite for comparison. Building's spectra only to the left

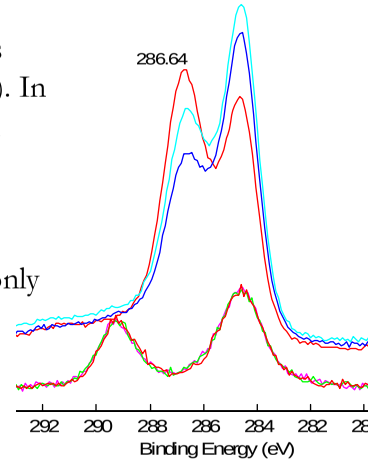

Building 441S (2005): Cu_2O, maybe C with Cl, N, S, or O with Si, N, P

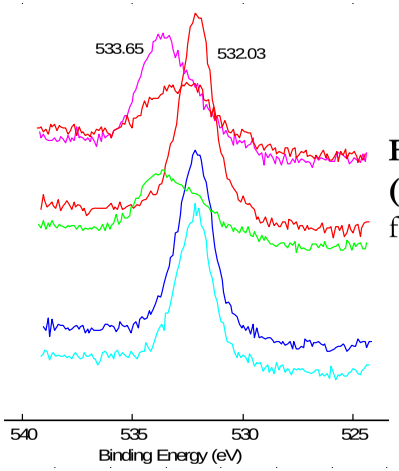

Figure H.66.
(left) O 1s peak for all samples

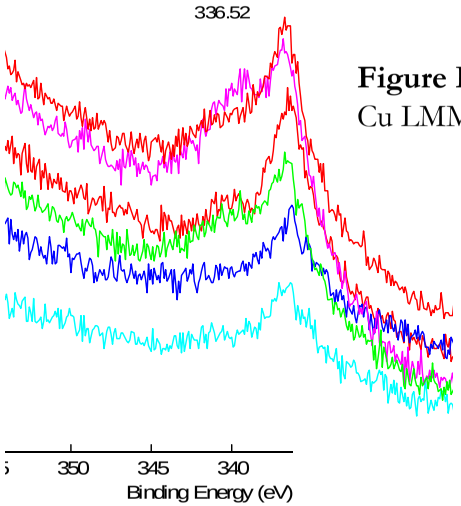

Figure H.67.
Cu LMM peak

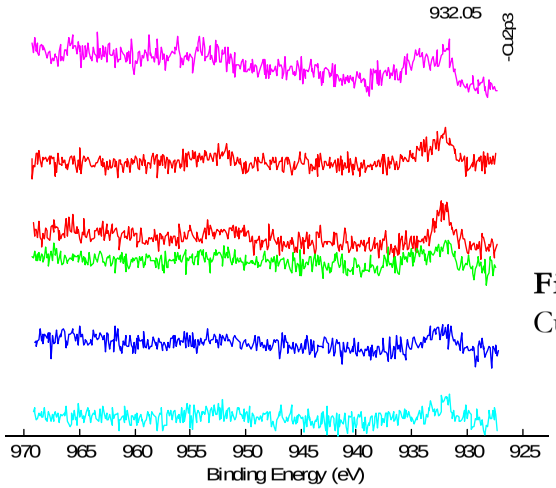

Figure H.69.
Cu 2p peaks

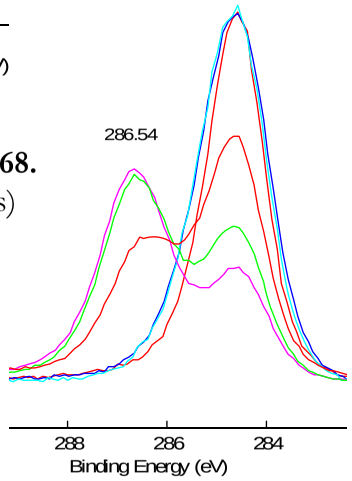

Figure H.68.
C 1s peak(s)

Appendix I

XPS Spectra of Malachite

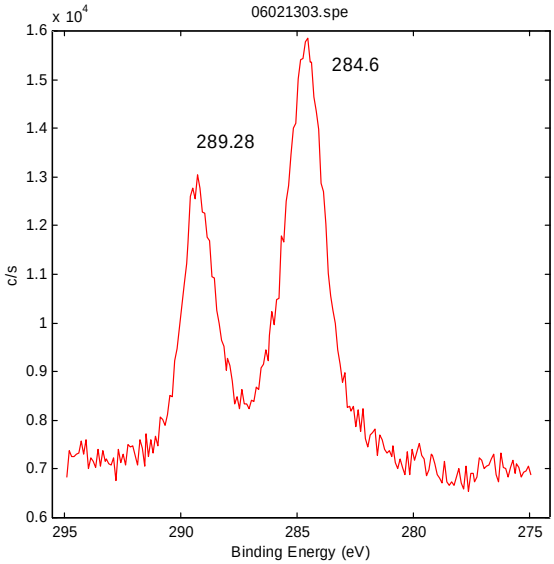

Figure I.1. C 1s peak for malachite. Carbon contamination corrected to 284.6 eV, and the carbonate peak is at 289.3 eV

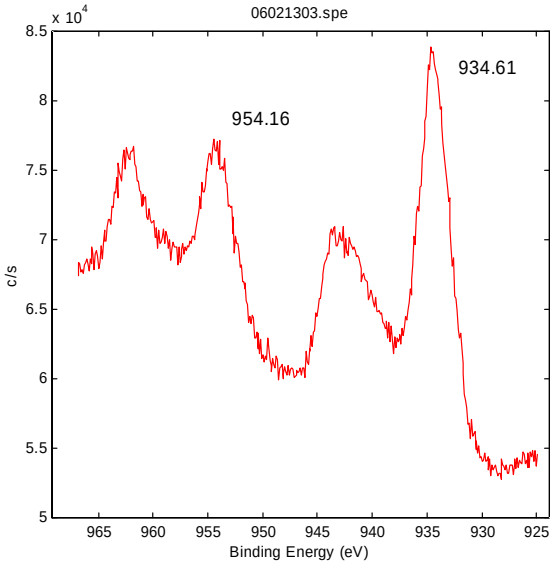

Figure I.2. Cu 2p peaks for malachite. The Cu 2p(3/2) peak is located at 934.6 eV and Cu 2p(1/2) peak at 954.2 eV

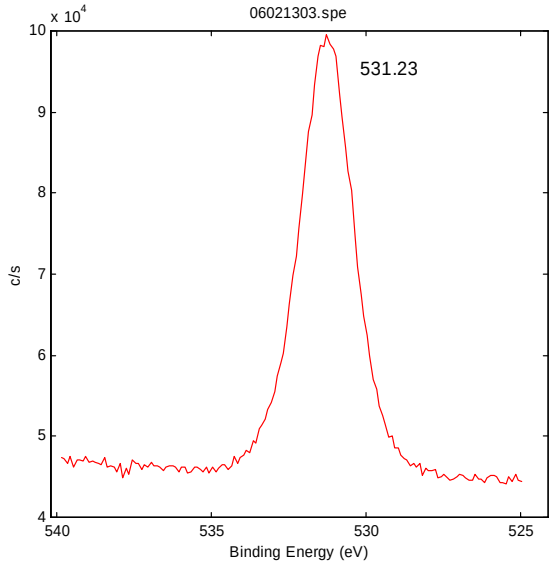

Figure I.3. O 1s peak for malachite, located at 531.2 eV

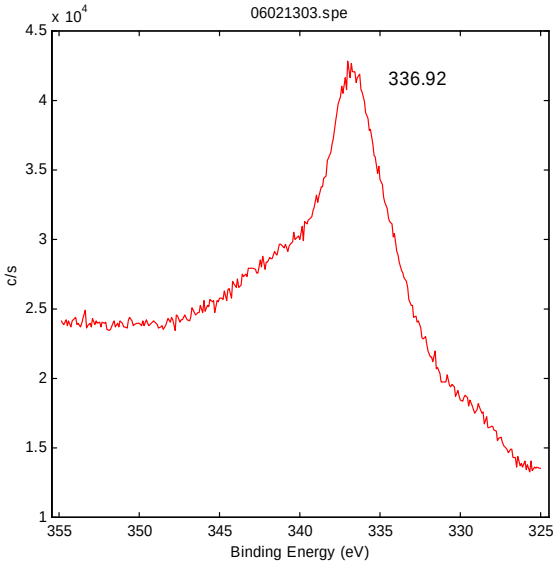

Figure I.4. Cu LMM peak for malachite, located at 336.9 eV

Figure I.5 Chemical State Plot: Malachite [$Cu_2CO_3(OH)_2$] with other Referenced Copper Species

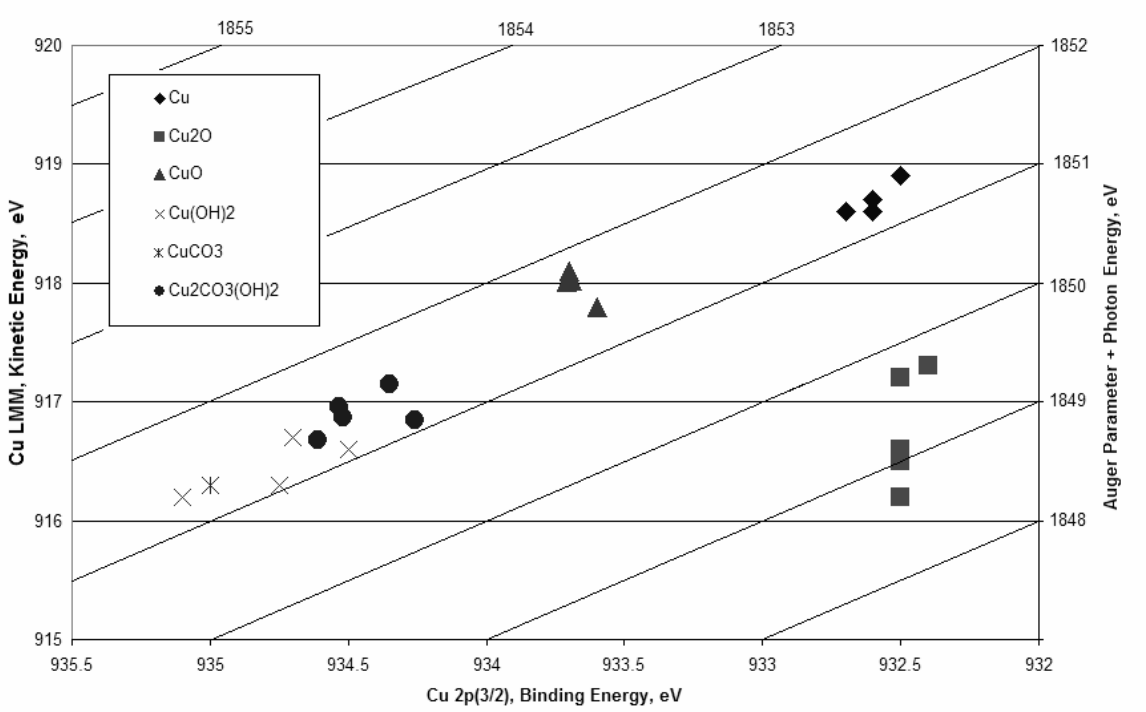

References

Adeloju, S. B. and Hughes, H. C. The corrosion of copper pipes in high chloride-low carbonate mains water. *Corrosion Science*. 26:10: 851-870 (1986).

American Society for Testing and Materials (ASTM). *Annual book of ASTM standards*. Vol. 11.01, Section 11. Philadelphia: American Society for Testing and Materials, 1994.

American Water Works Association (AWWA). *Internal Corrosion of Water Distribution Systems*. AWWA Research Foundation and DVGW-Forschungsstelle, (1985).

Boistelle, R. and Astier, J.P. Crystallization mechanisms in solution. *Journal of Crystal Growth.* 90: 14-30. (1988).

Boulay, N., and Edwards, M. Role of temperature, chlorine, and organic matter in copper corrosion by-product release in soft water. *Water Research*. 35:3: 683-690 (2001).

Brandenberg, B., Ross T., Elzufon, B., Malone, C., Grovhoug, T. *Contra Costa Central Sanitary District Residential Metal Study [Engineering Study Report]*. Davis CA: Larry Walker and Assoc. and CCCSD (July-August 1993).

Briggs, D. and Seah, M. P. Chapter 10: Uses of Auger Electron and Photoelectron Spectroscopies in Corrosion Science. *Practical Surface Analysis*. New York: John Wiley & Sons, 1983.

Brecevic, L. Crystal Growth Kinetics and Mechanisms. *Encyclopedia of Surface and Colloid Science.* NewYork: Dekker, 2002.

Broo, A. E., Berghult B., and Hedberg, T. Copper corrosion in drinking water distribution systems – the influence of water quality. *Corrosion Science,* 39:6: 1119-1132 (1997).

Cantor, A. G., Denig-Chakroff, D., Vela, R. R., Oleinik, M.G. Use of Polyphosphate in Corrosion Control. *Journal of the American Water Works Association,* 92:2: 95 (2000).

Chawla, S. K., Sankarraman, N., and Payer, J. H. Diagnostic spectra for XPS analysis of Cu-O-S-H compounds. *Journal of Electron Spectroscopy and Related Phenomena*, 61: 1-18 (1992).

Copper Development Association (CDA). *Industrial Applications – Corrosion Resistance*. http://www.copper.org/applications/plumbing/Overview/indl_appns.htm#corrnres. 29 July 2005

----. *Uses of Copper Compounds: Other Copper Compounds*. http://www.copper.org/applications/compounds/other_compounds.html. 20 February 2006

Deroubaix, G. and Marcus, P. X-ray photoelectron spectroscopy analysis of copper and zinc oxides and sulphides. *Surface and Interface Analysis*, 18: 39-46. (1992).

Eaton, A. D., Clesceri, L. S., Greenberg, A. E., Franson, M. H., American Public Health Association., American Water Works Association., Water Environment Federation. *Standard Methods for the Examination of Water and Wastewater, 18th Edition*. Washington, DC: American Public Health Association, 1992.

Edwards, M., Hidmi, L., and Gladwell, D. Phosphate inhibition of soluble copper corrosion by-product release. *Corrosion Science*, 44: 1057-1071 (2002).

Edwards, M., Schock, M. R., and Meyers, T. E. Alkalinity, pH, and Cu: Corrosion By-Product Release. *Journal of the American Water Works Association*, 88:3: 81 (1996).

Feng, Y., Teo, W. K., Siow, K. S., Tan, K. L., Hsieh, A. K. The corrosion behaviour of copper in neutral tap water. Part I: corrosion mechanisms. *Corrosion Science*. 38: 387 (March, 1996a).

Feng, Y., Teo, W. K., Siow, K. S., Hsieh, A. K. The corrosion behaviour of copper in neutral tap water. Part II: determination of corrosion rates. *Corrosion Science*. 38: 369 (March, 1996b).

Frost, D. C., Ishitani, A., and McDowell, C. A. X-ray photoelectric spectroscopy of copper compounds. *Molecular Physics*, 24:4: 861-877 (1972).

Hidmi, L. and Edwards, M. Role of Temperature and pH in $Cu(OH)_2$ Solubility. *Environmental Science & Technology*, 33: 2607-2710 (1999).

Iijima, Y., Niimura, N., and Hiraoka, K. Prevention of the reduction of CuO during x-ray photoelectron spectroscopy analysis. *Surface and Interface Analysis*, 24: 193-197 (1996).

Institute of Medicine of the National Academies. *Dietary Reference Intakes for Vitamine A, Vitamin K, Arsenic, Boron, Chromium, Copper, Iodine, Iron, Manganese, Molybdenum, Nickel, Silicon, Vanadium, and Zinc*. Washington DC: National Academies Press, 2000.

International Standards Organization (ISO). *ISO 8044:19999 Corrosion of metals and alloys -- Basic terms and definitions*. Author, 2004.

Introduction to Electrochemical Techniques. http://www.cp.umist.ac.uk/lecturenotes/Echem/intro.html. 15 August 2005

Ives, D. J., and Rawson, A. E. Copper Corrosion III: Electrochemical Theory of General Corrosion. *Journal of the Electrical Society*, 109:6: 458 (1962).

Kimbrough, D. E. Brass Corrosion and the LCR Monitoring Program. *Journal of the American Water Works Association*, 93:2: 81 (February 2001).

Klein, J. C., Li, C. P., Hercules, D. M., Black, J. F. Decomposition of copper compounds in x-ray photoelectron spectroscopy. *Applied Spectroscopy*, 38:5: 729-734 (1984).

Knobeloch, L. et al. Gastrointestinal Upsets and New Copper Plumbing: Is There a Connection? *Wisconsin Medical Journal*, 97: 49-53 (January 1998).

Lagos, G. E., Cuadrado C. A., Letelier, M. V. Aging of Copper Pipes by Drinking Water. *Journal of the American Water Works Association*, 93:11: 94 (November 2001).

Lagos, G. E., Maggi, L. C., Peters, D., Reveco, F. Model for estimation of human exposure to copper in drinking water. *The Science of the Total Environment*, 239: 49-70 (1999).

Lane, R. W. *Control of Scale and Corrosion in Building Water Systems.* New York: McGraw Hill, 1993.

Mattsson, E. *Basic Corrosion Technology for Scientists and Engineers.* West Sussex, England: Ellis Horwood, 1989.

McIntyre, N. S. and Cook, M. G. X-ray photoelectron studies on some oxides and hydroxides of cobalt, nickel, and copper. *Analytical Chemistry*, 47:13: 2208-2213 (1975).

McIntyre, N. S., Sunder, S., Shoesmith, D. W., and Stanchell, F. W. Chemical information from XPS—applications to the analysis of electrode surfaces. *Journal of Vacuum Science Technology*, 18:3: 714-721 (1981).

McNeill, L. S. and Edwards, M. Importance of Pb and Cu particulate species for corrosion control. *Journal of Environmental Engineering*, 130:2: 136-144 (February 2004).

Moulder, J. F., Stickle, W. F., Sobol, P. E., and Bomben, K. D. *Handbook of x-ray photoelectron spectroscopy*. Eden Prairie, MN: Physical Electronics, Inc, 1995.

Palit A. and Pehkonen, S. O. Copper corrosion in distribution systems: evaluation of a homogenous Cu_2O film and a natural corrosion scale as corrosion inhibitors. *Corrosion Science*, 42: 1801-1822 (2000).

Paparazzo, E. and Moretto L. X-ray photoelectron spectroscopy and scanning Auger microscopy studies of bronzes from the collections of the Vatican Museums. *Vacuum*, 55: 59-70 (1999).

Patterson, J. W., Bolce, R. E., and Marani, D. Alkaline Precipitation and Aging of Copper from Dilute Cupric Nitrate Solution. *Environmental Science & Technology*, 25: 1780-1787 (1991).

Pontius, F. W. Defining a safe level for copper in drinking water. *American Water Works Association Journal*, 90:7: 18 (July 1998).

Rajaratnam, G., Winder, C., An, M., Metals in drinking water from new housing estates in the Sydney area. *Environmental Research*, Section A 89: 165-170 (2002).

Schindler, P., Althaus, H., Hofer, F., and Minder, W. Löslichkeitsproduckte von Zinkoxid, Kupferhydroxid und Kupferoxid in Abhängigkeit von Teilchengrösse und molarer Oberfläche. Ein Beitrag zur Thermodynamik von Grenzflächen fest-flüssig. *Helvetica Chimica Acta*. 48:5: 1204-1215 (1965).

Schock, M. R., Lytle, D. A., Clement, J. A., and Black and Veatch. *Effect of pH, DIC, Orthophosphate and Sulfate on Drinking Water Cuprosolvency* (EPA 600-R-95-085). Cincinnati OH: National Risk Management Research Laboratory Office of Research and Development, US Environmental Protection Agency, 1995.

Schroeder, H. A., Nason, A. P., Tipton, B. A. and Balassa, J. J. Essential Trace Metals in Man: Copper. *J. Chronicle of Disease*, 19: 1007-1034 (1966).

Seiler, H. G., Sigel, A., and Sigel, H. *Handbook on metals in clinical and analytical chemistry*. New York: Marcel Drekkar Inc, 1994.

Settle, F. A. *Handbook of instrumental techniques for analytical chemistry*. Upper Saddle River, NJ : Prentice Hall, 1997.

Sharrett, A. R., Carter, A. P., Orheim, R. M. and Feinleib, M. Daily Intake of Lead, Cadmium, Copper, and Zinc from Drinking Water: The Seattle Study of Trace Metal Exposure. *Environmental Research*, 28: 456-475 (1982a).

Sharrett, A. R., Orheim, R. M., Carter, A. P., Hyde, J. E., and Feinleib, M. Components of Variation in Lead, Cadmium, Copper, and Zinc Concentration in Home Drinking Water: The Seattle Study of Trace Metal Exposure. *Environmental Research*, 28: 476-498 (1982b).

Shaw Environmental, Inc. *Investigation/Survey of Lead & Copper in Drinking Water at Child Care Development Centers.* Available from the Wright-Patterson Air Force Base, Civil Engineer Group, Environmental Flight, Dayton, OH 45433, (May 6, 2005).

Shim, J. J. and Kim, J. G. Copper corrosion in potable water distribution systems: influence of copper products on the corrosion behavior. *Materials Letters*, 58: 2002-2006 (2004).

Skoog, D. A. and West, D. M. *Principles of instrumental analysis*. New York: Holt, Rinehart and Winston, Inc, 1971.

Squarcialupi, M. C., Bernardini, G. P., Faso, V., Atrei, A, and Rovida, G. Characterization by XPS of the corrosion patina formed on bronze surfaces. *Journal of Cultural Heritage* 3: 199-204 (2002).

United States Congress (USC). *Code of Federal Regulations. Vol. 40, 141 & 142.* Federal Register 56:110:26462. Washington, DC: GPO, June 7, 1991.

-----. *Safe Drinking Water Act Amendments of 1986*. Public Law 99-339 Washington DC: GPO, 1986.

United States Department of Health and Human Services. *Toxicological profile for copper*. Agency for Toxic Substances and Disease Registry. (September 2004).

United States Environmental Protection Agency (USEPA). *Methods for the Determination of Inorganic Substances in Environmental Samples.* (EPA 600/R-93/100) Washington, DC: Author. (1993).

---. *Methods for the Determination of Metals in Environmental Samples.* (USEPA 600/4-91-010). Washington, DC: Author. (1994).

----. *Process design manual: land application of sewage sludge and domestic septage.* (EPA 625-K-95-001). Washington DC: Office of Research and Development, US Environmental Protection Agency. (September 1995).

----. *Lead and Copper Rule: A Quick Reference Guide* (USEPA 816-F-04-009). Washington, DC: Author. (March 2004).

Vehorn, C. J. Civil Engineer, 88 ABW/CECP. Personal interview. October 3, 2005.

Zhang, X., Simo, P.O., Kocherginsky, N., and Ellis, G. A. Copper corrosion in midly alkaline water with the disinfectant monochloramine. *Corrosion Science*, 44: 2507-2528 (2002).

Vita

Captain Nadja Frank Turek graduated from Chaminade-Julienne High School in Dayton, Ohio. She entered undergraduate studies at the University of Colorado in Boulder, Colorado where she graduated with distinction in December 2000, earning a Bachelor of Science degree in Civil Engineering. She was commissioned through the Detachment 105 AFROTC at the University of Colorado where she was recognized as a Distinguished Graduate.

Her first assignment was at Spangdahlem Air Base, Germany assigned to the 52nd Civil Engineer Squadron. There she served as the Protection Section Chief in the Environmental Flight and then as the Chief of Operations and Maintenance Programs in the Engineering Flight. In February 2003, she was assigned to the 78th Civil Engineer Group at Robins AFB, Georgia where she served as a Maintenance Engineer and as the Customer Service Flight Commander. In August 2004, she graduated with a Masters of Non-profit Management from Regis University in Denver, Colorado and in September 2004, she entered the Graduate School of Engineering and Management, Air Force Institute of Technology. Upon graduation, she will be assigned to the Civil Engineer and Services School at Wright-Patterson AFB, Dayton, Ohio, and an instructor.

REPORT DOCUMENTATION PAGE

Form Approved
OMB No. 074-0188

1. REPORT DATE *(DD-MM-YYYY)*	**2. REPORT TYPE**	**3. DATES COVERED** *(From – To)*
March 2006	**Master's Thesis**	Oct 2004 – Mar 2006

4. TITLE AND SUBTITLE

Investigation of Copper Contamination and Corrosion Scale Mineralogy in Aging Drinking Water Distributions Systems

5a. CONTRACT NUMBER

5b. GRANT NUMBER

5c. PROGRAM ELEMENT NUMBER

6. AUTHOR(S)

Turek, Nadja, F., Captain, USAF

5d. PROJECT NUMBER

5e. TASK NUMBER

5f. WORK UNIT NUMBER

7. PERFORMING ORGANIZATION NAMES(S) AND ADDRESS(S)
Air Force Institute of Technology
Graduate School of Engineering and Management (AFIT/EN)
2950 Hobson Way
WPAFB OH 45433-7765

8. PERFORMING ORGANIZATION REPORT NUMBER

AFIT/GES/ENV/06M-05

9. SPONSORING/MONITORING AGENCY NAME(S) AND ADDRESS(ES)
88 ABW/CE-2
Attn: Mr. Randy Parker
Building 11, Area A
WPAFB OH 45433 (937)257-6214

10. SPONSOR/MONITOR'S ACRONYM(S)

11. SPONSOR/MONITOR'S REPORT NUMBER(S)

12. DISTRIBUTION/AVAILABILITY STATEMENT
APPROVED FOR PUBLIC RELEASE; DISTRIBUTION UNLIMITED.

13. SUPPLEMENTARY NOTES

14. ABSTRACT

Research has shown higher levels of copper appear in drinking water conveyed through relatively new copper piping systems; older piping systems typically deliver lower copper levels in their drinking water. This research contributes field data from a real drinking water distribution system, providing a better understanding of this phenomenon, as it relates to treatment considerations and compliance with the Lead and Copper Rule. Copper pipes and copper levels were sampled from drinking water taps of 16 buildings with pipes ranging in age from less than 1 to 48 years. Water samples from each building were collected before and following a 16-hour stagnation period. A piece of domestic cold water pipe was cut from each building and analyzed to determine the mineralogy of the copper scale present using x-ray diffraction (XRD) and x-ray photoelectron spectroscopy (XPS) technologies. Results were compared to the predictions of the "cupric hydroxide model," developed by the Environmental Protection Agency. The samples showed remarkable variation in scale appearance and mineralogy, demonstrating the diversity of pipe scales present within a single distribution system. A mix of highly soluble and relatively insoluble copper phases were identified in the real world scale. Both stable scales, such as malachite, and relatively instable solids, such as cupric hydroxide appear in pipes irrespective of age. In many samples cupric hydroxide and cuprite appeared on the surface of the scale while malachite was in the bulk. Copper cyanide was also identified in two pipe scales. XPS and XRD are shown to be complimentary techniques for characterizing complex scales made up of a mixture of amorphous and crystalline solids.

15. SUBJECT TERMS
Copper, Corrosion, Scale, Mineralogy, X-ray Diffraction, X-ray Photoelectron Spectroscopy, Drinking Water, Lead and Copper Rule, Plumbing,
Water Distribution System

16. SECURITY CLASSIFICATION OF:			**17. LIMITATION OF ABSTRACT**	**18. NUMBER OF PAGES**	**19a. NAME OF RESPONSIBLE PERSON**
REPORT	**ABSTRACT**	**c. THIS PAGE**			Dr. Mark N. Goltz (ENV)
U	**U**	**U**	**UU**	207	**19b. TELEPHONE NUMBER** *(Include area code)* (937) 255-3636, ext 4638; e-mail: mgoltz@afit.edu

Standard Form 298 (Rev: 8-98)
Prescribed by ANSI Std. Z39-18